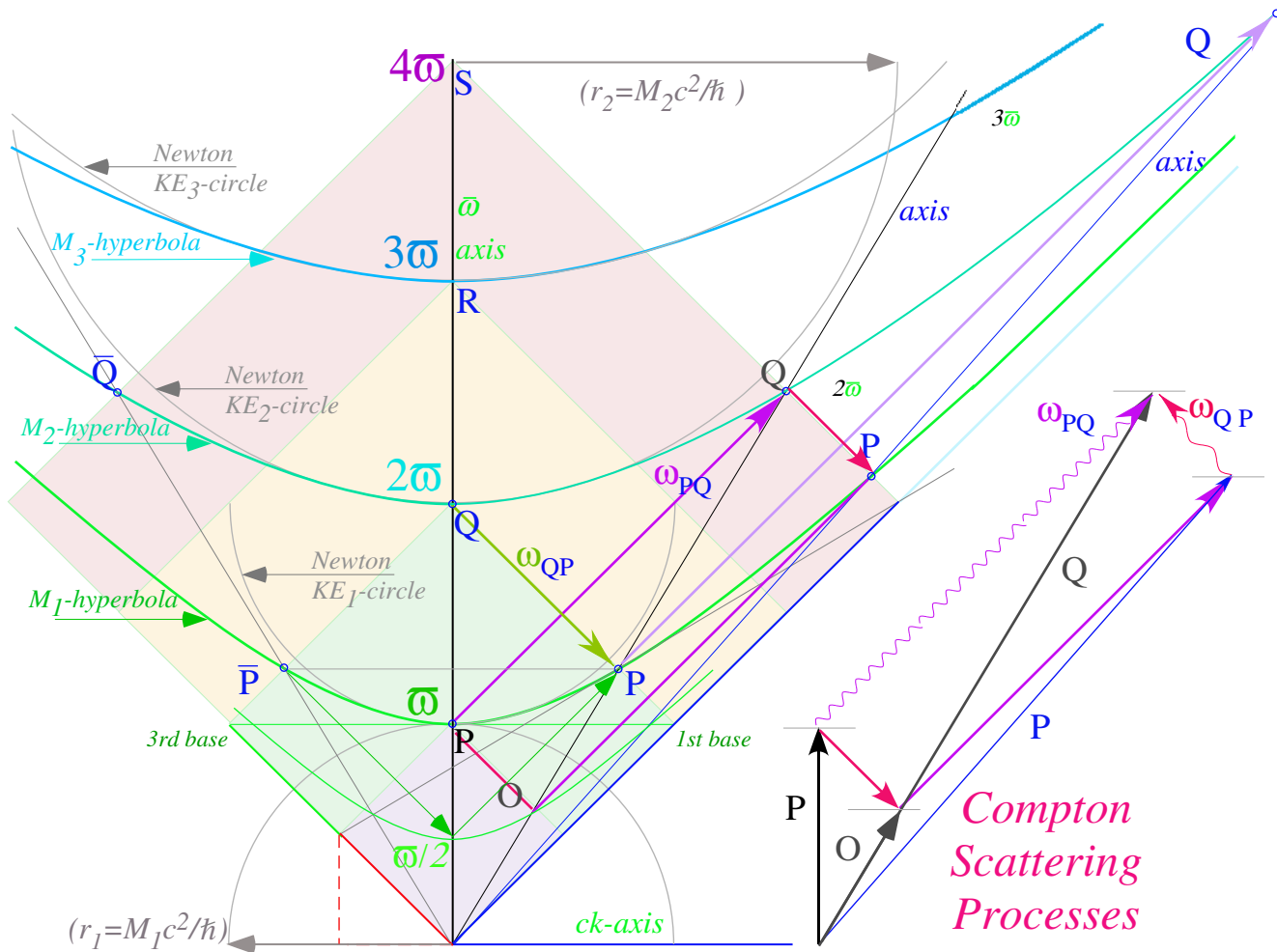


Physics by Geometry

A ruler & compass development of basics for classical and quantum physics



William G. Harter
 University of Arkansas
 Fayetteville

Harter-Soft

Elegant Educational Tools Since 2001

Spring 2008 Honors Colloquium Physics 3923H

Road Map for Physics by Geometry (2008)-version

*Euclid-
Aristotelean
World*

Unit 1:

Newton-Hamilton Classical World

(Think Bang-Bang particles ! Waves are Illusory.)

Concepts and Effects

Ways to visualize

Slope & Velocity (1-and-2-particles)	Velocity-velocity plots
Momentum (1-and-2-particles)	Space-time and space-space
Superball missiles	Energy shell (ellipse)
Rocket science & pileups	Matrix rotation & reflection
Kinetic Energy	F versus space work plots
Potential Energy	PE versus space
Force & PE Fields	Phase space
1D, 2D, & 3D oscillators	
Friction	Multi-velocity contours

Unit 2:

Maxwell-Lorentz View of Classical and Quantum Worlds

(Think resonance! Nature works by persuasion.)

Vibration and beats	Phasors
Action and phase	Momentum versus coordinate plot
Hysteresis	F versus time & work plots
1-Particle resonance	Lorentzian functions & Smith charts
2-Particle resonance	U(2) space & Stokes quasi-spin
n-Particle resonance (Waves)	Multiple phasors
Wave dispersion	Frequency vs. wavevector plots
Phase & group velocity	

Unit 3:

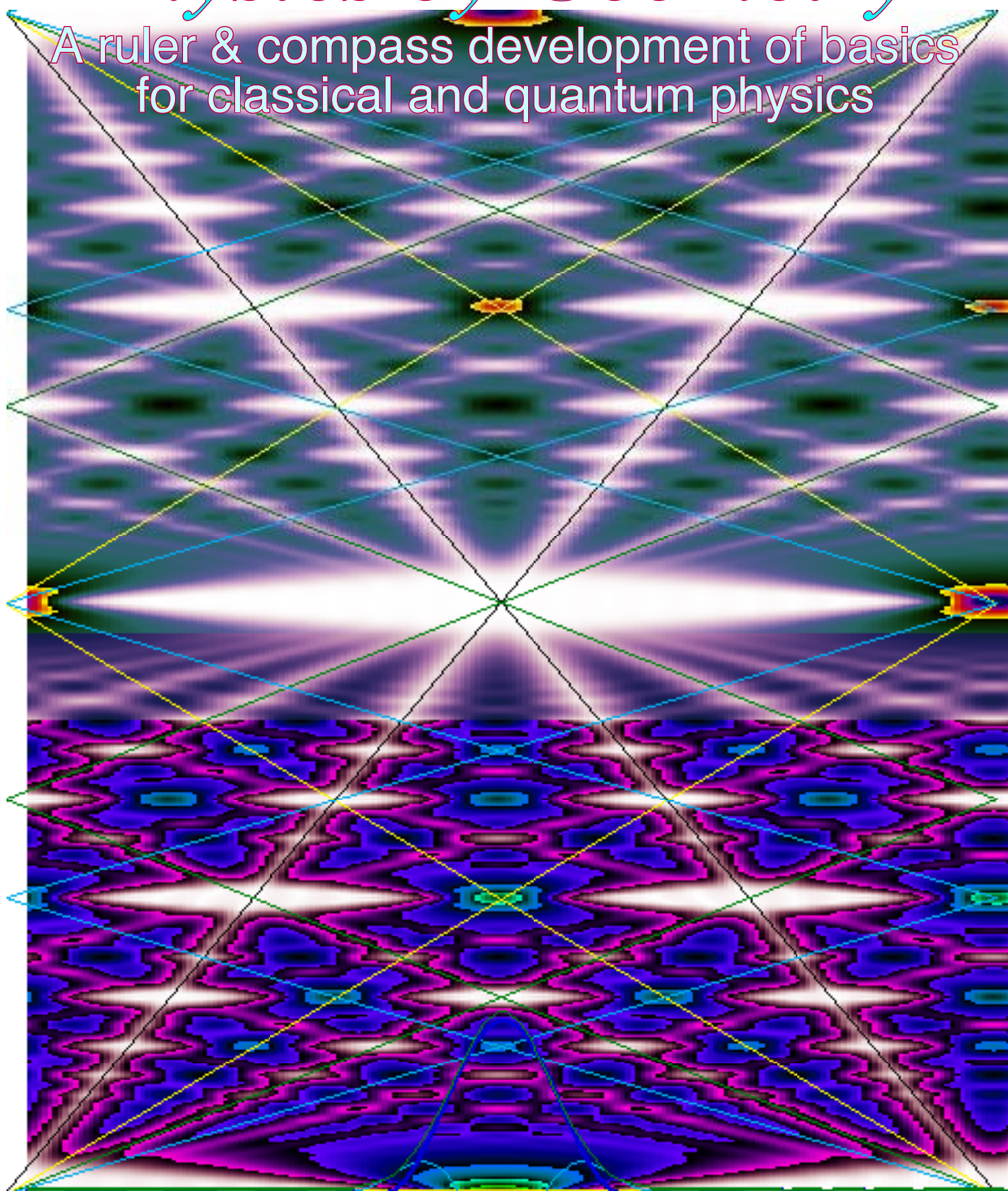
Einstein-Planck Relativity-Quantum World

(Think waves! Particles are Illusory.)

Space-Time by Wave Interference	Minkowski Spacetime graph
Doppler shifts tell all	Hyperbolic geometry
Energy Momentum Dispersion	Epstein x-proper time graph
Matter waves vs. No-Matter waves	
What is matter?	Dispersion graphs
Schrodinger's complaints	Wavevector geometry
Waves in accelerated frames	Angular momentum cones
Waves in nano-structures	RE surfaces
Spin and quantum angular momentum	
Correlation ("Entanglement")	The U(2) spinor slide rule
Bose vs. Fermi	

Physics by Geometry

A ruler & compass development of basics
for classical and quantum physics



William G. Harter
University of Arkansas

Harter-Soft

Elegant Educational Tools Since 2001

Introduction 7

- The triangle explosion..... 7
- Logos vs. mythos..... 8
- Science priests..... 8
- What’s the difference..... 8
- The weapons of math instruction 9
 - Toolbox 1: Euclidian plane geometry (Rule and compass)..... 9
 - Toolbox 2: Navigational geometry (Set 1+ protractor, ruler, divider, parallel rule) 9
 - Toolbox 3: Analytic geometry (Set 2+ graph paper, algebra, calculus, calculator) 9
 - Toolbox 4: Computer geometry (Set 3+ high resolution graphics, C++ etc.) 9
 - Toolbox 5: You 9
- Sketch of book units..... 11
- Some related books..... 11

UNIT 113

NEWTON-HAMILTON CLASSICAL MECHANICS.....13

Chapter 1. Velocity, slope geometry, and trigonometry.....15

- Right-handed Cartesian coordinates 17
- Change and delta variables..... 18
- Slope and delta ratios..... 18
- Slope angles and ratios..... 19
- Exercises for study of slope and trigonometry 21
- Arc functions 22
 - Know your calculator and ATAN, too! (atan2(y,x)) 24

Chapter 2. Velocity and momentum.....25

- Momentum exchange: a zero-sum game..... 25
- Deducing (perfect?) conservation from (ideal?) symmetry 27
 - Galilean time-reversal symmetry..... 27
 - Galilean relativity and spacetime symmetry 29
 - Geometry of Balance: Center of Momentum (COM) and Center of Gravity (COG)..... 30

Chapter 3. Velocity and energy.....31

- Time symmetry and energy conservation 31
 - Time symmetry 31
 - Kinetic Energy conservation 31
 - Kinetic energy ellipse and momentum line..... 32
 - Momentum vs. energy (Bang for the buck!)..... 34
 - Quick review of kinetic relations and formulas..... 34
 - Relations of energy W and space x..... 34
 - Relations of momentum P and time t..... 34
 - Quick construction of Energy ellipses..... 36

Chapter 4. Dynamics and geometry of successive collisions.....37

- Independent collision models (ICM)..... 38
 - Extreme and optimal cases 39
 - Integrating velocity plots to find position 40
 - Vector notation and space-space plots..... 44
 - Help! I’m trapped in a triangle..... 47
 - Two balls in 1D vs. one ball in 2D..... 47
 - Angle of incidence=Angle of reflection..... 47
 - Bang force..... 47
 - Kinematics versus Dynamics..... 48
 - Dynos and Kinos: Classical vs. quantum theory 48

Chapter 5 Multiple collisions and operator analysis.....51

- Doing collisions with matrix products 51
 - Rotating in velocity space: Ticking around the clock 53
 - Statistical mechanics: Average energy..... 54
 - Bonus: Rational right triangles 55

Reflections about rotations: It's all done with mirrors.....	55
Through the clothing store looking glass.....	57
How fundamental are reflections?.....	57
Chapter 6 Force and potential energy.....	61
MBM force fields and potentials.....	61
Isothermal model force laws.....	62
Adiabatic force laws.....	63
Conservative forces and potential energy functions.....	63
Is it +or-? Physicist vs. mathematician and the 3 rd law.....	63
Isothermal "Robin Hood" and "Fed rules".....	64
Oscillator force field and potential.....	65
The simplest force field $F=\text{const}$	66
Action is conserved (sort of).....	66
Monster mass M_1 and Galilean symmetry (It's deja vu all over, again.).....	69
Chapter 7 Interaction Forces and Potentials in Collisions.....	73
Geometry of superball force law.....	73
Dynamics of superball force: The Project-Ball story.....	74
The trip to Whammo.....	74
Eureka! Polka-dots save Project Ball.....	74
The "polka-dot" potential.....	75
Force geometry: Work and impulse vs. energy and momentum.....	77
Kiddy-pool versus trampoline.....	77
Linear force law, again (But, with constant gravity, too).....	79
Why super-elastic bounce?.....	81
RumpCo versus <i>Crap Corp.</i>	81
Seatbelts and buckboards.....	83
Friction and all that "dirty" stuff.....	84
Chapter 8 N-Body Collisions: Two's company but three's a crowd.....	87
The X3: Three-ball towers.....	87
Geometric properties of N-stage collisions.....	89
Supernovae super-duper-elastic bounce (SSDEB).....	89
Newton's balls.....	89
Friction, again: Inelastic energy-momentum quadratic equations.....	91
Geometric construction of elastic and inelastic energy ellipses.....	93
Ka-Runch-Ka-Runch-Ka-Runch-Ka-Runch-...:Inelastic pile-ups.....	95
Ka-pow-Ka-pow-Ka-pow-Ka-pow-...:Rocket science.....	97
Exercises.....	100
Chapter 9 Geometry and physics of common potential fields.....	101
Geometric multiplication and power sequences.....	101
Parabolic geometry.....	103
Coulomb and oscillator force fields.....	105
Tunneling to Australia: Earth gravity inside and out.....	107
To catch a falling neutron starlet.....	109
Starlet escapes! (In 3 equal steps).....	111
No escape: A black-hole Earth!.....	111
Oscillator phasor plots and elliptic orbits.....	111
Chapter 10 Exponentials, logarithms, and complex phasors.....	115
The story of e : A tale of great interest.....	115
Derivatives, rates, and rate equations.....	118
General power series approximations.....	119
Sine-wave power series.....	121
Euler's theorem and relations.....	123
Wages of imaginary interest: Phasor oscillation dynamics.....	124
What Good Are Complex Exponentials?.....	125
Complex numbers provide "automatic trigonometry".....	125
Complex exponentials $Ae^{-i\omega t}$ tracks position <u>and</u> velocity using Phasor Clock.....	125
Complex numbers add like vectors.....	125
Complex products provide 2D rotation operations.....	126

Complex products set initial values.....	126
Complex products provide 2D “dot”(•) and “cross”(x) products.....	127
Complex derivative contains “divergence”(∇•F) and “curl”(∇ _x F) of 2D vector field.....	127
Complex potential φ contains “scalar”(F=∇Φ) and “vector”(F=∇ _x A) potentials.....	127
Complex integrals ∫f(z)dz count “flux”(∫F _x dr) and “vorticity”(∫F•dr).....	129
Complex derivatives give 2D multipole fields.....	133
Complex power series are 2D multipole expansions.....	134
Cauchy integrals.....	137
Complex damped oscillator.....	139
Complex response to stimulus:Lorentz-Green’s function	140
Beats and lifetimes.....	143
Comparing resonant and non-resonant cases.....	147
High-q resonant and non-resonant cases.....	147
Appendix 1.A Vector product geometry.....	151
Determinants and triple products	152

Introduction

The triangle explosion

We are in an explosion of science and it starts with a triangle.

It has all been in a historical instant of a few hundred or a couple of thousand years. That is an eye-blink in human history and a lightning-flash in geological time. European Renaissance and Enlightenment periods are even more recent, just about 400 or 500 years ago.

There is an embarrassing 1500 years of time-out for the Middle Ages, but our story begins with Babylonian and Greek civilizations and the first recorded mathematical science including geometry of Pythagoras (~500BC) and Euclid (~300BC). Little evidence exists for higher math and science before that.

The 1500-year interruption after the burning of the libraries of Alexandria was a resumption of human business-as-usual, that is, fear, superstition, and feudal government by warlords. Thinking for yourself was an activity that was likely to get you “fired” and that didn’t mean just a pink slip!

You and your books got burned, literally.

During the European time-out the Middle Eastern and Arabic cultures flourished. They studied things saved from Babylonian and Greek geometry and made the first recorded development of algebra. Sadly, the Arabic cultures resumed business-as-usual just before Europe began its renaissance. Since then the Middle East remains in an unreasonable condition we see it today.

Also, during the European time-out, repositories of Babylonian and Greek culture were studied in monasteries of various Catholic sects. One notable scholarly monk is *William of Ockham* (~1285-1349) now known for Occam’s razor. He wrote, “*Pluralitas non est ponenda sine neccesitate*” (*Plurality should not be assumed without necessity*). It’s good advice.

Occam might be paraphrased, “*Keep it simple and make it powerful!*” It’s a logical idea of geometry and, indeed one may argue, of all science, mathematical or otherwise. It asks to begin a study of anything by first and finally collecting the smallest set of *axioms* that one needs to proceed.

Occam’s razor is supposed find ways to cut down any axiom set or *sine qua non* (without which there is nothing). It is amazing that such a “cutting” idea actually works! Perhaps, by reducing logical clutter we hack away unknowns and clear the way for new stuff. But, there is more to it than that.

By allowing thought to be driven by a need to undermine its premises, one is following a thought path that grows geometrically. An exponential explosion of science and mathematics results. Of course, Occam’s idea was heresy and he was nearly “fired.” Copernicus, Galileo, Bruno (who *was* burned at the stake), and others followed similar thought progression. Hacking sacred Churchly axioms or *mythos* is always trouble. Occam says, “Hack the axioms to save man.” The Church says, “Hack the man to save axioms.”

Logos vs. mythos

The battle between *logos* and *mythos* may be seen as a battle between portions of the human brain. An evolution through millions of years is seen in a magnetic resonance image (MRI) that shows the lower limbic (picean, reptilian, mammalian) lobes (LLL) below higher cerebral lobes (HCL). Little in the higher brain is fully functional at birth while the LLL “boots from the box.”

In fact, getting HCL up and running is at least a 20-year process called *education* and often a painful one. Most of our feelings of comfort and love are stimulated by the unconscious LLL and that goes double for feelings of fear, hatred and anger. The latter had proportionally greater survival value during countless millennia of animal and human evolution. Failure to educate ends in *synaptic mylenination*, an atrophy of unused HCL circuits. This is not good in school but just fine working for a local warlord.

Knowing a little history and physiology helps to understand how anger is generated by scientific reasoning in spite of reason’s obvious gifts. One understands an angry Martin Luther blurting, “That fool, Copernicus...” and sees why they forced Galileo to recant his logic and observations. Luther may have expressed it as succinctly as possible. His LLL explaterated the following in *The Lies of the Jews (1433)*.

“*Die verfluchte hure, vernunft.*” (*That damned whore, reason.*)

So, childish make-believe is just human business-as-usual as Al Gore, 2007 Peace Nobel, explains in *Assault on Reason (2005)*. Chris Mooney’s *Republican War on Science (2004)* adds further details.

Science priests

To win any “war” for scientific reason it is necessary to empower more thinking people with effective educational tools. This is something that scientists have largely failed to do. It is much easier to behave like a priest and say, “Trust me.” Many popular theoretical physics books leave readers more mystified than educated and more discouraged than enlightened. Quite a few textbooks suffer similarly.

What’s the difference

This book is different since it is a *geometric* approach to physics that allows you *practice* it starting with just a ruler & compass. (See *Weapons of Math Instruction* on the following pages.) Most important, is how this lets *you* check the math. Modern theory is great but it is always the *source* and *development* of ideas that is the most important idea of all. Ideas wax and wan. Idea development is a forever thing.

We will begin with ruler & compass reconstructions of car crashes to show symmetry principles that are key to classical mechanics. Symmetry principles, which I call *grown-up-geometry* provide doorways from classical mechanics to quantum mechanics, the currently reigning theory of our world. We use thought experiments and classical *analogy* to understand quantum and relativistic reality.

So we start by understanding car-crashes and work up to understanding photon-crashes.

The weapons of math instruction

When you've got a tough job you use *all* the tools you can find. We use tools listed below. (See Figure.) Each has advantages and disadvantages. There's no magic do-all "Swiss-Army knife" for physics.

Toolbox 1: Euclidian plane geometry (Rule and compass)

Note that Toolbox 1 has a *rule* not the ruler. That's in Toolbox 2. A *rule* is just a *straightedge*, a ruler without its inch or *mm* scale. Euclid's pretty strict about this. Formal plane geometry is kind of a game to see how much you can do drawing lines and circles with just these tools. And a pencil...did I forget the pencil? With an *eraser*, too. Very useful!

Toolbox 1 has limitations, at least by the formal rules of Mr. Euclid. You may have heard that you can't trisect an angle as Mr. Euclid wants it done, formally and *exactly* in a *finite* number of steps. When necessary, we'll do this and other "illegal" moves *approximately* and in a finite number of steps.

Toolbox 2: Navigational geometry (Set 1+ protractor, ruler, divider, parallel rule)

These were the tools used by the Portuguese, Spanish, Dutch, French, and English navigators who were at least indirectly responsible for many of us living in the American continent. These tools were also used by weekend sailors until the Global Positioning System made all but a six-pack obsolete.

Toolbox 3: Analytic geometry (Set 2+ graph paper, algebra, calculus, calculator)

The idea is not to discard algebra and other such formalisms but to *understand* them better. So one of the first things we do with each geometric graph is figure it out using algebra. This is called *analytic geometry* and is one of the quickest ways to understand calculus and its application to physics. This leads to complex algebra and geometry that is very important to physics. As a crutch for the arithmetically and algebraically challenged we include scientific calculators. (Most of these have complex algebra capability.)

Toolbox 4: Computer geometry (Set 3+ high resolution graphics, C++ etc.)

This is the "open" class of geometric analysis, and anything goes. A modern scientist without graphics programming is at a disadvantage. Current languages of greatest general usage, speed, and power are C++ and *Objective C* used to write simulations *BounceIt*, *BandIt*, etc. for this book. High-level languages such as Maple™, Mathematica™ are fine, too, though often they are jacks-of-all-trades and masters-of-few.

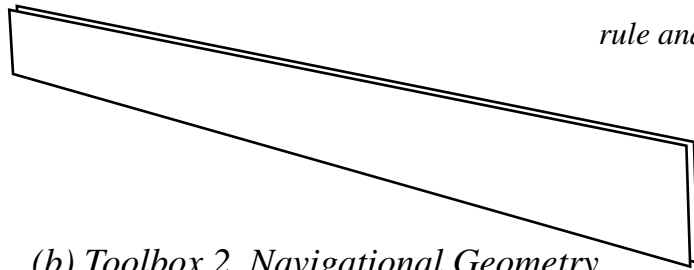
Toolbox 5: You

This is challenging stuff. Doing it will seem hard sometimes. Rome was not built in a day and neither was any understanding of Nature. So this book depends most on how much *you* like thinking and doing.

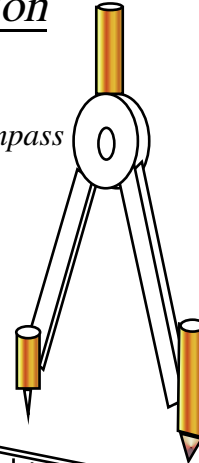
Ignorance about science is not a burden you must accept. It is a challenge you should overcome.

The Weapons of Math Instruction

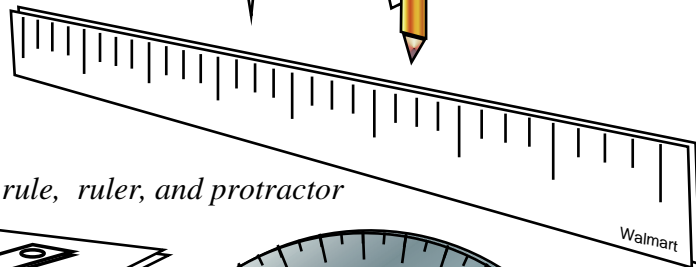
(a) Toolbox 1. Euclidian Geometry



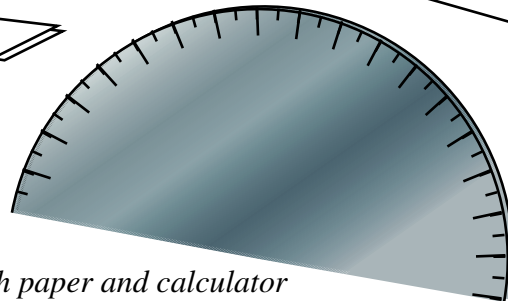
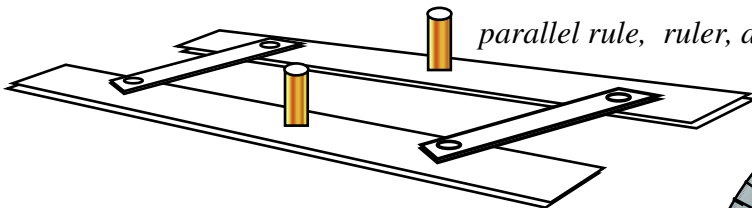
rule and compass



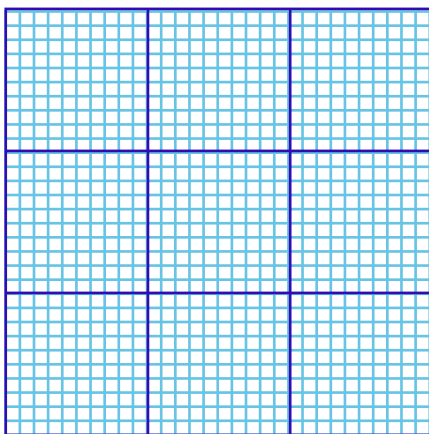
(b) Toolbox 2. Navigational Geometry



parallel rule, ruler, and protractor



(c) Toolbox 3. Analytical geometry

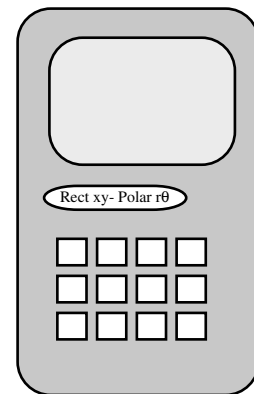


Graph paper and calculator

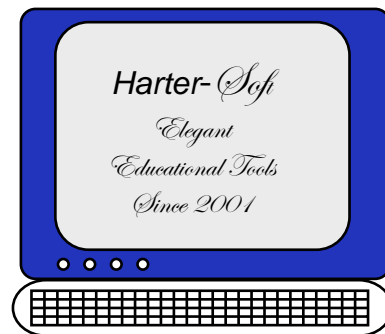
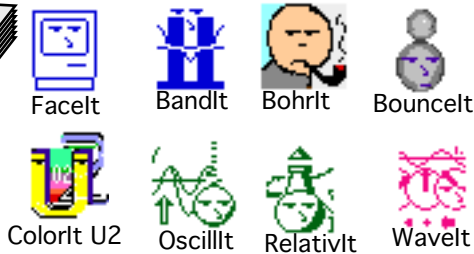
Complex algebra and calculus

$$1/z = r^{-1} e^{-i\theta}$$

$$\int 1/z dz = \ln z$$



(d) Toolbox 4. Computer geometry...Anything goes!



Sketch of book units

Unit 1 introduces classical mechanics of momentum and energy by geometry and symmetry while previewing subjects to come. Geometric approaches are direct and powerful so effects like super-elastic bounce and supernoval explosion can be analyzed by car-crash “slide-rules.” We introduce potential energy by oscillator and Coulomb models of Earth inside and out and construct elliptic orbits of a “neutron-starlet” by ruler & compass. The ellipse geometry then leads to an elegant development of resonance and beats in Unit 2, that is, in turn, a precursor to understanding relativity and quantum waves in Unit 3.

An ancient war machine called the *trebuchet* or *ingenium* is discussed near the end of Unit 1. The trebuchet is a super-catapult used between 3000 BC in China and 1500 AD that duplicates the human motions of throwing, reaping, chopping, and digging that built our culture. It also instructively models the motions used in modern sports of baseball, tennis, and golf while showing how one may improve one’s swing in any such sport (and ring the bell at the fair!)

Unit 2 introduces the concept of resonance, an alternative view of nature to the brutish bashing of particles seen in Unit 1. As we learn about fundamental processes it appears that Nature uses persuasion or resonance rather than so many punches. The concept of the oscillator phase and phasor-clock is introduced along with the mechanics of wave motion. The geometry of phasor clocks is used to introduce complex Fourier analysis discretely. Geometry again provides inside views of concepts often left unseen.

Unit 3 begins with light, a most common wave but most difficult to observe. Ancient geometry and Occam’s razor are used on Einstein’s postulate of light speed c . There results a new way to see relativity and quantum mechanics as one subject and dispel many mysteries about them. Optical Doppler frequency shift is seen to be a primary geometric source of relativistic quantum effects ranging from Lorentz transformation of spacetime to Compton scattering to the existence of mass-energy and classical Newtonian mechanics of Unit 1. A classical Newtonian mechanic might say, “Think *particles*. Waves are illusory.” A quantum mechanic should reply, “Think *waves*. Particles are illusory.” *Pluralitas non est ponenda sine neccesitate.*

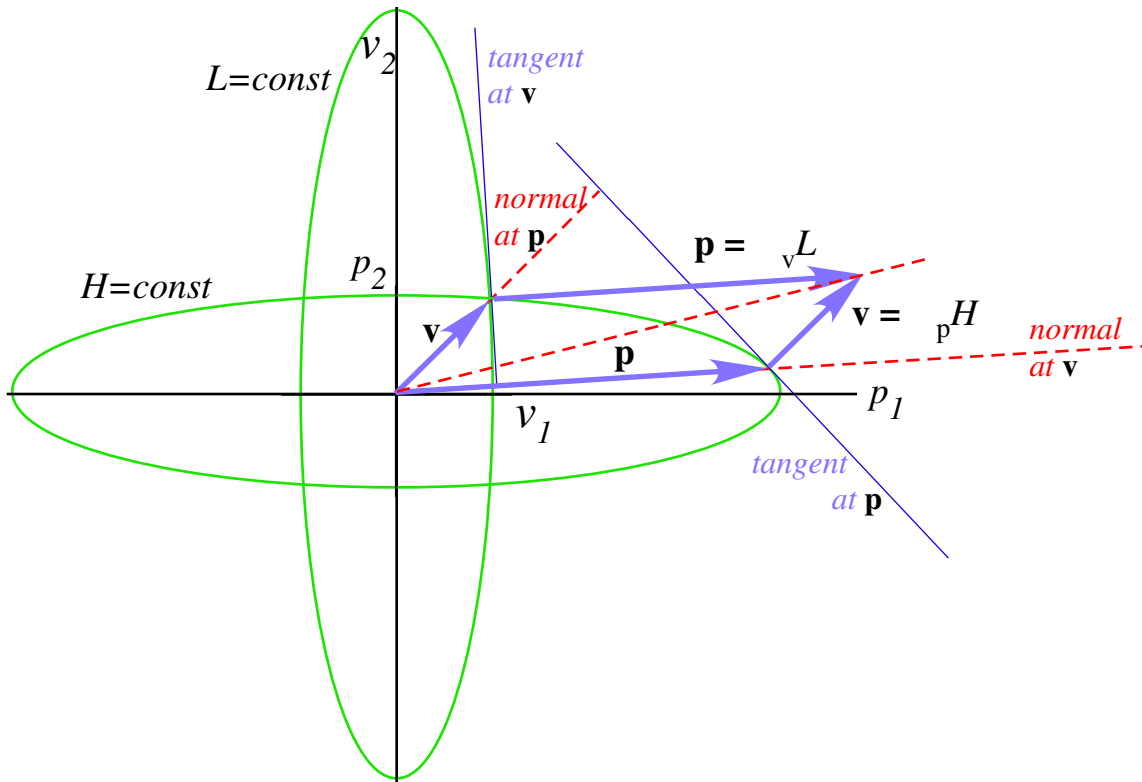
Some related books

This book is most in line with works that many regard as outside the mainstream including *Quantum Electrodynamics* by Feynman, *The Feynman Lectures* by Feynman, Leighton, and Sands, *The Berkeley Series on Physics 3. Wave Mechanics* by Frank Crawford, *Mechanics* by Landau and Lifshitz, and *Classical Mechanics* by Arnold. Hawkings “*God Created the Integers*” and Penrose’s “*Road to Reality*” are among recent additions to a list of readable books with depth.

William G. Harter
Fayetteville, Arkansas
January 2008

Unit 1

Newton-Hamilton Classical Mechanics



W. G. Harter

Basic ideas of velocity, momentum, and kinetic energy (KE) are reviewed using geometry of collision experiments between pairs of masses and extending it to many. Basic ideas of potential energy (PE) and force are introduced by defining PE as the KE of one or two balls that provides a force field for others. The two most famous PE functions, those of Coulomb and of a harmonic oscillator and linear (Hooke's Law) force are introduced. The elliptic orbits of the latter are reviewed in considerable geometric detail. This helps to clarify the basic axioms of classical mechanics.

Chapter 1. Velocity, slope geometry, and trigonometry

A 4-ton SUV going 60mph approaches a 1-ton VW going 10mph. (Fig. 1.1a.) The SUV driver is busy text-messaging on a cell-fax instead of watching the road ahead.

Ka-runch! The SUV rear-ends the VW. (Fig. 1.1b.) What happens then?

Well, both vehicles suddenly change speed. Our job is to figure out those speed changes. (See question marks in Fig. 1.1c.) The answers that we find later will depend upon whether the collision is a “ka-runch!” or a “ka-bong!” or (more likely) an intermediate “ka-whump!” as discussed shortly.

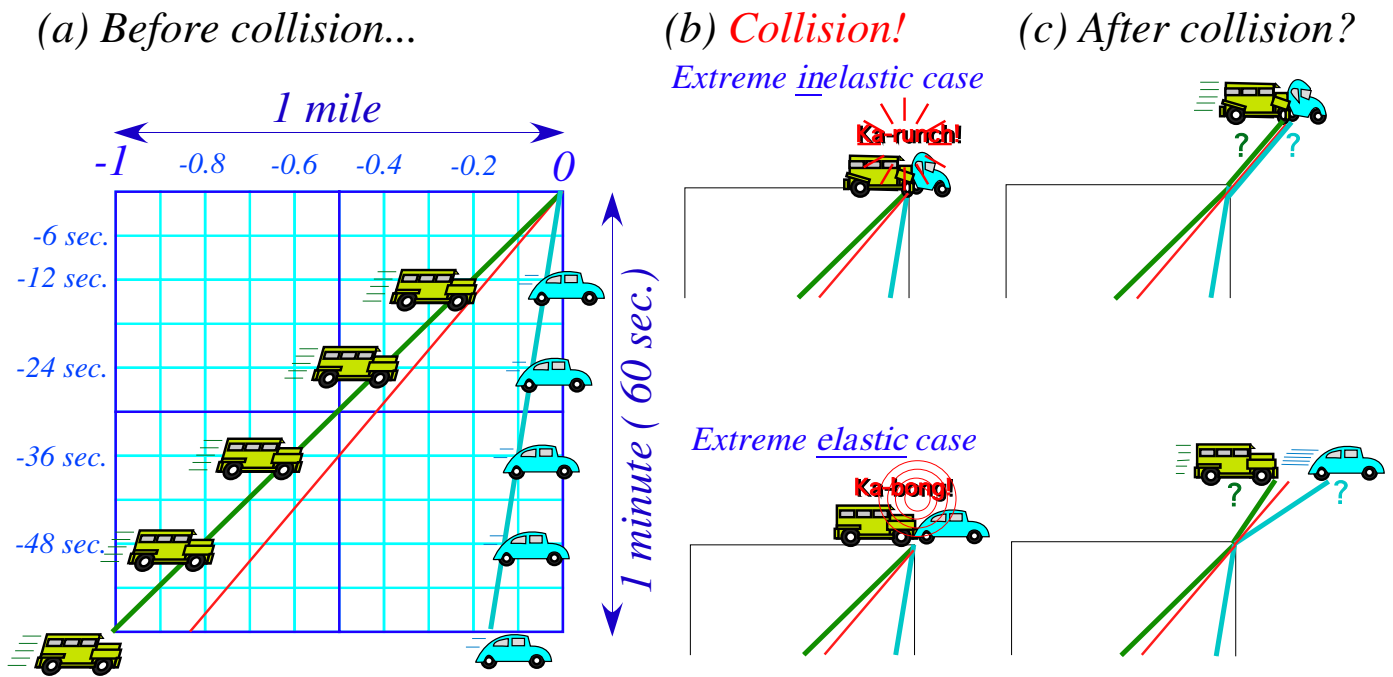


Fig. 1.1 Time vs. space graphs of (a) SUV (going 60mph) and VW (going 10mph), (b) collision, and (c) possible outcomes of two extreme cases: the inelastic “ka-runch!” and perfectly elastic “ka-bong!”

Our job is a lot easier than what first-responders, doctors, lawyers, insurance agents, ministers, or psychologists do to deal with *results* of such speed changes. Such difficult human problems are quite beyond our scope here. Also, I can’t say why so many people “need” *n*-ton SUV’s, but I do know you can get \$100,000 off 2007 taxable income by buying an SUV *provided it weighs over 6 (six) tons!*

My hope is that graphical analysis of physics and economics may help avoid injury due to either one. Graphs ought to give quantitative results while helping to expose logic. Our first graph (Fig. 1a) is a *time vs. distance plot*. It shows speed by *slope-from-vertical*. It has been used for space-time relativity since Herman Minkowski, one of Einstein’s math profs, suggested it. Calculus texts use a *distance vs. time plot* to show speed by *slope-from-horizontal* as Newton liked to do. Fig. 1.2 compares the two. They both use a 1:1 ratio ($45^\circ \text{slope} = 1/1$) to represent $60 \text{ mph} = 1 \text{ mile}/\text{min}$. in (a) but also $1 \text{ min.}/\text{mile}$ in (b).

(a) Time vs. space plot (Minkowski) (b) Space vs. time plot (Newton)

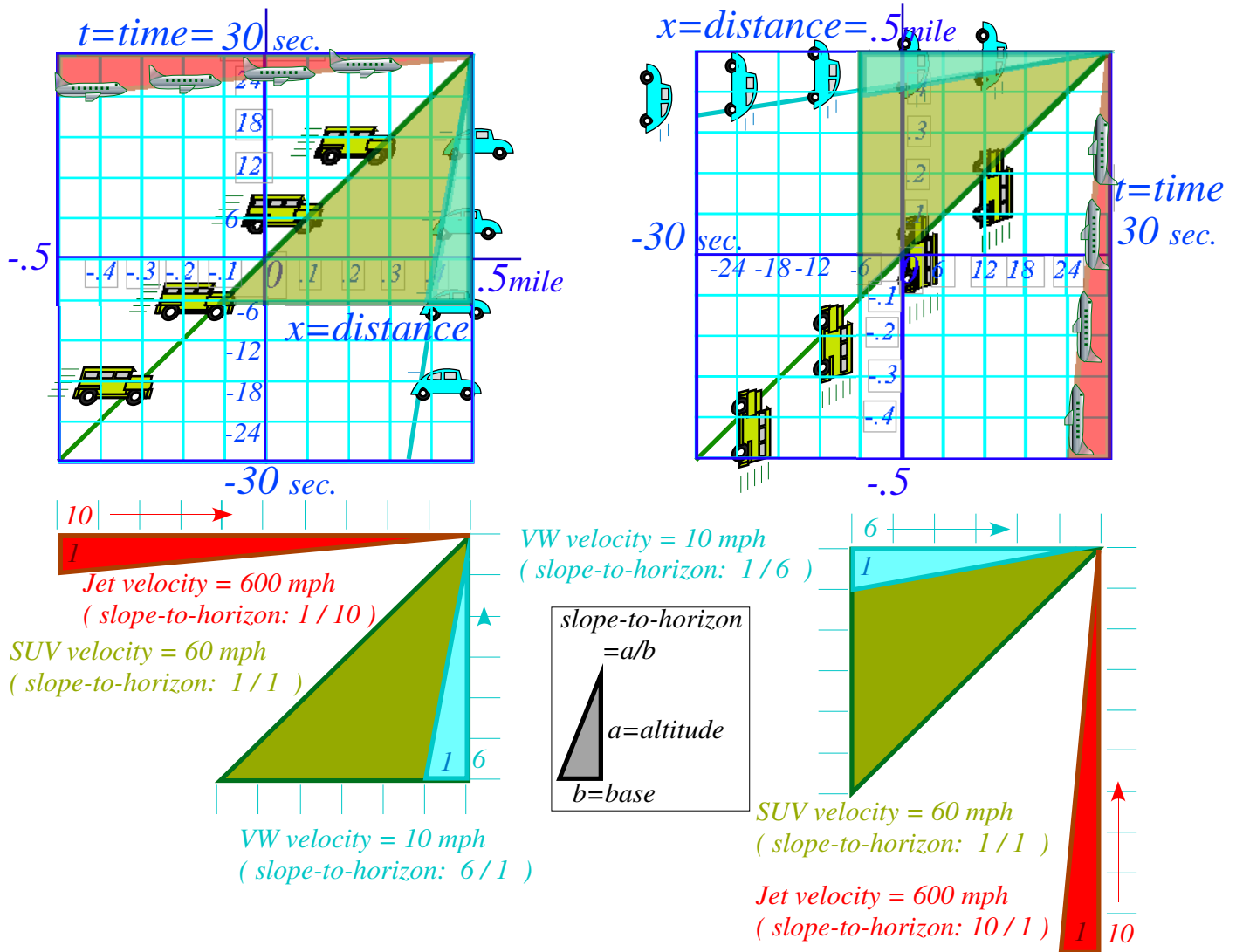


Fig. 1.2 Comparing slope (a) Minkowski time vs. space plots vs. (b) Newton's space vs. time plots.

The two plots (a) and (b) are equivalent; (a) is transformed into (b) by doing a mirror-reflection across the 45° diagonal (1:1)-SUV-line, the one line that is the same in (a) or (b). I prefer (a) for vehicular dynamics since cars usually go horizontally. (With (b) you might ask, “How do cars climb walls?”)

Now, *slope* is defined as the ratio $\Delta y/\Delta x$ of vertical altitude Δy per horizontal base Δx . This equals velocity $v = \Delta x/\Delta t$ for a horizontal time- t -axis and vertical space- x -axis like Fig. 1.2b. So horizontal x -axis and vertical time- t -axis of Fig. 1.2a has $slope = \Delta t/\Delta x = 1/v$ inverse to Fig. 1.2b slope. The lowest $slope = 1/10$ in Fig. 1.2a belongs to jet velocity $v = 600\text{mph}$ that is the highest $slope = 10/1$ in Fig. 1.2b, and a low VW velocity of $v = 10\text{mph}$ has a triangle of steep $slope = 6/1$ in Fig. 1.2a but in Fig. 1.2b that VW line is a low $slope = 1/6$.

Each unit graph square in Fig. 1.2a has a *horizontal scale factor* of $s_x = 0.1\text{mile}$ (per square) and a *vertical scale factor* of $s_y = 6\text{sec}$. (per square) and *vice versa* for Fig. 1.2b. If you multiply scale s_x by factor f_x and s_y by f_y then each graph slope $\frac{\Delta y}{\Delta x} = (n_y \text{ vert. squares}) / (n_x \text{ horiz. squares})$ changes to $(f_x/f_y) \frac{\Delta y}{\Delta x}$.

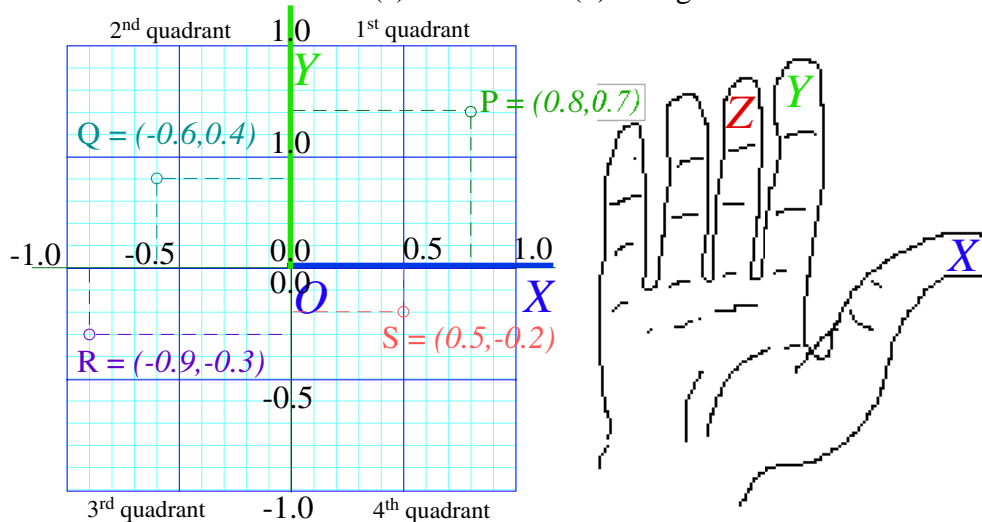
Right-handed Cartesian coordinates

Rene Descartes (1596-1650) is said to have invented (or discovered) the Cartesian graph and coordinate system. We usually call the two-dimensional (2D) version “XY-coordinates” and three-dimensional (3D) versions are “XYZ-coordinates.”

Four-dimensional (4D) space-time $(xyzt)$ -*Minkowski coordinates* after Herman Minkowski (who was Einstein’s math professor)[†] came later (1905-1908). The 2D projection of one space dimension (x or y or z) and time scale-by-lightspeed (ct) is called a *Minkowski graph*. Lightspeed $c=2.99792458$ m/s has velocity units so ct has distance units like x or y or z .

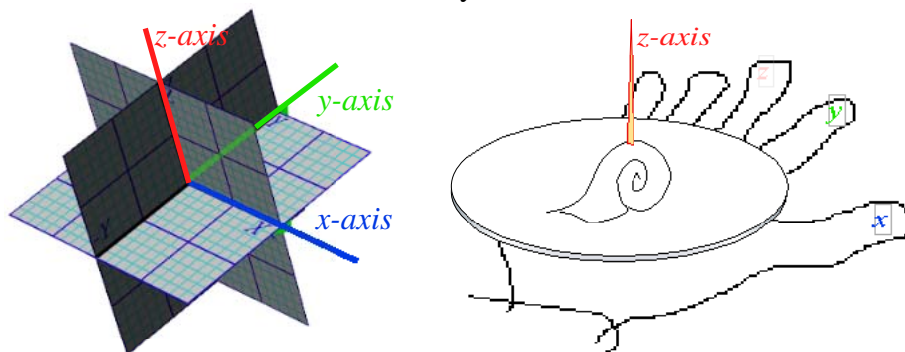
Two-dimensional (2D) XY-graphs often draw the primary X or x -axis along the horizontal direction with x increasing to the right, and then place the secondary Y or y -axis perpendicular or *normal* to the X-axis with y increasing vertically.

What (or which) physics variables should be “primary?” Well, that’s up to you. The choice between Minkowski(a) and Newton(b) in Fig. 1.2 is a matter of taste.



The graph above is called a *right-handed coordinate system* since it points like your thumb (X) and forefinger (Y) of your right hand as you extend to shake hands or hand someone a plate of *escargot*. (Descartes’ French cuisine is respected here.)

A toothpick sticking up from the *escargot* points in the Z or z -axis direction of a right-handed 3D Cartesian coordinate system as shown below.



[†] Minkowski (who was Polish) told Einstein (who was Swiss) that he was a “fat lazy boy.” Einstein never used Minkowski graphs. It is sad story since Herman’s graphs could help many more to visualize relativity and expose its geometric structure. We will certainly not repeat that sad mistake!

A. Einstein, *Annalen der Physik* 17, 891(1905).

H. Minkowski, *Mathematisch-Physikalische Klasse*, vol. 1, 53 (1908).

We do rescaling of dimensions whenever we change units. For example, changing miles to feet in Fig. 1.2a uses factor $f_x = 5,280 \text{ ft. per mile}$ (or $\frac{\text{ft.}}{\text{mile}}$) and changing minutes to seconds uses $f_y = 60 \frac{\text{sec}}{\text{min.}}$. The scale ratio (f_x/f_y) is 88, that is, 60mph equals $88 \frac{\text{ft.}}{\text{sec.}}$. SUV slope of l in Fig. 1.2b is 88 in a ft. vs. sec. plot. That's too high to plot 60mph accurately but a ft. vs. sec. or ft. vs. min. plot will be more appropriate for parking lot speeds.

Change and delta variables

The *delta notation*, such as Δx , Δv , Δt , and so forth, is confusing to one who has not had a calculus course (or has forgotten that stuff). Roughly speaking, the Greek upper case “D” or *delta* (Δ) stands for “difference” or *differential*, and Δx should be read as “change of x ” or *differential of x* and thought of as a single entity.

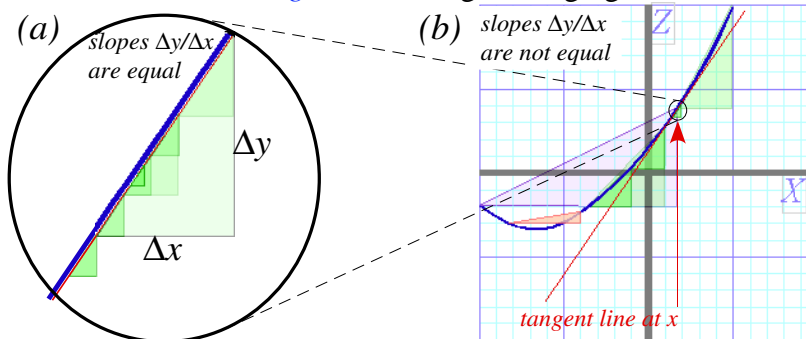
It is a common mistake to read Δx as “ Δ multiplied by x ” or “ Δ times x ” since, after all, product p of quantities a and x is written $p=ax$ or better $p=a \cdot x$. Instead, the mathematical *cognescenti* think of Δ as an *operation* that acts on a variable x or whatever to give whatever change has occurred in that variable.

When the letter Δ is used to denote an actual number or variable one should take care to write its product with another variable x as $\Delta \cdot x$ or (better) $x \cdot \Delta$ to avoid confusing it with Δx .

Slope and delta ratios

Slope ratio $\Delta y/\Delta x$ of a line or of a triangular hypotenuse is a key concept that is common to mathematics and physics beginning with Babylonian and Greek plane geometry of Euclid (300 BCE), and progressing through analytic geometry of Descartes (1620), the complex trigonometry of Euler (1700), the calculus of Newton (1720), the relativity of Einstein (1905), and the quantum mechanics of Planck (1900), Bohr (1920), Schrodinger (1925), and Dirac (1930). (That's a short list. A full one could take pages.) Physics uses slope like soup uses water. It's all based on slope and related triangular angles, areas, and ratios. *We must study slope!*

So far we have only talked about slope of straight lines in Fig. 1.1-2. For them triangle size or location makes no difference to ratio $\Delta y/\Delta x$. All triangles in the figure (a) below are *similar triangles*, but triangles hanging on a curve in figure (b) are not.



Slope of a triangle hanging on a curve depends on location x and base segment size Δx . Soon we will define slope of a *tangent line* to a curve in (b) by making its base segment Δx so small that the curve over it looks straight as in (a). Then (to graph accuracy) the tangent slope will only depend on location x on the curve.

Slope angles and ratios

Most of us learn to measure slope by *degrees*(°) of a *slope angle* σ . Greek “s” or *sigma* σ stands for *sector slope*. (We also use *theta* (θ) or *phi* (ϕ .) But, degrees are an *arbitrary* choice of 180° per (1/2)-turn or 360° per full turn. A better unit is *1 radian* $= 180/\pi \sim 57.3^\circ$. A $\sigma=1$ *radian*-sector on unit circle ($r=1$) (Fig. 1.3a) has *unit arc-length* ($\ell=\sigma \cdot r=1$) and *unit sector area* ($A=\sigma \cdot r^2=1$) based on $\pi=3.14159\dots$, not arbitrary numbers.

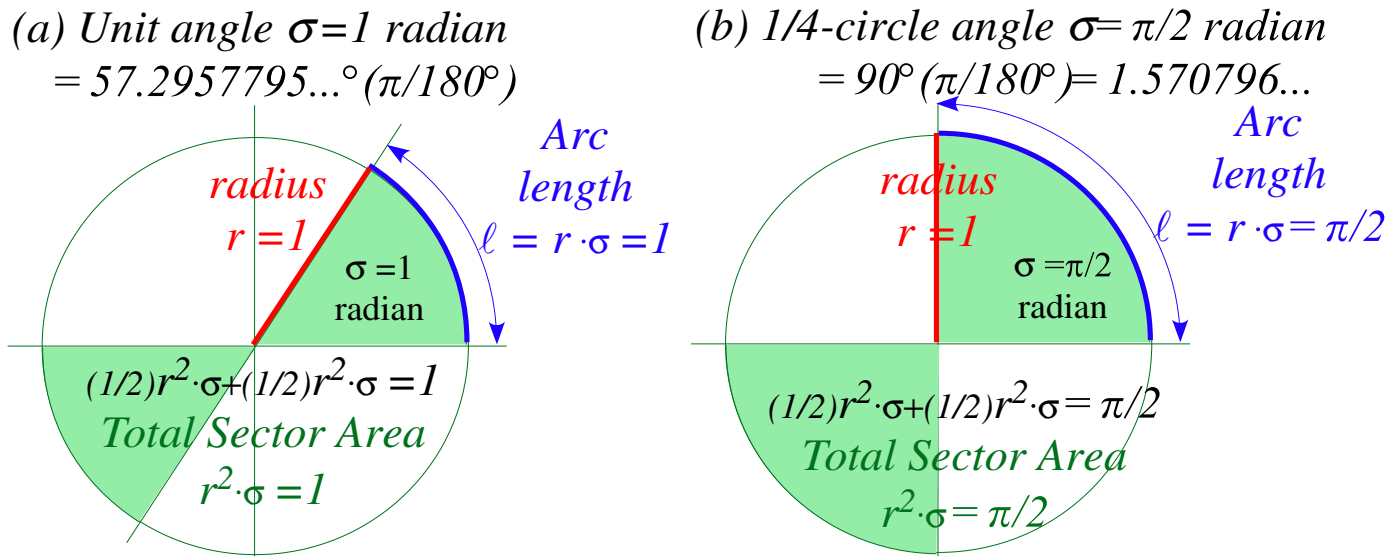


Fig. 1.3 (a) Definition of unit angle ($\sigma=1$) on unit circle ($r=1$) (b) A quarter turn sweeps half the area.

The trick here is that the sector slope line sweeps out *two* pieces of the pie to make a whole pie or area π if angle σ is π or 180° . The 1/4-circle angle $\sigma=\pi/2$ in Fig. 1.3b sweeps area $\pi^2/2=\pi/2$ of half a pie. It may not be how *you* serve pie, but it is how mathematicians serve π . (There (or their) pie (or pi) *are* square!)

Actual slope is the *tangent of angle* σ written $\tan\sigma$ and so called since it is the *length* of a line tangent to or “*touching*” a unit circle from angle σ to *x*-axis. (See Fig. 1.4b.) Another triangular ratio is the *sine* or $\sin\sigma$ that stands (*I think*) for “*s*lope over *i*ncline” or some such. While *tangent* in Fig. 1.4 is an *a:b* ratio ($\frac{\text{altitude}}{\text{base}} = \frac{a}{b} = \frac{\Delta y}{\Delta x} = \tan\sigma$), the *sine* is an *a:r* ratio ($\frac{\text{altitude}}{\text{radius}} = \frac{a}{r} = \frac{\Delta y}{\Delta r} = \sin\sigma$) that civil engineers use to “grade” roads.

$$\text{percent-grade} = 100 \cdot (\text{altitude } \Delta y \text{ gained}) / (\text{distance } \Delta r \text{ traveled}) = 100 \sin\sigma$$

High grades are *good* in school but *bad* for roads. An interstate highway would “flunk” anywhere its grade was above 5%. This changed in 2001 with the Bush administration’s “*No Road Left Behind*” policy.

Each triangle ratio switches places with its *codependent ratio* if you switch *x*-and-*y*-axes (or altitude-and-base) or switch Fig. 1.2a Minkowski plots to Fig. 1.2b Newton plots. For example, a *cotangent* ratio $\frac{\text{base}}{\text{altitude}} = \frac{b}{a} = \frac{\Delta x}{\Delta y} = \cot\sigma$ is codependent to $\tan\sigma$, and *cosine* ratio $\frac{\text{base}}{\text{radius}} = \frac{b}{r} = \frac{\Delta x}{\Delta r} = \cos\sigma$ is codependent to $\sin\sigma$.

In comparing (a) vs. (b) in Fig. 1.2 we saw that a slope (like 6/1) in (a) is inverse slope (1/6) in (b). (That was for the 10mph VW.) In other words, any slope $\frac{a}{b} = \tan\sigma$ in (a) becomes $\frac{b}{a} = \cot\sigma = 1 / \tan\sigma$ in (b). Also any slope angle σ in (a) becomes a *compliment* $\sigma_c = \frac{\pi}{2} - \sigma$ to angle σ in (b). (See Fig. 1.4a.)

From the two preceding paragraphs we deduce that any ratio like $\sin\sigma$ or $\tan\sigma$ for angle σ must equal its co-ratio for the compliment $\sigma_c = \pi/2 - \sigma$, and *vice versa*.

$$\sin\sigma = \cos\sigma_c, \quad \sin\sigma_c = \cos\sigma, \quad \tan\sigma = \cot\sigma_c = 1/\tan\sigma_c, \quad \tan\sigma_c = \cot\sigma = 1/\tan\sigma$$

Two other ratios use secant (or “sword-like”) lines that pierce the circle in Fig. 1.4b. The horizontal line is a *secant* ratio $\frac{\text{radius}}{\text{base}} = \frac{r}{b} = \frac{\Delta r}{\Delta x} = \sec\sigma = 1/\cos\sigma$ and its co-ratio is a *cosecant* ratio $\frac{\text{radius}}{\text{altitude}} = \frac{r}{a} = \frac{\Delta r}{\Delta y} = \csc\sigma = 1/\sin\sigma$.

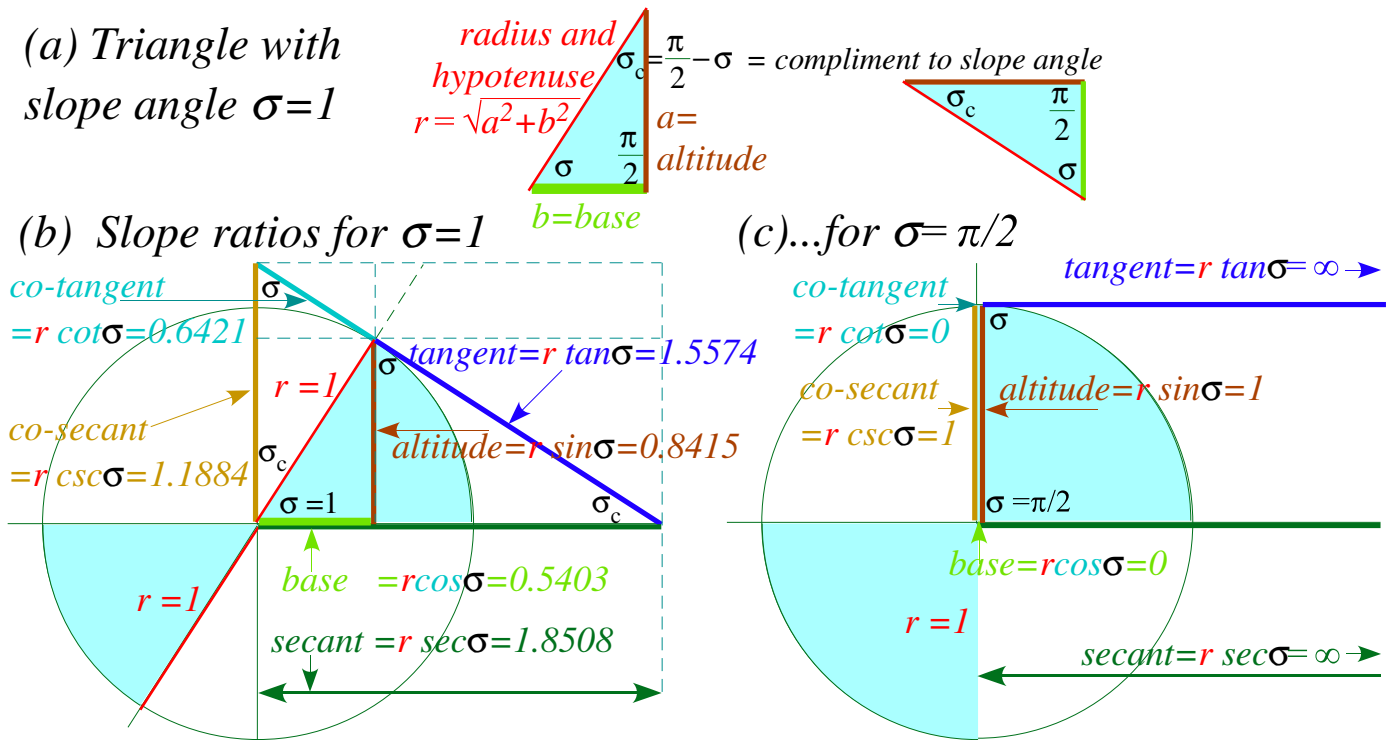


Fig. 1.4 (a) Right triangle geometry for $\sigma=1$ slope (b) Triangle ratios for $\sigma=1$ and (c) $\sigma=\pi/2$.

Fig. 1.4b has *eight* different but *similar* triangles with the same angles ($\sigma, \pi/2, \sigma_c$) as the triangle in Fig. 1.4a. Can you spot them? Whether big or small, similar triangles share ratios (sine, cosine, or tangent) if (and *only* if) they share angles. To do geometry problems we look for “hidden” similar triangles and hidden *right* triangles that form similar *rectangles*. Right triangles have relation $a^2 + b^2 = r^2$ of Pythagoras (~570 BC).

One secret is to visualize sequences of scale change or rotation transformation as in Fig. 1.5 where each rectangle is rotated by 90° and shrunk by a factor $\cot\sigma = 64.2\%$. Rectangle diagonals in Fig. 1.5a (and sides in Fig. 1.5b) give a *power sequence* ($\dots \tan^1\sigma, \tan^0\sigma = 1, (\tan\sigma)^{-1} = \cot^1\sigma, (\tan\sigma)^{-2} = \cot^2\sigma, (\tan\sigma)^{-3} = \cot^3\sigma, \dots$).

A power sequence is also called a *geometric sequence* since it is suggested by geometry. A rectangle sequence in Fig. 1.5a is lined up with the XY coordinates of the page, that is, each side has zero or infinite slope but the first diagonal ($\tan\sigma$) has a negative slope angle of $-\sigma_c = -1$ -radian or -57.3° . The sequence in Fig. 1.5b begins with a rectangle side ($\tan\sigma$) at angle -57.3° . Each sequential rotation in either figure is 90° clockwise around the original tangent point with rectangle size shrunk by factor $\cot\sigma = 64.21\%$ each time.

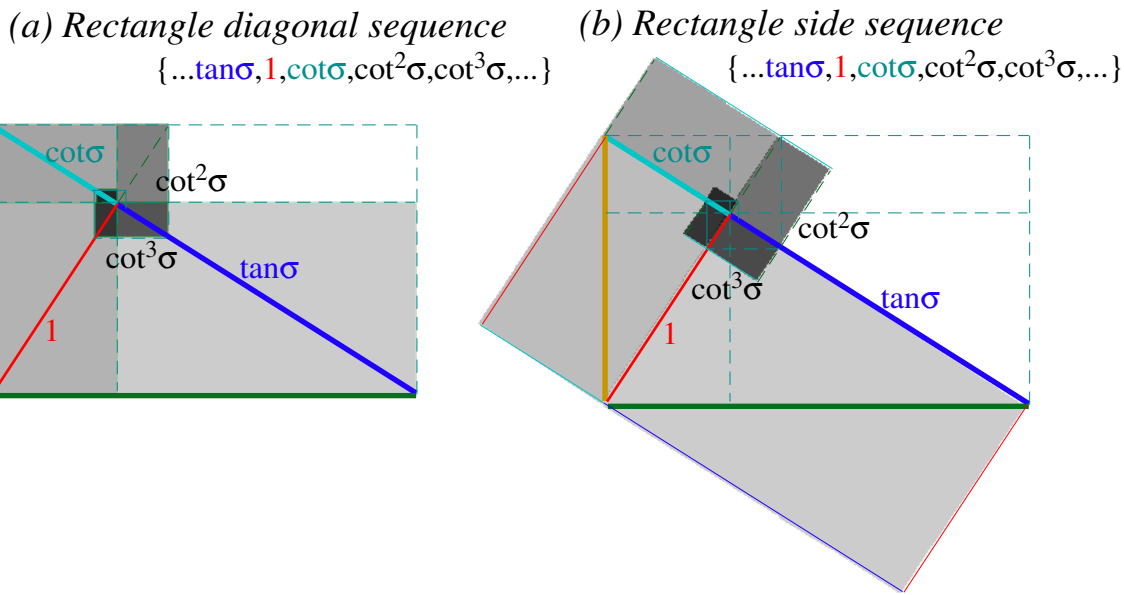


Fig. 1.5 Geometric $\cot\sigma=0.6241$ sequences of whirling rectangle segments based on slope angle $\sigma=1$.

Exercises for study of slope and trigonometry

1. Construct whirling square diagrams for 60° slope angle $\sigma=\pi/3$ without using protractor. First compare the precision of graph-derived values of $\sin\sigma$, $\cos\sigma$, $\tan\sigma$, etc. with algebraic^{and}/_{or} calculator-derived numbers.

Solution Hints:

Only certain angles have exact Euclid rule&compass construction and $\sigma=60^\circ$ is one of them. (But, $\sigma=1$ isn't!) If you could “straighten” the ($\ell=1$)-arc of a ($\sigma=1$)-sector (Fig. 1.3a) to one ($r=1$)-side of an equilateral triangle, its slope angle would grow from $\sigma=1=57.3^\circ$ to $\sigma=\pi/3=60^\circ$ as shown in Fig. 1.6b.

To construct a 60° slope *a’la* Euclid, draw a radius- $(r=1)$ circle by compass and use the same radius- r setting to strike an arc from **X** point- $(x=1,y=0)$ to locate **R** as in Fig. 1.6b. So now, theoretically, *arc-RX* is $\ell=\pi/3=1.0472\dots$ long *approximately* but *line-RX* has length- $(r=1)$ *exactly*. At 2-figure precision both have length 1.0, but at 3-figure precision, *arc-RX* length is 1.05, 5% greater than *line-RX* length 1.00.

Whether a math or physics theory is “correct” or not depends on our level of precision. As we will see, it is pretty tough to get level-3 absolute precision (1 part in 1,000) with ruler and compass construction but level-2 is pretty easy. By taping fishing line onto *arc-RX*, we can see that it is about 5% shorter than a unit line, but measuring 4.7% is challenging and 4.72% requires tools most don’t have.

We easily get level-9 precision by poking $\sin(\pi/3)$ into a calculator (or $\sin 60^\circ$ if set for degrees) to get $\sin(\pi/3)=0.866025403\dots$ but only can estimate 0.86 or 0.87 in Fig. 1.6b graph as indicated by ??? marks.

To construct the tangent declination by compliment angle $\sigma_c = \pi/2 - \pi/3 = \pi/6$ (or $90^\circ - 60^\circ = 30^\circ$) we strike a unit arc off the $-Y$ point to intersection point **Q** on the 4th quadrant-**YQX** of unit circle in Fig. 1.6c. The line **OQ** thru point **Q** is perpendicular or *normal* to original slope line **OR** since $\sigma_c + \sigma$ is $\pi/2(90^\circ)$ for any σ .

This line **OQ** drawn thru point **R** is the tangent decline we need for this problem. Just redo arc intersector **-YQO** to make sector **NPR** centered at **R** instead of **O**. Then draw tangent line **PR** so it extends down to secant point **S** on the **X** axis and up along the cotangent line to the cosecant point on the **Y** axis.

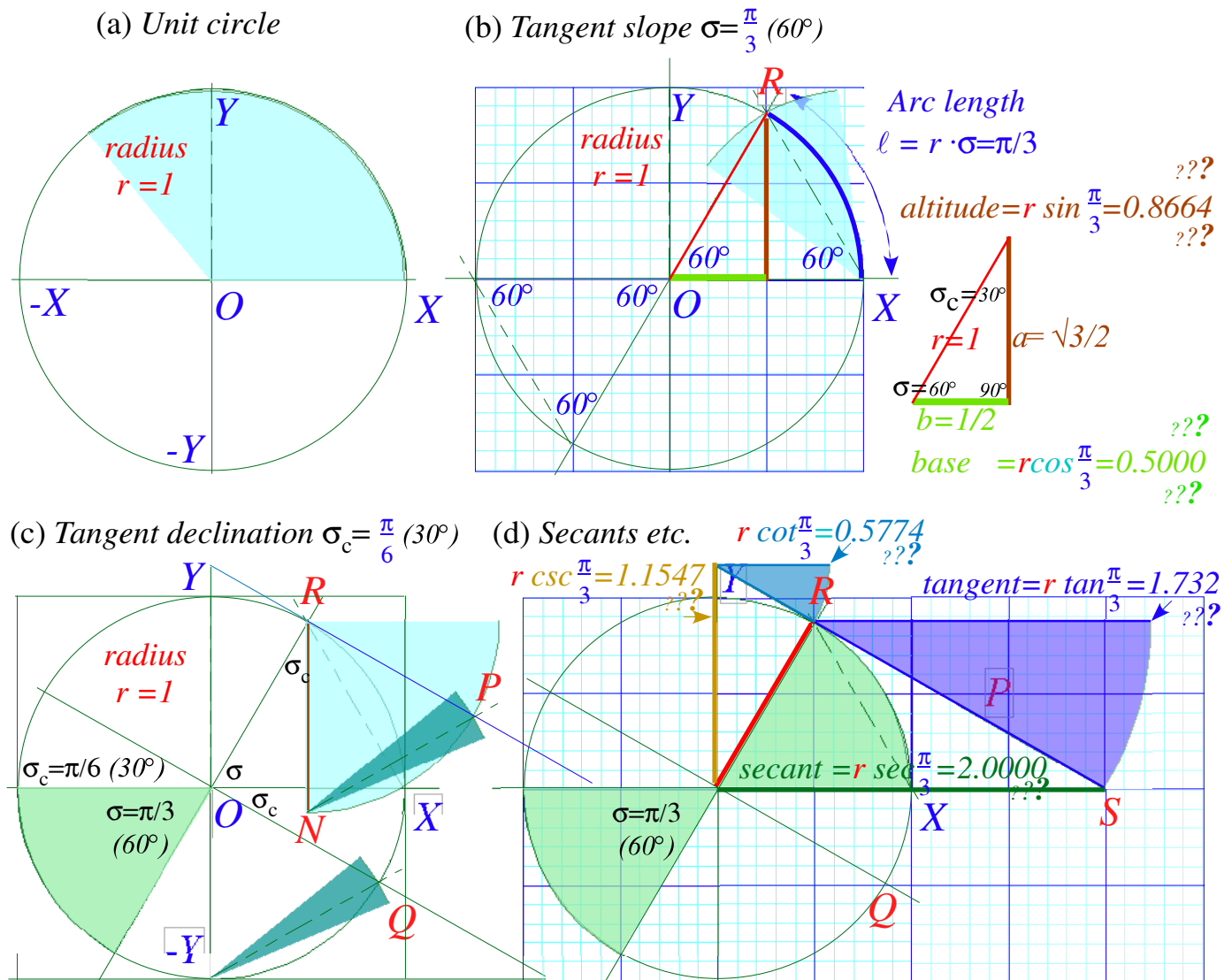


Fig. 1.6 Details of a geometric construction of Fig. 1.5 for slope angle $\sigma = \pi/3$ (60°)

Segments **OS** and **YR** provide numerical estimates of calculated values $\sec(\pi/3) = 2.000$ and $\csc(\pi/3) = 1.155$ along **X** and **Y** axes, respectively, in Fig. 1.6d. The value $\sec(\pi/3) = 2$ like its inverse $\cos(\pi/3) = 1/2$ is exactly rational, a nice feature of a $(30^\circ, 60^\circ, 90^\circ)$ -triangle with side ratios $(b:a:r) = (1:\sqrt{3}:2)$ (It is a right triangle, so: $a^2 + b^2 = r^2$.) The “30-60” is a famous right triangle students must learn. Others are “3-4-5” ($(a:b:r) = (3:4:5)$) and the “45” ($(45^\circ, 45^\circ, 90^\circ)$ or $(a:b:r) = (1:1:\sqrt{2})$). A “Golden” ratio $G = \frac{1}{2}(1 + \sqrt{5})$ triangle is very cool (and rich).

Arc functions

So far we give an angle or unit-circle arc σ and construct or calculate trigonometric functions of σ including $a = \sin \sigma$, $b = \cos \sigma$, $t = \tan \sigma$, $1/a = \csc \sigma$ or their co-functions. Now consider the reverse or inverse case: we are given a , or b , or t etc. and must come up with an arc σ (or arcs $\sigma_1, \sigma_2, \dots$) that gives a , etc. To do this we find *arc-functions* *arc-sine*, *arc-cosine*... or *inverse trig functions* \sin^{-1} , \cos^{-1} ... as follows.

$$\sigma = \arcsin(a) = \sin^{-1}(a), \sigma = \arccos(b) = \cos^{-1}(b), \sigma = \arctan(t) = \tan^{-1}(t), \dots$$

The exponential (⁻¹)-notation seems to confuse $\sin^{-1}(a)$ with $(\sin(a))^{-1}=1/(\sin(a))$ that we do *not* want here. (However, it is conventional to write $(\sin(a))^n=\sin^n(a)$ or any power but (⁻¹.)

Algebra of arc-functions is trickier than algebra of functions themselves. Geometric constructions of \sin^{-1} , \cos^{-1} ...etc. are not so tricky but quite simple and revealing. To find $\sin^{-1}(0.5)$, for example, we draw a horizontal line at $y=0.5$ and see where it intersects the unit circle. (Fig. 7a) Nothing to that! Except, we see there are *two* angles $\sigma_1=\pi/3$ and $\sigma_2=2\pi/3$ that give $\sin\sigma_1=0.5=\sin\sigma_2$. The same applies to $\cos^{-1}(0.5)$ except now the angles are $\pm\pi/3$. (Fig. 1.7b) Note the *antipodal* ($\pm 180^\circ$) angles that equal $\tan^{-1}(0.5)$. (Fig. 1.7c)

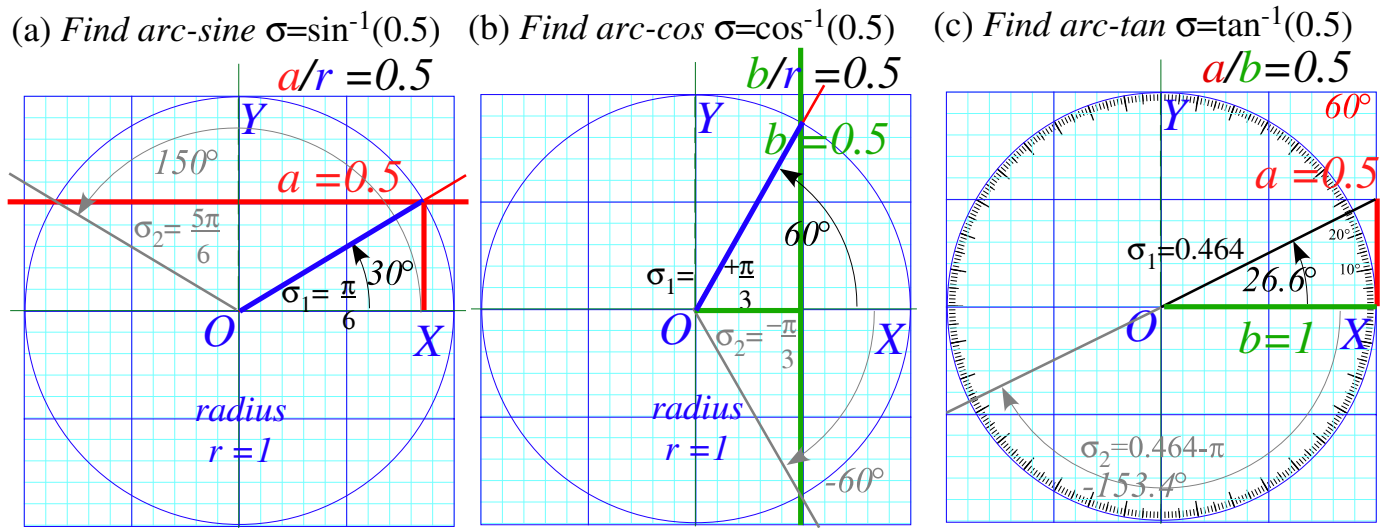


Fig. 1.7 Geometric construction of arc-trig functions of $0.5=\frac{1}{2}$. (a) $\sin^{-1}(\frac{1}{2})$ (b) $\cos^{-1}(\frac{1}{2})$ (c) $\tan^{-1}(\frac{1}{2})$

More challenging is finding *arc-secant* (say, $\sec^{-1}3.0$) by geometry. Try it first without looking at the answer.

Solution Hints:

We need to find the tangent that goes from 3.0 to touch the circle. A circle of radius $r=3.0$ concentric to the unit circle has rectangle tangents of that size that we copy from $x=3.0$ to touch unit circle.

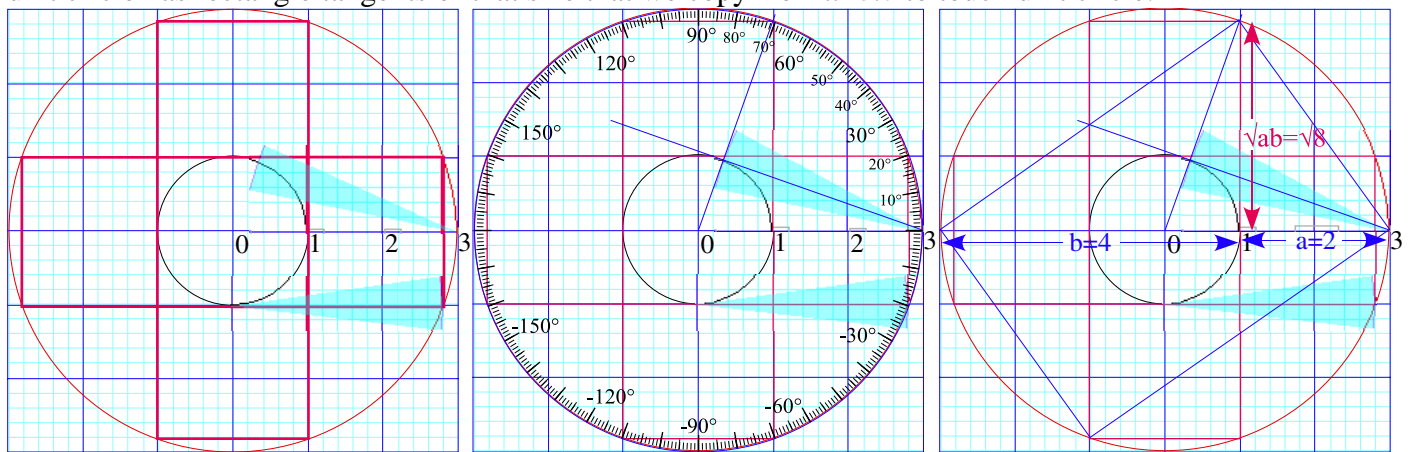


Fig. 1.8 Geometric construction of arc tangent, arc secant, and geo-mean square-root.

Or else we simply draw rectangle diagonal thru unit circle. This leads to *Euclid's Geometric Mean* construction of a product square root $\sqrt{(a \cdot b)}$ that is $\sqrt{8}=2.82\dots$ and is the desired tangent in this case.

Know your calculator and ATAN, too! (atan2(y,x))

Scientific calculators do not always give the solution you want for arc-function $\sin^{-1}(a)$, $\cos^{-1}(b)$, or $\tan^{-1}(b/a)$. For one thing, they never give an angle in the 3rd quadrant (*minus-x, minus-y*) so you could be wrong 25% of the time.

But it is worse than that. “Blind” arc-calculations are wrong *half* the time.

As you vary altitude $a=y$ from (+1) to (-1) values in Fig. 1.7a the 1st arc-solution $\sigma_1 = \sin^{-1}(a/r)$ sweeps the unit circle in the right-half plane while its x -reflection is the 2nd solution σ_2 is in the left-half plane. The calculator ignores σ_2 .

As you vary base $b=x$ from (+1) to (-1) values in Fig. 1.7b the 1st arc-solution $\sigma_1 = \cos^{-1}(b/r)$ sweeps the unit circle in the upper-half plane while its y -reflection is the 2nd solution σ_2 is in the lower-half plane. Again, the calculator ignores σ_2 .

Varying either altitude $a=y$ or base $b=x$ from (+1) to (-1) in Fig. 1.7c gives a full range of solutions $\sigma_1 = \tan^{-1}(a/b)$ but a calculator cannot distinguish between the first solution and the 2nd *antipodal* solution $\sigma_2 = \tan^{-1}(-a/-b)$ since $a/b = -a/-b$.

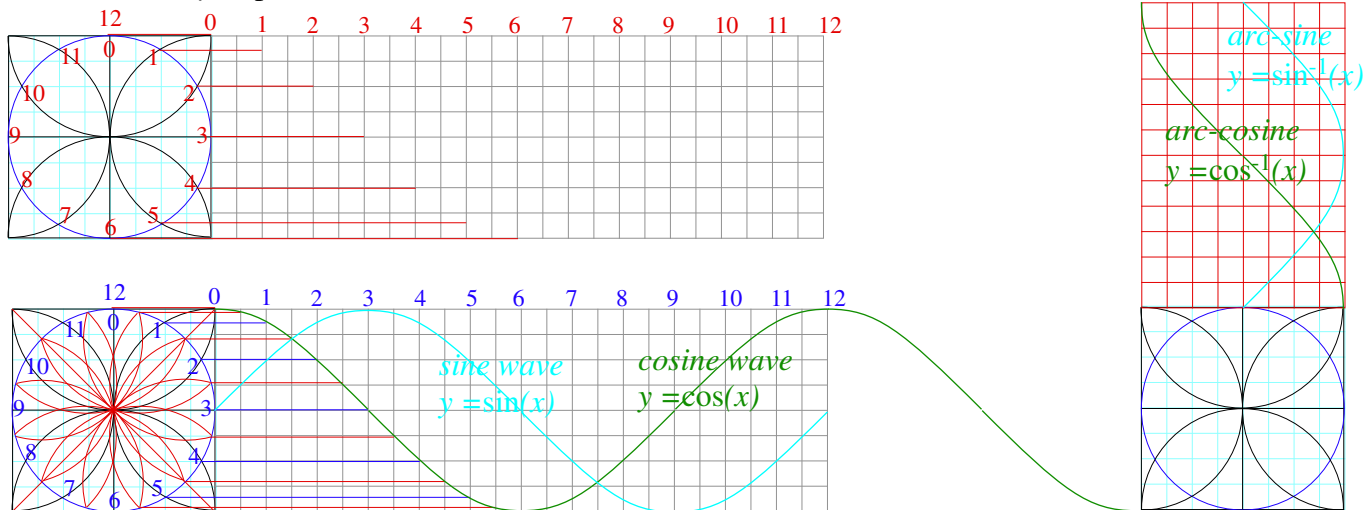
So the calculator plays it safe and gives the *acute angle* solution in the arc-range -90° and $+90^\circ$, that is $(-\frac{\pi}{2} \leq \sigma \leq +\frac{\pi}{2})$. The *obtuse angle* solution is ignored for ranges $+90^\circ$ to $+180^\circ$ (2nd quadrant: $+\frac{\pi}{2} < \sigma \leq +\pi$) or -90° and -180° (3rd quadrant: $-\frac{\pi}{2} > \sigma \geq -\pi$)

A correct solution is the sure-fire **atan2**(y,x) function that requires you to give both the altitude $a=y$ and the base $b=x$ (with correct signs, of course) so it knows which quadrant you’re in. The **atan2**, built into calculators gives what is called the *rect-to-polar coordinate conversion* often labeled by a $(x, y) \rightarrow (r, \theta)$ -button.

Plug in x and y and out comes $r = \sqrt{x^2 + y^2}$ and $\theta = \tan^{-1}\frac{y}{x}$. The θ is our correct σ .

Trig function plotting exercises

Use ruler&compass to plot the function $y=\cos(x)$ and $y = \cos^{-1}(x)=\arccos(x)$. Do $y=\sin(x)$ and $y=\sin^{-1}(x)$. Begin by constructing a 12-pt “clock” circle. Repeat using 45° diagonals to make a 24-hr clock. Then you project the 24 points horizontally for $y=\cos(x)$ and vertically $y=\cos^{-1}(x)=\arccos(x)$. Shift the plot by 3 hours (90°) to get the sine and arc-sine functions. Each “hour” is angle 15° or $\pi/6$. These are *really* important curves!



Chapter 2. Velocity and momentum

Recall the car-crash problems discussed first in Chapter 1 regarding Fig. 1.1. The first one involves a text-messaging driver of 4-ton SUV going 60mph SUV rear-ending a dawdling 1-ton VW going 10mph. (Fig. 1.1b.) What happens then? What velocity or velocities do the cars have just afterwards?

As sketched in Fig. 1.1b, the answer depends on whether it's "Ka-Runch" or "Ka-Bong" or some more generic noise like "Ka-whump". By "Ka-Runch" we mean the cars crumpled enough to become interlocked into one hunk of metal weighing 5 tons. ($4+1=5$) This is a simple problem that is solved by drawing a line of slope $(-4/1)$ on a velocity vs. velocity graph from before-crash-point ($V_{SUV}^{INITIAL} = 60, V_{VW}^{INITIAL} = 10$) to where that line intersects the red 45° ($V_{SUV}=V_{VW}$)-line at the after-crash-point ($V_{SUV}^{FINAL} = 50, V_{VW}^{FINAL} = 50$). (Fig. 2.1)

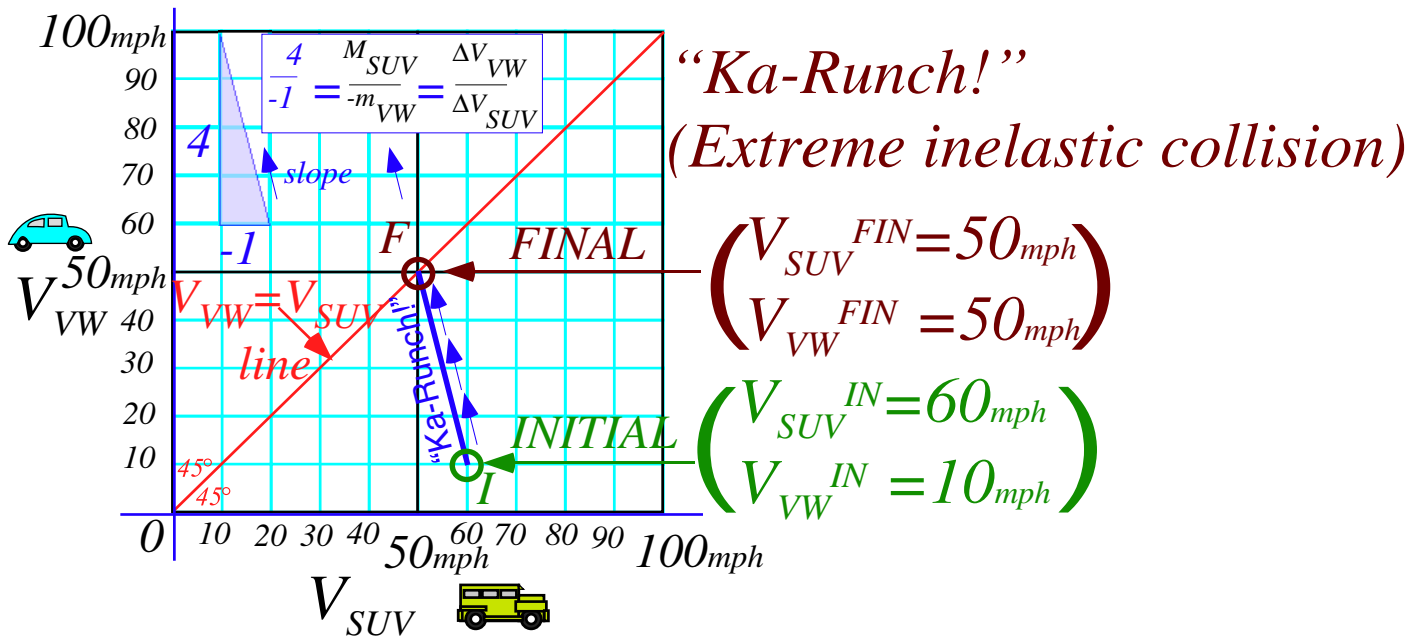


Fig. 2.1 Anatomy in velocity space of a "Ka-runch!" that is an extreme inelastic collision.

The logic behind a ($V_{SUV}=V_{VW}$)-line is that interlocked vehicles have equal velocity. The logic behind a *Ka-Runch*-line of slope $(-4/1)$ is subtler. It is due to *Newton's 1st axiom* or "law" that says Nature conserves so-called *momentum*, a sum of products of each mass with its velocity. It's a law we can live with but, how? *Momentum exchange: a zero-sum game*

During the car crash the velocity coordinate pair (V_{SUV}, V_{VW}) change very rapidly in moving from initial point *I* at (60,10) to final point *F* at (50,50) in Fig. 2.1. The *Ka-Runch* takes less than $1/50^{\text{th}}$ of a second! During that time, SUV will only lose one unit of velocity for every *four* units gained by VW since SUV is *four* times heavier than VW. Newton writes this as a *total momentum conservation* equation.

$$P_{SUV} + P_{VW} = M_{SUV} \cdot V_{SUV} + m_{VW} \cdot V_{VW} = P_{Total} = constant \tag{2.1}$$

Checking (2.1) with Fig. 2.1 gives a total momentum $P_{Total} = 250$ that the poor SUV and VW can't change.

$$4 \cdot 60 + 1 \cdot 10 = 4 \cdot V_{SUV} + 1 \cdot V_{VW} = 4 \cdot 50 + 1 \cdot 10 = P_{Total} = 250 \tag{2.2}$$

The *change* of P_{Total} must be zero ($\Delta P_{Total} = 0$) before, during, or after the crash. It's a zero-sum game.

$$M_{SUV} \Delta V_{SUV} + m_{VW} \Delta V_{VW} = \Delta P_{Total} = 0 \tag{2.3}$$

Dividing by SUV change-of-velocity (ΔV_{SUV}) and VW mass (m_{VW}) gives the slope relation in Fig. 2.1.

$$\frac{M_{SUV}}{m_{VW}} + \frac{\Delta V_{VW}}{\Delta V_{SUV}} = 0 \text{ or: } \frac{\Delta V_{VW}}{\Delta V_{SUV}} = -\frac{M_{SUV}}{m_{VW}} \tag{2.4}$$

P_{Total} is also conserved in an ideal *Ka-Bong* of Fig. 2.2. Here cars bounce off each other without damage. That’s unlikely at 60mph speeds! So Fig. 2.2 is rescaled to units of *feet per minute*. Then initial $v_{SUV}^{IN} = 60 \text{ feet per minute} = 1 \text{ ft. per sec.}$ is more like a parking lot speed, and insurance claims are less as the VW is bumped from an initial $v_{VW}^{IN} = 10 \text{ ft per min}$ to $v_{VW}^{FIN} = 90 \text{ ft per min} = 1.5 \text{ fps} = 1.02 \text{ mph}$. To find v_{VW}^{FIN} in Fig. 2.2, draw an arc from initial *I*-pt (60,10) to hit final *F*-pt (40,90). Arc-center is *Center of Momentum COM* pt-(50,50) on the 45° line. (It’s the *final* point if cars get “stuck” to each other as they do in a *Ka-Runch* like Fig. 2.1.)

“Ka-Bong!” (Ideal elastic collision)

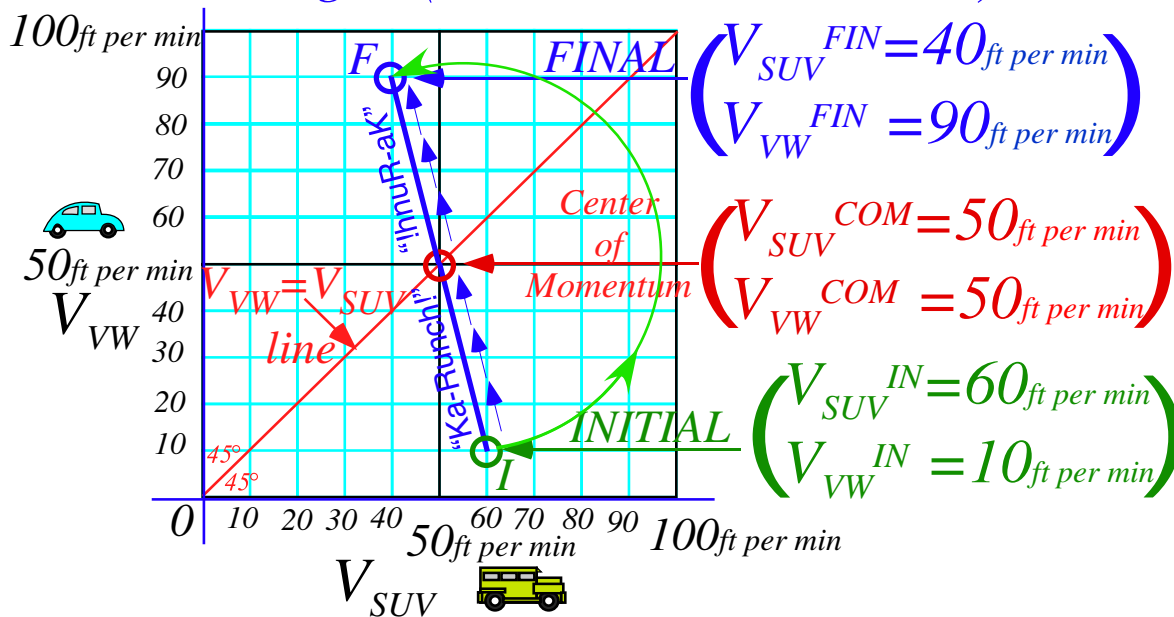


Fig. 2.2 Anatomy in velocity space of a “Ka-Bong!” that is an extreme or ideal elastic collision.

The *Ka-Bong* in Fig. 2.2 is like the *Ka-Runch* in Fig. 2.1 followed by an equal but opposite rebound or *hcnuR-aK* (*un-crash*) that undoes the “damage” by the *Ka-Runch*. Now you might ask, “Is this possible outside of the cartoon world or a video game?” Well, *certainly not* at high speeds and *not quite* at low speeds.

Only in a quantum nano-world do *perfectly* elastic processes exist. Any collision of classical objects, however gentle, will permanently disturb or exchange thousands or millions of atoms and electrons. We call this “wear&tear” or *entropy growth* and ignore it until it has gone too far. (Then, we discard the objects!)

Even gentle bumps like the one starting at initial *pt-I* in Fig. 2.2 cannot quite go *exactly* to final *pt-F* on the *COM* circle, but collisions with no appreciable damage pass as (*almost*) *elastic* or *time reversible* bumps. A video of the Fig. 2.2 $I \rightarrow F$ bump played backwards looks like an $F \leftarrow I$ bump that is not extraordinary. But a reversed video of the Fig. 2.1 crash looks like a crazy “*un-crash*” where ruined cars get reborn like new.

Deducing (perfect?) conservation from (ideal?) symmetry

Newton's momentum or P -conservation axiom or "law" is one of the most strictly enforced laws in classical physics. (It's also quasi-conserved in quantum physics that so often seems to get away with utter mayhem!) Momentum is like some kind of fluid that you can buy and sell but never can create or destroy. In our car bumps or crashes the zero-sum-rule says, "Whatever P the VW gains (or loses) the SUV loses (or gains.)"

A classical law without classical proof remains an axiom until deeper theory may rule on it. Quantum theory has ruled and can shed some light on origin and properties of this mysterious " P -fluid." It also shows how to cheat P -conservation and other classical "laws" a little. This will be discussed in later units.

In the meantime it is possible to deduce P -conservation using more fundamental axioms that are called *symmetry principles*. This is a grown-up geometric approach that is also *very* useful in the quantum world. Most importantly, symmetry helps deduce principles of energy E and E -conservation as discussed below.

Symmetry means "same-etry" or "similarity" or "smoothness" and other "s" words like *simplicity*. The fancy technical term is *isotropy* or *isometry* with *iso* meaning *same*. For example, the most *symmetric* ball would be a *sphere* since it is *isotropic* and has the *same* radius everywhere. A most-isotropic plane or most-symmetric plane is *flat* and *bump-free*. Some would say *symmetry* means *Beauty*, but others might say it means *Boring*. Think of a seemingly endless *Kansas* prairie for either response.

Symmetry can refer to *sameness* in time as well as in space and often the two are related. (Think of *driving* across *Kansas*.) The idea of being *time reversible* is an example from the preceding page. Another is Galileo's relative-velocity symmetry or *Galilean relativity*. Both are behind Fig. 2.3 and Fig. 2.4 below.

Galilean time-reversal symmetry

Suppose a traffic cop is going *50mph* in a lane adjacent to the one occupied by the SUV and VW. He or she records (using radar) the SUV coming up at *60mph*, and puts on the blue-light to stop it for exceeding the *20mph* limit in a school zone. Just then *Ka-Runch!* SUV+VW becomes a single 5-ton hunk going *50 mph*, the same speed as the cop. (The cop can just reach across to hand SUV a cyber-ticket for (1) speeding in a school zone, (2) improper following, and (3) driving while faxing. C-tickets are *costly* even for SUVites!)

The V_{VW} vs. V_{SUV} graph for the *Ka-Runch* is shown in Fig. 2.3 as viewed by the *50mph* cop. It is the same as Earth-frame-view in Fig. 2.1 except the cop's speed of *50mph* is subtracted from both V -scales. The cop sees a final 5-ton SUV-VW hunk going *0 mph* relative to cop-frame or *COM frame* of SUV+VW.

The V_{VW} vs. V_{SUV} graph for the *Ka-Bong* in Fig. 2.4 is viewed in the *50mph* cop-frame or *COM*-frame. Again, it's just Fig. 2.2 with *50mph* subtracted off V -scales. Cop or *COM*-frame view shows *simplicity* and *symmetry*. Velocity values simply change sign as the *Ka-Bong* crosses the whole *COM*-circle diameter.

Initial I -pt (10, -40) \rightarrow (reflection thru *COM* pt-(0,0)) \rightarrow final F -pt (-10, 40)

Reversing time ($\Delta t \rightarrow -\Delta t$) makes (-)velocity ($V = \frac{\Delta x}{\Delta t} \rightarrow -\frac{\Delta x}{\Delta t} = -V$) and crosses the diameter oppositely.

Initial I -pt (-10, 40) \rightarrow (reflection thru *COM* pt-(-0, -0)) \rightarrow final F -pt (10, -40)

That is just Fig. 2.4 with blue time-direction arrows reversed. (*INITIAL I* switches places with *FINAL F*.)

Elastic collisions (Fig. 2.4) are *symmetric* and *balanced* to t -reversal, but inelastic *Ka-whump*'s are *unbalanced* if they stop short of the *COM* circle. A *Ka-Runch* (Fig. 2.3) is *unbalanced to an extreme*.

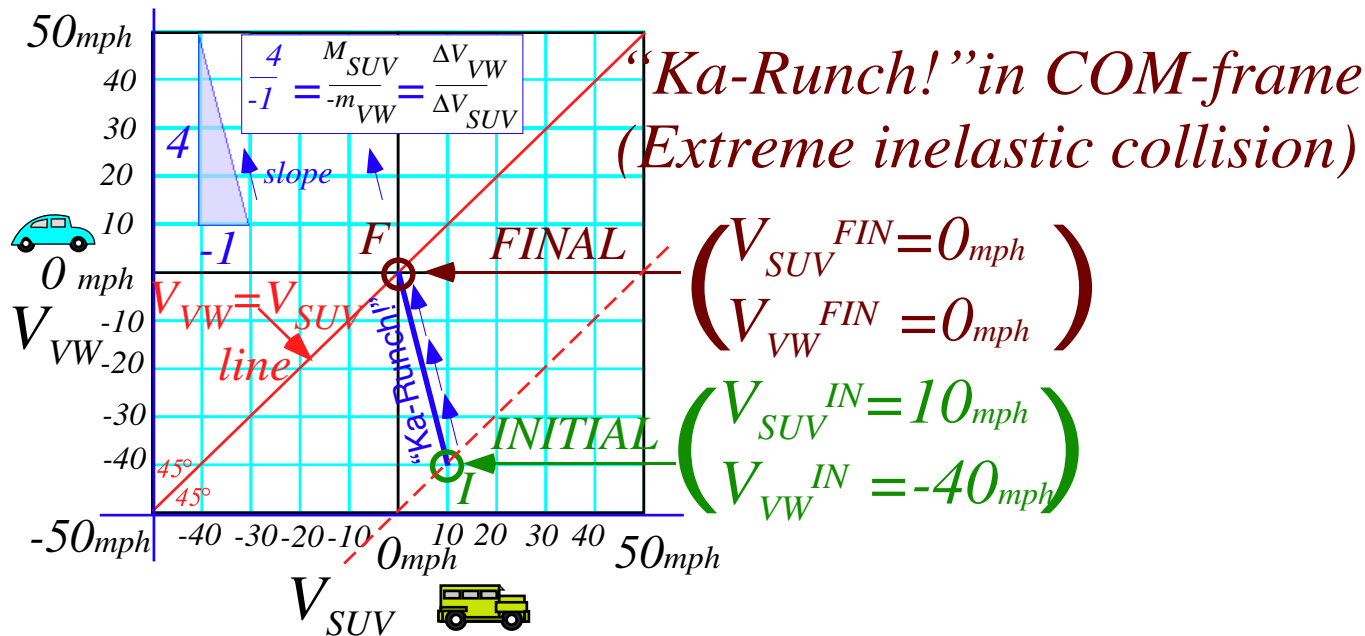


Fig. 2.3 COM-frame or 50mph cop-frame view of a “Ka-runch” inelastic collision of Fig. 2.1.

“Ka-Bong!” (Ideal elastic collision in COM-frame)

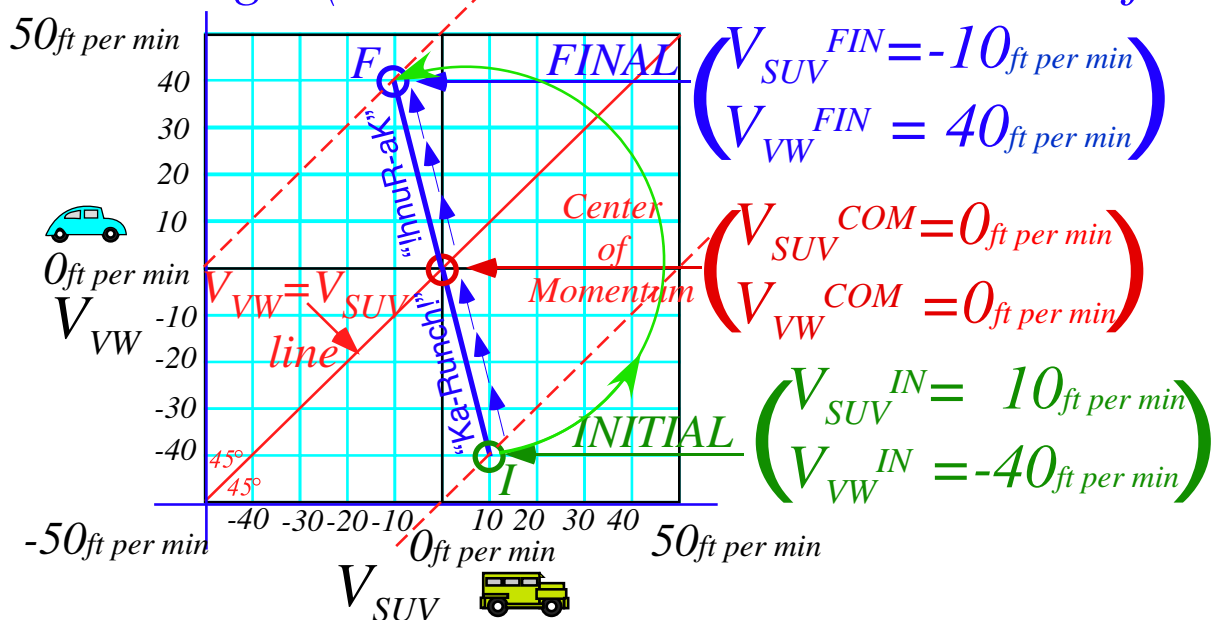


Fig. 2.4 COM-frame or 50mph cop-frame view of a “KaBong” elastic collision of Fig. 2.2.

This is a common situation in physics. The real (or generic) world lies between extreme ideals that are easiest to quantify. On one hand, we’ll say a *Ka-whump* that ends up close to its initial *COM*-circle is *elastic* or *Ka-Bong*-like and, on the other hand, a *Ka-whump* that stops near its *COM*-point is *inelastic* or *Ka-Runch*-like.

Galilean relativity and spacetime symmetry

Galileo grew up in Renaissance Italy as it flourished from its sea trade. Perhaps, watching ships of trade glide smoothly in the harbor led him to ideas about relativity of velocity. In any case he wrote about comparing what a sailor sees in a ship-frame with what is seen in the Earth-frame. He noted how apparent velocity of an object decreases by subtracting the velocity of the observer’s frame.

Subtraction of the cop’s velocity $V_{cop}=50$ from Earth-frame velocity $(V_{SUV}, V_{VW})=(60, 10)$ of SUV and VW in Fig. 2.2 gives their initial velocity $(60, 10)-(50, 50)=(10, -40)$ in cop-frame. (Fig. 2.4) Such a subtraction (or addition if the cop goes the other way) is a *Galilean relativity transformation*. Fig. 2.4 is a redrawing of Fig. 2.2 with new (V_{SUV}, V_{VW}) scales, each reduced by 50mph . Or else, you may start with Fig. 2.2 and slide each velocity point down its 45° -line by 50mph , (*COM* and cop-frame Earth-relative velocity) as in Fig. 2.5a.

This becomes a “slide-rule” in Fig. 2.5b that quantifies several Galilean frames. The initial VW frame $(VW(I))$ is found where the 45° -*I*-line hits the horizontal $(V_{VW}=0)$ axis. VW starts in frame- $VW(I)$ and is hit by a $(V_{SUV}=50)$ -SUV that knocks VW into a new frame- $VW(F)$ of final $V_{VW}=80$ as SUV slows to a final $V_{SUV}=30$.

Next a final SUV frame $(SUV(F))$ intersects the 45° -*F*-line on the vertical $(V_{SUV}=0)$ axis where a final $(V_{SUV}, V_{VW})=(0, 50)$ -point- $F_{SUV(F)}$ results if initially a $(V_{SUV}=20)$ -SUV *Ka-Bongs* a $(V_{VW}=-30)$ -VW at point- $I_{SUV(F)}$.

Note that seven *Ka-Bong* lines in Fig. 2.5 show seven different-frame views of the same *Ka-Bong*. In four frames, one car has $V=0$ either before or after the *Ka-Bong*. One frame, the *COM* has $V_{COM}=0$ before and after. That *COM*-frame is balanced to velocity reversal $(+V \leftrightarrow -V)$. Other frames have distinct V -reversed twins with *INITIAL I* and *FINAL F* switched. For example, $I_{SUV(F)} \leftrightarrow F_{SUV(F)}$ and $F_{SUV(I)} \leftrightarrow I_{SUV(I)}$ are symmetry twins.

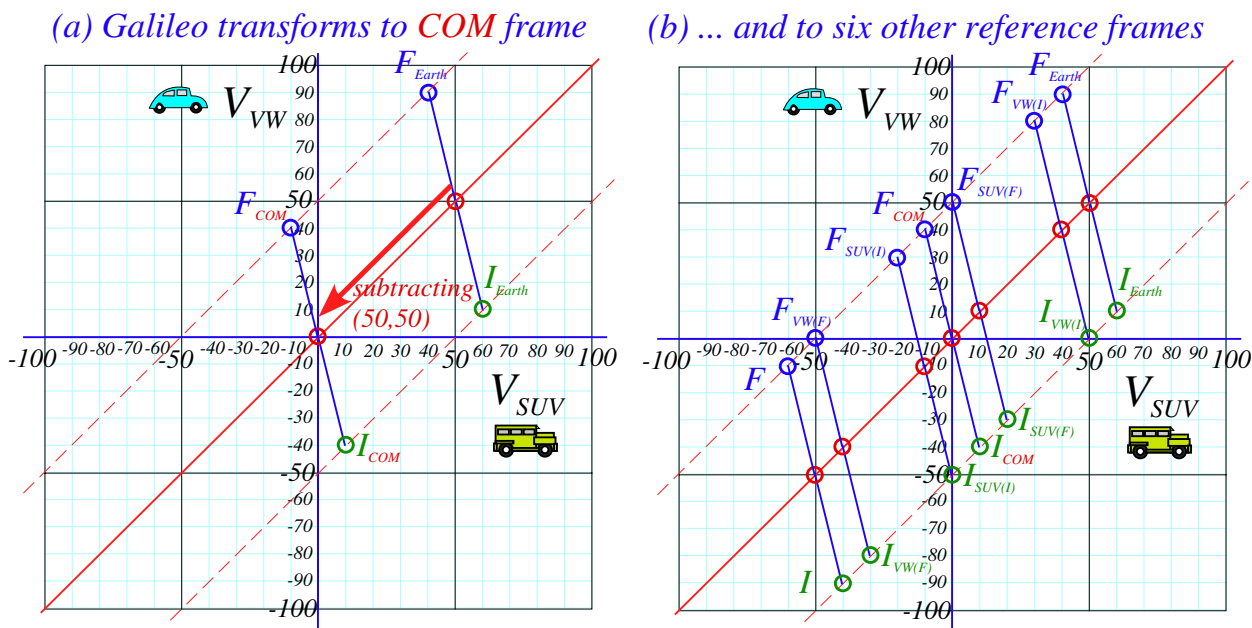


Fig. 2.5 Galilean transform of “KaBong” in Fig. 2.2 to (a) COM-frame and (b) to other frame views.

V_{COM} identifies a frame and is the *weighted average* of any V_{SUV}, V_{VW} pair (*initial, final, or en flagrante delecti!*) on its *IF*-line. V_{COM} is zero for the *COM* frame so its *IF*-line is the same for $+V$ or $-V$. ($V_{COM}=\pm 0$)

Geometry of Balance: Center of Momentum (COM) and Center of Gravity (COG)

The uniqueness and constancy of a **COM** for the SUV and VW is connected with underlying space-time symmetry or geometry of spatial balance in Newton’s equation (2.1) repeated here in different forms.

$$P_{Total} = P_{SUV} + P_{VW} = M_{SUV} \cdot V_{SUV} + m_{VW} \cdot V_{VW} = M_{TOTAL} \cdot V_{COM} = constant \quad (2.5a)$$

Total momentum is a product of V_{COM} and total mass $M_{TOTAL} = M_{SUV} + m_{VW}$ of a 5-ton SUV-VW “hunk”. This holds whether the “hunk” forms permanently in a *Ka-Runch* or the cars bounce off in a *Ka-Bong* or *Ka-whump*. Both $P_{Total} = M_{TOTAL} \cdot V_{COM}$ and V_{COM} are constant throughout the collision regardless of “auto-elasticity.”

$$V_{COM} = \frac{M_{SUV} \cdot V_{SUV} + m_{VW} \cdot V_{VW}}{M_{SUV} + m_{VW}} = \frac{M_{SUV} : m_{VW}}{\text{weighted average of } V_{SUV} \text{ and } V_{VW}} = \frac{constant}{M_{TOTAL}} \quad (2.5b)$$

Weighted average V_{COM} of (V_{SUV}, V_{VW}) is fixed as V go from *initial* to *in-between* to *final* values. Collisions in Fig. 2.1 thru Fig. 2.5 all have $V_{COM} = 50$ in the Earth frame. The 4:1-weighted average of each coordinate pair $(40, 90), (50, 50), (60, 10), (70, -30), etc.$ on the slope-(-1:4)-line (in Fig. 2.6a below) is $V_{COM} = 50$.

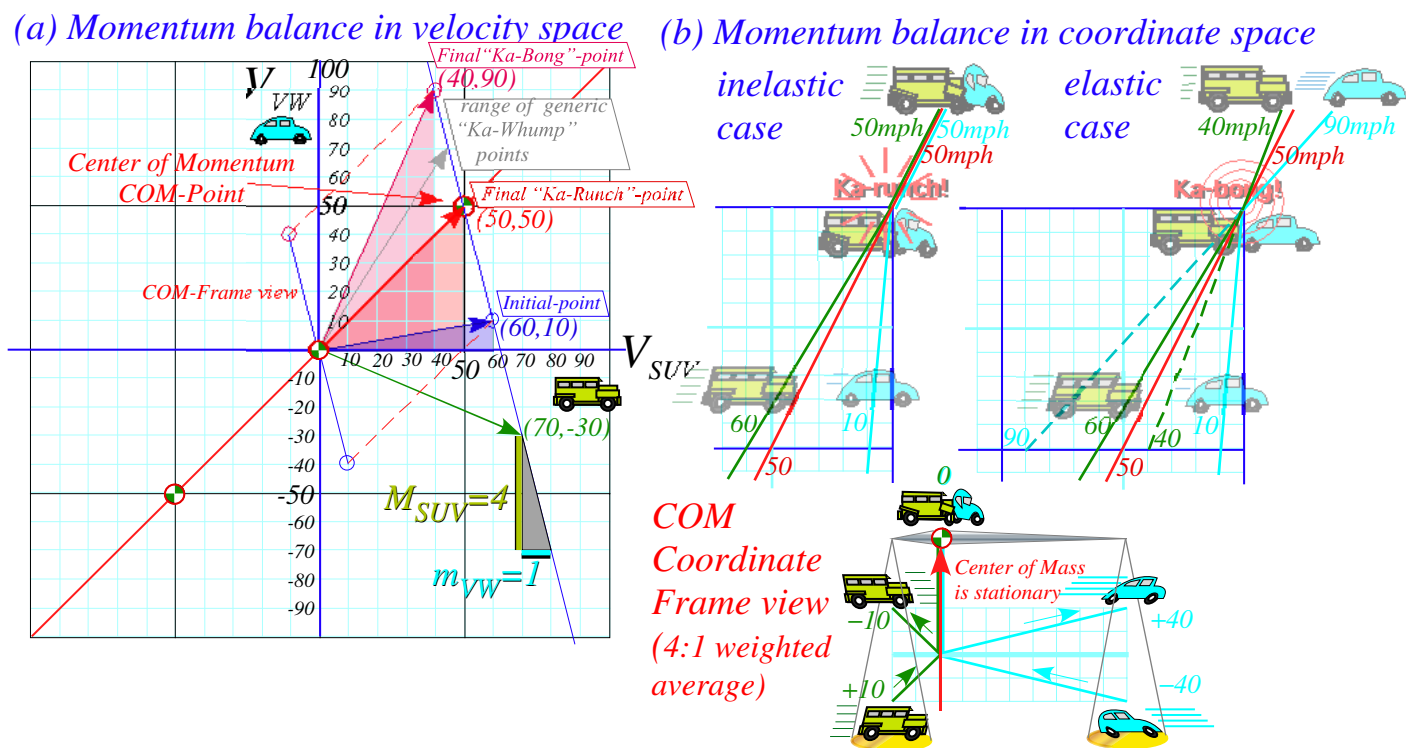


Fig. 2.6 Geometry of (a) 4:1-weighted velocity average (b) 4:1-weighted coordinate average.

Balance between velocity V_{SUV} and V_{VW} in (2.5b) relates to balance between position x_{SUV} and x_{VW} .

$$x_{COM} = \frac{M_{SUV} \cdot x_{SUV} + m_{VW} \cdot x_{VW}}{M_{SUV} + m_{VW}} = \frac{M_{SUV} : m_{VW}}{\text{weighted average of } x_{SUV} \text{ and } x_{VW}} \quad (2.5c)$$

As SUV and VW close, collide, bounce, or stick, the *Center of Mass* x_{COM} stays at a constant velocity V_{COM} . In the **COM** frame that velocity is zero as sketched in the lower part of Fig. 2.6b. The weighted average (2.5c) of coordinates is also a *Center of Gravity* and is cartooned by a 4:1 Greek balance.

Chapter 3. Velocity and energy

We noted that reflection symmetry or balance in *space* is connected with *momentum* or $P=m \cdot V$ conservation. Uniformity or “sameness” of coordinate and velocity space means the SUV can lose a unit of momentum only if the VW gains that unit, and *vice versa*. Momentum is a zero-sum game that does not depend on whether the two protagonists bounce elastically or crumple in-elastically during their collisions.

Time symmetry and energy conservation

Now we consider symmetry or balance in *time*. This is connected with a something called *energy* that also plays a conservation zero-sum game but, unlike momentum, requires elastic (*Ka-Bong!*) collisions. While momentum conservation is *axiomatic*, energy conservation can be *derived* from the former. Let’s do that.

Time symmetry

Symmetry balance in Fig. 2.6 is between pairs of velocity values (V_{SUV}, V_{VW}) or spatial coordinates (x_{SUV}, x_{VW}) of the colliding SUV and VW. Weighted average (2.5b) equals the same V_{COM} for the initial pair ($V_{SUV}^{IN}, V_{VW}^{IN}$), the final pair ($V_{SUV}^{FIN}, V_{VW}^{FIN}$), or a pair ($V_{SUV}(t), V_{VW}(t)$) at anytime t . (Recall (2.1) and (2.5), too.)

$$P_{Total} = M_{Total} V_{COM} = M_{SUV} V_{SUV}^{IN} + M_{VW} V_{VW}^{IN} = M_{SUV} V_{SUV}^{FIN} + M_{VW} V_{VW}^{FIN} = etc. \quad (3.1a)$$

We subtract *IN*’s from *FIN*’s to isolate SUV terms from VW terms and redo *zero-sum relation* (2.3).

$$0 = P_{Total} - M_{SUV} V_{SUV}^{IN} - M_{VW} V_{VW}^{IN} = M_{SUV} (V_{SUV}^{FIN} - V_{SUV}^{IN}) + M_{VW} (V_{VW}^{FIN} - V_{VW}^{IN}) \quad (3.2a)$$

$$0 = M_{SUV} \cdot (\Delta V_{SUV}) + M_{VW} \cdot (\Delta V_{VW}) \quad (3.2b)$$

(Ch.1 introduces *Delta* notation $\Delta V = V^{FIN} - V^{IN}$.) Here is another way to write the zero-sum relation.

$$M_{SUV} (V_{SUV}^{FIN} - V_{SUV}^{IN}) = M_{VW} (V_{VW}^{IN} - V_{VW}^{FIN}) \quad (3.3)$$

Now consider balancing *IN* vs. *FIN* pair ($V_{SUV}^{IN}, V_{SUV}^{FIN}$) for SUV or ($V_{VW}^{IN}, V_{VW}^{FIN}$) for VW. Elastic (*Ka-Bong!*) cases in Fig. 2.2 or Fig. 2.6 show how V_{COM} is a balanced *IN*-vs.-*FIN* pair-average of *both* SUV *and* VW.

$$V_{COM} = \frac{1}{2} (V_{SUV}^{FIN} + V_{SUV}^{IN}) = \frac{1}{2} (V_{VW}^{FIN} + V_{VW}^{IN}) \quad (3.4)$$

This is an algebraic statement of a *time reversal symmetry* axiom or *IN vs. FIN balance* mentioned earlier. For ideal elastic (*Ka-Bong!*) collisions, *IN* and *FIN* points balance around the *COM* point. Switching past and future gives a similar *Ka-Bong* and not a miraculous “*un-crash*” that shows up for V^{FIN} closer to V_{COM} than V^{IN} .

Kinetic Energy conservation

A definition of energy is derived by multiplying *space and time balance equations* (3.3) with (3.4)

$$\begin{aligned} \frac{1}{2} (V_{SUV}^{FIN} + V_{SUV}^{IN}) M_{SUV} (V_{SUV}^{FIN} - V_{SUV}^{IN}) &= \frac{1}{2} (V_{VW}^{FIN} + V_{VW}^{IN}) M_{VW} (V_{VW}^{IN} - V_{VW}^{FIN}) \\ \frac{1}{2} M_{SUV} (V_{SUV}^{FIN})^2 - \frac{1}{2} M_{SUV} (V_{SUV}^{IN})^2 &= \frac{1}{2} M_{VW} (V_{VW}^{IN})^2 - \frac{1}{2} M_{VW} (V_{VW}^{FIN})^2 \end{aligned}$$

Then adding the (-)-terms to both sides isolates *IN*-terms, and a *FIN*-sum is proved to equal an *IN*-sum.

$$\frac{1}{2} M_{SUV} (V_{SUV}^{FIN})^2 + \frac{1}{2} M_{VW} (V_{VW}^{FIN})^2 = \frac{1}{2} M_{VW} (V_{VW}^{IN})^2 + \frac{1}{2} M_{SUV} (V_{SUV}^{IN})^2 \quad (3.5a)$$

This $\frac{1}{2} M \cdot V^2$ is *kinetic energy (KE)* and it is conserved by a relation like (2.5a) for *momentum* $P=M \cdot V$.

$$constant = KE_{Total} = KE_{SUV}^{FIN} + KE_{VW}^{FIN} = KE_{SUV}^{IN} + KE_{VW}^{IN} \quad \text{where: } KE = \frac{1}{2} M \cdot V^2 \quad (3.5b)$$

$$constant = P_{Total} = P_{SUV}^{FIN} + P_{VW}^{FIN} = P_{SUV}^{IN} + P_{VW}^{IN} \quad \text{where: } P = M \cdot V \quad (2.5a)_{repeated}$$

Conservation relations are insensitive to overall factors. So is factor $\frac{1}{2}$ in (3.5a) fortuitous? Well, KE can be defined by integral relation $KE = \int V \cdot dP$. (See below.) A V vs. P plot is a triangle with base $P = M \cdot V$, altitude V , and area $KE = \frac{1}{2} P \cdot V = \frac{1}{2} M \cdot V^2$. With $\bar{V} = (V^{IN} + V^{FIN})/2$ our product (3.3)·(3.4) above is $\bar{V} \cdot \Delta P = \int V \cdot dP = \frac{1}{2} M \cdot V^2$.

Kinetic energy ellipse and momentum line

Momentum-conservation relation (2.5a) is rearranged for plot geometry.

$$m_{VW} \cdot V_{VW} + M_{SUV} \cdot V_{SUV} = (M_{SUV} + m_{VW}) \cdot V_{COM} \text{ becomes: } V_{VW} - V_{COM} = -\frac{M_{SUV}}{m_{VW}} (V_{SUV} - V_{COM}) \quad (3.6a)$$

The V_{SUV} -vs- V_{VW} -plot of (3.6a) in Fig. 3.1 is a line of slope $-M_{SUV}/m_{VW}$ thru the COM -point (V_{COM}, V_{COM}) .

$$y - y_0 = m \cdot (x - x_0) \text{ where: } \begin{cases} (x, y) = (V_{SUV}, V_{VW}) \\ (x_0, y_0) = (V_{COM}, V_{COM}) \end{cases} \text{ and: } m = -\frac{M_{SUV}}{m_{VW}} \quad (3.6b)$$

Energy conservation relation (3.5a) is rearranged by placing KE and masses into denominator.

$$\frac{1}{2} M_{SUV} \cdot V_{SUV}^2 + \frac{1}{2} m_{VW} \cdot V_{VW}^2 = KE \text{ becomes: } \frac{V_{SUV}^2}{\left(\frac{2 \cdot KE}{M_{SUV}}\right)} + \frac{V_{VW}^2}{\left(\frac{2 \cdot KE}{m_{VW}}\right)} = 1 \quad (3.7a)$$

The V_{SUV} -vs- V_{VW} -plot (3.7a) in Fig. 3.1 is KE -ellipse (3.7b) of x -radius a and y -radius b to match (3.7a).

$$\frac{x^2}{a^2} + \frac{y^2}{b^2} = 1 \text{ where: } \begin{cases} (x, y) = (V_{SUV}, V_{VW}) \\ (a, b) = \left(\sqrt{\frac{2 \cdot KE}{M_{SUV}}}, \sqrt{\frac{2 \cdot KE}{m_{VW}}} \right) \end{cases} \quad (3.7b)$$

Fig. 3.1 also shows a smaller inelastic Ka -runch- IE -ellipse and a tiny KE -ellipse seen in the COM -frame.

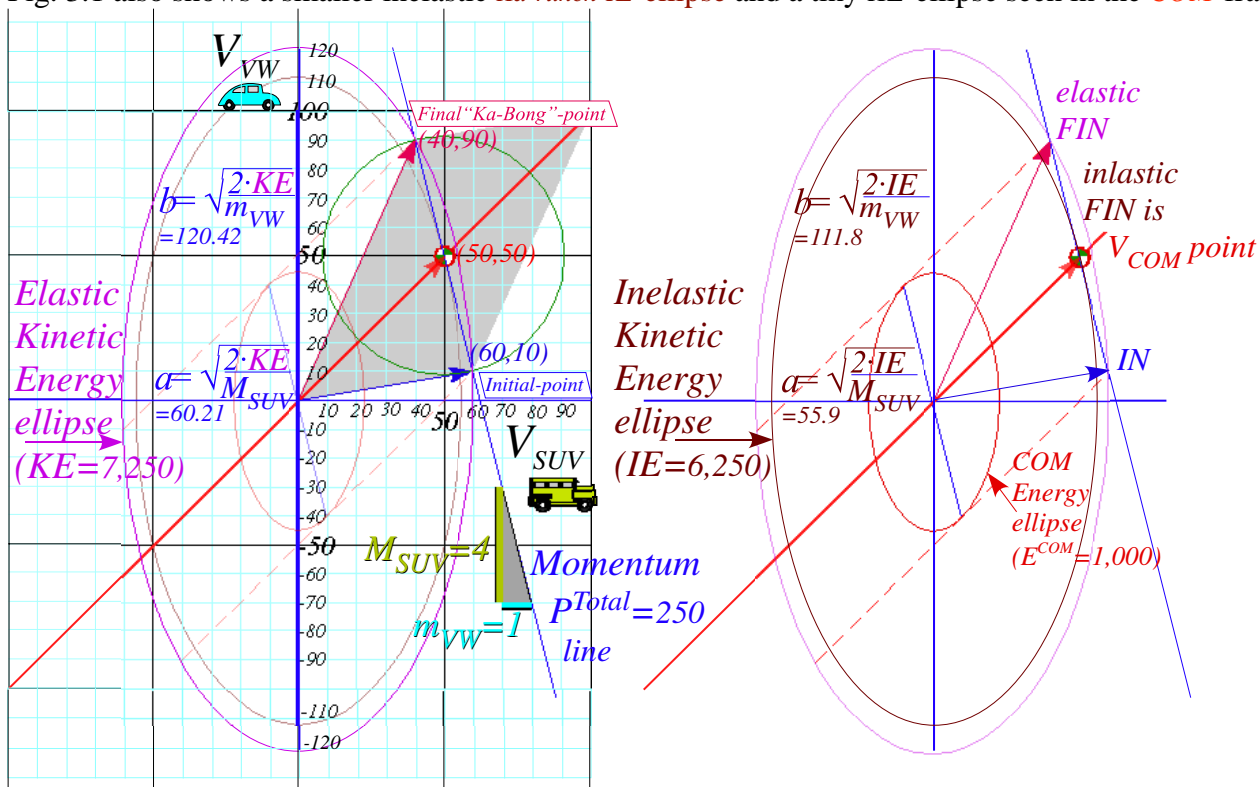


Fig. 3.1 Elastic KE -ellipse hits (P^{Total}) -line at IN and FIN pts. Inelastic IE -ellipse hits only at V_{COM} pt.

Elastic $KE (V_{SUV}=60, V_{SUV}=10)$, inelastic $IE(50, 50)$, and $E^{COM}(10, 40)$ in COM frame is worked out for Fig. 3.1.

$$\frac{1}{2}4\cdot60^2 + \frac{1}{2}1\cdot10^2 = 7,250 \quad \frac{1}{2}4\cdot50^2 + \frac{1}{2}1\cdot50^2 = 6,250 \quad \frac{1}{2}4\cdot10^2 + \frac{1}{2}1\cdot40^2 = 1,000 \quad (3.8)$$

The difference in energy between the two extreme types of collision, *Ka-Bong* and *Ka-runch*, is 1,000 units in the Earth frame and 1,000 units in the COM frame. But, only in the COM frame does the *Ka-runch!* take all the kinetic energy and leave both cars standing still. Galilean symmetry says “cost” of damage is the same in all frames. Cost of a generic *Ka-whump* is measured by what fraction of $E^{COM}=1,000$ is lost to inelastic crumpling.

A fine point of Fig. 3.1 geometry deserves notice. The tangent slope to the IE -ellipse at pt-(50, 50) on the 45° (slope-1)- COM -line is that of the momentum line, namely $-M_{SUV}/m_{VW}=-4$. Conversely, slope of dashed tangent lines to the $E^{COM}(10, 40)$ -ellipse on (slope= $-M_{SUV}/m_{VW}$)-line is that of the COM -line, namely slope-1. This beautiful duality is an important part of mechanics, both classical and quantum. Here it has *IN* and *FIN* points stay on a (slope= $-M_{SUV}/m_{VW}$)-line even as they coalesce to a tangent point of non-collision!

Head-on ($V_{SUV}^{IN} = 3, V_{VW}^{IN} = -4$) collisions are plotted in Fig. 3.2 below showing increasing inelasticity in parts (b) and (c). (These involve an $M_1=6$ ton SUV satisfying Bush gas-hog entitlement.) The final KE-ellipse shrinks from the initial elastic *Ka-Bong* ellipse to a smaller inelastic *Ka-whump* ellipse ($E^{whump}=23^{1/3}$ in Fig. 3.2b) and to the totally inelastic *Ka-runch*-ellipse ($IE=14$ in Fig. 3.2c).

The “in-between-ideal” or generic *Ka-whump* cases will each have two possible final F -points where the momentum line cuts the *Ka-whump* ellipse. The top F_{whump} point represents the partial rebound. Below is its symmetry point $F_{Pass-thru}$ that represents cars *passing through each other*. Fortunately, that’s not a usual highway event and certainly not a survivable one. But in the quantum world that’s business-as-usual.

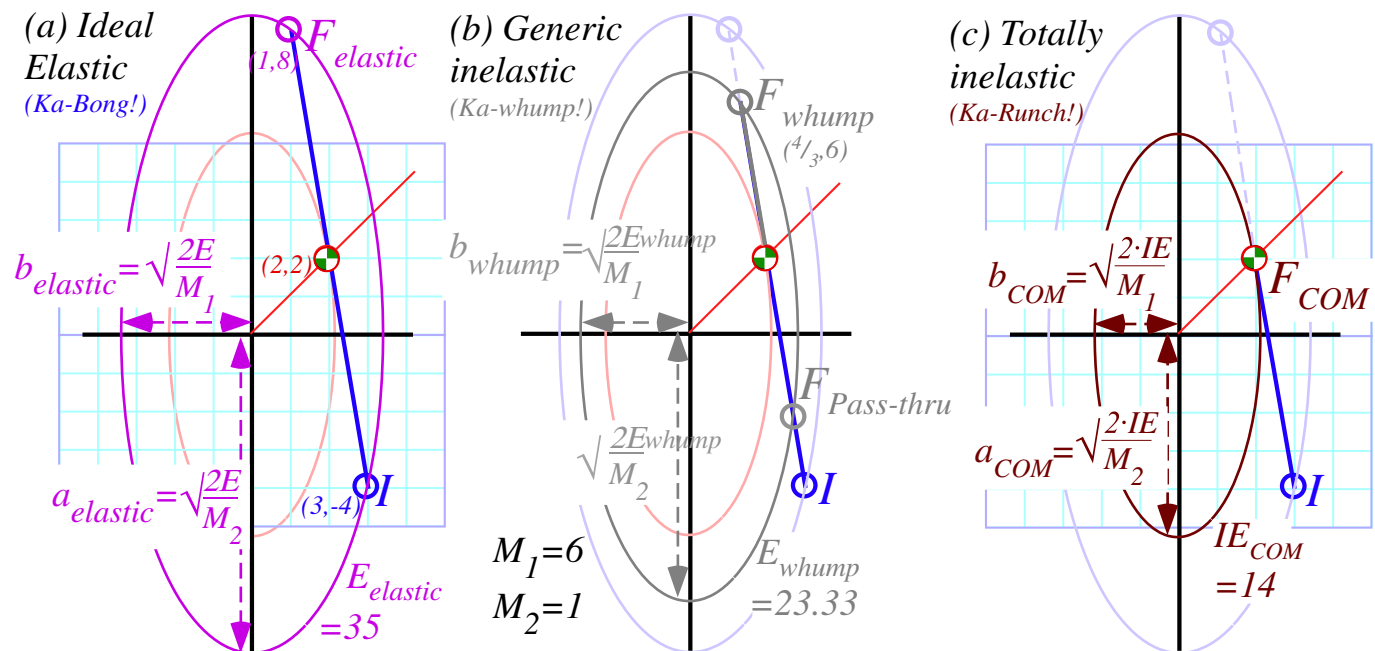


Fig. 3.2 ($V_1=3, V_2=-4$) collisions. (a) Elastic ($E^{loss}=0$). (a) Generic ($E^{loss}=11^{2/3}$). (a) Inelastic ($E^{loss}=21=E^{COM}$).

Momentum vs. energy (Bang for the buck!)

What are *momentum P* and *energy E*, really? A flippant answer is *Bang!* and *\$Buck\$*. We pay (a lot) for the latter in order to get the former. A less flippant answer based on space-time relativity and quantum wave theory must wait until Unit 3. But, we can discuss relations involving $P=M \cdot V$ and $E=M \cdot V^2/2$ in the meantime.

Also, there's the notion of *Force*. That's the *rate* of being banged in *bangs per second*, if you will. And, there's *Power*, the *rate* of being bucked in *\$bucks\$ per second*, if you will. (Or, maybe you won't.)

What we're trying to say is that *force F* is the slope $F = \frac{\Delta P}{\Delta t}$ on a graph of *momentum P* vs. time *t*.

Also, we're trying to say that *power Π* is the slope $\Pi = \frac{\Delta E}{\Delta t}$ on a graph of *energy E* vs. time *t*.

And, do not ever forget that *velocity V* is the slope $V = \frac{\Delta x}{\Delta t}$ on a graph of *position x* vs. time *t*.

These and other relations (in calculus form) are collected below in preparation for lots of discussion later on.

Quick review of kinetic relations and formulas

The suffix *kinetic* refers to energy connected directly to velocity of motion (“kinos” means *moving*). Kinetic energy *KE* is distinct from *potential energy (PE)* is “stored” energy) or entropic energy (*entropy* is chaotic or “trashed” energy like *heat*) that will be introduced later.

We now give a quick algebraic run-down of energy-related formulas to be introduced with more detail and geometry soon. Readers with calculus or physics knowledge might use this to review and connect our geometrical development to more conventional ones. Novice readers: Patience. Logical relief is coming.

Relations of energy W and space x

Energy or *work* may be defined by a delta-*work* product $\Delta W = F \cdot \Delta x$ of force *F* and *distance-Δx*-pushed. More precisely, *W* is an integral $\int_0^{\Delta x} F \cdot dx$, the area of a *F* vs. *x* work-plot. *Power*, a time rate $\Pi = \frac{\Delta W}{\Delta t}$ of energy production, is the product $\Pi = F \cdot V$ of force and velocity $V = \frac{\Delta x}{\Delta t} = \frac{dx}{dt}$. So, $\Delta W = \Pi \cdot \Delta t$ or $W = \int_0^{\Delta t} \Pi \cdot dt = \int_0^{\Delta t} F \cdot V \cdot dt = \int F \cdot dx$.

Relations of momentum P and time t

Momentum may be defined by a delta-*momentum* product $\Delta P = F \cdot \Delta t$ of force *F* and *time interval Δt*. More precisely, *P* is an integral $\int_0^{\Delta t} F \cdot dt$, the area of a *F* vs. *t* plot. *Force*, a time rate $F = \frac{\Delta P}{\Delta t} = \frac{dP}{dt}$ of momentum production, is a product $F = M \cdot a$ of mass and *acceleration* $a = \frac{\Delta V}{\Delta t}$. ($F = M \cdot a$ is called *Newton's "2nd Law."*)

With $F = \frac{dP}{dt}$, energy integral $W = \int_0^{\Delta t} \Pi \cdot dt = \int_0^{\Delta t} F \cdot V \cdot dt$ is $W = \int_0^{\Delta t} F \cdot V \cdot dt = \int_0^{\Delta t} \frac{dP}{dt} \cdot V \cdot dt = \int V \cdot dP$, the area under a *V* vs. *P* plot where $P = M \cdot V$ is momentum. For a single mass *M* this area is kinetic energy: $\frac{1}{2} M \cdot V^2$.

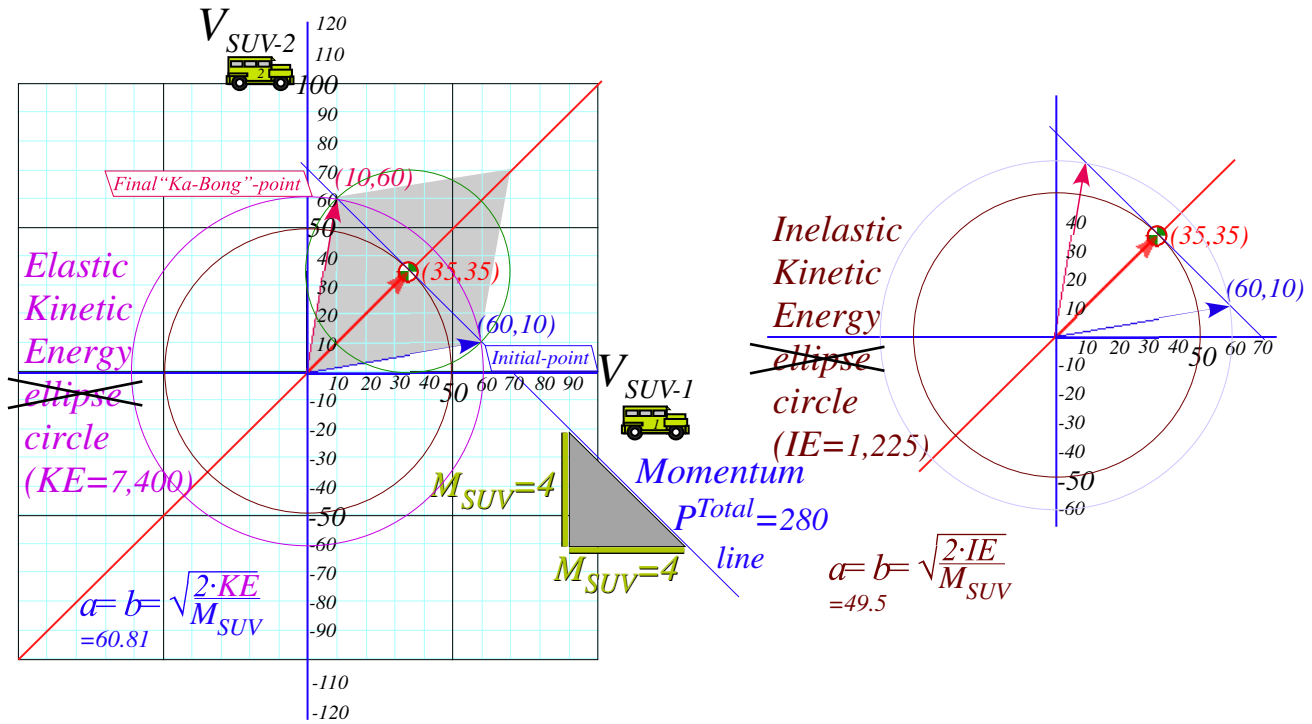
Table of kinetic relations

	<i>Position or space</i>	<i>Velocity or time-rate</i>	<i>Acceleration or time-rate</i>	
	$x = \int V \cdot dt$	<i>of position</i> : $V = \frac{dx}{dt}$	<i>of velocity</i> : $a = \frac{dV}{dt}$	(3.9)
<i>Work or Energy</i>	<i>Power or time-rate</i>	<i>Impulse or momentum</i>	<i>Force or time-rate</i>	
$E = \int \Pi \cdot dt = \int F \cdot dx$	<i>of Energy</i> : $\Pi = \frac{dE}{dt}$	$P = \int F \cdot dt \approx M \cdot V$	<i>of momentum</i> : $F = \frac{dP}{dt} = M \cdot a$	
$= \int F \cdot V \cdot dt$				
$= \int V \cdot dP = \frac{1}{2} M \cdot V^2$	(3.10a)	(3.10b)	(3.10c)	

Exercise

Don't look at figure below! Try the exercise yourself first.

Plot a $(V_{SUV-1}, V_{SUV-2}) = (60, 10)$ collision like Fig. 3.1 but with an identical $M=4$ SUV replacing the VW.

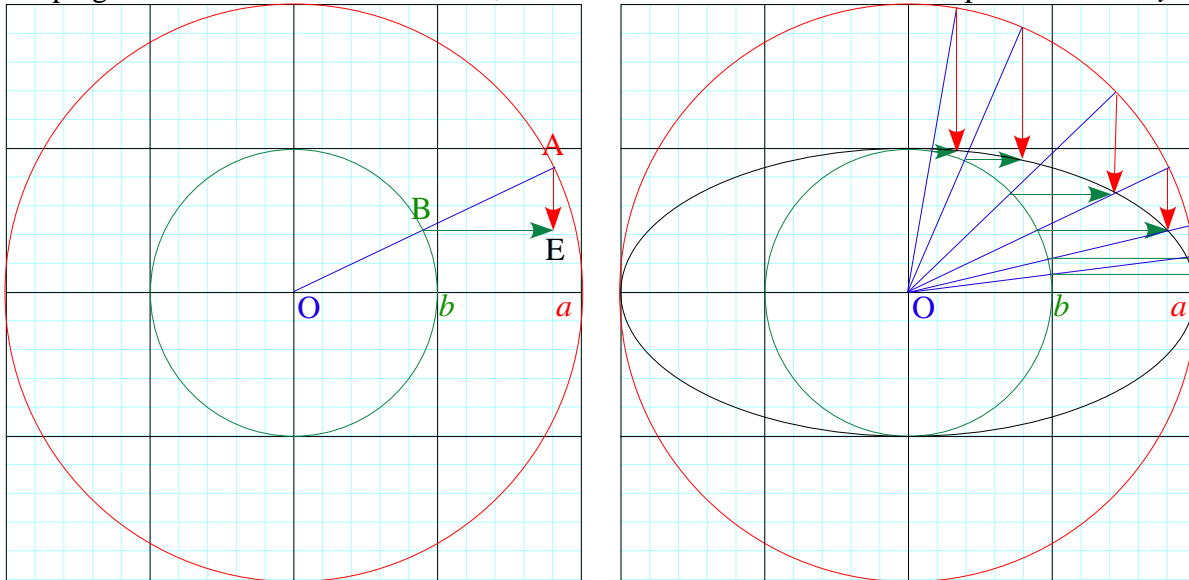


Exercise Fig. 3.3 Equal mass $M=4$ SUV collision geometry for elastic and inelastic cases.

Quick construction of Energy ellipses

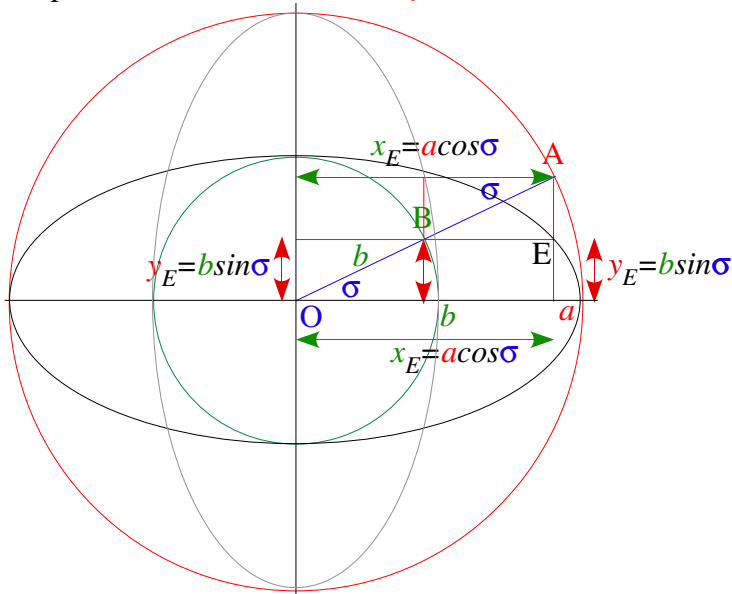
Graph paper facilitates construction of energy ellipses given the two radii a and b in (3.7). The first step is to draw concentric circles of radius a and b . Then any radial line OB “points” to a point E on the ellipse. Ellipse point E lies at the intersection of a vertical line AE thru radial intersection A with circle a and a horizontal line BE thru radial intersection B with circle b .

Graph grid “finds” E for a radius OB , no need to draw AE or BE . You can pick x and find y or *vice-versa*.



Exercise Fig. 3.4 Ellipse construction

Ellipse coordinates $(x_E = a \cdot \cos \sigma, y_E = b \cdot \sin \sigma)$ are rescaled base and altitude $(x_r = r \cdot \cos \sigma, y_r = r \cdot \sin \sigma)$ of Fig. 1.4.



Exercise Fig. 3.5 Analytic ellipse geometry

Verify that the values $(x = a \cdot \cos \sigma, y = b \cdot \sin \sigma)$ satisfy an ellipse equation (3.7b).

A dual or complimentary (gray) ellipse results if complement angle $\sigma_c = \pi/2 - \sigma$ is used so x and y values switch.

Chapter 4. Dynamics and geometry of successive collisions

Mechanics gets difficult for many collisions, dimensions, or masses. A single one-dimensional two-mass (1D-2-body) collision occupies Ch. 2-3. Now we do more dangerous things such as an X2-super bouncer from *Project Ball*, our 1969 class project. (*Am. J. Phys.* **39**, 656 (1971)) See the product liability disclaimer in Fig. 4.1.

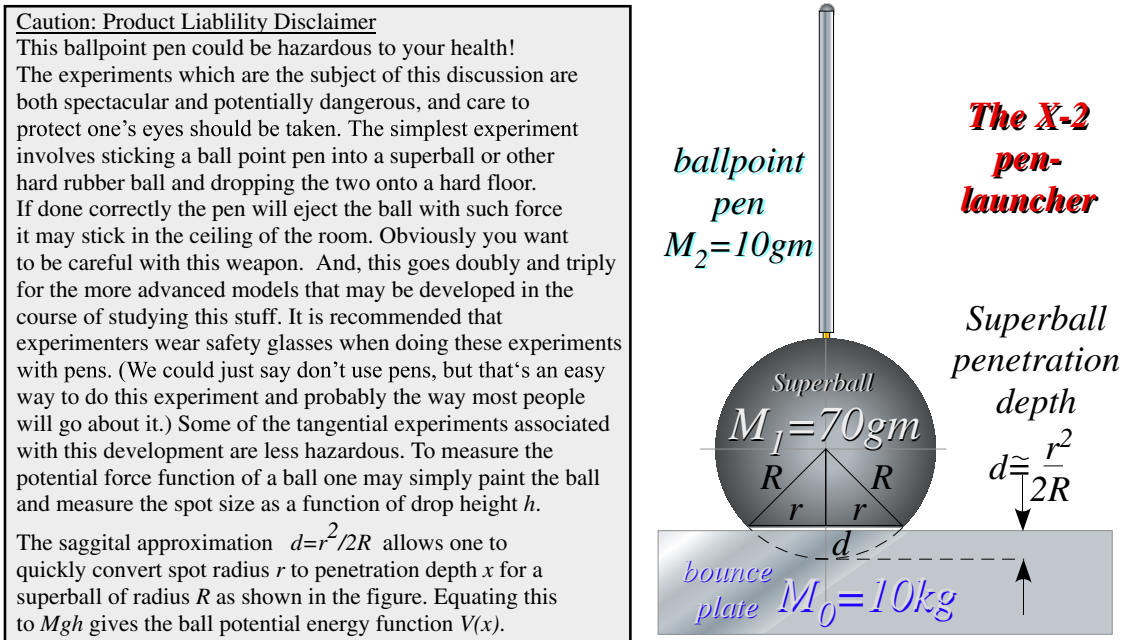


Fig. 4.1 The X2-pen launcher with product liability disclaimer.

At first, the X2 looks like a 1D-2-body device. A *superball*(TMWhammo Corp.) of mass $M_1 = 70gm$ launches a ballpoint pen of mass $M_2 = 10gm$. But, it has a 3rd body, bounce plate mass- $M_0 = 10kg$ shown by a rectangle in Fig. 4.1. Actually the third body most responsible for this experiment is old Mother Earth of mass $M_{\oplus} = 6 \cdot 10^{24} kg$. (Earth mass M_{\oplus} and solar mass $M_{\odot} = 2 \cdot 10^{30} kg$ are good-to-2-figure numbers to remember. More precisely: $M_{\oplus} = 5.9742 \cdot 10^{24} kg$ and $M_{\odot} = 1.9891 \cdot 10^{30} kg$.)

Collisions of very large or very small masses suggest thorny questions (Like, “What IS mass?”) and how do we deal with it. As a mass ratio M_1/M_2 approaches zero or infinity the slope of the P -conservation line in (V_1, V_2) -space (Recall Fig. 3.2.) approaches infinity or zero, respectively, as drawn in Fig. 4.2(a-b).

Geometric construction in Fig. 4.2a of final velocity for an elastic collision is a vertical reflection thru the **COM** point ($V_1=V_2$) on the P -line if $M_1 \gg M_2$ or else a horizontal reflection in Fig. 4.2b if $M_1 \ll M_2$. Inelastic final points approach the **COM** point more closely if inelasticity is significant. (Recall Fig. 3.2.)

You should understand how a relatively large mass may give huge momentum to a smaller one but transfer only tiny amounts of energy. Each P -line in Fig. 4.2 is part of a KE-ellipse. In the **COM** frame (where the **COM** point is at origin) the P -line sits on top of an entire E -ellipse as the ratio M_1/M_2 approaches (a) infinity or (b) zero. I visualize **COM** P -lines as ultra-thin ellipses between I_0 and F_0 and other P -lines in Fig. 4.2 as segments of a KE-ellipse that has (a) a huge V_2 -axis $\sqrt{2E / M_2}$ or (b) a huge V_1 -axis $\sqrt{2E / M_1}$.

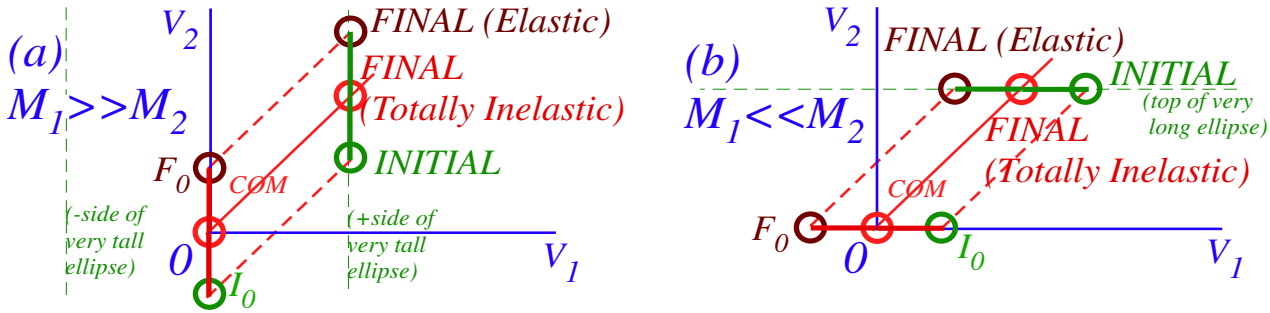


Fig. 4.2 Extreme mass-ratio collisions (a) M_1/M_2 approaches infinity. (b) M_1/M_2 approaches zero.

Fig. 4.2a reflects our common experience of a bouncy ball of mass M_2 hitting the Earth of mass M_\oplus with velocity $-V_0$ (point I_0) and being reflected with velocity $+V_0$ (point F_0). While standing in the Earth frame, one is very nearly in the COM frame, too. Earth’s COM velocity is a tiny fraction M_2 / M_\oplus of the apparent ball velocity V_0 . For super-balls of mass $M_2=60gm$, the fraction M_2 / M_\oplus is $0.06/(6 \cdot 10^{24})=10^{-26}$.

Bounce momentum absorbed by Earth is $2 M_2 V_0$ (or $M_2 V_0$ if the ball goes “*Ka-runch!*”) but Earth absorbs at most a tiny KE of $\frac{1}{2} M_\oplus (V_0 M_2 / M_\oplus)^2$, that is, a fraction 10^{-26} of ball KE: $\frac{1}{2} M_2 (V_0)^2$. Moreover, for elastic collisions, Mother Earth returns *all* the KE to M_2 but absorbs *double* momentum $P=2 M_2 V_0$.

However, common experience does not prepare us for X2 easily rebounding M_2 with more than *twice* its drop velocity in Fig. 4.3. (That means M_2 rises to more than *four* times its drop height!)

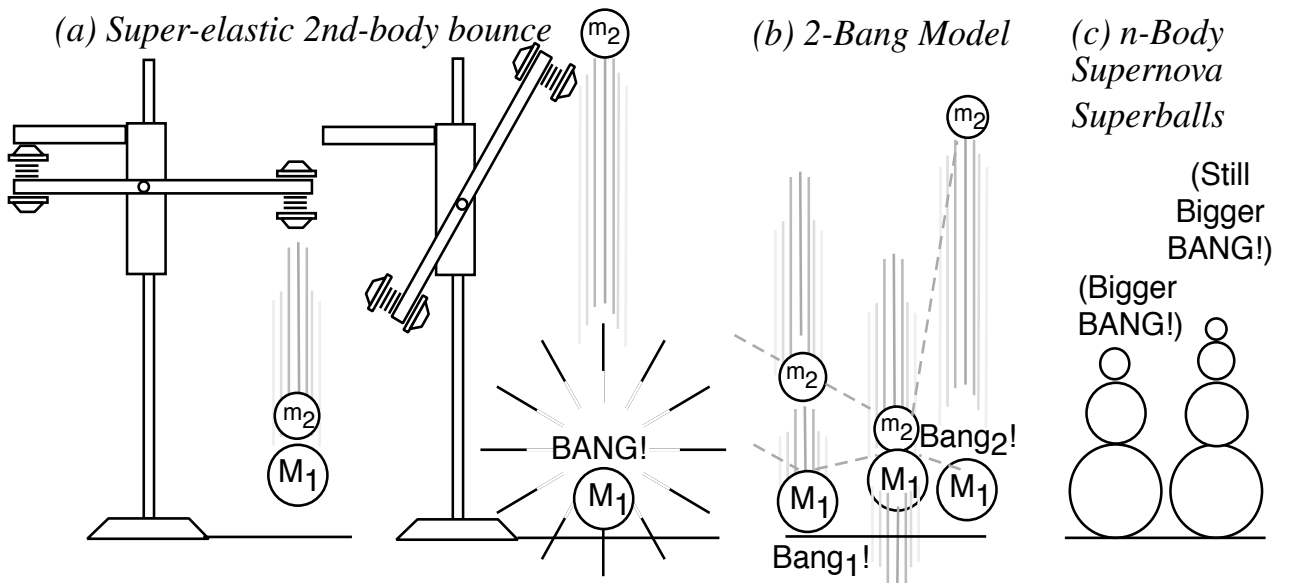


Fig. 4.3 n-Body collision experiments. (a) X-2 drop. (b) Independent collision model. (c) Ball towers.

Independent collision models (ICM)

To compute final velocities of M_1 and M_2 it helps to idealize the collision of three bodies M_1 , M_2 , and M_\oplus as a sequence of two separate 2-body collisions that are completely determined by P and KE conservation. First

M_1 bounces off Earth M_\oplus . Only then does M_1 knock M_2 to a faster speed as in Fig. 4.3b. The first collision is labeled *Bang-1*₍₀₁₎ in Fig. 4.4a followed by *Bang-2*₍₁₂₎ in Fig. 4.4b. The first *Bang-1*₍₀₁₎ between Earth M_\oplus and M_1 has a horizontal line like the I_0F_0 line in Fig. 4.2b. The second *Bang-2*₍₁₂₎ between mass M_1 and M_2 has a line of slope $-M_1/M_2 = -7$ for a $M_1 = 70\text{gm}$ and $M_2 = 10\text{gm}$ (that of a superball and pen, respectively). The *Bang-2*₍₁₂₎ line is like the IF line in Fig. 3.1 or Fig. 3.2.

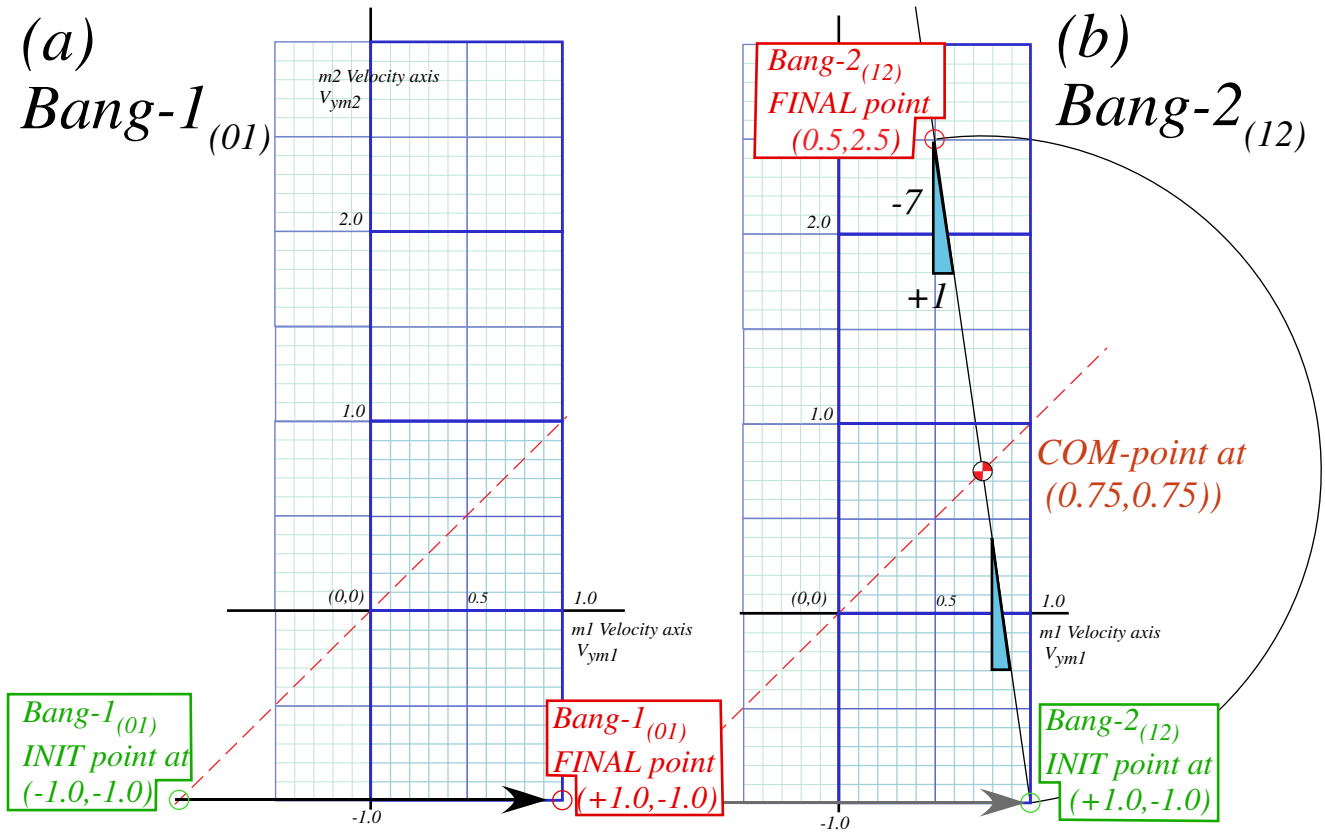


Fig. 4.4 (V_1 - V_2)-plot of 2-Bang collision. (a) M_1 bounces off floor. (b) M_1 hits M_2 head-on.

This approximation is called an *independent collision model (ICM)* and is one secret to analyzing such 1D-3-body bang-up that otherwise has one too many unknown velocities to be found by just two equations $\Delta P=0$ and $\Delta KE=0$ alone. ICM is exactly true if we initially separate M_1 and M_2 so three M_1 , M_2 , and M_\oplus never collectively bargain for available momentum and energy. ICM also applies to n -ball towers in Fig. 4.3c. They give very high-energy ejections and serve as classical models for supernovae. (N -body bangs are in Ch.8.)

Velocity geometry suggests a family of X2 solutions as shown in Fig. 4.5 for a range of mass ratio M_1/M_2 . This is an advantage of geometric solutions. Just a few points in Fig. 4.5a show all elastic (V_1 - V_2) points lie on the 45°-line CPL . Extreme or optimal cases are located in Fig. 4.5b.

Extreme and optimal cases

First, the upper limit for elastic final velocity is $V_2=3 \cdot V_0$ at pt- I for infinite mass ratio $M_1/M_2 \rightarrow \infty$. If no energy is lost, a particle of dust on a superball could be ejected three times the speed that the ball hits the

floor. (And, it could go *nine* ($9=3^2$) times the drop height. However, the elastic ICM model is not so good for tiny M_2 due to molecular and static charge. So bouncing balls do not usually embed dust in ceilings!)

Second, an optimal performance case is shown by pt- M where the collision achieves a 100% transfer of energy to projectile M_2 . The M -point is the intersection of the CPL line with the V_2 -axis on which the M_1 -ball velocity is zero. ($V_1=0$) There mass ratio is $M_1/M_2=3.0$, the slope of the M -line.

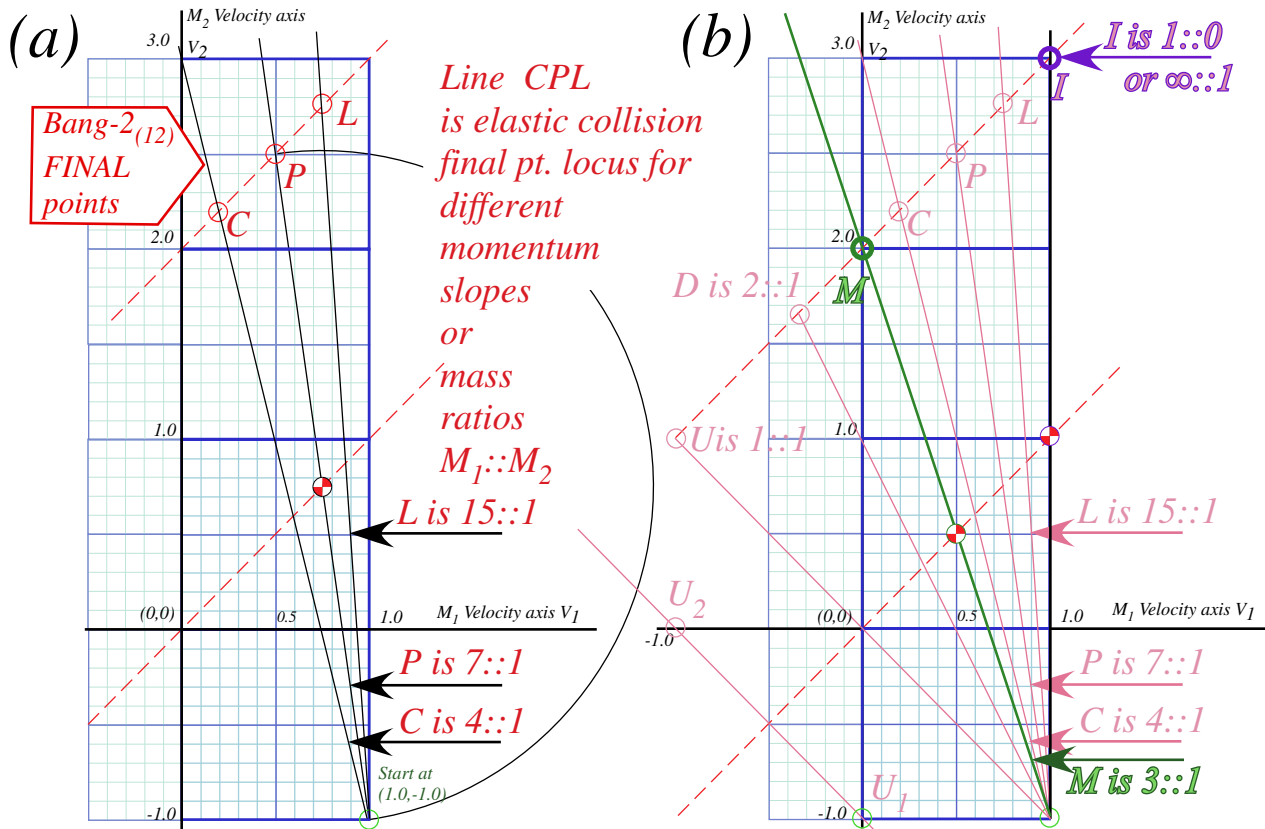


Fig. 4.5 X2-Final (V_1, V_2) (a) Final point locus. (b) Infinite ratio pt. I and maximum transfer pt. M.

Another singular point U is for unit ratio $M_1/M_2=1$, a familiar ratio for players of billiards or pool. U undergoes inversion of velocities $(+1, -1) \rightarrow (-1, +1)$. (Its COM point lies at origin.) If the U -line is boosted by (-1) to $(0, -2) \rightarrow (-2, 0)$ it is like a straight elastic pool shot. A 100% of KE transfers from a moving ball to an equal sized ball that was stationary. The same process at half that speed is $(0, -1) \rightarrow (-1, 0)$ shown by the Galileo-shifted line $U_1 \rightarrow U_2$ in the lower left hand side of Fig. 4.5b.

Points D between U and M have ball M_1 knocked to negative velocity by the down-coming M_2 . Then M_1 hits the floor (Earth) at velocity $-v$ to rebound at $+v$. For unit ratio case U , M_1 and M_2 rebound quite like a rigid body. Below U , ball M_1 rebounds at a speed faster than M_2 to hit M_2 again. In cases of low mass ratio, ($M_1/M_2 \ll 1$) mass M_1 must hit M_2 many times to turn it around. We will study this effect shortly.

Integrating velocity plots to find position

It is important to see how velocity values of Fig. 4.4b are turned into space-time position plot lines. Consider the first collision (*Bang-1₍₁₀₎*) in Fig. 4.6a and corresponding space-time paths in Fig. 4.6b.

Initial velocity $V_{y1}(0)=-1.0$ gives a slope (*distance*)/(*time*) of an M_1 path but doesn't tell *where* is the path or particle. The same for velocity $V_{y2}(0)=-1$ of M_2 in Fig. 4.6a. The paths need location, location,...

Initial position values such as $(y_1(0)=1, y_2(0)=3)$ locate the paths as shown in Fig. 4.6b. Each path keeps its slope until a collision (*Bang-1*₍₁₀₎) between M_1 and the floor occurs at $y_1(t=1)$ where its path and the floor intersect. Then, according to Fig. 4.6a, M_1 bounces its slope from $V_{y1}=-1$ up to $V_{y1}=+1$. Meanwhile, the upper path (M_2) maintains its down slope of $V_{y2}=-1$ until it intersects the rising path of M_1 .

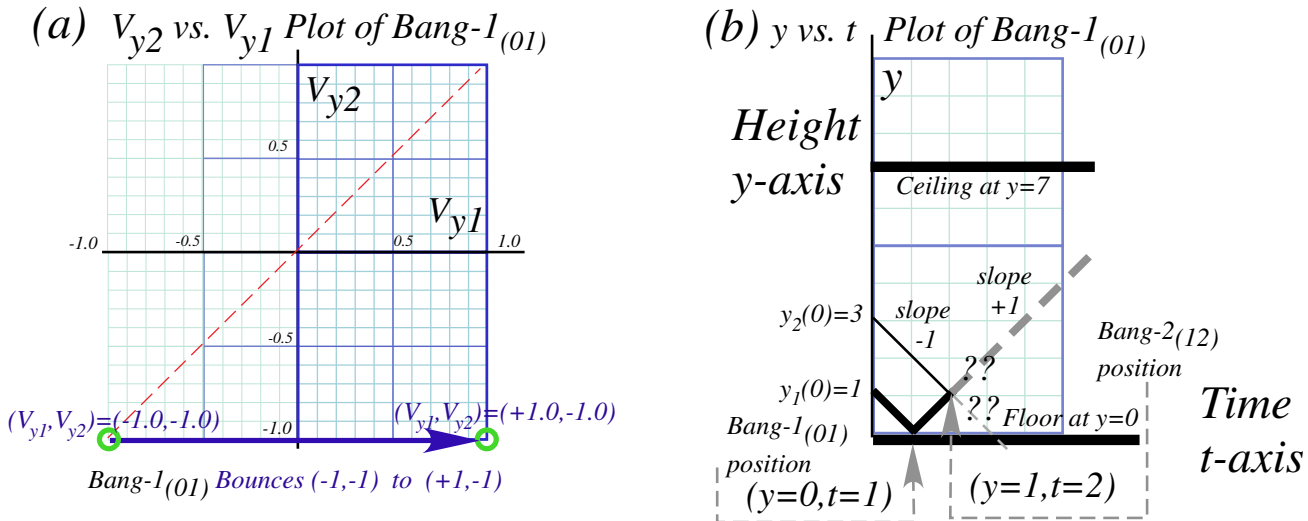


Fig. 4.6 Plots of 1st collision (*Bang-1*₍₁₀₎). (a) Velocity-velocity plot. (b) Space-time plot.

At time ($t=2$) there is an intersection of paths and the 2nd collision (*Bang-2*₍₁₂₎) between M_1 and M_2 at space-time point $(y_1(2)=1, y_2(2)=3)$. This gives $V_{y1}=0.5$ and $V_{y2}=2.5$ in Fig. 4.4b or in Fig. 4.7a-b below. Then to keep M_2 from flying away we install an elastic ceiling at $y=7$.

The game becomes more interesting as *Bang-3*₍₂₀₎ between the ceiling (part of Earth M_0) is shown in Fig. 4.7b by a vertical arrow (like an *IF* line in Fig. 4.2a) reflecting M_2 to speed $V_{y2}=-2.5$. Then M_2 has *Bang-4*₍₁₂₎ between M_1 and itself that sends it back to the ceiling at a blistering speed of $V_{y2}=+2.7$ as M_1 returns more slowly toward the floor with velocity $V_{y1}=-0.5$.

The high speed of M_2 lets it go to the ceiling for *Bang-5*₍₂₀₎ and return to knock M_1 down once more (*Bang-6*₍₁₂₎) before M_1 hits the floor at $V_{y1}=-0.9$. (*Bang-7*₍₁₀₎) Then M_2 having lost speed to $V_{y2}=+1.5$ hits the ceiling (*Bang-8*₍₀₂₎) and returns for *Bang-9*₍₁₂₎ with M_1 rising at $V_{y1}=+0.9$.

Masses are treated as point-masses that travel along straight lines between collisions in space-time plots. This is an ideal gravity-free ICM approximation with only straight lines in *VV*-plots. So we may derive motion without having to integrate the kinetic equations at the end of Ch. 3.

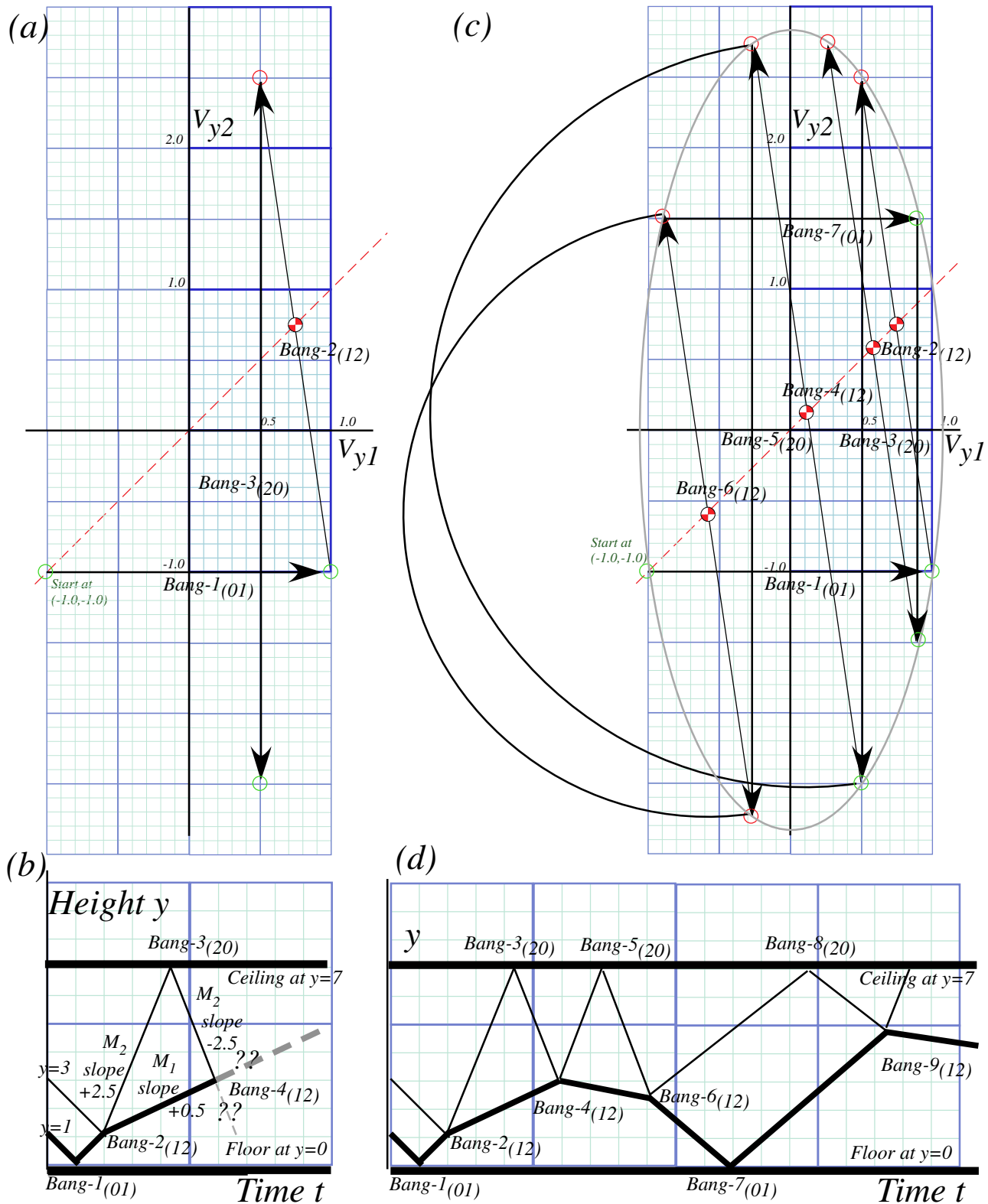


Fig. 4.7 Collision sequence. (a-b) Up to Bang-4(12), (c-d) Up to Bang-9(12).

For comparison, a force-law simulation using *BounceIt* of the bang sequence of Fig. 4.7 is shown in Fig. 4.8. It assumes balls instead of ideal point particles yet compares quite well. (So far.)

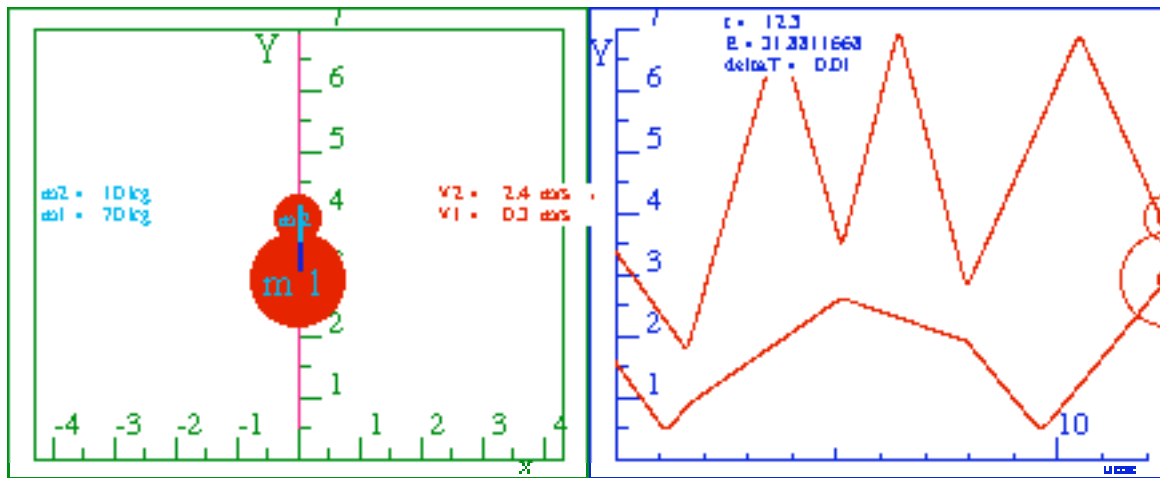


Fig. 4.8 BounceIt simulation up to Bang-9₍₁₂₎ in space-time plot.

Bang sequences can be very sensitive to ceiling height and initial ball values. In fact, we see examples of extreme *sensitivity to initial values* and parameters. Often this leads to *classical chaos* in which every slip in accuracy may grow exponentially so that classical mechanics loses predictability.

Running BounceIt simulation of the 1:7 system for 69 steps fills up the V-V screen with dots that forms an oval as shown in Fig. 4.9. Among other things, it shows *conservation of energy* in the form of the KE ellipse (3.7). Bang P-lines (IF-lines) in Fig. 4.7b must terminate on a KE-ellipse of energy as shown.

$$KE(\text{unit}V_1, V_2) = \frac{1}{2} M_1 V_1^2 + \frac{1}{2} M_2 V_2^2 = \frac{1}{2} \cdot 8 \quad (\text{for } M_1=7 \text{ and } M_2=1)$$

The major and minor radii are $a = \sqrt{2 \cdot KE / M_z} = 2\sqrt{2} = 2.828$ and $b = \sqrt{2 \cdot KE / M_y} = 2\sqrt{2/7} = 1.069$ and this checks with Fig. 4.9. The IF-line geometry provides a strange way to construct an ellipse. Later this geometry shows some deep relations between velocity, momentum and energy.

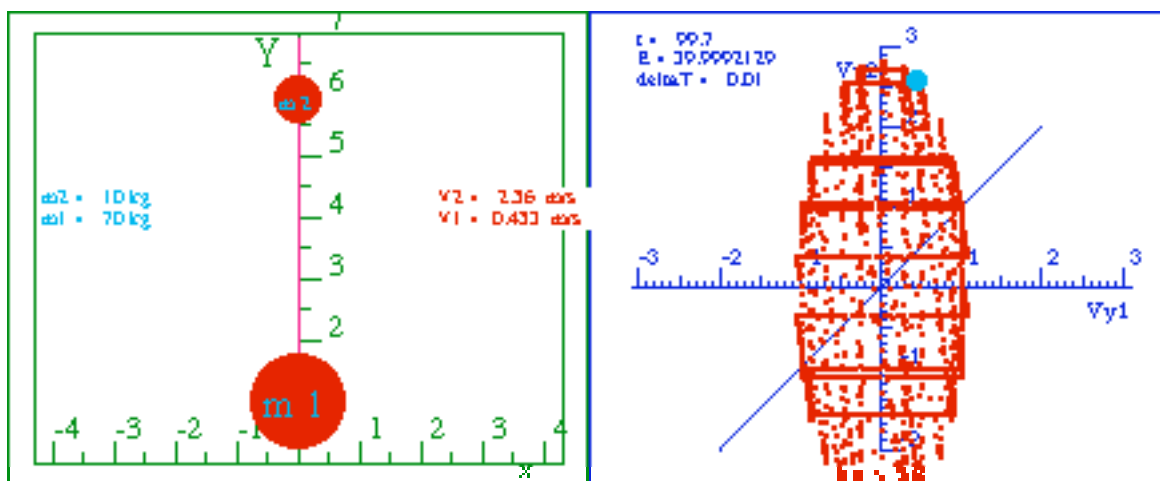


Fig. 4.9 BounceIt simulation up to Bang-69₍₁₂₎ in velocity-velocity plot.

Vector notation and space-space plots

Balance equation (3.4) concisely sums up preceding constructions or plots of elastic collisions.

$$\begin{aligned} (V_1^{FIN} + V_1^{IN}) / 2 = V^{COM} \\ (V_2^{FIN} + V_2^{IN}) / 2 = V^{COM} \end{aligned} \quad \text{or:} \quad \begin{aligned} V_1^{FIN} = 2V^{COM} - V_1^{IN} \\ V_2^{FIN} = 2V^{COM} - V_2^{IN} \end{aligned} \quad (3.4)_{repeated}$$

More concise notation uses *vector* equations or arrays.

$$\begin{aligned} v_1^{FIN} = 2V^{COM} - v_1^{IN} \\ v_2^{FIN} = 2V^{COM} - v_2^{IN} \end{aligned} \quad \text{is written:} \quad \begin{pmatrix} v_1^{FIN} \\ v_2^{FIN} \end{pmatrix} = \begin{pmatrix} 2V^{COM} - v_1^{IN} \\ 2V^{COM} - v_2^{IN} \end{pmatrix} = 2 \begin{pmatrix} V^{COM} \\ V^{COM} \end{pmatrix} - \begin{pmatrix} v_1^{IN} \\ v_2^{IN} \end{pmatrix} \quad (4.1)$$

It saves writing two (=)'s and two (-)'s. Also, each *column vector* may be labeled by a “fat” letter.

$$\mathbf{v}^{FIN} = \begin{pmatrix} v_1^{FIN} \\ v_2^{FIN} \end{pmatrix} = \vec{v}^{FIN}, \quad \mathbf{V}^{COM} = \begin{pmatrix} V^{COM} \\ V^{COM} \end{pmatrix} = \vec{V}^{COM}, \quad \mathbf{v}^{IN} = \begin{pmatrix} v_1^{IN} \\ v_2^{IN} \end{pmatrix} = \vec{v}^{IN}. \quad (4.2)$$

Each fat-letter stands for an arrow vector in Fig. 4.10. The *Gibbs vector form* of equation (1.1.3) or (4.1) uses fat- \mathbf{v} or over-arrow- \vec{v} .

$$\mathbf{v}^{FIN} = 2 \mathbf{V}^{COM} - \mathbf{v}^{IN}, \quad \text{or:} \quad \mathbf{V}^{COM} = \frac{\mathbf{v}^{IN} + \mathbf{v}^{FIN}}{2}. \quad (4.3)$$

Algebra *and* geometry are helped by fat- \mathbf{v} (vector) notation. Fig. 4.10 shows how vector \mathbf{V}^{COM} is half the vector-sum $\mathbf{v}^{IN} + \mathbf{v}^{FIN}$ of *IN* velocity \mathbf{v}^{IN} and *FIN* velocity \mathbf{v}^{FIN} . (Since this is an elastic collision, the labels *IN* and *FIN* may be switched.) \mathbf{V}^{COM} lies on a $(\mathbf{v}^{IN} + \mathbf{v}^{FIN})$ -parallelogram diagonal. The opposite diagonal (dashed M_1/M_2 line) bisects $(\mathbf{v}^{IN} + \mathbf{v}^{FIN})$ to give $\mathbf{V}^{COM} = (\mathbf{v}^{IN} + \mathbf{v}^{FIN})/2$.

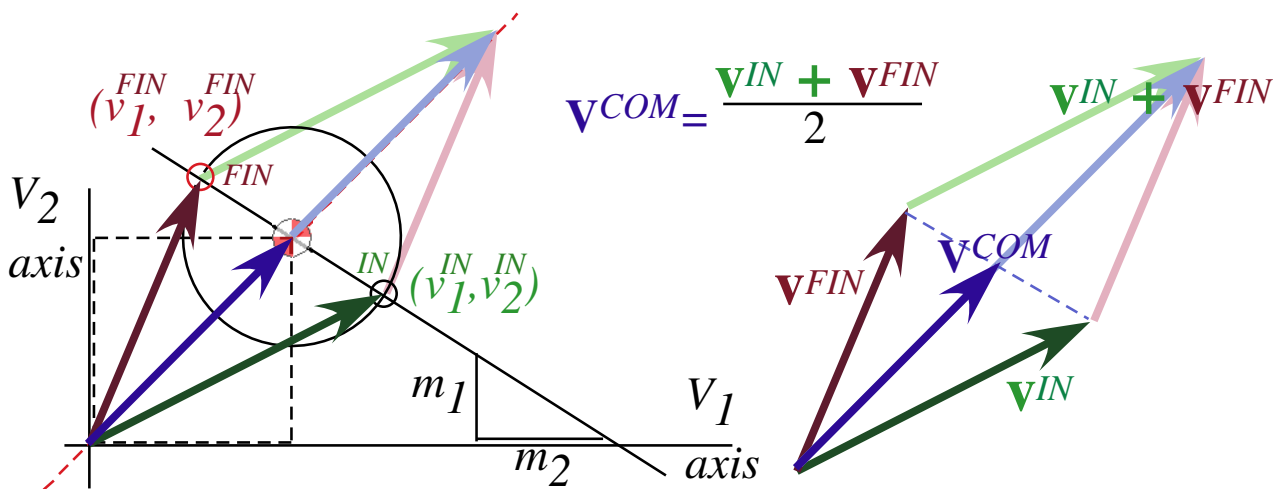


Fig. 4.10 Vector collision velocity diagrams (After equation (4.1).)

Note the distinction between vectors $\mathbf{v}=(v_1, v_2)$ above for *two* particles each in *one*-dimension and more common vectors $\mathbf{v}=(v_x, v_y)$ (or $\mathbf{v}=(v_x, v_y, v_z)$) for *one* particle in *two*-dimensions (or three dimensions).

Fig. 4.11 shows how vectors help analyze the results of *Bang-1*₍₀₁₎ and *Bang-2*₍₁₂₎ collisions done before in Fig. 4.7. What's new is a *space-space* y_2 vs. y_1 or *position-vector* \mathbf{y} -plot whose paths are called *spatial-trajectories* or just plain *trajectories*. They are made like the space-time paths in Fig. 4.7 by transferring velocity slopes over to the space plot, but vectors in Fig. 4.11 simplify this geometry.

As the construction steps in Fig. 4.11 show, one easily transfers each velocity vector $\mathbf{v}(\mathbf{n})$ from the V_2 vs. V_1 plot so it points away from start point $\mathbf{y}(\mathbf{n})$ in the y_2 vs. y_1 plot. *Step-0* does this by drawing initial velocity $\mathbf{v}(\mathbf{0})=(-1,-1)$ to point away from our given initial position $\mathbf{y}(\mathbf{0})=(1,3)$. Then you extend that \mathbf{v} -vector until it hits the floor (as $\mathbf{v}(\mathbf{0})$ does at $\mathbf{y}(\mathbf{1})=(0,2)$), or hits the collision line ($y_2=y_1$) (as $\mathbf{v}(\mathbf{1})$ does at $\mathbf{y}(\mathbf{2})=(1,1)$), or hits the ceiling (as $\mathbf{v}(\mathbf{2})$ does at $\mathbf{y}(\mathbf{3})=(2,2,7)$). Each such "hit" is a Bang, *Bang-1*₍₀₁₎ at $\mathbf{y}(\mathbf{1})$, *Bang-2*₍₁₂₎ at $\mathbf{y}(\mathbf{2})$, or *Bang-3*₍₂₀₎ at $\mathbf{y}(\mathbf{3})$. Then from each *Bang-n* position point $\mathbf{y}(\mathbf{n})$ is drawn the next $\mathbf{v}(\mathbf{n})$ -velocity vector from the V_2 vs. V_1 plots. This process continues in Fig. 4.12.

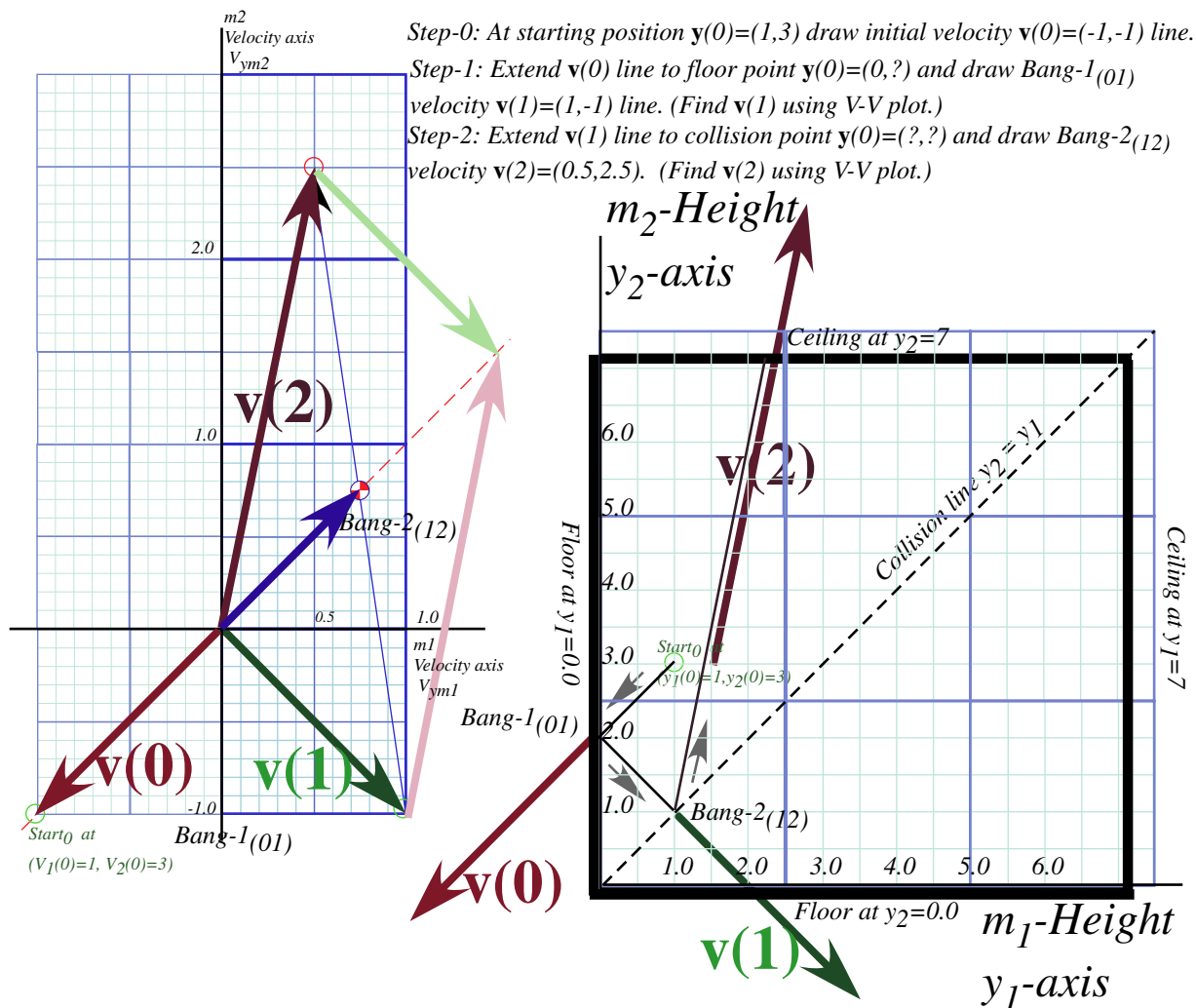


Fig. 4.11 Vector collision velocity diagrams with Velocity-Velocity space and space-space.

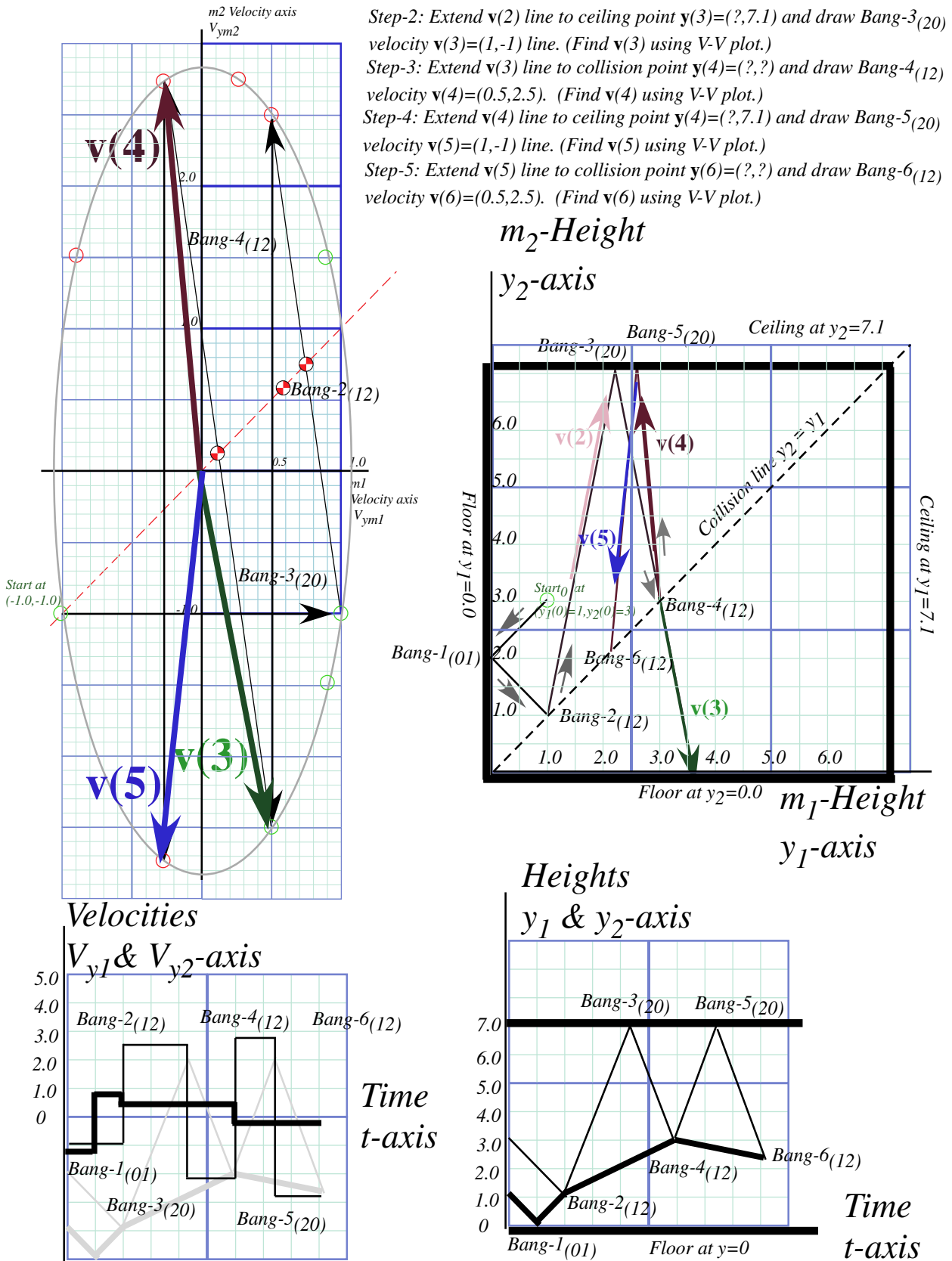


Fig. 4.12 Vector collision diagrams continued with velocity-time and space-time plots added.

Some remarks about space-space plots are in order. First, position $\mathbf{y}(\mathbf{n})$ -vectors of the *Bang-n* points are not drawn in Fig. 4.12 to avoid clutter. Also, ideal (small) masses called *point masses* are assumed.

Help! I'm trapped in a triangle.

The trajectory in these figures is confined to the triangle above the 45° -collision line. Our model keeps m_2 above m_1 . The right-hand “ceiling” in the figures never is hit because m_1 always is knocked down by m_2 before it touches the ceiling, and m_2 never sees the floor because m_1 is in the way. (Quantum theory doesn't encourage this feature. Quantum objects pass easily through each other!)

Two balls in 1D vs. one ball in 2D

For ball-Earth collisions involving ceiling or floor, the paths bounce in the space-space plot as though they're inside a box. Only one component V_1 or V_2 changes each time and only by changing \pm sign. Off the floor: (V_1, V_2) changes to $(-V_1, V_2)$, off of ceiling: (V_1, V_2) changes to $(V_1, -V_2)$. It is like a *single* particle bouncing around a pool table. Here (V_1, V_2) acts like (V_X, V_Y) in *two* dimensions, so *two* particles in *one*-dimension use graphs similar to *one* particle in *two* dimensions, a useful analogy in quantum theory.

Angle of incidence=Angle of reflection

When paths bounce off the floor and ceiling in the space-space plot, the angle of incidence equals the angle of reflection just as light rays reflect off mirrors. (Newton imagined little light *corpuscles* bouncing.) It is customary to measure path angles from the *normal* or perpendicular to a mirror so a normal bisects the angle between the incident and reflected paths.

For m_1 - m_2 *Bangs* off the 45° -collision line, the bisecting line has the slope $-M_1/M_2=-7$. It is like having mirror facets at slope $M_2/M_1=1/7$ along the 45° -collision line. For equal-mass- $(M_1=M_2)$ balls, or *one* ball in *two* dimensions, the bisecting line slope at the 45° -collision line is -1 or -45° and the collision line acts like a unit-slope mirror on a triangular billiard table. It is not quite that simple if $M_1 / M_2 \neq 1$.

Consider the two collisions *Bang-3*₍₂₀₎ and *Bang-4*₍₁₂₎ in Fig. 4.12. Velocity $\mathbf{v}(\mathbf{2})$ bounces off the ceiling in *Bang-3*₍₂₀₎ into $\mathbf{v}(\mathbf{3})$, whose velocity slope is close to the mass-ratio M_1/M_2 which is $7:1$ here. So the next collision *Bang-4*₍₁₂₎ bounces $\mathbf{v}(\mathbf{3})$ off the diagonal into $\mathbf{v}(\mathbf{4})$ which is close to $-\mathbf{v}(\mathbf{3})$. It's followed by another ceiling bounce *Bang-5*₍₂₀₎ into $\mathbf{v}(\mathbf{5})$ heading down for another collision *Bang-6*₍₁₂₎.

Bang force

Lower Fig. 4.12 has a *velocity vs. time* plot next to a space-time plot. (A y - t plot in gray is under the V - t plot, too.) Each *Bang* means a change in velocity for any particle involved in the collision. By *Newton's 2nd law* (1.1.9) each change in velocity, \mathbf{v} to $\mathbf{v}+\Delta\mathbf{v}$, or better, each change in *momentum*, $m\mathbf{v}$ to $m(\mathbf{v}+\Delta\mathbf{v})$, requires a force impulse $\mathbf{F}\cdot\Delta t= m(\Delta\mathbf{v})$ on each mass that changes. Shortly, we study ways to deal with this \mathbf{F} .

Kinematics versus Dynamics

The velocity-velocity (v_1, v_2) plots, such as the left side of Fig. 4.12, fall in a category known as *kinematics*, or *momentum analysis*, which is concerned with how things are going, where they're headed, or what is their *velocity* or *momentum* and *energy*. (*kinos* means movement.)

In contrast, the space-time plots, such as the right side of Fig. 4.12, fall in a category known as *dynamics*, or *coordinate analysis*, which is concerned with how things are located, where they are, or what are their *coordinate* or *position* and *time* schedules. (*dynos* means change.) We introduced the *space-space* (x_1, x_2) *plot*, another geometric or *trajectory* representation of dynamics.

Before going on, let's compare how *kinos* and *dynos* play out in classical Newtonian physics versus their corresponding roles in quantum physics. This is a preview for later chapters, mainly ones in Unit 3.

Dynos and Kinos: Classical vs. quantum theory

In Newtonian physics, a precise position plot (y_k vs. time) lets you find a precise velocity plot, too, and, a velocity plot (V_k vs. time) lets you find a position plot if you know starting position values. (We did just that in Fig. 4.7 and Fig. 4.12.) In calculus, finding position from velocity values is called *integration*, and finding velocity from position values is called *differentiation*. Of the two, the latter is formally easier but numerically more sensitive and error prone.

In quantum physics, having a precise velocity plot renders a position plot meaningless and *vice-versa*! Werner Heisenberg was the first to state this quantum idea, now known as Heisenberg's Principle. If you know momentum exactly, that means a uniform wave is everywhere, and all positions are equally possible. If you know position exactly, that means every momentum is possible, implying a "wave-bomb" about to blow up the universe! (Fortunately, neither of these extremes readily exist.)

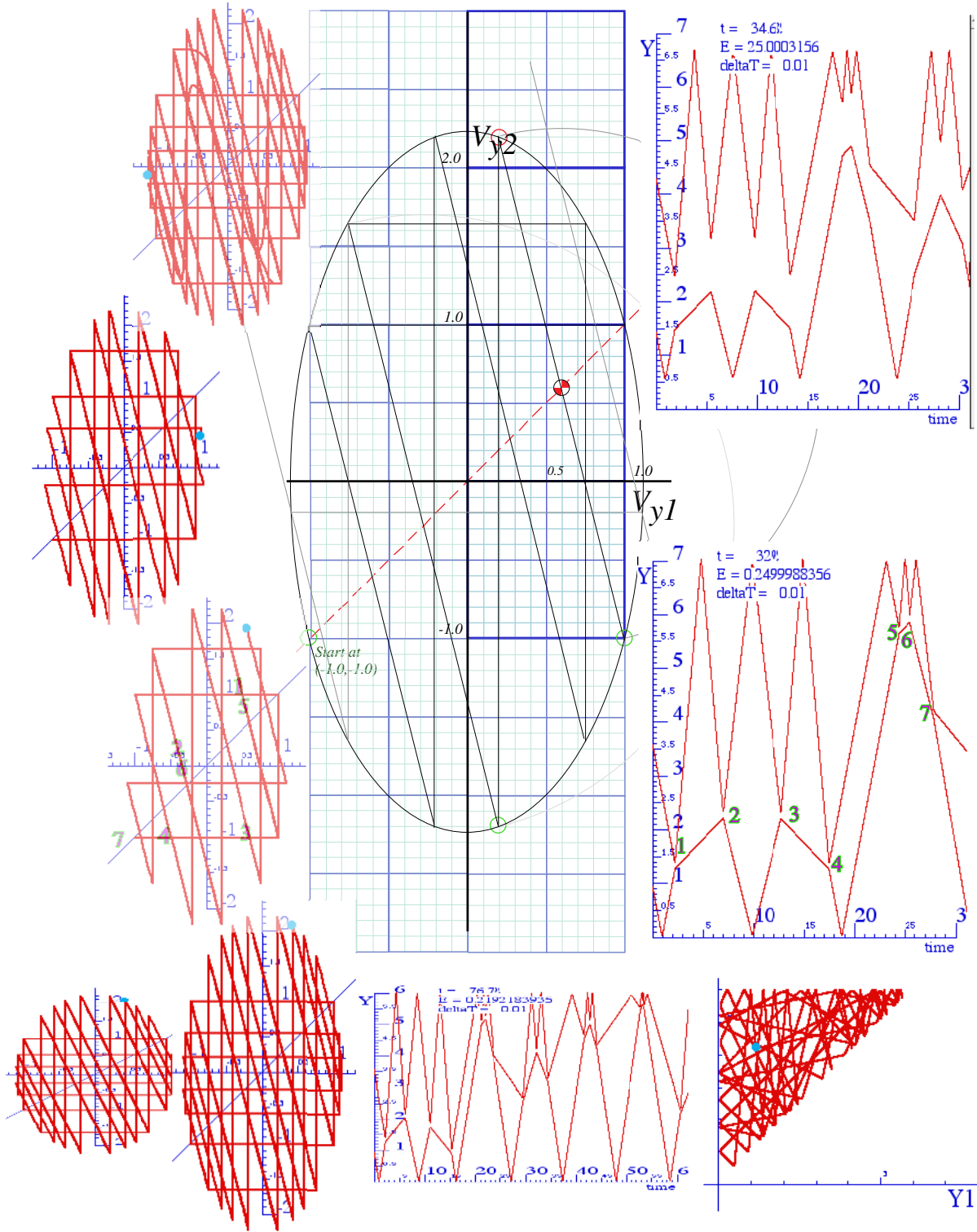
All this sounds crazy to most of us who are born-and-bred Aristotelean-to-Newtonian students. It is difficult enough to go from Aristotle's what-you-see-is-what-you-get (*WYSIWYG*) universe to Newton's corpuscular one. A quantum universe is yet another step removed on the *WYSIWYG* scale.

A way to see the quantum universe (Perhaps, it is *the* way.) is to learn about *wave* kinematics and dynamics without Newtonian corpuscles and see how waves *mimic* corpuscles and do so quite cleverly. The quantum universe is a *WYDAWYG* (*waves-you-don't see-are-what-you-get*) world!

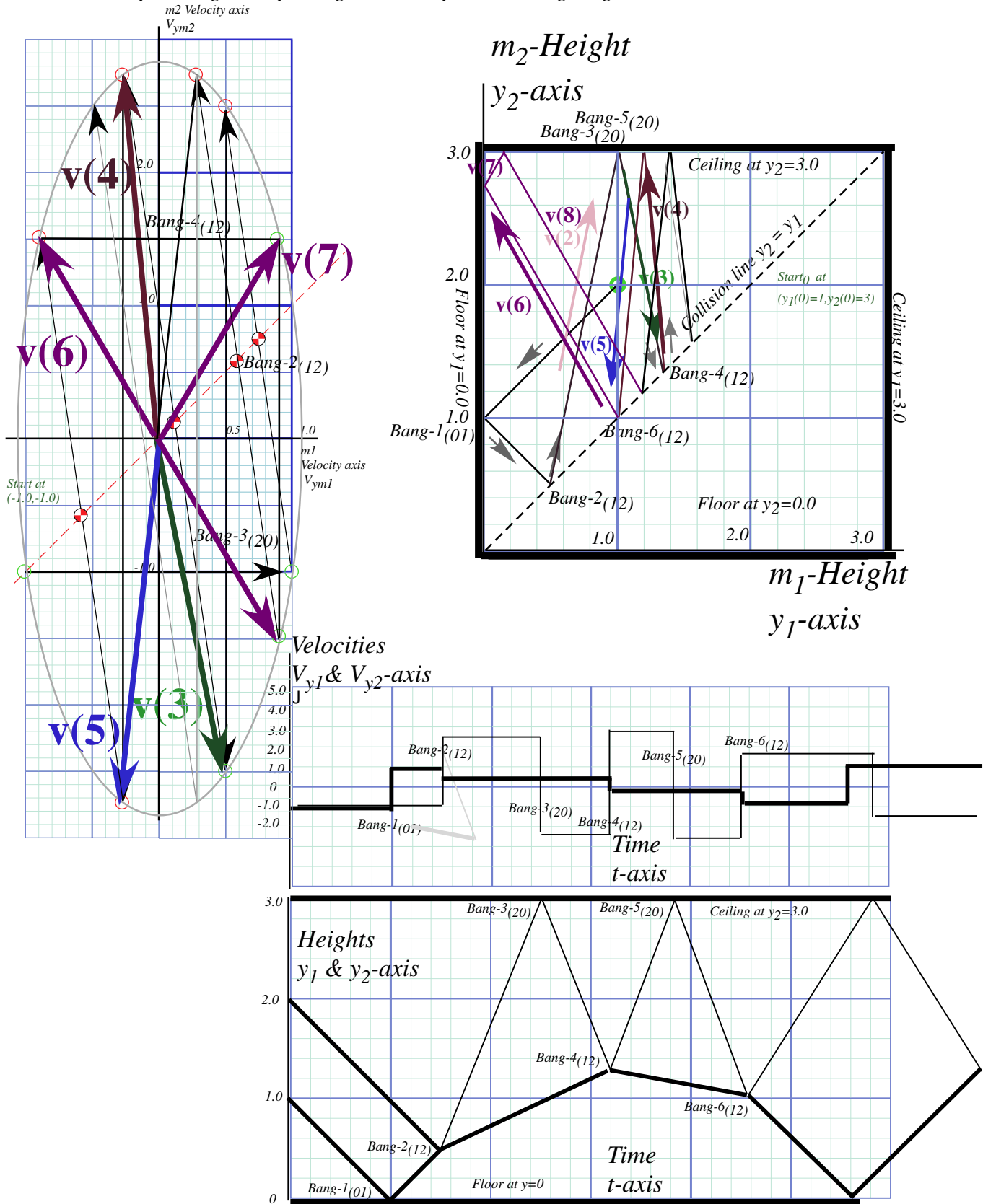
So our plan is to cast classical Newtonian kinematics and dynamics in a form that carries over into vibration and wave kinematics and dynamics. It is done by *analogy* with classical waves such as sound waves, water waves, and (most important) light waves. Many classical wave analyses invoke corpuscles (including, for Newton, light waves) so these analogies, like any analogy, need critical use of an Occam's razor that must be sharp. Above all, symmetry principles must be taken seriously.

Exercise: Construct a history of a 4:1 mass ratio bounce. $x_1(0)=1.5, x_2(0)=3.0, v_1(0)=-1, v_2(0)=-1$

Ceiling height=7.0.(For bottom row: Ceiling height=6.0) The 4:1 mass ratio case is surprisingly periodic.



Exercise: Complete Fig. 4.12 past “gameover” point. Ceiling height=3.0



Chapter 5 Multiple collisions and operator analysis

Analysis of many collisions with very different masses requires an advanced kind of geometry and algebra involving matrices and symmetry operators. Similar analysis is needed for quantum theory so this is a good opportunity to learn about these concepts using a classical bang physics that is quite clear-cut.

Doing collisions with matrix products

Fig. 5.1 shows a big mass $m_2=49$ bang a little mass $m_1=1$ more than ten times off the ceiling before being halted. This tests our collision precision! To check our results we use our previous vector equation (4.1) to make a *matrix equation* in (5.1) with $V^{COM} = (m_1v_1 + m_2v_2)/M$ and total mass $M = m_1 + m_2$.

$$\begin{pmatrix} v_1^{FIN} \\ v_2^{FIN} \end{pmatrix} = \begin{pmatrix} 2V^{COM} - v_1^{IN} \\ 2V^{COM} - v_2^{IN} \end{pmatrix} \quad (4.1)_{repeated} \quad \begin{pmatrix} v_1^{FIN} \\ v_2^{FIN} \end{pmatrix} = \begin{pmatrix} 2\frac{m_1v_1 + m_2v_2}{m_1 + m_2} - v_1 \\ 2\frac{m_1v_1 + m_2v_2}{m_1 + m_2} - v_2 \end{pmatrix} = \frac{1}{M} \begin{pmatrix} m_1v_1 - m_2v_1 + 2m_2v_2 \\ 2m_1v_1 + m_2v_2 - m_1v_2 \end{pmatrix} \quad (5.1a)$$

(Let $v_1^{IN}=v_1$ and $v_2^{IN}=v_2$ here.) Vector equation (5.1a) is converted to matrix equation $\mathbf{v}^{FIN} = \mathbf{M} \cdot \mathbf{v}$ in (5.1b).

$$\begin{pmatrix} v_1^{FIN} \\ v_2^{FIN} \end{pmatrix} = \frac{1}{M} \begin{pmatrix} m_1 - m_2 & 2m_2 \\ 2m_1 & m_2 - m_1 \end{pmatrix} \begin{pmatrix} v_1 \\ v_2 \end{pmatrix} \quad (5.1b)$$

Each *IN-to-FIN* bang is a $\mathbf{v}^{FIN} = \mathbf{M} \cdot \mathbf{v}^{IN}$ operation (5.2a). Matrix product $\mathbf{M} \cdot \mathbf{N}$ (5.4b) is bang- \mathbf{M} following bang- \mathbf{N} .

$$\mathbf{M} \cdot \mathbf{v} = \begin{pmatrix} A & B \\ C & D \end{pmatrix} \begin{pmatrix} a \\ b \end{pmatrix} = \begin{pmatrix} Aa + Bb \\ Ca + Db \end{pmatrix} \quad (5.2a)$$

$$\mathbf{M} \cdot \mathbf{N} = \begin{pmatrix} A & B \\ C & D \end{pmatrix} \begin{pmatrix} a & c \\ b & d \end{pmatrix} = \begin{pmatrix} Aa + Bb & Ac + Bd \\ Ca + Db & Cc + Dd \end{pmatrix} \quad (5.2b)$$

Matrix \mathbf{M} operates column-by-column on another matrix \mathbf{N} as it does on a vector \mathbf{v} . The off-the-ceiling matrix $\mathbf{C} = \begin{pmatrix} 1 & 0 \\ 0 & -1 \end{pmatrix}$ changes (v_1, v_2) to $(v_1, -v_2)$ (*Odd-n Bang-n(02)*) A 2-ball collision matrix \mathbf{M} (*Even-n Bang-n(12)*) and

ceiling bang \mathbf{C} act p -times in matrix products $\mathbf{v}^{FIN-p} = (\mathbf{C} \cdot \mathbf{M})^p \cdot \mathbf{v} = (\mathbf{C} \cdot \mathbf{M}) \cdot (\mathbf{C} \cdot \mathbf{M}) \cdot (\mathbf{C} \cdot \mathbf{M}) \cdot \dots \cdot (\mathbf{C} \cdot \mathbf{M}) \cdot \mathbf{v}$ to give Fig. 5.1.

$$\mathbf{C} \cdot \mathbf{M} = \begin{pmatrix} 1 & 0 \\ 0 & -1 \end{pmatrix} \frac{1}{M} \begin{pmatrix} m_1 - m_2 & 2m_2 \\ 2m_1 & m_2 - m_1 \end{pmatrix} = \frac{1}{M} \begin{pmatrix} m_1 - m_2 & 2m_2 \\ -2m_1 & m_2 - m_1 \end{pmatrix} = \begin{pmatrix} 1 & 0 \\ 0 & -1 \end{pmatrix} \begin{pmatrix} 0.96 & 0.04 \\ 1.96 & -0.96 \end{pmatrix} = \begin{pmatrix} 0.96 & 0.04 \\ -1.96 & 0.96 \end{pmatrix} \quad (5.3)$$

(5.4) shows ($p=5$) double-bangs $\mathbf{C} \cdot \mathbf{M} = \begin{pmatrix} 0.96 & 0.04 \\ -1.96 & 0.96 \end{pmatrix}$ following a floor-bounce $\mathbf{F} = \begin{pmatrix} -1 & 0 \\ 0 & +1 \end{pmatrix}$ or *11* bangs in all.

$$\begin{pmatrix} v_1^{FIN-11} \\ v_2^{FIN-11} \end{pmatrix} = \begin{pmatrix} 1 & 0 \\ 0 & -1 \end{pmatrix} \cdot \begin{pmatrix} 0.96 & 0.04 \\ 1.96 & -0.96 \end{pmatrix} \cdot \begin{pmatrix} 1 & 0 \\ 0 & -1 \end{pmatrix} \cdot \begin{pmatrix} 0.96 & 0.04 \\ 1.96 & -0.96 \end{pmatrix} \cdot \begin{pmatrix} 1 & 0 \\ 0 & -1 \end{pmatrix} \cdot \begin{pmatrix} 0.96 & 0.04 \\ 1.96 & -0.96 \end{pmatrix} \cdot \begin{pmatrix} 1 & 0 \\ 0 & -1 \end{pmatrix} \cdot \begin{pmatrix} 0.96 & 0.04 \\ 1.96 & -0.96 \end{pmatrix} \cdot \begin{pmatrix} -1 & 0 \\ 0 & +1 \end{pmatrix} \begin{pmatrix} v_1^{IN} = -1 \\ v_2^{IN} = -1 \end{pmatrix}_{(INITIAL (0))}$$

$$\begin{pmatrix} v_1^{FIN-11} \\ v_2^{FIN-11} \end{pmatrix} = \begin{pmatrix} 0.96 & 0.04 \\ -1.96 & 0.96 \end{pmatrix} \cdot \begin{pmatrix} 0.96 & 0.04 \\ -1.96 & 0.96 \end{pmatrix} \cdot \begin{pmatrix} 0.96 & 0.04 \\ -1.96 & 0.96 \end{pmatrix} \cdot \begin{pmatrix} 0.96 & 0.04 \\ -1.96 & 0.96 \end{pmatrix} \cdot \begin{pmatrix} 0.96 & 0.04 \\ -1.96 & 0.96 \end{pmatrix} \begin{pmatrix} v_1 = 1 \\ v_2 = -1 \end{pmatrix}_{(after Bang-1)}$$

$$\begin{pmatrix} v_1^{FIN-11} \\ v_2^{FIN-11} \end{pmatrix} = \begin{pmatrix} 0.96 & 0.04 \\ -1.96 & 0.96 \end{pmatrix} \cdot \begin{pmatrix} 0.96 & 0.04 \\ -1.96 & 0.96 \end{pmatrix} \cdot \begin{pmatrix} 0.96 & 0.04 \\ -1.96 & 0.96 \end{pmatrix} \cdot \begin{pmatrix} 0.96 & 0.04 \\ -1.96 & 0.96 \end{pmatrix} \begin{pmatrix} v_1 = 0.92 \\ v_2 = -2.92 \end{pmatrix}_{(after Bang-3)} \quad \text{Note: } \begin{pmatrix} 0.92 \\ -2.92 \end{pmatrix} = \begin{pmatrix} 0.96 & 0.04 \\ -1.96 & 0.96 \end{pmatrix} \begin{pmatrix} 1 \\ -1 \end{pmatrix} \quad (5.4)$$

$$\begin{pmatrix} v_1^{FIN-11} \\ v_2^{FIN-11} \end{pmatrix} = \begin{pmatrix} 0.96 & 0.04 \\ -1.96 & 0.96 \end{pmatrix} \cdot \begin{pmatrix} 0.96 & 0.04 \\ -1.96 & 0.96 \end{pmatrix} \cdot \begin{pmatrix} 0.96 & 0.04 \\ -1.96 & 0.96 \end{pmatrix} \begin{pmatrix} v_1 = 0.7664 \\ v_2 = -4.606 \end{pmatrix}_{(after Bang-5)} \quad \text{Note: } \begin{pmatrix} 0.7664 \\ -4.606 \end{pmatrix} = \begin{pmatrix} 0.96 & 0.04 \\ -1.96 & 0.96 \end{pmatrix} \begin{pmatrix} 0.92 \\ -2.92 \end{pmatrix}$$

$$\begin{pmatrix} v_1^{FIN-11} \\ v_2^{FIN-11} \end{pmatrix} = \begin{pmatrix} 0.96 & 0.04 \\ -1.96 & 0.96 \end{pmatrix} \cdot \begin{pmatrix} 0.96 & 0.04 \\ -1.96 & 0.96 \end{pmatrix} \begin{pmatrix} v_1 = 0.5515 \\ v_2 = -5.924 \end{pmatrix}_{(after Bang-7)} \quad \text{Note: } \begin{pmatrix} 0.5515 \\ -5.924 \end{pmatrix} = \begin{pmatrix} 0.96 & 0.04 \\ -1.96 & 0.96 \end{pmatrix} \begin{pmatrix} 0.7664 \\ -4.606 \end{pmatrix}$$

$$\begin{pmatrix} v_1^{FIN-11} \\ v_2^{FIN-11} \end{pmatrix} = \begin{pmatrix} 0.96 & 0.04 \\ -1.96 & 0.96 \end{pmatrix} \begin{pmatrix} v_1 = 0.2925 \\ v_2 = -6.768 \end{pmatrix}_{(after Bang-9)} \quad \text{Even after 9 bangs, big } m_1 \text{ still has a small upward velocity } v_1=0.2925.$$

After *Bang-11*₍₀₂₎ big m_1 is nearly stopped and little m_2 is coming down at $v_2=-7.071$ with *all the energy*!

$$\begin{pmatrix} v_1^{FIN-11} \\ v_2^{FIN-11} \end{pmatrix} = \begin{pmatrix} v_1 = 0.0100 \\ v_2 = -7.071 \end{pmatrix}_{\text{(after Bang-11)}} \tag{5.5}$$

Look out below! As m_1 turns back it crosses $v_1=0$ axis in Fig. 5.1a. The greatest curvature (acceleration or force) for m_1 is between *Bang-8* and *Bang-14* in Fig. 5.1b just when m_2 is busiest. Geometry works, too!

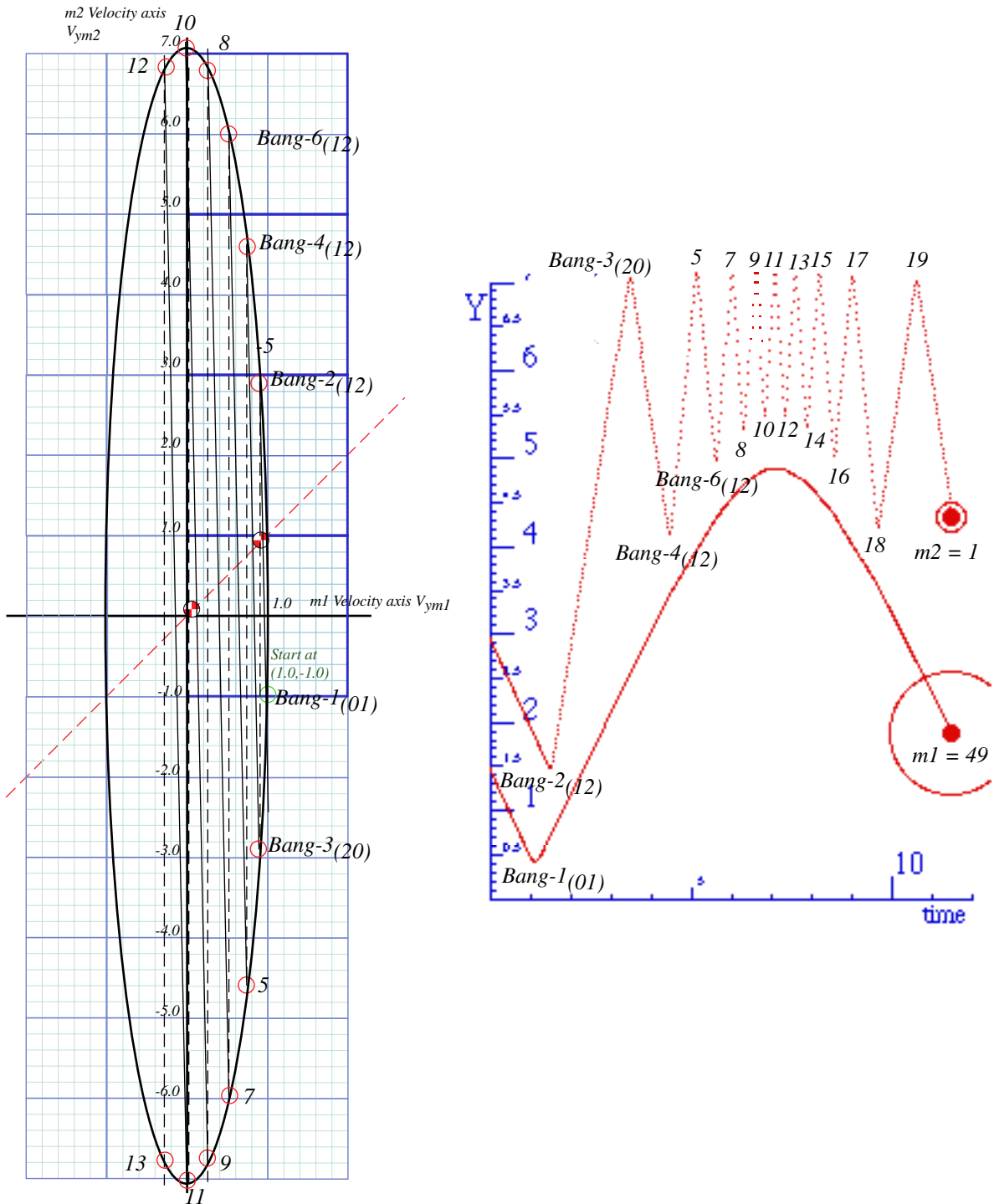


Fig. 5.1 Multiple Bangs of the $m_1=49$ and $m_2=1$ superball system. (a) V vs V plot. (b) Y vs time.

Big m_1 descends rapidly after being pushed down by m_2 hits. Soon hits by an exhausted m_2 become less frequent. At some point m_2 ends up slower than m_1 and can't hit it again. With no floor both would fall below $y=0$ with no further bangs. (We'll call this a *game-over* point. As an exercise, you should find it.)

However, if a floor intervenes, then a 2nd floor-bounce matrix $\mathbf{F} = \begin{pmatrix} -1 & 0 \\ 0 & +1 \end{pmatrix}$ changes (v_1, v_2) to $(-v_1, v_2)$ and bounces ball- m_1 back up to start the whole process over again. Ball- m_1 does another graceful up-then-down time trajectory very much like the one shown on the right-hand side of Fig. 5.1.

Except for floor bounces, the m_1 -ball in Fig. 5.1 experiences smoother flight than in Fig. 4.12 where a more massive m_2 -ball jerks it severely. A smaller mass m_2 has less momentum-per-bang. The result is a gentler and smoother force cushion for m_1 . Force and potential field theory will be derived from this.

Rotating in velocity space: Ticking around the clock

Here is an example of geometry and slope ratios being helpful. If you view the ellipse in Fig. 5.1a lower-edge-on (and do the exercise to finish it!) you may see it as a circular clock with each double-bang (*odd*-bangs 1,3,5,...) rotating the \mathbf{v} -vector like a clock hand ticking equal-angle jumps around a dial.

This suggests making energy ellipses ($2E = m_1 v_1^2 + m_2 v_2^2$) into energy *circles* ($2E = \mathbf{V}_1^2 + \mathbf{V}_2^2$) using rescaled velocity $(\mathbf{V}_1, \mathbf{V}_2)$, as shown here and in Fig. 5.2(a-b).

$$\mathbf{V}_1 = v_1 \sqrt{m_1}, \quad \mathbf{V}_2 = v_2 \sqrt{m_2} \quad \text{where: } 2E = m_1 v_1^2 + m_2 v_2^2 = \mathbf{V}_1^2 + \mathbf{V}_2^2 \quad (5.6)$$

Big-V variables replace little- v 's by setting $(v_1 = \mathbf{V}_1 / \sqrt{m_1}, v_2 = \mathbf{V}_2 / \sqrt{m_2})$ in matrix relation (5.1).

$$\begin{pmatrix} v_1^{FIN_1} \\ v_2^{FIN_1} \end{pmatrix} = \frac{1}{M} \begin{pmatrix} m_1 - m_2 & 2m_2 \\ 2m_1 & m_2 - m_1 \end{pmatrix} \begin{pmatrix} v_1 \\ v_2 \end{pmatrix} \quad (5.1)_{repeated} \quad \begin{pmatrix} \mathbf{V}_1^{FIN_1} / \sqrt{m_1} \\ \mathbf{V}_2^{FIN_1} / \sqrt{m_2} \end{pmatrix} = \frac{1}{M} \begin{pmatrix} m_1 - m_2 & 2m_2 \\ 2m_1 & m_2 - m_1 \end{pmatrix} \begin{pmatrix} \mathbf{V}_1 / \sqrt{m_1} \\ \mathbf{V}_2 / \sqrt{m_2} \end{pmatrix} \quad (5.7)$$

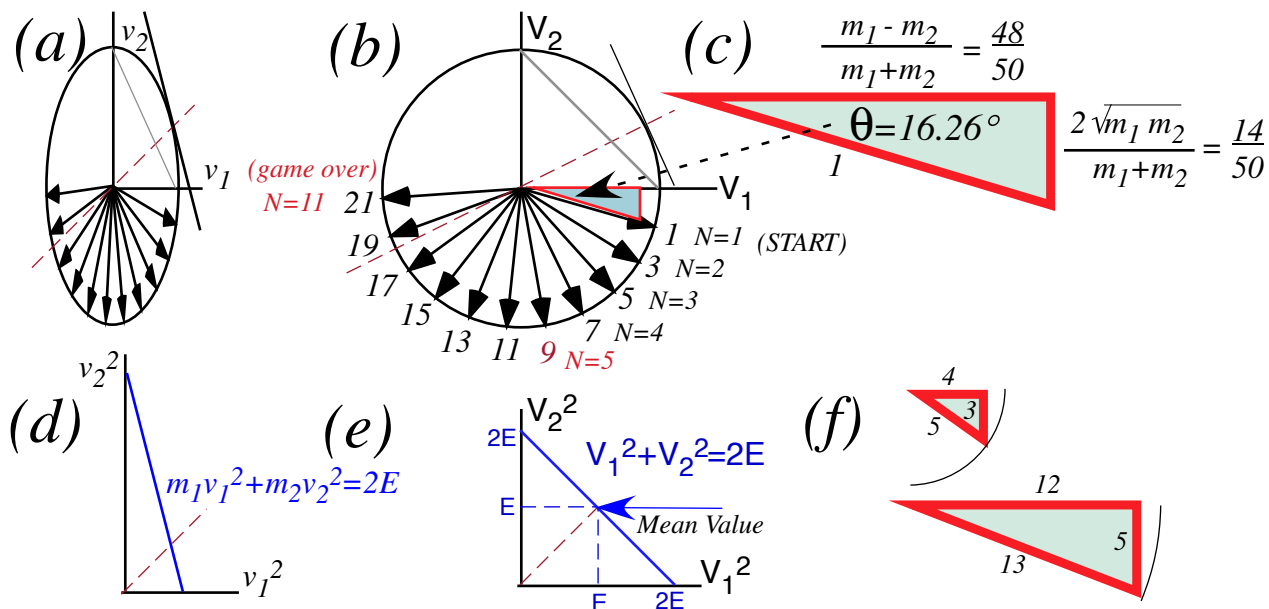


Fig. 5.2 Velocity-velocity clocks. (a) Energy ellipse (As in Fig. 5.1) (b-c) Energy bang-clock angles (d) Velocity-squared E-plot. (e) Mass-scaled V-squared E-plot. (f) Integral right triangles

Clearing scale factors $\sqrt{m_k}$ gives big- \mathbf{V} matrix relations so (5.10) below replaces (5.5) above.

$$\mathbf{v}^{FIN_1} = \begin{pmatrix} \mathbf{v}_1^{FIN_1} \\ \mathbf{v}_2^{FIN_1} \end{pmatrix} = \frac{1}{M} \begin{pmatrix} m_1 - m_2 & 2\sqrt{m_1 m_2} \\ 2\sqrt{m_1 m_2} & m_2 - m_1 \end{pmatrix} \begin{pmatrix} \mathbf{v}_1 \\ \mathbf{v}_2 \end{pmatrix} = \mathbf{M} \cdot \mathbf{v} \quad (5.8) \quad \mathbf{v}^{FIN_2} = \begin{pmatrix} \mathbf{v}_1^{FIN_2} \\ \mathbf{v}_2^{FIN_2} \end{pmatrix} = \frac{1}{M} \begin{pmatrix} m_1 - m_2 & 2\sqrt{m_1 m_2} \\ -2\sqrt{m_1 m_2} & m_1 - m_2 \end{pmatrix} \begin{pmatrix} \mathbf{v}_1 \\ \mathbf{v}_2 \end{pmatrix} = \mathbf{C} \cdot \mathbf{M} \cdot \mathbf{v} \quad (5.9)$$

The trick is to notice a Pythagorean relation $x^2 + y^2 = 1$ for the circular bang-matrix components.

$$\left(\frac{m_1 - m_2}{M} \right)^2 + \left(\frac{2\sqrt{m_1 m_2}}{M} \right)^2 = \frac{m_1 + m_2}{m_1 + m_2} = 1 \quad (5.10a)$$

So the matrix can be defined using $\sin\theta$ and $\cos\theta$. Our example $m_1=49$ and $m_2=1$ is plotted in Fig. 5.2(c).

$$\text{Define: } \cos\theta \equiv \left(\frac{m_1 - m_2}{M} \right) \quad \text{and: } \sin\theta \equiv \left(\frac{2\sqrt{m_1 m_2}}{M} \right) \quad (5.10b)$$

A 1-Bang matrix is a *reflection* by θ . Our 2-Bang matrix is a *rotation* by angle $-\theta = -16.26^\circ$ in big- \mathbf{V} space.

$$\begin{pmatrix} \mathbf{v}_1^{FIN_1} \\ \mathbf{v}_2^{FIN_1} \end{pmatrix} = \begin{pmatrix} \cos\theta & \sin\theta \\ \sin\theta & -\cos\theta \end{pmatrix} \begin{pmatrix} \mathbf{v}_1 \\ \mathbf{v}_2 \end{pmatrix} \quad (5.11)$$

$$\begin{pmatrix} \mathbf{v}_1^{FIN_2} \\ \mathbf{v}_2^{FIN_2} \end{pmatrix} = \begin{pmatrix} \cos\theta & \sin\theta \\ -\sin\theta & \cos\theta \end{pmatrix} \begin{pmatrix} \mathbf{v}_1 \\ \mathbf{v}_2 \end{pmatrix} = \begin{pmatrix} 0.96 & 0.04 \\ -1.96 & 0.96 \end{pmatrix} \begin{pmatrix} \mathbf{v}_1 \\ \mathbf{v}_2 \end{pmatrix} \quad (5.12)$$

(5.12) is a big help in N -double-bang calculations like (5.4). Instead of multiplying the matrix (5.9) by itself N -times, we just replace $\theta = 16.26^\circ$ in (5.12) by $N\theta = 81.30^\circ$ (for $N=5$) and get answers in (5.13) below *pronto!*

$$\begin{pmatrix} \mathbf{v}_1^{FIN_{2N}} \\ \mathbf{v}_2^{FIN_{2N}} \end{pmatrix} = (\mathbf{C} \cdot \mathbf{M})^N \cdot \mathbf{v} = \begin{pmatrix} \cos N\theta & \sin N\theta \\ -\sin N\theta & \cos N\theta \end{pmatrix} \begin{pmatrix} \mathbf{v}_1 \\ \mathbf{v}_2 \end{pmatrix} = \begin{pmatrix} \cos 5\theta & \sin 5\theta \\ -\sin 5\theta & \cos 5\theta \end{pmatrix} \begin{pmatrix} \mathbf{v}_1 \\ \mathbf{v}_2 \end{pmatrix} = \begin{pmatrix} 0.1512 & 0.9885 \\ -0.9885 & 0.1512 \end{pmatrix} \begin{pmatrix} \mathbf{v}_1 \\ \mathbf{v}_2 \end{pmatrix} \quad (\text{for } N=5) \quad (5.13a)$$

Relating \mathbf{V} 's to v 's by $(\mathbf{V}_1 = v_1 \sqrt{m_1}, \mathbf{V}_2 = v_2 \sqrt{m_2})$ gives (5.1b). Here $(\mathbf{C} \cdot \mathbf{M})^N$ is *after floor F* gives $(v_1, v_2) = (1, -1)$.

$$\begin{pmatrix} v_1^{FIN_{2N}} \\ v_2^{FIN_{2N}} \end{pmatrix} = \begin{pmatrix} \cos N\theta & \sqrt{\frac{m_2}{m_1}} \sin N\theta \\ -\sqrt{\frac{m_1}{m_2}} \sin N\theta & \cos N\theta \end{pmatrix} \begin{pmatrix} v_1 \\ v_2 \end{pmatrix} = \begin{pmatrix} \cos 5\theta & \frac{1}{7} \sin 5\theta \\ -7 \sin 5\theta & \cos 5\theta \end{pmatrix} \begin{pmatrix} v_1 \\ v_2 \end{pmatrix} = \begin{pmatrix} 0.1512 & 0.1412 \\ -6.9194 & 0.1512 \end{pmatrix} \begin{pmatrix} 1 \\ -1 \end{pmatrix} = \begin{pmatrix} 0.010 \\ -7.071 \end{pmatrix} \quad \text{for } \begin{cases} N=5 \\ m_1=49 \\ m_2 \end{cases} \quad (5.13b)$$

Without a 2nd floor-bounce-back operation \mathbf{F} , this sequence ends near bang-21 or “game-over.” (How? Do the exercise!) Matrices can do collision sequences easily and even can “engineer” them.

Statistical mechanics: Average energy

If two balls of mass $m_2=1$ and $m_1=7$ bounce back and forth between wall the small ball goes faster on the average than the bigger one. How much faster? Let's assume that arrows on the scaled velocity clock in Fig. 5.2(b) get uniformly distributed around its circle after many collisions. (Fig. 5.2(b) shows only m_1 - m_2 -bounce arrows. m_2 -ceiling-bounce-arrows fill up the upper half.) A ball's velocity and momentum must sum and average to zero otherwise it will not stay in the region between the floor and the ceiling.

But, what is average squared-velocity v^2 of each ball? An energy plot in the space $(V_1)^2$ vs $(V_2)^2$ of scaled velocity-squared helps to answer this. The result is a 45° line shown in Fig. 5.2(e). In other words points on the circle in Fig. 5.2(b) get mapped onto the 45° line in Fig. 5.2(e) by KE conservation.

$$(V_1)^2 + (V_2)^2 = 2 KE = m_1(v_1)^2 + m_2(v_2)^2$$

The average of all points on the 45° line is its bisector.

$$(V_1)^2 = KE = (V_2)^2 \quad \text{or:} \quad m_1(v_1)^2 = KE = m_2(v_2)^2$$

This gives the average velocities or *root-mean-square-speeds* v_1^{rms} and v_2^{rms} of m_1 and m_2 .

$$v_1^{rms} = \sqrt{KE / m_1} \quad v_2^{rms} = \sqrt{KE / m_2} \quad (5.14)$$

Each ball, regardless of mass, gets equal share (50% if there are just two) of the total energy. So, if m_1 is 7 times m_2 then the mean speed of m_2 is $\sqrt{7}=2.65$ times faster than that of m_1 . The 1st bang in Fig. 4.4 gives 2.5.

Bonus: Rational right triangles

Geometry often offers interesting numerics. In this case, the general right triangle in Fig. 5.2(c) makes integer or rational fraction solutions to the Pythagorean sum $a^2 + b^2 = c^2$ such as the famous $(a=3, b=4, c=5)$ right triangle. Perfect-square mass values (m_1 and $m_2=1, 4, 9, 16, 25, 36, 49, 81, 100, \dots$) will give integral valued right triangle altitude $a=\sqrt{4 m_1 \cdot m_2}$, base $m_1 - m_2$, and hypotenuse $m_1 + m_2$. Examples in Fig. 5.2 are $(a=14, b=48, c=50)$ for $(m_1=49, m_2=1)$ and $(a=12, b=5, c=13)$ for $(m_1=9, m_2=4)$.

Reflections about rotations: It’s all done with mirrors

In 1843 Hamilton discovered his *quaternion algebra* $\{1, i, j, k\}$, a mathematical jewel. In 1930 Pauli found related *spinor matrices* $\{1, \sigma_x, \sigma_y, \sigma_z\}$. We label Pauli matrix σ_z as *sigma-A* $=\sigma_A$ (*A for Asymmetric*) and σ_x as *sigma-B* $=\sigma_B$ (*B for Balanced*). They are Hamilton’s **k** and **i** with an imaginary factor $i=\sqrt{-1}$ attached.

$$\sigma_A = \begin{pmatrix} 1 & 0 \\ 0 & -1 \end{pmatrix} = \sigma_z = i\mathbf{k} \quad (5.15a)$$

$$\sigma_B = \begin{pmatrix} 0 & 1 \\ 1 & 0 \end{pmatrix} = \sigma_x = i\mathbf{i} \quad (5.15b)$$

Other matrices, *sigma-C* $=\sigma_C$ (*C for Circular*) and *sigma-0* $=\sigma_0$ (*0 for “Origin”*) are products like $\sigma_A\sigma_B$ or σ_A^2 .

$$\sigma_A\sigma_B = \begin{pmatrix} 1 & 0 \\ 0 & -1 \end{pmatrix} \cdot \begin{pmatrix} 0 & 1 \\ 1 & 0 \end{pmatrix} = \begin{pmatrix} 0 & 1 \\ -1 & 0 \end{pmatrix} = i\sigma_C = i\sigma_y = -\mathbf{j} \quad (5.15c)$$

$$\sigma_A\sigma_A = \sigma_B\sigma_B = \sigma_C\sigma_C = \begin{pmatrix} 1 & 0 \\ 0 & 1 \end{pmatrix} = \sigma_0 = \mathbf{1} = \mathbf{1} \quad (5.15d)$$

Hamilton’s $\{i, j, k\}$ square to **-1**. ($i^2=j^2=k^2=-1$) That is like $i^2=-1$. But, Pauli- σ ’s square to **+1**. ($1=\sigma_x^2=\sigma_y^2=\sigma_z^2$.)

We now relate σ -matrices to simple super-ball collision reflections and rotations shown in Fig. 5.2. For example, the σ_A is our “ceiling bounce” **C** in (5.3) and our “floor bounce” **F** in (5.3) is just $-\sigma_A$.

$$\sigma_A = \begin{pmatrix} 1 & 0 \\ 0 & -1 \end{pmatrix} = \mathbf{C} \quad (5.15a)$$

$$-\sigma_A = \begin{pmatrix} -1 & 0 \\ 0 & 1 \end{pmatrix} = \mathbf{F} \quad (5.15b)$$

A geometric view of σ_A (or $-\sigma_A$) is *mirror reflection* thru Cartesian x -(or y) axes in Fig. 5.3a while σ_B (or $-\sigma_B$) is reflection thru mirror planes tilted at angle $\pi/4$ (or $-\pi/4$) *between* x - y axes in Fig. 5.3b. General reflection σ_ϕ thru a mirror plane tilted at angle $\phi/2$ (Fig. 5.3c) is a sum (5.15c) of $\sigma_A \cos \phi$ and $\sigma_B \sin \phi$. We now verify this.

$$\sigma_\phi = \sigma_A \cos \phi + \sigma_B \sin \phi = \begin{pmatrix} 1 & 0 \\ 0 & -1 \end{pmatrix} \cos \phi + \begin{pmatrix} 0 & 1 \\ 1 & 0 \end{pmatrix} \sin \phi = \begin{pmatrix} \cos \phi & \sin \phi \\ \sin \phi & -\cos \phi \end{pmatrix} \quad (5.15c)$$

Like all reflections, σ_ϕ must square-to-one. ($\sigma_\phi^2=\mathbf{1}$) It does so because $\sigma_A^2=\mathbf{1}=\sigma_B^2$ and $\sigma_A\sigma_B=-\sigma_B\sigma_A$.

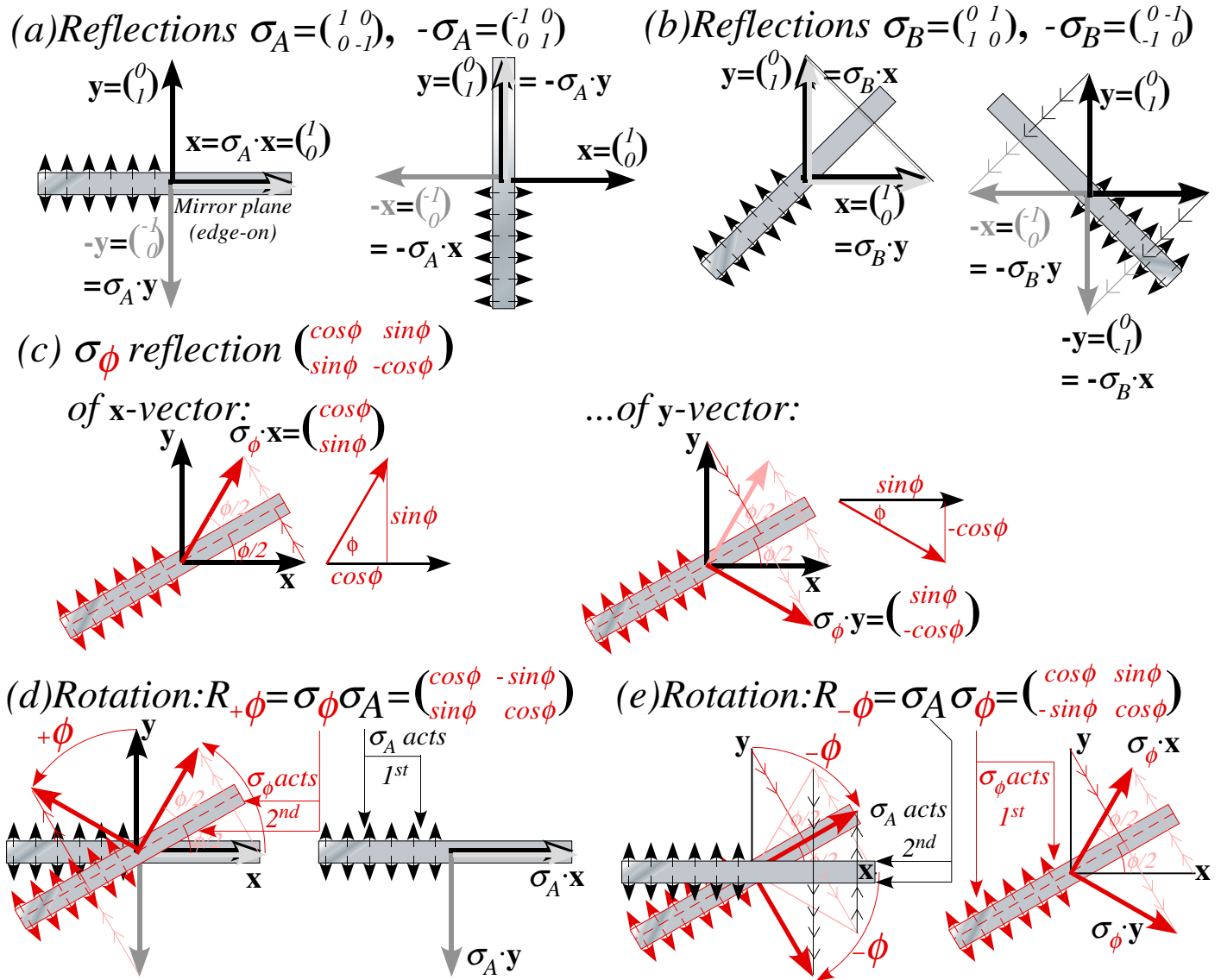


Fig. 5.3 Mirror-reflection geometry (a) $\pm\sigma_A$, (b) $\pm\sigma_B$, (c) σ_ϕ . Right-and-left-handed rotation (e) $\sigma_\phi\sigma_A$ (f) $\sigma_A\sigma_\phi$.

We test σ_ϕ on unit vectors $\hat{x} = \begin{pmatrix} 1 \\ 0 \end{pmatrix}$ and $\hat{y} = \begin{pmatrix} 0 \\ 1 \end{pmatrix}$ and see that matrix algebra checks with geometry in Fig.5.3c.

$$\sigma_\phi \cdot \hat{x} = \begin{pmatrix} \cos\phi & \sin\phi \\ \sin\phi & -\cos\phi \end{pmatrix} \cdot \begin{pmatrix} 1 \\ 0 \end{pmatrix} = \begin{pmatrix} \cos\phi \\ \sin\phi \end{pmatrix} \quad (5.16a)$$

$$\sigma_\phi \cdot \hat{y} = \begin{pmatrix} \cos\phi & \sin\phi \\ \sin\phi & -\cos\phi \end{pmatrix} \cdot \begin{pmatrix} 0 \\ 1 \end{pmatrix} = \begin{pmatrix} \sin\phi \\ -\cos\phi \end{pmatrix} \quad (5.16b)$$

Geometry Fig. 5.3d also shows that a product $\sigma_2\sigma_1$ of any two reflection matrices is a *rotation matrix R*.

In Fig. 5.3d $\sigma_\phi\sigma_A$ is right-hand rotation $R_{+\phi}$ but $\sigma_A\sigma_\phi=R_{-\phi}$ in Fig. 5.3e is left handed. Rotation angle ϕ is twice the angle $\phi/2$ between mirrors. Direction of rotation $\sigma_2\sigma_1$ is from 1st mirror (of σ_1) to 2nd mirror (of σ_2).

$$\sigma_\phi \cdot \sigma_A = \begin{pmatrix} \cos\phi & \sin\phi \\ \sin\phi & -\cos\phi \end{pmatrix} \cdot \begin{pmatrix} 1 & 0 \\ 0 & -1 \end{pmatrix} = \begin{pmatrix} \cos\phi & -\sin\phi \\ \sin\phi & \cos\phi \end{pmatrix} \quad (5.17a)$$

$$\sigma_A \cdot \sigma_\phi = \begin{pmatrix} 1 & 0 \\ 0 & -1 \end{pmatrix} \cdot \begin{pmatrix} \cos\phi & \sin\phi \\ \sin\phi & -\cos\phi \end{pmatrix} = \begin{pmatrix} \cos\phi & \sin\phi \\ -\sin\phi & \cos\phi \end{pmatrix} \quad (5.17a)$$

For example, rotation $\sigma_B\sigma_A$ is by $+90^\circ$ and $\sigma_A\sigma_B$ is by -90° . Rotation $\sigma_A(-\sigma_A)=(-\sigma_A)\sigma_A$ is by $\pm 180^\circ$.

Through the clothing store looking glass

The rotation in V_1 vs V_2 space of Fig. 5.2b is a product of ceiling bounce and m_1 - m_2 collision that are each a reflection. An even simpler example of paired-reflection rotation is a clothing store mirror in Fig. 5.4a. It lets you swing two mirrors like doors to view multiple images of yourself. If you set the angle between mirrors to $\phi/2=30^\circ$ as in Fig. 5.3 d-e or to 60° as in Fig. 5.4a then you see yourself rotated by twice that angle. Images are turned 120° counter-clockwise in the right mirror and clockwise (-120°) in the left mirror of the latter.

The sketches in Fig. 5.4a oversimplify the actual images shown by photos of a real mirror pair. The single reflections for σ_A are not shown in the sketch but clearly visible in photos where the σ_A and σ_ϕ images both have backwards text and a left hand image of the original right hand. This is corrected in the (-120°)-rotated $\sigma_A\sigma_\phi$ image and the ($+120^\circ$)-rotated $\sigma_\phi\sigma_A$ image.

A special case is rotation $\sigma_A(-\sigma_A)=(-\sigma_A)\sigma_A$ by $\pm 180^\circ$ due to setting mirrors at exactly $\phi/2=90^\circ$ as in Fig. 5.4b. The result is known as a *corner-reflector image*. Wherever you stand while viewing a 90° corner you see your image centered and rotated $\pm 180^\circ$ to face you but it is *not reflected*. A 90° corner image is as others see you, complete with a readable monogram on your jacket and your right hand on the right side.

How fundamental are reflections?

A product of two reflections is a rotation $\mathbf{R}_\phi=\sigma_2\sigma_1$, but two rotations just give another rotation $\mathbf{R}_{\phi+\theta}=\mathbf{R}_\phi\mathbf{R}_\theta$ and never a reflection. This makes reflections more basic and productive than rotations.

On the other hand, you cannot do a reflection of a real solid object without entering an Alice-in-Wonderland looking-glass-world. Moving every atom in a classical object to a reflected position (without destroying it) is unthinkable! Yet, we easily rotate semi-solid objects (like your eyeballs while reading this).

Waves, on the other hand, are very *un-solid* and do reflection effortlessly. Rotation takes twice the effort as seen in the looking glass images of Fig. 5.4. This is why reflection operations are so basic to the study of wave mechanics, quantum theory, and relativistic symmetry as we will see in later Units 2 and 3.

Symmetry operation \mathbf{R} or σ is defined by what it does to unit vectors $\hat{x}=\begin{pmatrix} 1 \\ 0 \end{pmatrix}$ and $\hat{y}=\begin{pmatrix} 0 \\ 1 \end{pmatrix}$ as σ_ϕ (5.16) is done in Fig. 5.3c. That matrix does that same operation to any and all vectors $\mathbf{v}=\begin{pmatrix} v_1 \\ v_2 \end{pmatrix}=v_1\hat{x}+v_2\hat{y}$ in the space.

$$\sigma_\phi \cdot \mathbf{v} = v_1 \sigma_\phi \cdot \hat{x} + v_2 \sigma_\phi \cdot \hat{y} = v_1 \begin{pmatrix} \cos \phi \\ \sin \phi \end{pmatrix} + v_2 \begin{pmatrix} \sin \phi \\ -\cos \phi \end{pmatrix} = \begin{pmatrix} \cos \phi & \sin \phi \\ \sin \phi & -\cos \phi \end{pmatrix} \begin{pmatrix} v_1 \\ v_2 \end{pmatrix} \quad (5.18)$$

A way to distinguish rotation and reflection operators is by the *determinant* $\det|\mathbf{M}|$ of their matrices.

$$\det|\mathbf{M}| = \det \begin{vmatrix} a & b \\ c & d \end{vmatrix} = a \cdot d - b \cdot c \quad \det \begin{vmatrix} u_x & v_x \\ u_y & v_y \end{vmatrix} = u_x \cdot v_y - v_x \cdot u_y = |\mathbf{u}| |\mathbf{v}| \sin \angle_{\mathbf{u}}^{\mathbf{v}}$$

A determinant of matrix \mathbf{M} quantifies the space (area in this case) enclosed by vectors in \mathbf{M} 's rows or columns (\mathbf{u} and \mathbf{v} enclose a parallelogram in this case).

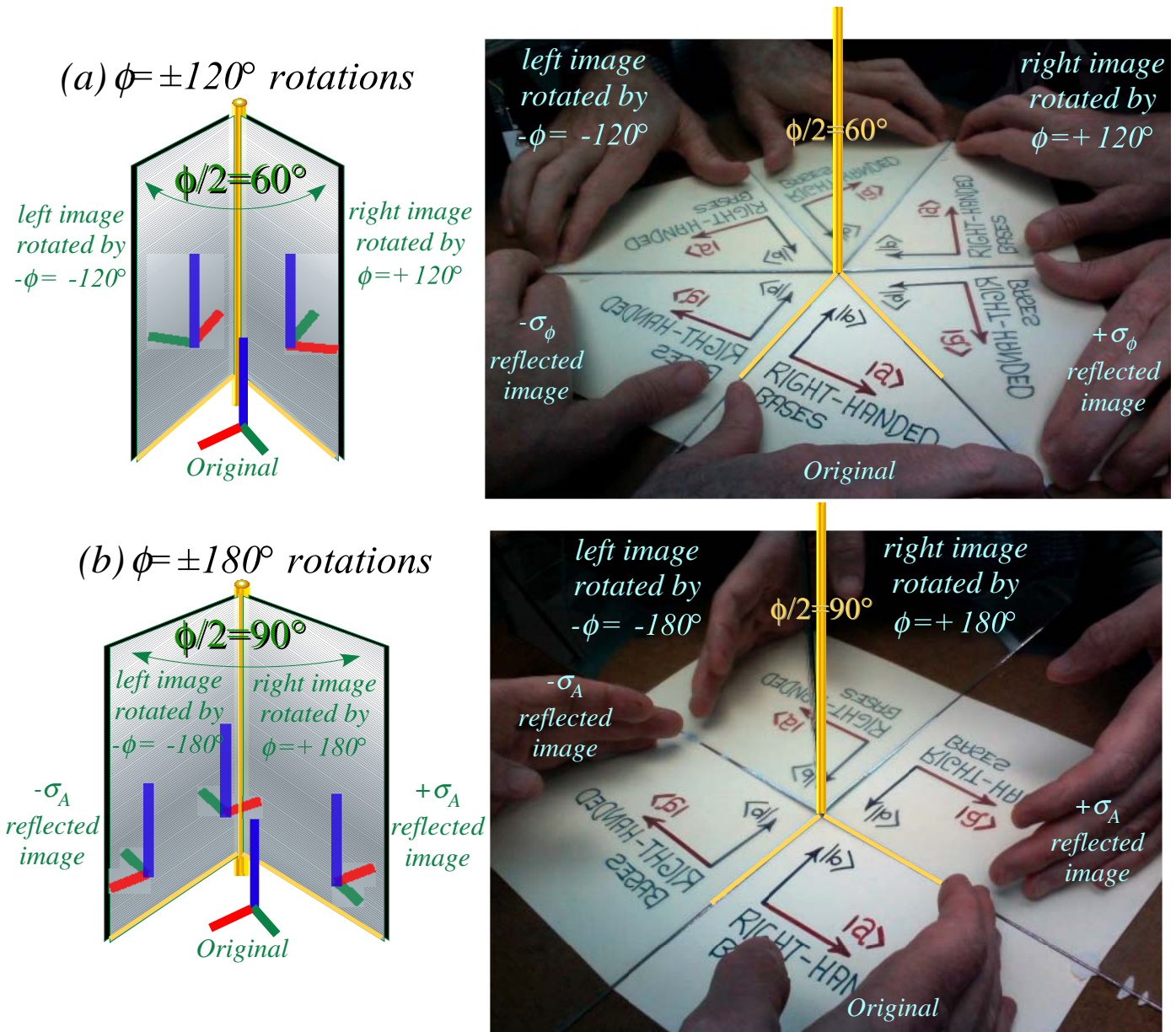


Fig. 5.4 Mirror reflections and their rotations with relative angle: (a) 60° (b) 90° (corner reflector images).

A rotation determinant is +I, but a reflection determinant is -I. Reflected area or angle in Fig. 1.3 is negative.

$$\det|\mathbf{R}_\phi| = \det \begin{pmatrix} \cos \phi & \sin \phi \\ -\sin \phi & \cos \phi \end{pmatrix} = \cos^2 \phi + \sin^2 \phi = +1$$

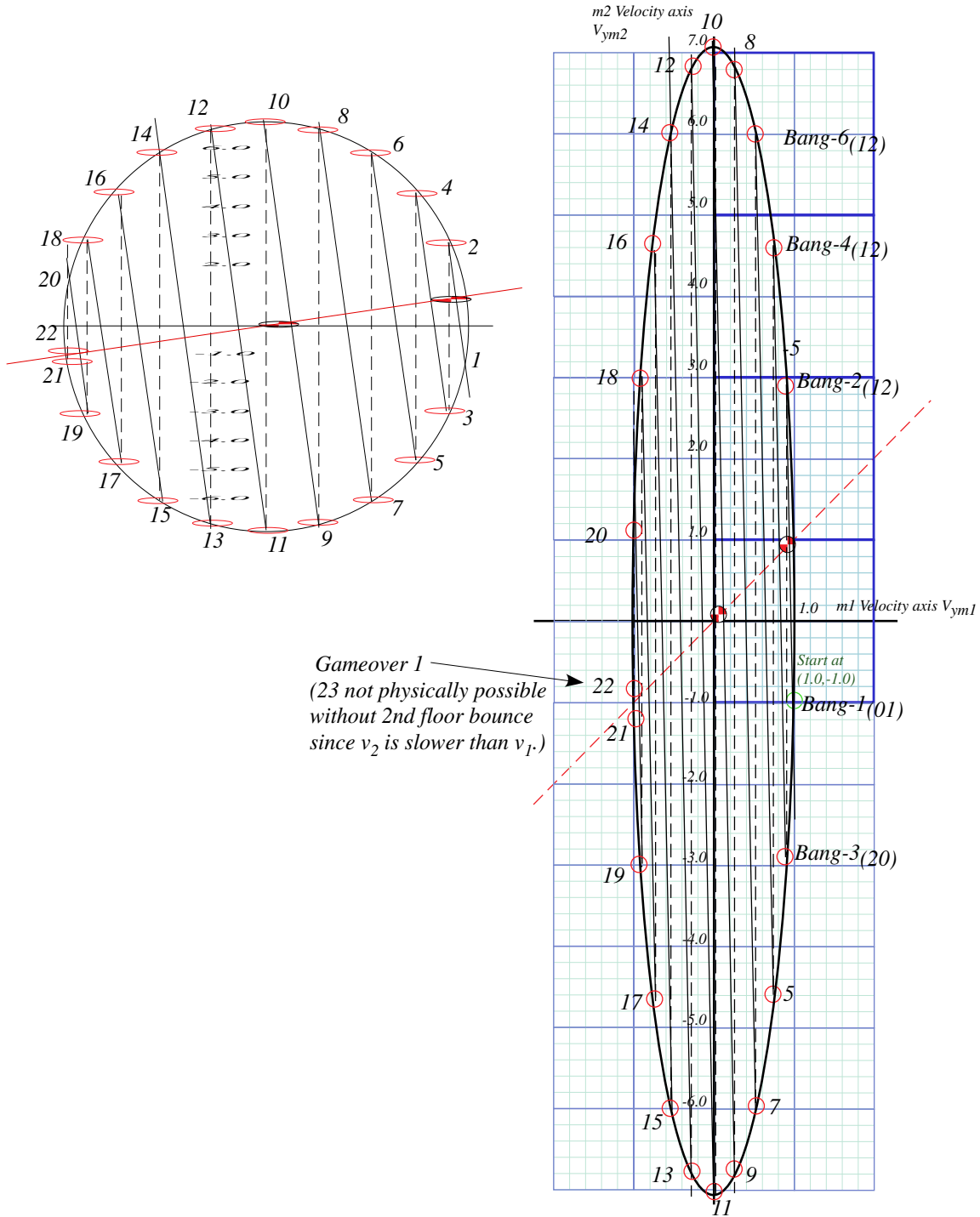
$$\det|\boldsymbol{\sigma}_\phi| = \det \begin{pmatrix} \cos \phi & \sin \phi \\ \sin \phi & -\cos \phi \end{pmatrix} = -\cos^2 \phi - \sin^2 \phi = -1$$

Determinants track the multiplication of matrices. The determinant of a product is a product of determinants.

$$\det|\mathbf{M}\cdot\mathbf{N}| = (\det|\mathbf{M}|)(\det|\mathbf{N}|) = \det|\mathbf{N}\cdot\mathbf{M}|$$

Thus, two reflections each with $\det/\sigma = -1$ form a product of $\det/\sigma_1\sigma_2 = (-1)(-1) = +1$, that of a rotation. This also shows a product of rotations cannot make a negative-det-matrix and so cannot be a reflection.

Exercise Complete Fig. 5.1 to the game-over point where sequence ends without floor bounce.



Chapter 6 Force and potential energy

Analysis of *force* is one of the trickier parts of Newtonian mechanics and one that Aristotle seems to have not done so well. We, like Aristotle, feel we know force after being pushed and pulled around by it most of our conscious lives. Aristotle related force directly to mass and its motion. If he ever wrote equations then, perhaps, Aristotle's equation would be $F=Mv$.

NOT! Mv is *momentum*, not force. Galileo and Newton seem to be among the first to realize that force should be equated to a *change* in momentum. A famous equation $F=Ma$ equates force to mass or *inertia* M times *acceleration* a , the *rate of change* of velocity. (This is called *Newton's 2nd law* or *NEWTON-TWO*.)

$$F = \frac{dP}{dt} = M \frac{dV}{dt} = M \cdot a \quad (6.0)$$

MBM force fields and potentials

Motion of m_1 in Fig. 5.1b suggests a *kinetic model* and a *potential force field*. Boltzman used this to derive gas force laws for volume, temperature, and pressure. As a big m_1 -ball squeezes space (*volume*) for a tiny m_2 -ball in Fig. 6.1, the speed v_2 and energy $\frac{1}{2} m_2 v_2^2$ of m_2 increases. So does the *momentum transfer rate* or *bang-force* on m_1 . Energy is related to *temperature* and bang-force is related to *pressure*. A furiously bouncing m_2 is like a single-atom gas getting hot when its Y -space is compressed as in Fig. 6.1b.

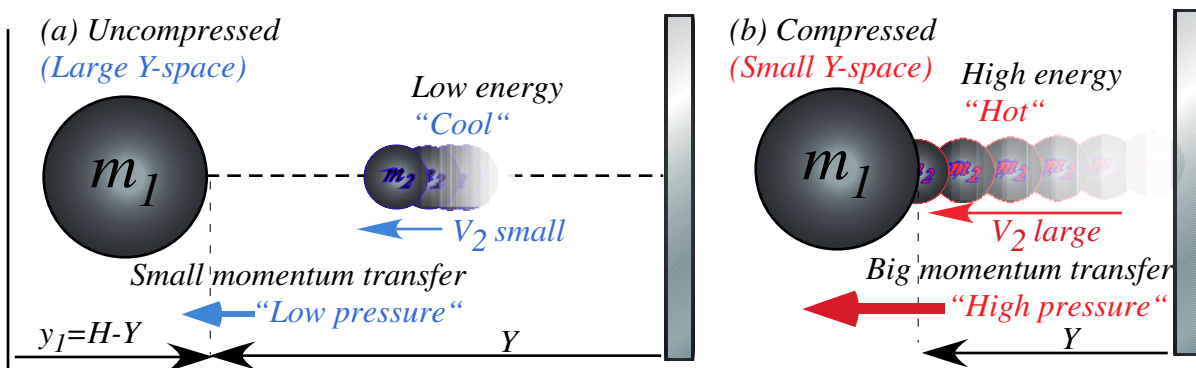


Fig. 6.1 Big mass- m_1 ball feeling "force-field" or "pressure" of small ball rapidly bouncing to-and-fro.

A "double-whammy" hits the m_1 -ball as it closes in with velocity v_1 toward m_2 and the ceiling:

- (1) Bang rate B with m_2 increases with shrinking distance $2Y$ traveled by m_2 back-and-forth to the ceiling.
- (2) Increased velocity v_2 (due to v_1) increases momentum $m_2 v_2$ and ΔP transferred to m_1 by each bang.
- (3) Increased velocity v_2 (due to v_1) increases bang rate even more. It's really a *triple whammy*!

If m_1 is huge (say 1kg) compared to atom or molecule m_2 (say $(2/3) \cdot 10^{-27}\text{kg}$ for an H-atom), the speed v_1 of the macro-mass m_1 may be negligible compared to typical atomic speeds v_2 of 10^3 m/s . Then we ignore effects (2) and (3) due to tiny v_1 in a so-called *isothermal* model. An *adiabatic* model includes them.

Isothermal model force laws

Atom m_2 in Fig. 6.1 travels distance $2Y$ back & forth between m_1 and ceiling at Y for each bang m_1 . If v_1 is slow, the time Δt between bangs is $2Y$ divided by velocity v_2 of m_2 . **Bang rate B** is the inverse: $B=1/\Delta t$.

$$\Delta t = 2Y/v_2 \text{ (bangs per sec)} \quad (6.1a) \qquad B = 1/\Delta t = v_2/2Y \text{ (seconds per bang)} \quad (6.1b)$$

Each head-on bang of big m_1 on small m_2 changes velocity of m_2 from $-v_2$ to $+v_2^{FIN}$ as shown in Fig. 6.2.

$$\text{(for: } m_1 \gg m_2\text{):} \qquad v_2^{FIN} = v_2 + 2v_1 \qquad (\approx v_2 \text{ for: } v_2 \gg v_1) \quad (6.2)$$

Added speed for m_2 is $2v_1$, twice that of incoming m_1 . (See V - V -plot Fig. 6.2 for large- m_1 .) The change ΔP of momentum m_2v_2 is the difference between FIN value $+m_2v_2^{FIN}$ and IN value $-m_2v_2$.

$$\Delta P = (+m_2v_2^{FIN}) - (-m_2v_2) = 2m_2v_2 + 2m_2v_1 \qquad (\approx 2m_2v_2 \text{ for: } v_2 \gg v_1) \quad (6.3)$$

So, if “atomic” velocity v_2 is large compared to v_1 it gives a **bang-force** $F=B \cdot \Delta P = \Delta P/\Delta t$ on m_1 .

$$BP = \Delta P/\Delta t = F = 2m_2v_2(v_2/2Y) = m_2v_2^2/Y \quad (6.4)$$

So a **force field** $F=2 \cdot KE/Y$ on m_1 due to m_2 is proportional to $KE = \frac{1}{2}m_2v_2^2$ or temperature T of m_2 . **Boltzman’s constant k** of proportionality ($KE=kT$) gives an **isothermal** force law $FY=2kT$. It is a 1-D version of **Boyle’s ideal gas law**: $PV=2kT$. Here a ceiling tries to keep energy or “temperature” of m_2 constant in spite of m_1 .

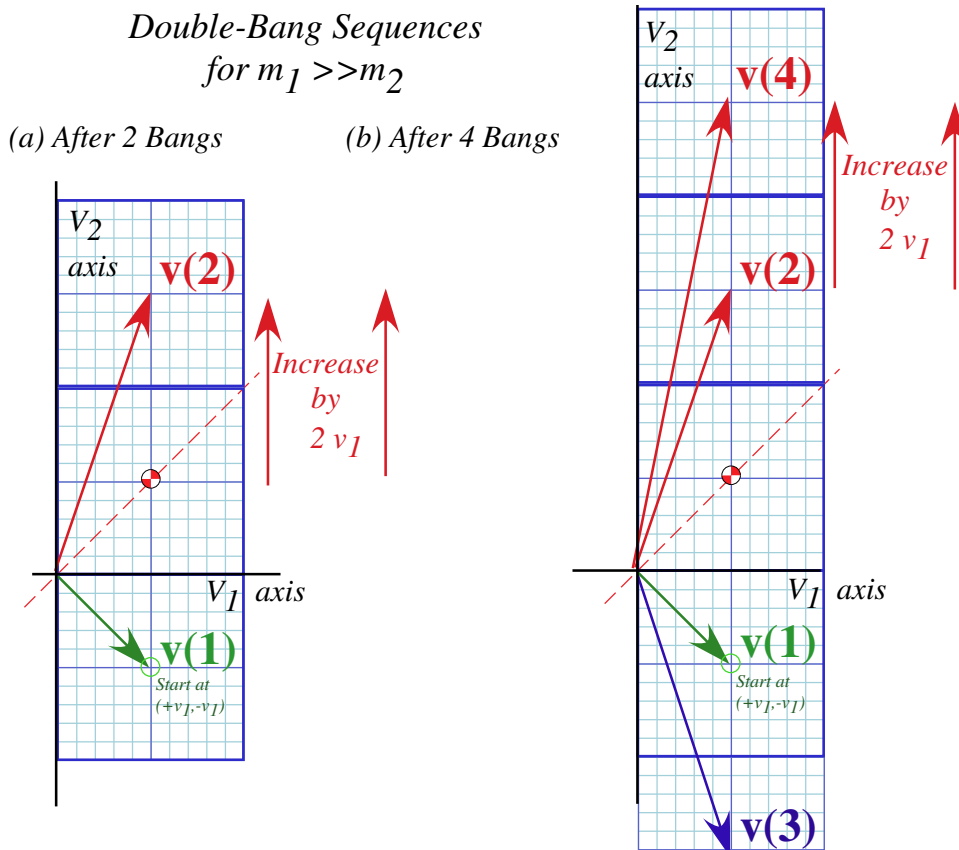


Fig. 6.2 Large mass-ratio ($m_1/m_2 \gg 1$) bounce sequence. (Compare to Fig. 4.2a.)

Adiabatic force laws

An elastic ceiling can't give or take energy so each m_1 bang adds velocity $2v_1$ to v_2 at rate $B=v_2/2Y$ (6.1). As m_1 closes at speed v_1 it reduces distance $2Y$ that m_2 travels. So bang rate B grows due to more v_2 and less Y .

$$\frac{dv_2}{dt} = 2v_1 B = 2v_1 \frac{v_2}{2Y}, \quad y = v_1 t = H - Y, \quad \frac{dy}{dt} = v_1 = -\frac{dY}{dt} \quad (6.5a)$$

We cancel time and v_1 to show this force is inverse- Y -cubed. That's a lot "harder" than inverse- Y in (6.4).

$$\frac{dv_2}{dt} = \left(\frac{dY}{dt} \frac{dv_2}{dY} = -v_1 \frac{dv_2}{dY} \right) = 2v_1 \frac{v_2}{2Y}, \quad \frac{dv_2}{v_2} = -\frac{dY}{Y}, \quad v_2 = \frac{\text{const.}}{Y} = \frac{v_2^{\text{IN}} Y(t=0)}{Y}, \quad F = \frac{m_2 v_2^2}{Y} = m_2 \frac{(\text{const.})^2}{Y^3} \quad (6.5b)$$

This is called an *adiabatic* or "fast" force law. Collisions are so fast that an isothermal-seeking "Robin Hood" in the ceiling hasn't time to steal m_2 's energy when it's judged too energy-rich or give energy back when m_2 becomes energy-poor. So m_2 can get hotter and hit m_1 harder and more often as gap Y shrinks.

Conservative forces and potential energy functions

Each force law (5.9) and (6.5) actually conserves the energy of the big- m_1 ball in the long run. By that we mean that m_1 will come out with practically the same energy that it had when it went in.

The adiabatic case is easier to see. Each bang conserves energy as demanded by the kinetic energy (KE) conservation relation (3.5a). Little-ball velocity $v_2 = \text{const.}/Y$ from (6.5b) is used here.

$$E = \frac{1}{2} m_1 v_1^2 + \frac{1}{2} m_2 v_2^2 = \frac{1}{2} m_1 v_1^2 + \frac{1}{2} m_2 \left(\frac{\text{const.}}{Y} \right)^2 = \text{const.} \quad (6.6)$$

The first term is m_1 's *kinetic energy* KE_1 . The second term, which is really m_2 's kinetic energy, is called m_1 's *potential energy* PE_1 or just plain *PE*, and it is labeled $U(Y)$ since it varies according to height Y only.

$$E = KE_1 + PE = \frac{1}{2} m_1 v_1^2 + U(Y) \quad \text{where: } PE = U(Y) = \frac{1}{2} m_2 \left(\frac{\text{const.}}{Y} \right)^2 \quad (6.7)$$

The *PE* is energy that m_1 lends to m_2 each time m_1 moves a distance ΔY closer so m_1 does a little bit of *work* ΔW on m_2 . *Work* is defined as *force times distance*. ($\Delta W = F \cdot \Delta Y$) *Power*, the rate of work done, is defined as *force times velocity*. Here distance is a small ΔY and the force F in (6.5b) is $m_2 \text{const.}^2/Y^3$. But "work" force might be plus-or-minus (\pm) $m_2 \text{const.}^2/Y^3$. Which sign? (+) or (-)? Conflicting sign conventions make force-physics confusing. The sign depends on how *force* and *direction* are defined. (It's all relative!)

Is it +or-? Physicist vs. mathematician and the 3rd law

A physicist's force F^{phys} is what is felt by a free object (Here that's m_1 .) whose motion is driven by force field $F = F^{\text{phys}}$. A mathematician's force F^{math} is what is needed to hold back the object in the force field. (How *apropos*! A physicist lets it *go* but a constipated mathematician holds it *back*!) They differ by (\pm) sign

only, that is, $F^{math} = -F^{phys}$, and F^{math} is the equal-but-opposite force by an object (m_1 here) on its field or force agent(s) (m_2 here). (This is essentially *Newton's 3rd law*. (NEWTON-THREE))

Force is momentum flow. Momentum is stuff that's conserved, so the flow rate F^{phys} of this stuff into an object m_1 must be balanced by an equal-but-opposite negative flow, $F^{math} = -F^{phys}$, out of the forcing agent(s) (m_2 here), and, *vice versa*, whatever flows out of m_1 flows into m_2 . Momentum $\mathbf{p} = m\mathbf{v}$ and force \mathbf{F} are both vector quantities and a \pm sign gives direction to-or-fro, another confusing (\pm) sign to bother us. But, whatever the flow rate F^{phys} seen by m_1 , then m_2 sees the opposite rate $F^{math} = -F^{phys}$.

Let's define positive Y and F direction to be away from the ceiling in Fig. 6.1. So incoming m_1 has negative velocity $v_1 = -\Delta Y/\Delta t$, but after m_1 reverses $V = \Delta Y/\Delta t$ is positive. Positive $V = -v_1$ (increasing Y) and positive F^{phys} means both momentum and energy of m_1 are being *increased* by force F^{phys} . Each bit of energy or work $\Delta W = F^{phys} \Delta Y$ gained by m_1 is energy lost by the force-field's potential "bank" that is m_2 . ($\Delta U = -\Delta W$)

$$\Delta W = F^{phys} \cdot \Delta Y = -\Delta U \quad \text{where: } F^{phys} = F(Y) = m_2 \frac{(const.)^2}{Y^3} \tag{6.8}$$

In other words, power $\Pi = F^{phys} \cdot V$ into m_1 is power ($-\Delta U/\Delta t$) out of the field. ($V = \Delta Y/\Delta t$ is m_1 's velocity.)

$$\Pi = F^{phys} \cdot V = -\frac{\Delta U}{\Delta t} = -\frac{\Delta U}{\Delta Y} \frac{\Delta Y}{\Delta t} = -\frac{\Delta U}{\Delta Y} V \quad \text{where: } F^{phys} = -\frac{\Delta U}{\Delta Y} \tag{6.9}$$

But is this consistent? Does force F^{phys} in (6.8) really equal minus the slope of potential (6.7)? We check.

$$F^{phys} = m_2 \frac{(const.)^2}{Y^3} \quad \begin{matrix} \text{consistent} \\ \text{with:} \end{matrix} \quad F^{phys} = -\frac{\Delta U}{\Delta Y} = -\frac{d}{dY} \frac{1}{2} m_2 \left(\frac{const.}{Y} \right)^2 = m_2 \frac{(const.)^2}{Y^3} \tag{6.10}$$

Well, *Yes!!* Note that $F = -\Delta U/\Delta Y$ needs that $1/2$ to be in kinetic energy $1/2 m_2 v_2^2$. (See discussion of (3.5).)

Isothermal "Robin Hood" and "Fed rules"

The isothermal case is a weird one. The little "force-field agent" m_2 maintains its kinetic energy at around the same initial value $1/2 m_2 v_2^2$ no matter how much the big mass m_1 loses or gains kinetic energy.

It's as though a "Robin-Hood" in the ceiling acts like a big Federal Reserve Bank. ("The Fed.") Whatever energy m_2 earns from m_1 over and above a some fixed deposit $1/2 (m_2 v_2^2)$ is taken and stored away, but if m_2 's deposits falls below that value, the Fed makes up the difference. This energy or deposit limit is determined by a prevailing allowed "temperature" of the ceiling or the current money supply. (I'm not making this up. It's what happens in nature and very roughly what happens in our economy. It becomes a problem if the Fed stops being Robin Hood and becomes robbing hood!)

Under ideal conditions, force agent m_2 makes a much "softer" $1/Y$ force field $F = m_2 v_2^2 / Y$ given by (5.9). Definition (6.9) of force F as negative- U -slope $-\Delta U/\Delta Y$ then gives a $\log_e Y = \ln Y$ potential.

$$F^{phys} = m_2 \frac{v_2^2}{Y} = -\frac{\Delta U}{\Delta Y} \quad \text{implies:} \quad U = -m_2 v_2^2 \ln(Y) \quad (6.11)$$

It may seem weird that we can define a useful potential while energy-funds are being siphoned in and out. Nevertheless, the ceiling “Robin Hood” is true to his word. (Analogy with “The Fed” ends here!) He puts back all the energy that m_1 gave up to m_2 (the potential U) on the way in, so that, except for small-change or “tips” left with m_2 after the final parting collision, m_1 recovers the energy it originally had. Such a force field, if determined by such a reliable potential, is also a *conservative* one. We discuss later the details of what is needed for general multi-dimensional fields to be labeled conservative.

Oscillator force field and potential

Consider a mass m_1 between two walls and two little speeding m_2 masses as in Fig. 5.5. m_1 feels a force like that of an oscillator. As m_1 moves distance x off center the left wall space expands to $Y+x$ and the right wall space shrinks to $Y-x$. Two opposing forces (6.11) then are unbalanced. (Only x^2, x^4, \dots terms cancel.)

$$F^{total} = \frac{f}{1+x} - \frac{f}{1-x} = f[1-x+x^2-x^3\dots] - f[1+x+x^2+x^3\dots] = -2f \cdot x - 2f \cdot x^3 -$$

Here we let $Y=1$ be a unit interval and assume an isothermal kinetic constant $k \equiv 2f = 2m_2 v_2^2$ for each side. For small x ($x \ll 1$) the force F^{total} has a linear or Hooke’s law form, and the potential U^{total} is quadratic.

$$F^{total} \approx -k \cdot x = -\frac{\partial U^{total}}{\partial x}$$

$$U^{total} \approx \frac{1}{2} k \cdot x^2 = -\int F^{total} dx \quad (6.12)$$

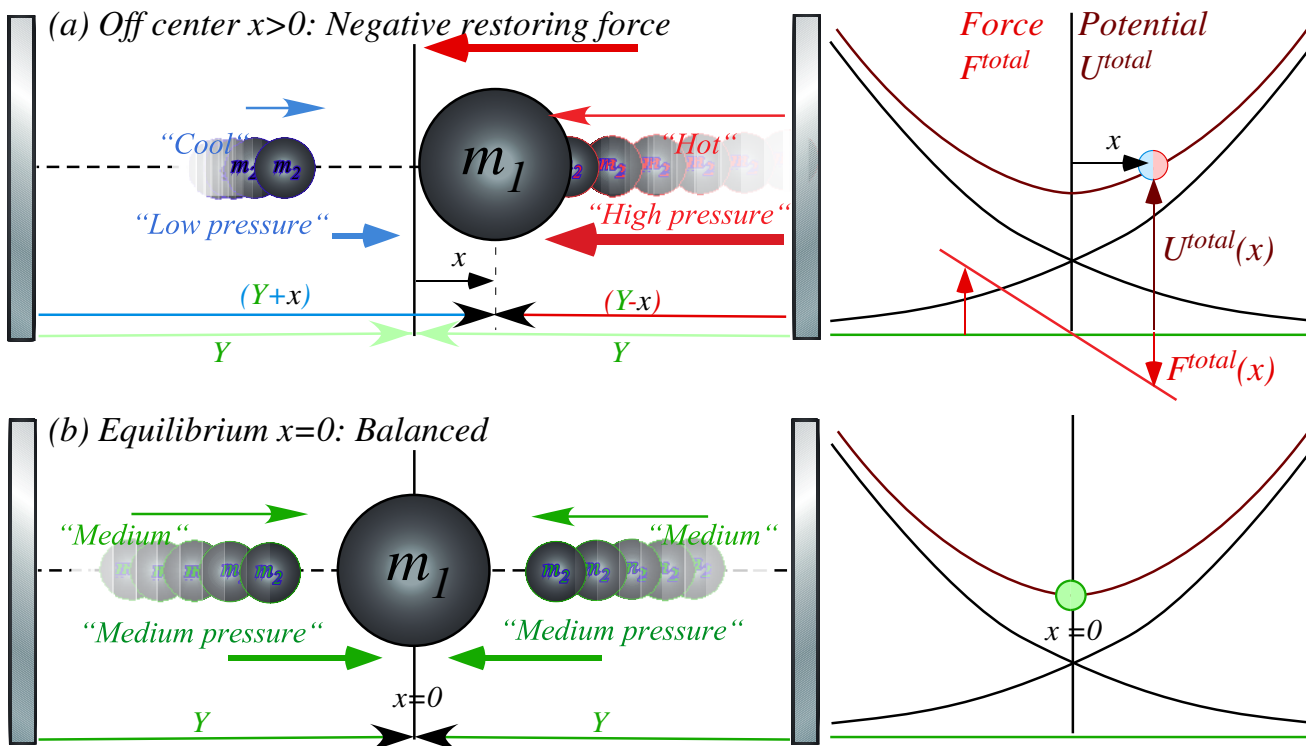


Fig. 6.3 Oscillator force and potential (a) Off center with (-)force (b) On center at equilibrium.

Harmonic oscillator forces and potentials are, perhaps, the most famous and useful ones in all of physics and come up more often in this book than any other. Normally, they are introduced as a mass on a spring, rubber band, or pendulum, only rarely (if ever) as three bouncy masses like Fig. 6.3. The 2nd most useful field is probably the Coulomb potential $U=-k/r$ and force $F=k/r^2$. (See Ch. 7 for electrostatics and Earth gravity, which also have oscillator potentials at their cores.) After that, the 2D Coulomb $U=k \cdot \ln(r)$ and $F=k/r$ may be the next most useful field. (The latter is like (6.11). A pair of them underlies Fig. 6.3.)

You should be warned that an oscillator like Fig. 6.3 is not as simple as it might appear, and as we will see, neither are springs, rubber bands, or pendulums. Also, balls bouncing against moving objects are particularly dicey devices. A simple model with one ball and one oscillating wall is called a *Fermi oscillator*, and is quite chaotic. The thing in Fig. 6.3 can be even more devilish if m_2 is not very small. *Caveat emptor!*

The simplest force field $F=const$.

We have mentioned power-law forces $F_{adiab}=k/y^3=ky^{-3}$ (6.5), $F_{Coul}=k/y^2=ky^{-2}$, $F_{isoT}=k/y=ky^{-1}$ (6.4), and lastly $F_{osc}=-ky$ (6.12), but have forgotten the simplest, namely *zero* power law $F_{const}=k=ky^0$. This last one is like a constant near-Earth-surface gravity force $F_{\odot}=-\frac{\partial U}{\partial y}=mg=-m/g$ on a mass m . ((-) sign for downward.) Acceleration of gravity near Earth's surface is nearly -10 meters per second per second and *very* nearly -9.8 . ($g=-9.7997m/s^2$) All terrestrial objects experience this whether they are bundled together or not.

All power-law forces $F=ky^p$ have power-law potentials $U=-\int F \cdot dy = -ky^p/(p+1)$, except for $p=-1$ where $F_{isoT}=k/y$ has a logarithmic $U_{isoT}=-k \ln(y)$. (6.11) Earth-surface potential $U_{\odot} = mgh$ is *linear* in height $y=h$. This we use to compute height of a superball toss by equating its floor level $KE=1/2mV^2$ to maximum $PE=mgh$.

$$gh_{max} = \frac{1}{2} V_{floor}^2 \quad (6.13a)$$

$$V_{floor} = \sqrt{2gh_{max}} \quad (6.13b)$$

Ejection height goes as the *square* of ejection velocity. A 3-fold velocity gain means $3^2=9$ -fold height gain.

Action is conserved (sort of)

It is remarkable that a bouncing mass has a physical property called *action* $S = \oint P \cdot dx$ that is more or less constant even if its position x momentum P and kinetic energy KE are driven crazy. Action is defined by the area of a one-cycle loop swept out in a momentum vs position *phase-plot* (P vs x). That is analogous to an energy or *power-plot* of force vs position (F vs x) whose loop area $\oint F \cdot dx$ is work per cycle.

Conservation of momentum and conservation of energy are each a rigorously obeyed axiom or theorem for an isolated classical system. However, conservation of action is “more or less” or “sort of” and “it depends” *for a driven system*. The concept of action is both subtle and deep and it lies at the heart of quantum theory for how we affect and are affected by the world around us.

Here we use a geometric construction of a bouncing ball trajectory to quantify action conservation or lack thereof. We suppose the little mass m_2 is caught as before in Fig. 5.1 and Fig. 6.1 between a rock and a hard place, that is, bouncing between a big mass m_1 (moving in at a constant velocity $v_1 = 1$ from the left) and a hard elastic wall. The big ball path is indicated in Fig. 6.4 by a line of slope=1= v_1 that hits an initially fixed m_2 following a vertical line (slope=0= v_2) that then gets knocked up to a line of slope=2= v_2 (after Bang(1)). Throughout the imagined collision sequence we suppose the ball is so much more massive that its change in velocity is not noticeable. This is in spite of the fact that it is absorbing more and more momentum from the little ball with each bang. (Surely *something* breaks eventually!)

Each time the small ball is banged elastically by the big one it picks up two more units of velocity that it maintains, apart from change in sign, through its subsequent bang with the elastic wall. Each time it returns for more, is banged again, and increases its speed by two units.

The horizontal dashed lines in Fig. 6.4 indicate the range Δx available to the small ball at each instant of its bang with the wall. Note that the product of the range Δx and the speed v_2 is a constant three units even as spatial range Δx rapidly decreases and the velocity range $\Delta v = 2/v_2$ increases just as rapidly.

$$\Delta x v_2 = 3.0 = \Delta x \Delta v / 2$$

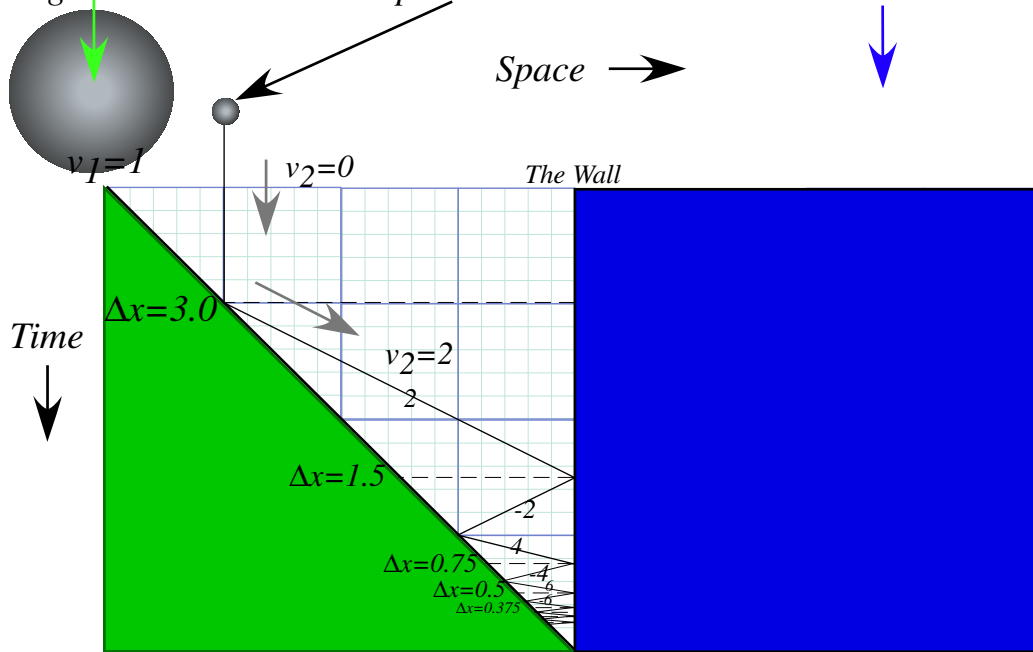
This is an example of conservation of action mentioned before. If we define the small ball's "range of velocity" by $\Delta v = 2/v_2$ then this relation takes the form of a weird kind of uncertainty relation, that is, it looks like Heisenberg's famous *minimum uncertainty relation* $\Delta x \Delta p = \hbar = (\text{constant})$ for position and momentum. It happens that the two are related even though the constant used by Heisenberg is an unimaginably tiny Planck constant ($\hbar \sim 10^{-34} \text{Js}$) compared to a constant 3.0 appearing above. (Ours has *gadzillions* of wave quanta!)

The geometry behind this relation is exposed in Fig. 6.4 (b). It is obtained by considering intersections between lines of integral speeds or slopes $v_2 = \pm 1, \pm 2, \pm 3, \pm 4, \pm 5, \pm 6, \pm 7, \dots$ that are relevant to the bang sequence. They are also relevant to quantum theory where the speeds of a particle in a box are indeed quantized to integers times a tiny number. (This is where that tiny \hbar comes in.) That is simply a reflection (pun intended) of the fact that mutually reflecting waves require that an integral (or half-integral) number of the wavelengths fit perfectly between mirroring containment walls or cavities.

Now we might ask if the action area $\Delta x \Delta v$ in Fig. 6.4c-e stays the same if the big-ball speed v_1 varies. Action variance was argued hotly by Einstein and the "quantum gang" at the 1920 Solvay Conference. They imagined a hotel chandelier being jerked up and down by a clerk upstairs. They concluded that if the clerk could not detect the swinging pendulum phase, then he would only rarely change its action.

Action and its wiggly antics will be discussed later, particularly in Unit 2 and 3.

(a) Big ball moves in and traps small ball between it and The Wall



(b) Trajectory geometry exposed

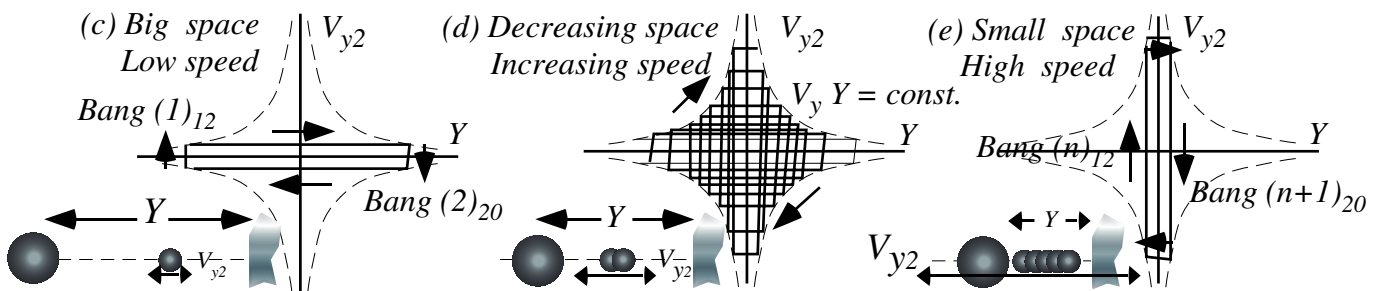
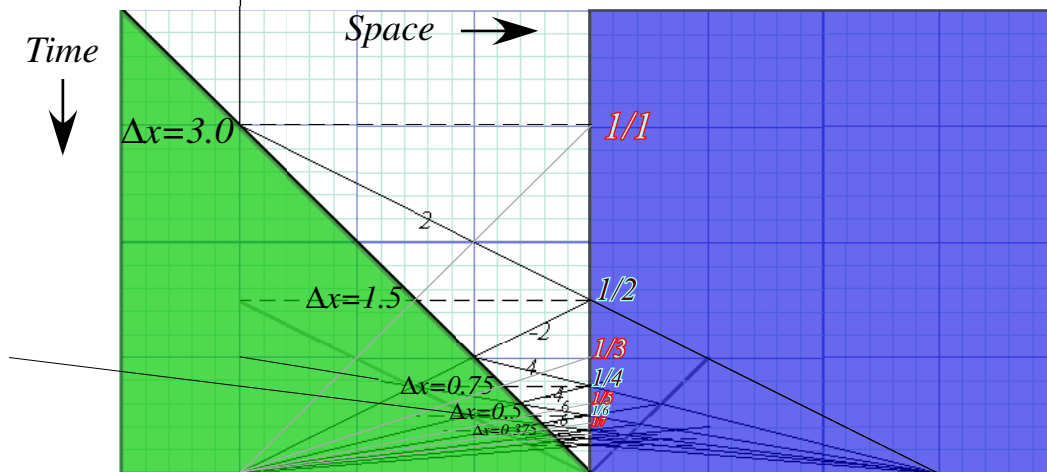


Fig. 6.4 Bang sequence for small ball between big ball and wall. (a) Spacetime paths. (b) Geometry

Monster mass M_1 and Galilean symmetry (It's *deja vu* all over, again.)

“Monster mass” M_1 bongs hapless m_2 -atoms in Fig. 6.4 using Galilean symmetry. To show symmetry we imagine two head-on monster M_1 's going at $\pm V_1 = \pm 1$ in Fig. 6.5. A mirror image of Fig. 6.4 lies in extended m_2 -path lines. The red paths of even integral velocity $v_2 = 0, \pm 2, \pm 4, \dots$ are copies of Fig. 6.4 paths. Odd integral velocity $v_2 = \pm 1, \pm 3, \dots$ paths mesh with even ones to make a full grid. Any initial v_2 between $\pm V_1$ has a path on the grid. A blue path is drawn thru a series of bongs with $v_2 = -0.2, +2.2, -4.2, +6.2, \dots$ in Fig. 6.5.

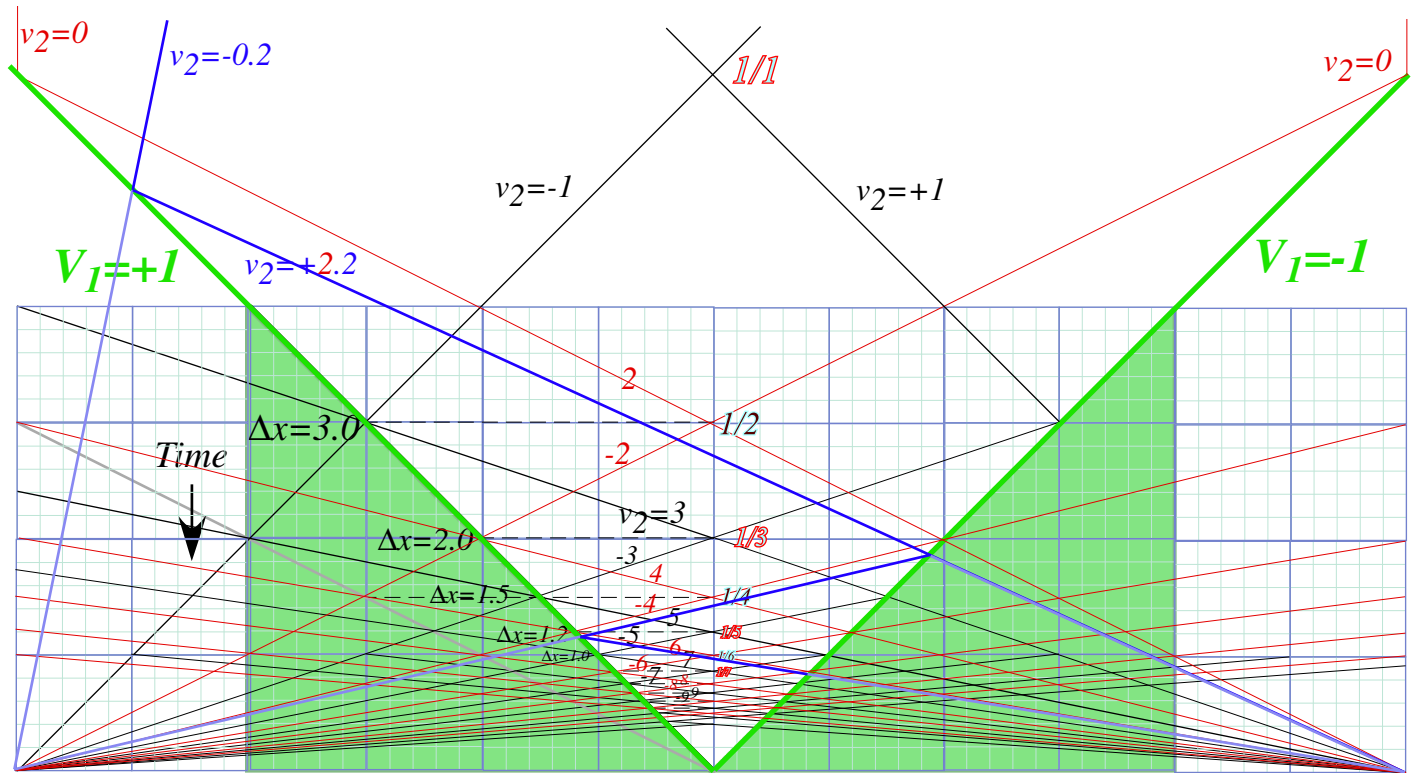


Fig. 6.5 Symmetric pair of head-on $V_1 = \pm 1$ monster- m_1 -masses pong tiny- m_2 -atoms to higher speeds.

Monster M_1/m_2 -ratios have simple V_1-v_2 -plots shown in Fig. 6.6a. (Recall Fig. 6.2.) It simply adds $2V_1$ to incoming speed v_2 of atom m_2 and M_1 bounces m_2 out at that speed. Monster M_1 is the COM and its path bisects in-and-out paths as it balances v^{IN} and v^{FIN} paths of atom m_2 . (In its COM frame each bong is simply a change of sign for velocity. Recall balance in Fig. 2.6.)

The geometry of adding slope $2V_1$ to speed v_2 is shown in Fig. 6.6a. It is based on the unit square and unit velocity $V_1 = 1$. Incoming $-v^{IN}_2$ is an altitude of a right triangle with vertical base $V_1 = 1$, and it is reflected thru the square diagonal to $+v^{IN}_2$ then added to $2V_1$ to give sum $v^{FIN}_2 = v^{IN}_2 + 2V_1$ as long side of the triangle with right side vertical base $V_1 = 1$ in Fig. 6.6a. The hypotenuse is the final path with final slope v^{FIN}_2 . Each m_2 -path and slope originates at $pt-B_-$ or else $pt-B_+$ ends of unit square base bisected by unit slope path of M_1 at B_0 . Fig. 6.6.c shows quadrilateral $B_+B_-A_+A_-$ bisected by M_1 path B_0CA_0 . Similar triangles explain multiple coincidences.

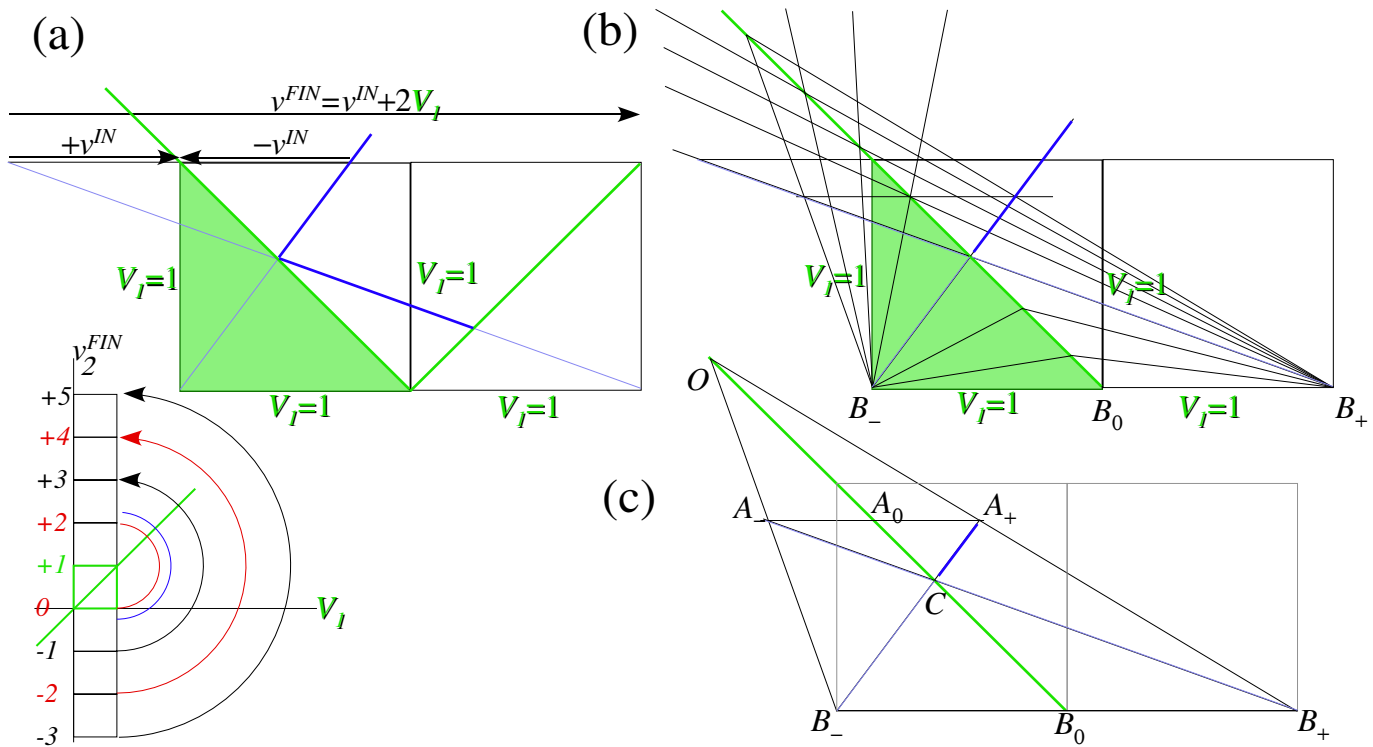


Fig. 6.6 Bisection geometry of Fig. 6.5.

Fig. 6.5 contains time plots for paths in different Galilean reference frames. An excerpt plot in Fig. 6.7a shows how Fig. 6.4 (copied in Fig. 6.7b) appears to a frame traveling at $V=1$ with each velocity in Fig. 6.7b reduced by $V=1$ in Fig. 6.7a. Also shown in Fig. 6.7a is the extension of lines connecting the two plots and this highlights this remarkable symmetry. All collision times in Fig. 6.7a match perfectly with ones in Fig. 6.7b though all velocities are shifted. This is as Galileo's symmetry would have it.

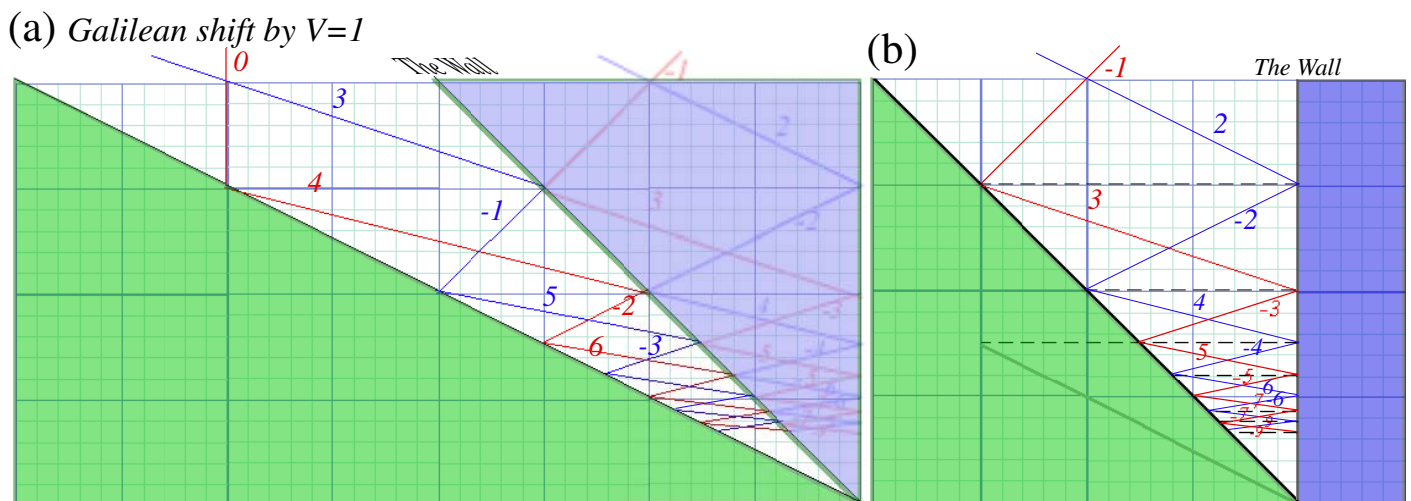


Fig. 6.7 (a) Galilean frame shift by frame velocity $V=1$ of collision sequence in Fig. 6.4 (shown in (b)).

Chapter 7 Interaction Forces and Potentials in Collisions

Derivation of force field potentials in Ch. 6 used elementary bangs by tiny m_2 's on a big M_1 . (Ch.5) We predicted elementary bangs between a ball and floor, ceiling, or another ball without knowing potentials. However, three (or more) objects having a *ménage a trois* are not so easy to predict, and outcomes of *3-body interactions* depend sensitively on whatever interaction potential or force law exists between participants.

Geometry of superball force law

When a superball or any elastic sphere hits the floor or ceiling it dents itself and, maybe it dents the surface it's hitting a little bit, too. But, if the floor, wall, or ceiling is much harder than the ball, we might assume only the ball develops a “flat-tire” as shown in the Figure 7.1a below.

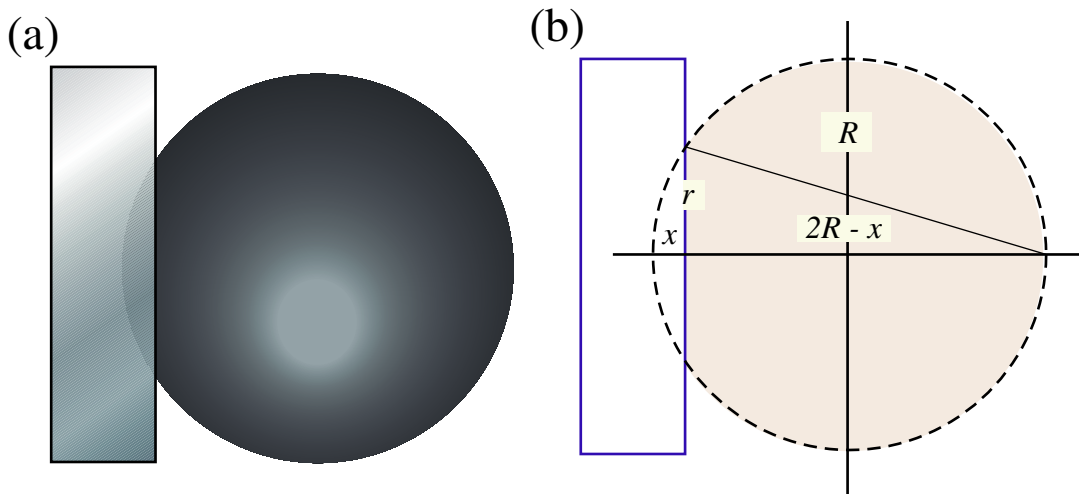


Fig. 7.1 Superball collides with solid wall. (a) “flat” (b) Saggital (“Bow”) mean geometry

The radius r of the ball's “flat” is indicated by an altitude in Fig. 7.1b and is the geometric mean of the depression distance x and the remainder $2R-x$ of the ball diameter. (Recall Fig. 1.4.8.)

$$r = \sqrt{x(2R-x)} \quad \left(\approx \sqrt{2Rx} \text{ for } x \ll R \right) \quad (7.1a)$$

Solving approximately for depression x gives the Saggital (“bow”) formula. (It's used for thin lenses.)

$$x \approx \frac{r^2}{2R} \quad \text{for } x \ll R \quad (7.1b)$$

How much force $F(x)$ is needed to depress the ball by distance x ?

The answer is, “It depends.” A hollow rubber ball or balloon with pressure differential P would push back with a force equal to the product of pressure P and area of contact $A = \pi r^2$.

$$F_{\text{balloon}}(x) = PA = P \pi r^2 \approx 2\pi PRx \quad (7.2)$$

This is a *linear force law* like the gravity law (1.4.11) inside the Earth sketched in Fig. 1.4.12.

However, the pressure and force in a superball or any solid varies non-linearly with x . Even if force varies only linearly with volume of the x -dent in Fig. 7.1b, it's still non-linear in x .

$$\begin{aligned}
 \text{Volume}(X) &= \int_0^X \pi r^2 dx = \int_0^X \pi x(2R-x) dx \\
 &= \int_0^X 2R\pi x dx - \int_0^X \pi x^2 dx = R\pi X^2 - \frac{\pi X^3}{3} \approx \begin{cases} R\pi X^2 & (\text{for } X \ll R) \\ \frac{4}{3}\pi R^3 & (\text{for } X = 2R) \end{cases} \quad (7.4)
 \end{aligned}$$

(Here we check that our integral gives the whole ball volume $4\pi r^3/3$ for $x=2R$. That's the equivalent of crushing the superball into a black hole (or black sheet). It's likely to complain before we get that far!)

Dynamics of superball force: The Project-Ball story

One of the interesting things to come out of *Project Ball* was the superball's peculiar force law behavior. The USC mechanical engineering department took an interest in this crazy project when it showed up on NBC News "Ray Duncan Reports." They offered to measure the superball force curve on a precise tension meter. But, that curve never worked. It didn't predict the bounces the students were observing. Nothing was making any sense even though we had a big analog computer working it all out.

That was a low point in the project. Even with all this fancy experiment, computers, and theory, I looked like I didn't know what the heck I was doing. So, what's new? That's science most of the time! But, to make things worse we got kicked out of the Project Ballroom, the old basement Lab 69 that we'd squatted in. It was up to be repainted so we had to drag all our stuff out of there and store it down the hall.

Well, after that I had to do something with the students so I arranged for a visit to Whammo Mfg. Co. in San Gabriel, California, where superballs and other goofy stuff was made. The Whammo man said maybe we could talk business about selling our super-elastic effects as a toy. So, a day or so later, with \$\$-signs in our eyes, we piled into our cars and drove down to the plant.

The trip to Whammo

By the time we got there, the inventors were on an all-day alpha-wave break. That's a 60's fad where you try to increase your creativity by looking at your brain waves. I said, "Maybe, I could use some of that stuff!" But, the company lawyer wanted to show us around. After awhile, he said he thought our invention was cool, but its product liability potential looked too high to make a commercial toy.

We all must have looked pretty sad after hearing that. So he went in a back room and dragged out a big collection of superballs that had been rejected for one reason or another. "Here, take as many as you want!" We thanked him and loaded the balls into some boxes and headed back to USC.

When we got back to Rm 69, the painters were done but the paint wasn't quite dry. So I said, "Let's drop off our new balls so we're ready for tomorrow." The students took "drop" to mean literally and dumped them out of the boxes into the empty room. Right away the balls bounced into the wet paint and made lots of little polka-dot spots all over the floor and wall. What fun! What a mess.

Eureka! Polka-dots save Project Ball

But, suddenly, it occurred to me what was wrong with our force analysis and how we might fix it. The engineers had carefully and slowly produced a static or *isothermal* force curve, but what we *really* needed was a fast-response or *adiabatic* force curve. I thought, "*Maybe that force law can be told by the polka-dots!*"

From a polka-dot radius r made by a superball of mass M and radius R dropped from a height h we could relate gravitational potential energy Mgh to an *adiabatic* superball potential energy U , that is, find a $U(x)$ curve for each value of $x=r^2/2R$ in formula (7.1b) by plotting height h against x given by dot radius r . Then the adiabatic force curve $F(x)$ can be found from the slope $dU(x)/dx$ of a $U(x)$ curve.

Just as the adiabatic $F=1/Y^3$ in (6.5) force curve is steeper and curvier than the isothermal $F=1/Y$ in (6.4) so was the polka-dot bounce curve steeper than what we had been using. We stuck our new $F(x)$ on the analog computer's diode function generator and started getting good predictions. Now we could work out the deadly *Model-X3*, a 3-ball super tower! (This is described Chapter 8.)

The “polka-dot” potential

First, let's look carefully at this “polka-dot” potential theory. What we did, like most of physics, was an approximation. Using gravitational potential to estimate superball $U(x)$ is a neat trick only if the superball forces are large and quick compared to the gravitational force or weight mg of the ball.

Fig. 7.2a shows a massive (Bowling-ball sized) superball at its ($V=0$) drop point h , where potential energy is mgh . Kinetic energy rises from zero as the ball falls down until it passes a point where the upward floor force cancels the ball's downward weight mg . That point- x_{static} of *static equilibrium* is at the bottom of the total potential energy curve in Fig. 7.2b. The ball would sit still if put gently at x_{static} with no kinetic energy. It's a point of zero slope since total force $F(x_{static})$ is zero there.

After passing x_{static} the ball slows down due to negative $F(x < x_{static})$. Finally it will have to stop at its maximum penetration point x_{max} where the energy line intersects the total potential line in Fig. 7.2c. Now the ball's gravity potential mg has been converted completely into potential energy $U(x_{max})$ (and frictional heat that we're ignoring) due to compressing rubber a distance x_{max} into the ball.

In the example, the ball's weight is almost as large as the inertial bang-force driving the ball into the floor. An indication of this is how flat the ball is in Fig. 7.2 b when its weight and compressive force are equal. A standard superball sits stiffly on a table with no noticeable depression, and mg is a tiny part of the total force, and because it's so stiff, its bang force is hundreds of times its weight and lasts only a few hundredths of a second. Very stiff rebounding potentials are shown in the later Fig. 7.3 and Fig. 7.4 b in which gravity is a negligible force after such a stiff rebound begins.

By comparison, the ball in Fig. 7.2 is heavy and its potential is not so stiff. Instead it is so soft it has a big “flat” if sits still with zero KE at x_{static} just as it does when passing that point in Fig. 7.2 b. The collision shown in Fig. 7.2 a-c is less like a bang and more like a lingering smooch! Similarly soft collision energy for a linear rebound force and quadratic potential is shown in parts (d) and (e) of Fig. 7.4.

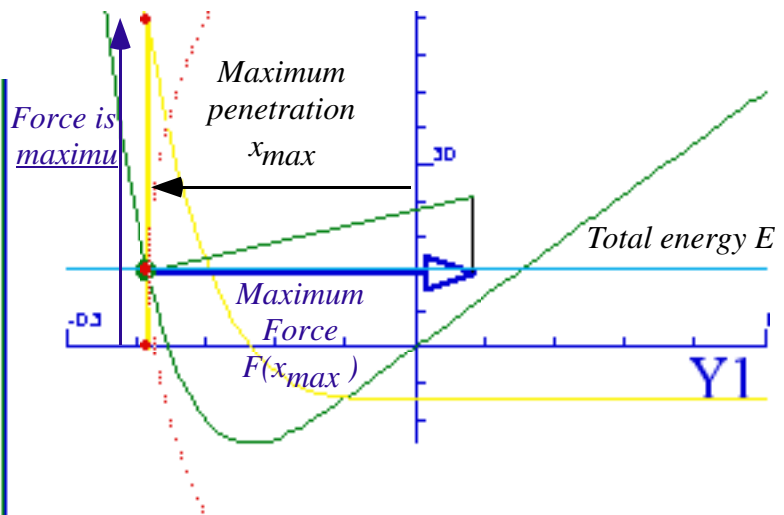
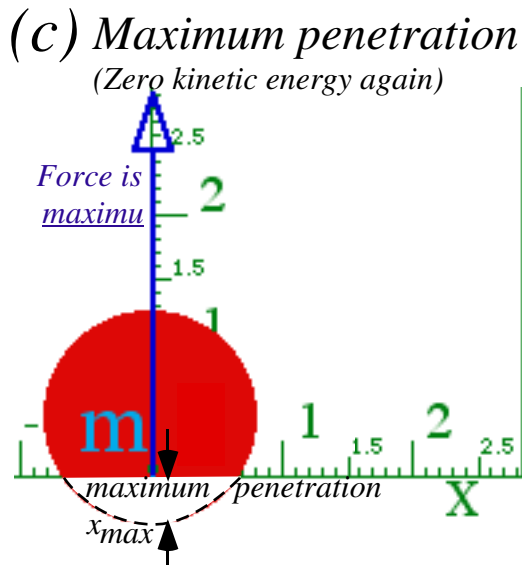
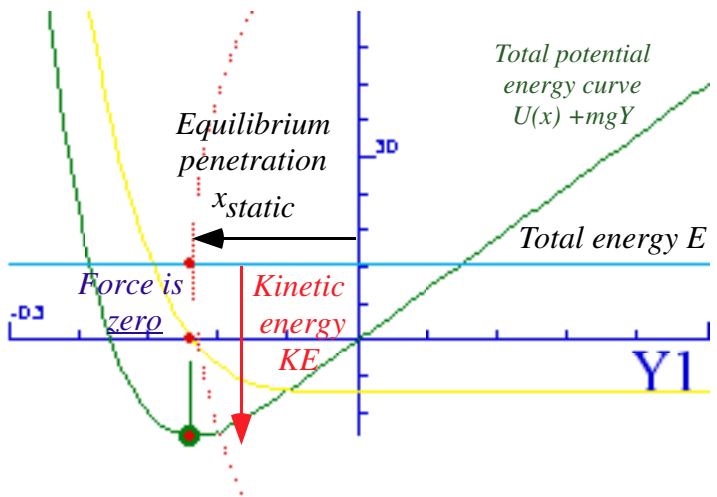
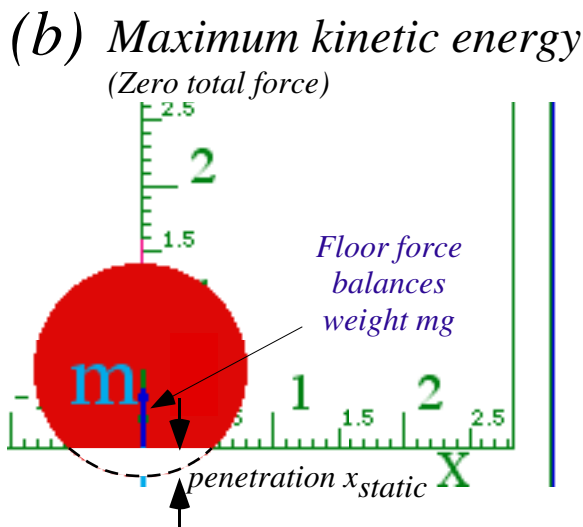
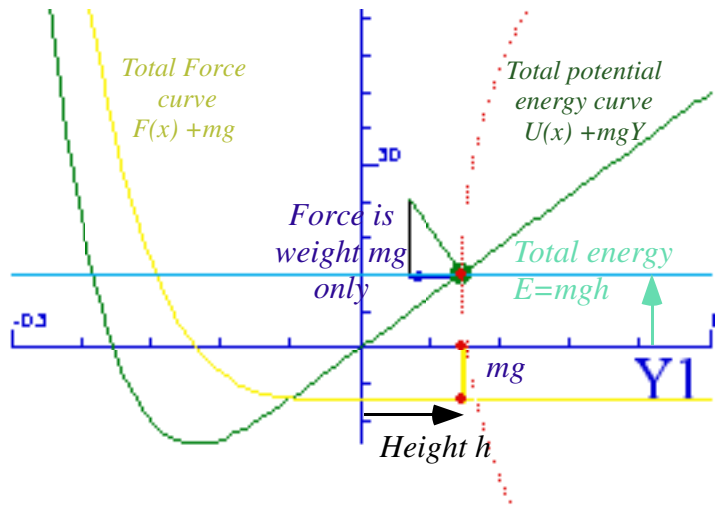
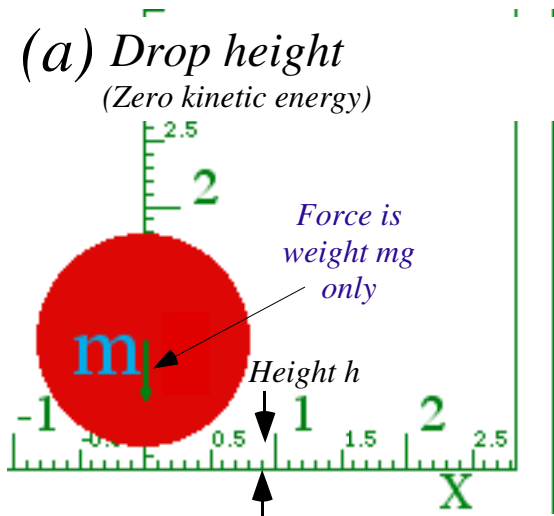


Fig. 7.2 Details of ball hitting floor (a) Ball is dropped. (b) Ball at max speed. (c) Ball at low point.

Force geometry: Work and impulse vs. energy and momentum

TV daredevils jump off 30-meter towers and belly-flop into kiddy-pools that are less than 1 meter deep. What a way to earn a buck! And, how do they ever survive such stunts?

Two important physical quantities tell about survival chances. The first is the product $F \cdot x$ of force-times-distance, or, more precisely, the integral $\int F dx$ of force over distance. The second is the product $F \cdot t$ of force-times-time, or, more precisely, the integral $\int F dt$ of force over time. (Recall the fundamental Galileo-Newton relations (3.10) and (6.0).)

The first quantity $\int F dx$ is *work* done or *energy* $-U(x)$ acquired. $U(x)$ is area under an $-F$ vs. x plot.

$$\text{Work} = W = \int F(x) dx = \text{Energy acquired} = \text{Area of } F(x) = -U(x) \quad (7.5a)$$

If energy is stored as potential energy $U(x)$, then force $-F(x)$ is the slope of a $U(x)$ plot at point x .

$$F(x) = -\frac{dU(x)}{dx} \quad (7.5b)$$

(Recall the discussion of force and potential leading up to (6.10).)

A second quantity $\int F dt$ is *impulse* done or *momentum* $P(t)$ acquired and area under an F vs. t plot.

$$\text{Impulse} = P = \int F(t) dt = \text{Momentum acquired} = \text{Area of } F(t) = P(t) \quad (7.5c)$$

If momentum is stored in kinetic velocity $V(t) = P(t)/M$ then force $F(t)$ is slope of the $P(t)$ plot at time t .

$$F(t) = \frac{dP(t)}{dt} \quad (7.5d)$$

The time equation (7.5c-d) is just Newton's 2nd law first given by (6.0). The space force law (7.5a-b) is just the slope rule first stated (with the physicist's minus-sign) in (6.9). Both laws deal with conserved stuff. If you, a daredevil, acquire x of this stuff (energy or momentum) sooner or later you are going to have to find something or someone help you get rid of x . Or else!

A daredevil falling 30 meters acquires energy equal to gravity force (body weight Mg) times *thirty* meters. Fig. 7.3a-b plots a constant $F = -Mg$ and a linear potential $U(y) = Mg y$ from $y=30$ to $y=0$. The 1m kiddy-pool must get rid of the $30Mg$ (*Newton meters*) of energy in *one* meter, by applying a force of $30Mg$ (*Newtons*) *steadily* over the *entire meter* from $y=0$ to $y=-1$. (That's a $30g \sim 300ms^{-2}$ deceleration. Human survivability is somewhere around $50g$.) An alternative is to get rid of that energy in the concrete below the pool in about *1 millimeter*, a *30 thousand g* deceleration. (That is *not* survivable!)

Kiddy-pool versus trampoline

Suppose the daredevil falls onto a special trampoline that applies exactly the same constant force as the kiddy-pool, but stores the energy as potential instead of dissipating it all by dousing the audience with a huge splash. The trampoline could then toss the daredevil back up to the 30 m tower to do the fall over again. (My gosh! What a daredevil has to do to satisfy a sated TV audience these days!) Such a potential is plotted by a steep-slope line $U(y) = -30y$ in Fig. 7.3b.

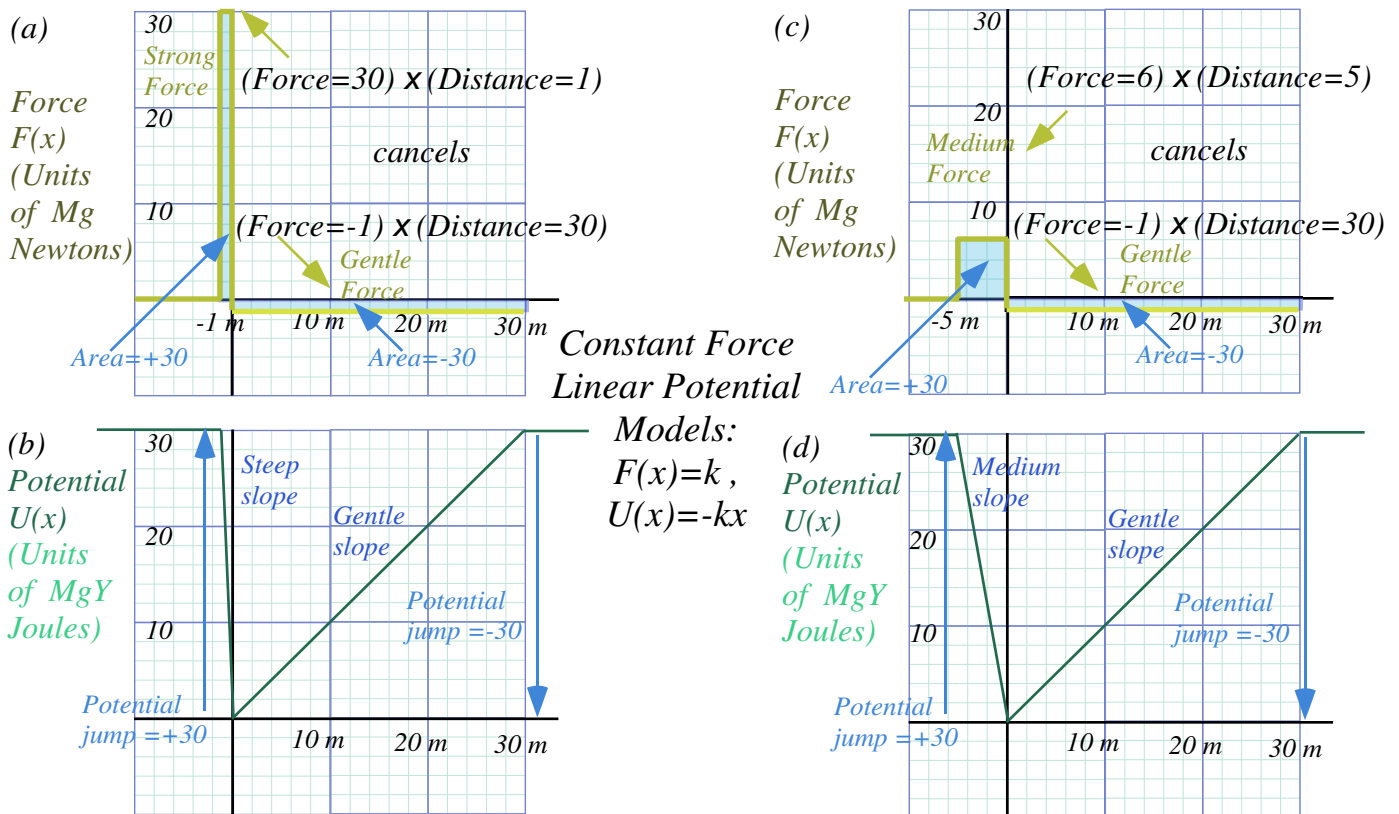


Fig. 7.3 Force and potential plots. (a-b) Strong (30g) deceleration. (c-d) Medium (6g) deceleration.

Suppose the Americans for Humane Daredevilry (AHD) demand that the deceleration distance be increased from 1 meter to 5 meters. (That’s what Olympic divers get for a 10 m fall.) As shown in Fig. 7.3c this reduces the deceleration by a factor of 5 from 30g to only 6g. (A walk in the park!) The sloping $U(x)$ lines are tallying the area-accumulation under the $F(x)$ lines. Starting on the right hand side, $U(x)$ drops by 30 units in 30 meters in Fig. 7.3b to correspond to the -30 units of area under the gravitational $F=-1$ unit line for the same distance in Fig. 7.3a. The daredevil’s kinetic energy must increase by 30 units to conserve total energy. So trampoline or pool is hit at 24 meters per sec. or 55 mph. (Recall (6.13).)

$$\frac{1}{2} M V^2 = 30 Mg \quad \text{or: } V = \sqrt{60g} = \sqrt{588} = 24.2 \text{ m/sec.}$$

Getting rid of this 30 J potential deficit means climbing a steep 30 J high slope between $y=0$ and -1 in Fig. 7.3b or a medium slope of the same height between $y=0$ and -5 in Fig. 7.3d. Both cases have the same +30 J area under a force line, but having 5 meters instead of just one reduces the force to $30/5=6$.

Time functions $F(t)$ and $MV(t)=P(t)$ relate to $F(x)$ and $U(x)$ using *Newton II*: $F=M^{dV}/_{dt}$ in (7.5d).

$$-U(x) = \int F(x) dx = \int M \frac{dV}{dt} dx = \int M \frac{dx}{dt} dV = \int MV dV = M \frac{V^2}{2} - \text{const.} \quad \text{or: } M \frac{V^2}{2} + U(x) = \text{const.} \quad (7.6a)$$

$$P(t) = \int F(t) dt = \int M \frac{dV}{dt} dt = \int M dV = MV + \text{const.} \quad \text{or: } P(t) - MV(t) = \text{const.} \quad (7.6b)$$

The first relation is *total energy conservation* ($KE+PE=\text{const.}$) first stated in (6.6) and (6.7).

Linear force law, again (But, with constant gravity, too)

Let's imagine the AHD demands further protection of daredevils from themselves by outlawing constant-force targets that turn on a full force suddenly upon entry. Claiming that "high-jerk" is bad, the AHD requires *linear-force* targets, instead. Physicists comply happily since a harmonic-oscillator linear-force-quadratic-potential (6.12) is the favorite force law. It also describes inside-Earth oscillation in Chapter 9.

Plots of linear-force-quadratic-potentials are shown in Fig. 7.4. Just like the preceding Fig. 7.3, a constant gravitational force $F_{grav} = -Mg$ is present both in and out of the ($y < 0$)-region where the linear $F = -ky$ force and the $U(y) = \frac{1}{2}ky^2$ potential exist as a sum of constant and linear forces for ($y < 0$).

$$F^{Total} = F^{grav} + F^{target} = \begin{cases} -Mg & (y \geq 0) \\ -Mg - ky & (y < 0) \end{cases} \quad U^{Total} = U^{grav} + U^{target} = \begin{cases} Mg y & (y \geq 0) \\ Mg y + \frac{1}{2}ky^2 & (y < 0) \end{cases} \quad (7.7a) \quad (7.7b)$$

If a linear potential $b \cdot y$ is added to a quadratic $a \cdot y^2$ potential we get the same parabolic curve $U = a \cdot y^2$, but that curve is shifted to the left by $y_{shift} = -b/2a$ and down by $U_{shift} = -b^2/4a$ as follows.

$$U^{Total}(y) = ay^2 + by = a \left(y + \frac{b}{2a} \right)^2 - \frac{b^2}{4a} = a(y - y_{shift})^2 + U_{shift} \quad (7.8a)$$

$$y_{shift} = -\frac{b}{2a}, \quad U_{shift} = -\frac{b^2}{4a} = -a \left(\frac{b}{2a} \right)^2 = -U(y_{shift}) \quad (7.8b)$$

The nose or tip of the parabola, which is the equilibrium resting point, follows an upside-down copy of the U -parabola itself! This important geometric fact is shown in Fig. 7.4. The geometry does not reveal itself until we look in Fig. 7.4e at a "soft ball" that is soft enough to clearly show its gravitational shifts. A hard superball is more like Fig. 7.4b that barely shows such a small shift.

Hardball total potential is $u(y) = 8y^2 + y$ with a total force function $f(y) = -16y - 1$ in graph units of Fig. 7.4(a-b). A medium total potential is $u(y) = y^2 + y$ with a total force function $f(y) = -2y - 1$ is plotted in Fig. 7.4(c-d). The latter clearly shows the equilibrium or lowest "sag" point of zero force. The softball total potential is $u(y) = (1/4)y^2 + y$ with a total force function $f(y) = -(1/2)y - 1$ in Fig. 7.4e. The hardball potential requires about 6 meters ($Y = -6$ or $y = -0.6$) to cancel the energy from the 30 meter fall (from $Y = 30$ or $y = 3$) and maximum force of about $F = 10$. This is much more than the constant $F = 6$ that stopped the same daredevil in 5 meters in Fig. 7.3c because a linear force has only the area under a triangle which has a factor of $1/2$. Here $\frac{1}{2}(F = 10)(Y = -6)$ gives the necessary energy of 30 Joules. So the AHD ruling has actually *increased* the maximum force on the daredevil! (But, only during the final milliseconds is F large.)

Note that the focus of the $U(y)$ parabola is on the y -axis because we plot gravity with $slope = 1$. Can you find a geometrical a way to locate that focus given some allowed stopping distance?

Parabolic geometry of an oscillator potential subject to a uniform (or nearly uniform) force field is an important one in physics. Electronic charges pinned to an atomic potential well behave like oscillators in an electric field of a passing light wave. Generally the light wavelength of 0.5 micron ($0.5E-6m$) is several thousand times as long as the atomic radius of a few Angstrom ($1E-10m$). So the effective potential is a rigid parabola like Fig. 7.4e shifting to and fro and up and down at some frequency.

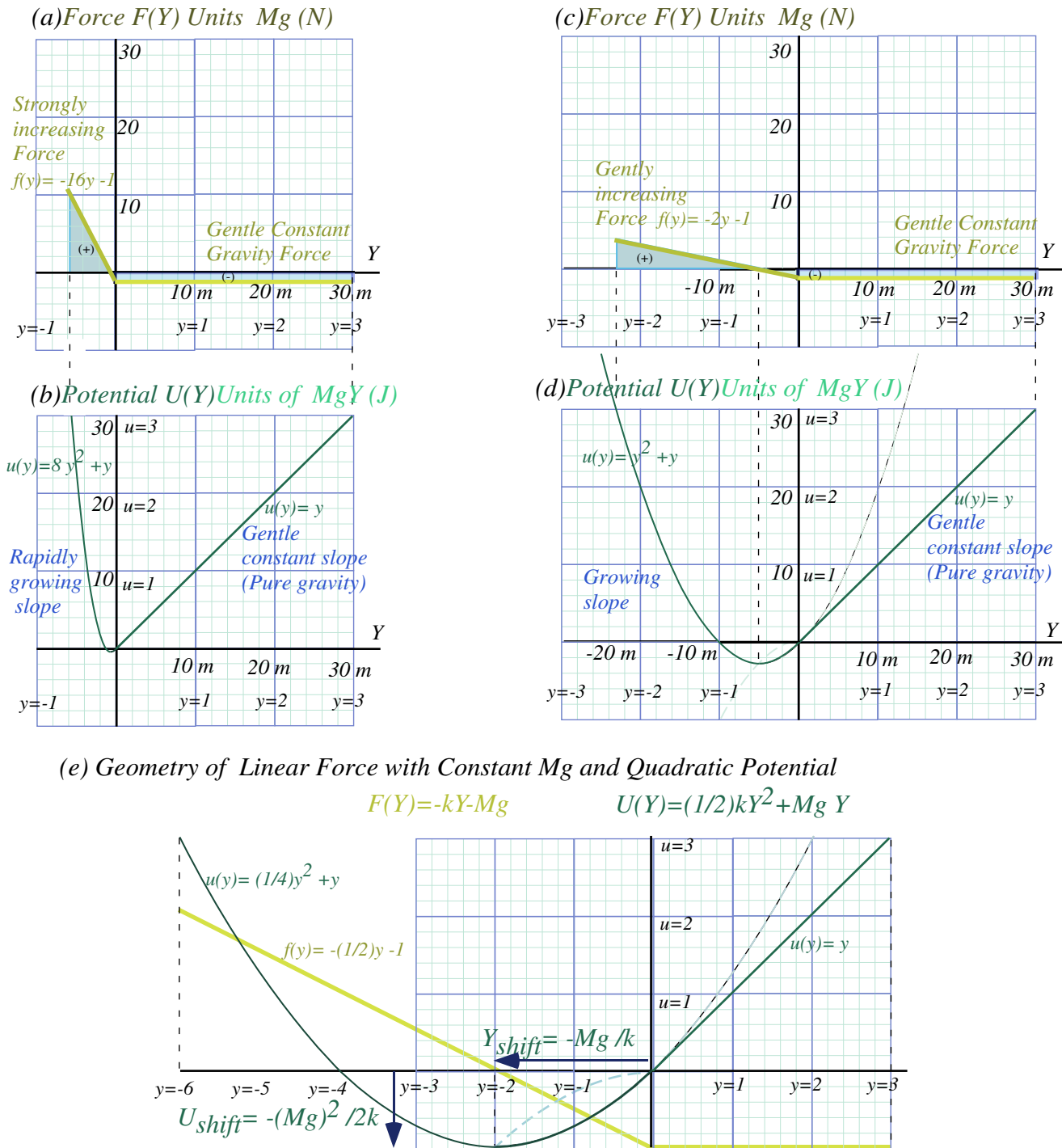


Fig. 7.4 Linear deceleration force after constant falling force. (a-b) Hard (c-d) Medium (e) Soft

As mentioned before, a superball force function is non-linear and approximated by $F_{ball}(y) \sim y^4$ as plotted in Fig. 7.2 and Fig. 7.5 below. Compare this to the linear balloon-like force curve $F_{balloon}(y) \sim y^1$ in Fig. 7.4e above. (Recall (7.2).) Note that $F_{balloon}(y)$ is a pair of straight lines bent at contact point $y=0$, while $F_{ball}(y)$ has a long flat region below $y=0$. A flat in $F(y)$ assures super-elastic bounce as we'll see. For either case, the force integrals $\int F^{total}(y) dy$ and the areas they represent cancel between any two points $y=h$ and

$y=y_{max}$ that have the same potential energy $U(h)=E=U(y_{max})$. If that energy is the total energy E then these points $y=h$ and $y=y_{max}$ are the *classical turning points* where the mass M stops with zero KE and zero speed to turn around and fall backward or forward, respectively, into the potential valley in between the turning points. This is a common feature of most oscillatory motion or vibration.

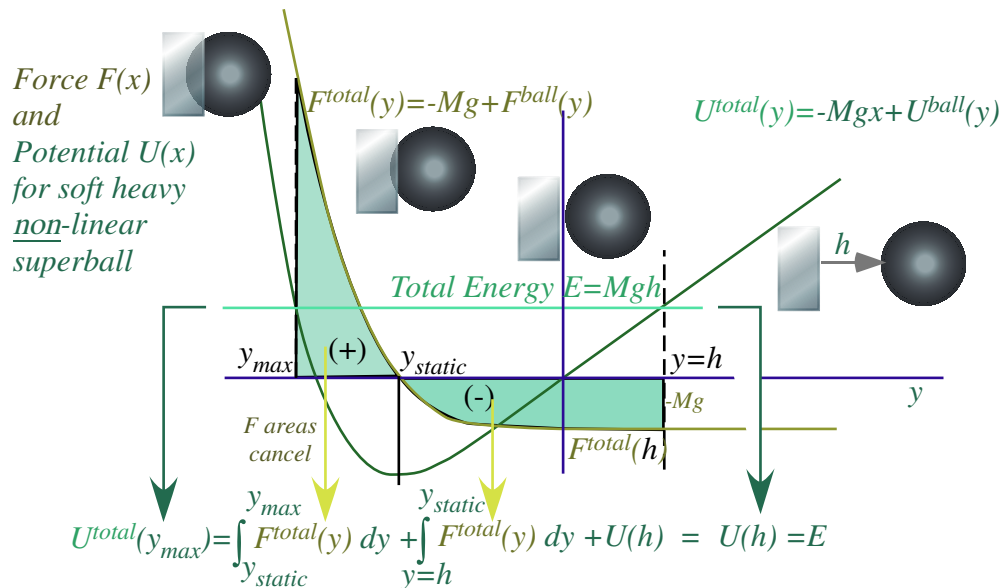


Fig. 7.5 Force and potential for soft nonlinear ($F=ky^4$) superball dropped from height h

Why super-elastic bounce?

Super-elastic bounce involving two balls was introduced way back in Fig. 4.5 and “explained” by the 2-Bang model sketched there. Is that the only explanation? Certainly not! Is it even right? Well, yes and no. Here is a chance to discuss how science works or doesn’t work. It is, after all, a human endeavor. (*To err is...*)

RumpCo versus Crap Corp

Let’s imagine a big scientific fight between two research groups something like real ones I’ve seen. We’ll imagine it’s about superball dynamics. On one side is a small but creative group working for the Rumpny Company® that first discovers the effect and explains it with the 2-Bang model. But their small budget limits them to things you can do cheaply with a ruler and compass.

On the other side is the huge Crap Corporation®. With unlimited military contracts, Crap Corp can afford any kind of computer or lab equipment. They hear about RumpCo’s discovery and decide to develop and sell it to the Army as a bomb detonation system.

I hope you’ll excuse a scatological nomenclature and contempt for shortsighted and mindless goals often associated with post-modern cash-flow-science. My allegorical objective is to encourage curiosity-driven-science that is now becoming regarded as quaint. I do believe that humans are capable of creating much more than fertilizer and should be strongly encouraged to do better. If earning gets in the way of learning, then humans do poorly. I have watched big labs in government, industry, and university die of a pernicious groupthink fueled by the acquisitive rather than the inquisitive human drives. People lose ability to reflect

and become happy to merely genuflect. A novel *Radiance* by Carter Scholz (Picador 2002) is a “Star Wars” *romaine a’clef* exposing foibles of scientists at Livermore and Los Alamos.

On one side of our allegory is poor but resourceful little RumpCo full of ideas but nowhere to go. Their 2-Bang model of super-elastic bounce is simple, elegant, but appears wrong. The powerful *Crap Corp.*, on the other hand, knows where it’s going and what’s right. It has every resource imaginable. Except wisdom.

Crap Corp.’s first move is to discredit RumpCo’s work. They set up a computer that uses lab observed potential functions to fully analyze a 2-ball bounce. Let’s compare two competing vu-graphs side-by-side.

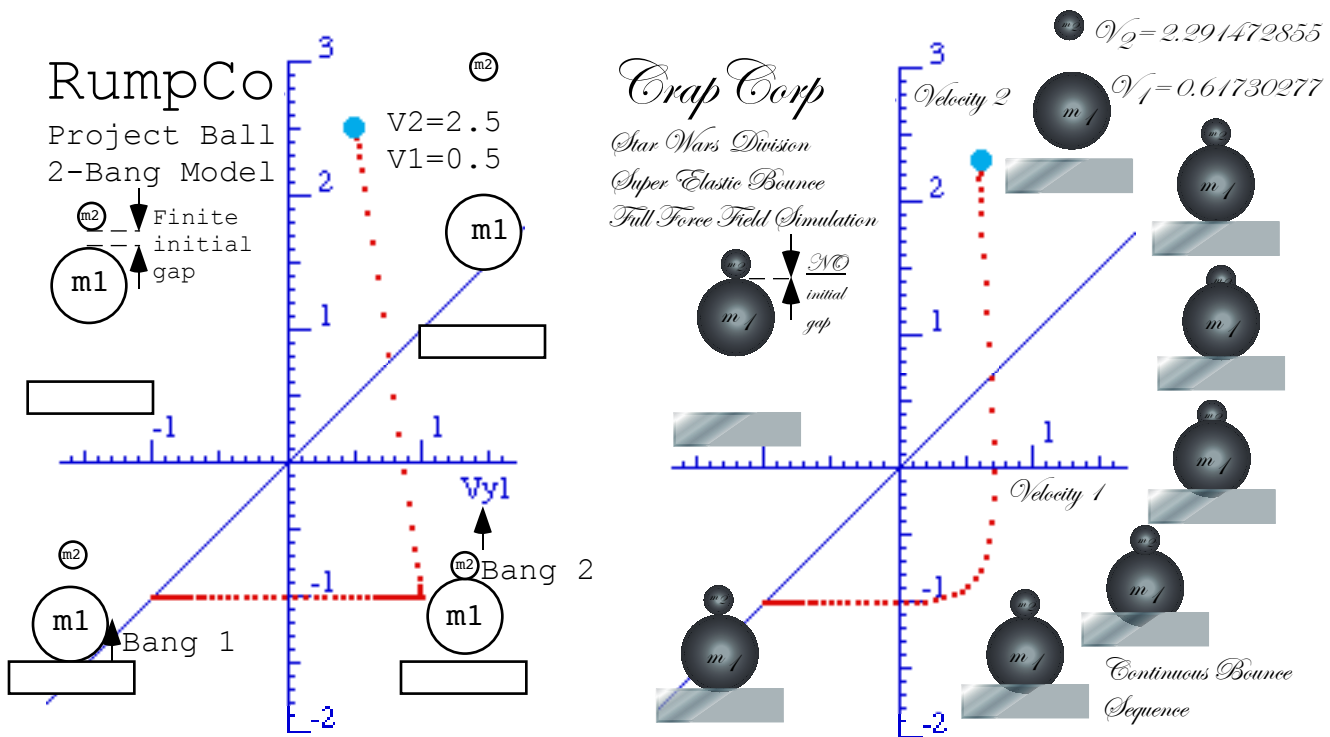


Fig. 7.6 RumpCo theory versus *Crap Corp.*’s simulation. (RumpCo) Finite initial gap (*Crap Corp.*) NO gap

One thing is clear. *Crap Corp.* does fancy-schmancy vu-graphs! They resemble wedding invitations. And, while *Crap Corp.*’s 10-figure precision is dubious, we note their $V_1=0.62$ and $V_2=2.29$ disagree with RumpCo’s predictions (Recall Fig. 4.4.) of final $V_1=0.5$ and $V_2=2.5$ by a little. Furthermore, RumpCo uses an independent 2-ball bang model. They assume or idealize an initial gap separating mass m_1 from m_2 so *Bang-1* of m_1 with the floor is independent of *Bang-2* between m_1 and m_2 . So V_1 and V_2 result from 2-body energy-momentum conservation. RumpCo’s results are not sensitive to force functions.

Crap Corp. can compute the difficult *3-body collision* between m_2 , m_1 , and m_0 (the Earth) all together just like what’s really happening on the floor. *Crap Corp.*’s curvy V_1 vs. V_2 plot in Fig. 7.6 is very sensitive to each force function $F(y)$ between each pair of colliding bodies. When (and if) *Crap Corp.* values check out with experiment, they’ll happily sneer at the primitive pair of straight lines in the RumpCo velocity plot.

Does RumpCo have nearly the right (V_1, V_2) for wrong reasons? Not entirely. The reason a 2-Bang model works at all is that the force function for these balls is highly *non-linear*. A quartic function $F(y)=y^4$ has

a flat bottom as noted before Fig. 7.5. That allows the floor- m_1 collision to nearly finish before the m_1 - m_2 bang really gets going.

Realizing this, the RumpCo researchers suggest that *Crap Corp* try a linear force $F(y)=y^1$ simulation to see if super-elastic bounce disappears. They do, it does, and the rest is history. As seen in Fig. 7.7, m_1 and m_2 bounce up in unison. It's a *pax de deus*. Super-elastic bounce goes away!

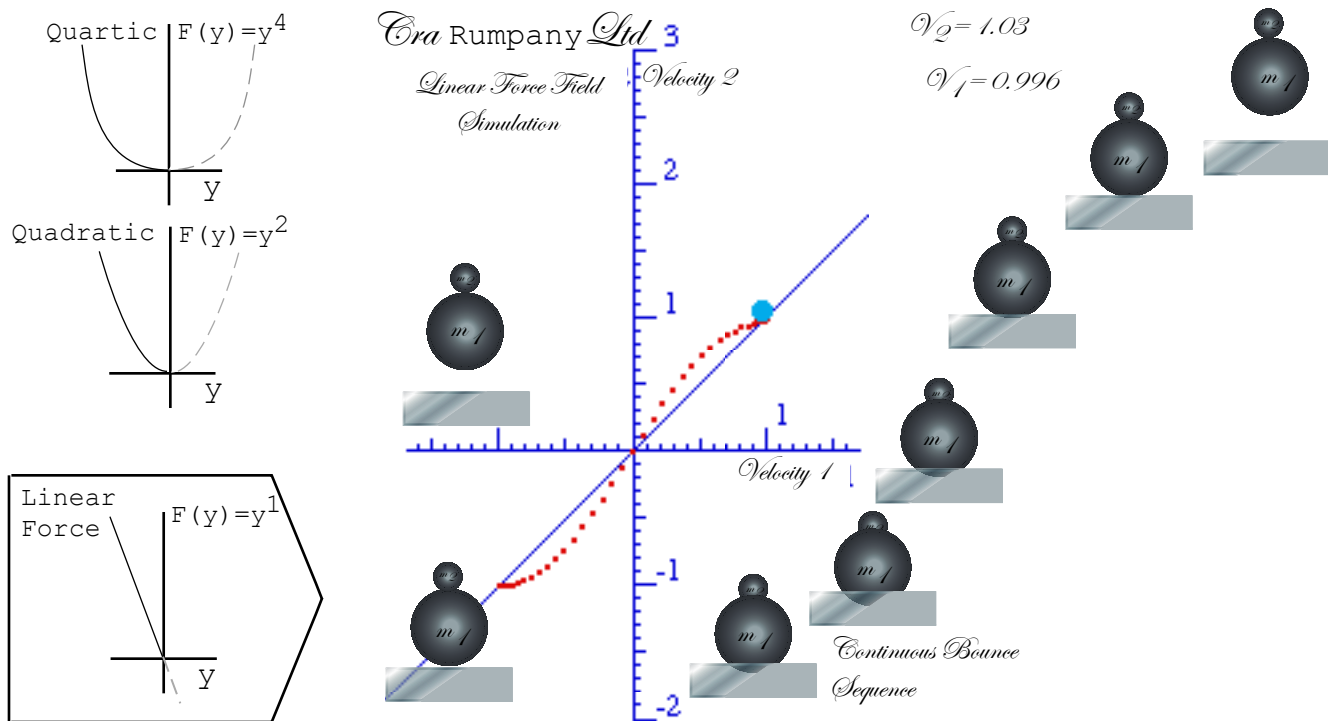


Fig. 7.7 Linear force kills super-elastic bounce. (Collaborative effort.)

The two groups decide to stop feuding and join forces. A corporate merger results in a multi-national conglomerate *Carumppany Ltd.* based in the Caymans. They lived happily ever after. (Sort of.)

Seatbelts and buckboards

Another important physics lesson from this section is, “Fasten your seatbelts...tightly!” To avoid great and damaging force you need to avoid non-linear force functions and fasten yourself with linear ones that can start working off your kinetic energy and momentum most immediately after a collision. The non-linear force with its “flat” region applies little or no force at first but then has to make up for its procrastination with deadly high force after it’s too late. Note how nonlinear force in Fig. 7.5 finishes much higher than the linear force in Fig. 7.4. Even worse is having no seatbelt at all. That’s like a very non-linear force of, say, $F(x)=kx^{100}$. It’s a flat gap with a practically vertical wall waiting to crush you!

One of the most dangerous vehicles in the Wild West of the early US was the *buckboard*, a wagon with no suspension except for a set of springs right under the rider’s seat. When the buckboard hit a bump it generally lived up to its name. Unfortunate riders ended up like a little m_1 superball knocked skyward by a big m_2 wagon. A safer and more comfortable ride is had in a car with a body as much heavier than the wheels and suspension as possible. Monster trucks have the worst kind of ratio possible for stability.

Friction and all that “dirty” stuff

Slowly we have put back some of the “real-world” features of the superball collisions that our idealized “Bang-Bang” models of Ch.4 ignored in order to make the problems more easily solvable. The effects of gravity during collision have been introduced and applied to interacting zero-gap superballs. More such effects will be studied in what follows since interacting linear forces are very common in nature and there are ways to make them easily solvable, too. The oscillating neutron star in Ch. 9 provides a taste of what is to come in the study of waves and oscillation in Unit 3.

But even the neutron star model neglects what is the bane of the purist physicist, the dreaded *frictional forces*. These are among the most neglected and poorly treated physical effects in physics. If anything goes wrong with a theory, we just blame it on friction! Often we have little choice in this matter.

Friction is a result of having more particles than we’d like to admit. Consider one $m_1=72$ gram superball. That’s about a *mole* of Carbon C_6 rings and a mole has $6.02E23$ (That’s *Avogadro’s number*.) of these C_6 molecules. So we’re dealing with not *one* mass m_1 particle but an enormous heap with an unimaginably huge number $60,200,000,000,000,000,000,000$ of particles that individually are (mostly) friction-free and well behaved, but their mob-behavior is just plain abominable!

You’ve got to get down to at least the individual molecular level before “internal-friction” is pretty much a non-existent phenomena due to quantum mechanics. So what we call “frictional loss” is simply poor accounting of 60.2 gazillion chiseling thieves stealing bits of energy that turn up later as “heat.” In conservative economics the effect is known as “supply side” or “trickle-down.” Let’s see if we can account for energy chiseled by just *three* thieves. (And, then we’ll hire more thieves until we bankrupt the whole operation!)

Chapter 8 N-Body Collisions: Two's company but three's a crowd

Without knowing force and potential effects on superball collisions, it is often impossible to even approximately predict the outcome for $N=3, 4$, or more balls. But, if all N masses have independent one-on-one collisions with the floor, the ceiling, and each other, prediction can be done “Bang-by-Bang” as in Ch.5. Difficulty arises when three or more collide at once. Then prediction may need precise and detailed treatment of their interactive force laws. Elastic binary or one-on-one collisions in *one* dimension are solved completely by momentum conservation alone as we've done since Ch. 4. But, as we'll see, anything more complicated may require more work, and often it requires a *lot* more work!

The X3: Three-ball towers

One of the goals of *Project Ball* at USC was to optimize final velocity for superball towers with three or more balls stacked up like a pyramid as in a multi-stage rocket. One dumb idea was a cheap satellite launcher. It's dumb because, even if you could achieve 8 km/s (See discussion in Ch. 9.), you'd burn it up in the atmosphere. (Well, OK, but on the *moon*...?)

Actually we were happy just to break the theoretical 2-ball limit of 3.0-times-initial. (Recall discussion of the INF limit in and after Fig. 4.5.) As seen in Fig. 8.1a that is done quite easily by a 3-stage tower which achieves a velocity that is $V_3=3.41$ times initial drop-speed ($V_n(0)=1$ for $n=1,2,3$).

An even better final speed of $V_3=3.62$ is had in independent collisions caused by setting initial gaps between the falling balls as shown in Fig. 8.1(b) so each collision can be completed before the next one begins. Then the result becomes independent of the force law governing the detailed trajectory within each collision, and a geometric construction in Fig. 8.1(b), based on momentum conservation, finds velocity accurately if collisions are independent. This requires force non-linearity or large initial gaps that are enough to reduce or eliminate N -body contact effects for $N>2$.

Conversely, zero initial gaps often reduce the final velocity maximum below independent collision values. This is particularly true if the force law is linear as shown in Fig. 8.1(c). The 3-ball linear case comes out very much like the linear case for a 2-ball tower in Fig. 7.7. No single mass gains much speed over its neighbors. Super-elastic bounce is essentially squelched.

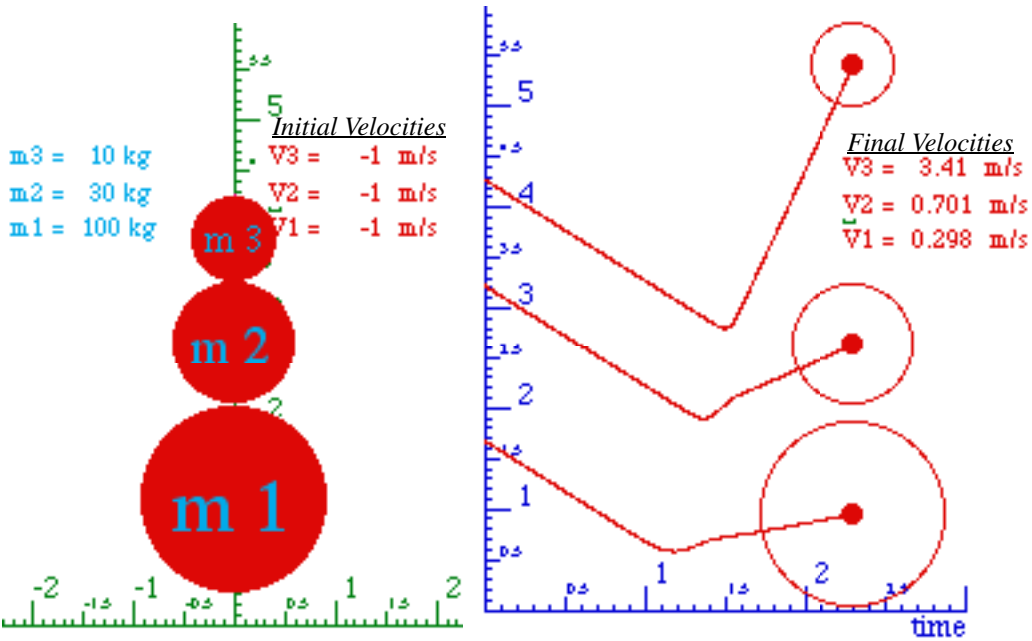
The American Journal of Physics[†] paper produced by *Project Ball* contains a discussion of attempts to optimize super-elastic bounce in towers of 3 or 4 balls. Progress was made but the theory needs work. As we will see later, this dynamics is somewhat analogous to wave motion in a varying channel. An early AJP paper^{††} has an analogy between a trumpet and a chain of sliding balls whose masses increase geometrically. It's also analogous to tsunami wave build-up. A rule-of-thumb is that optimum-velocity chains satisfy a geometric-mean mass relation $m_2=\sqrt{(m_1 m_3)}$ as is approximately so in Fig. 8.1. Later on, some of this technology was developed into a toy by Stirling Colgate (astrophysicist and toothpaste heir) and company.

[†] Class of WGH, *Am. J. Phys.* **39**, 656 (1971).

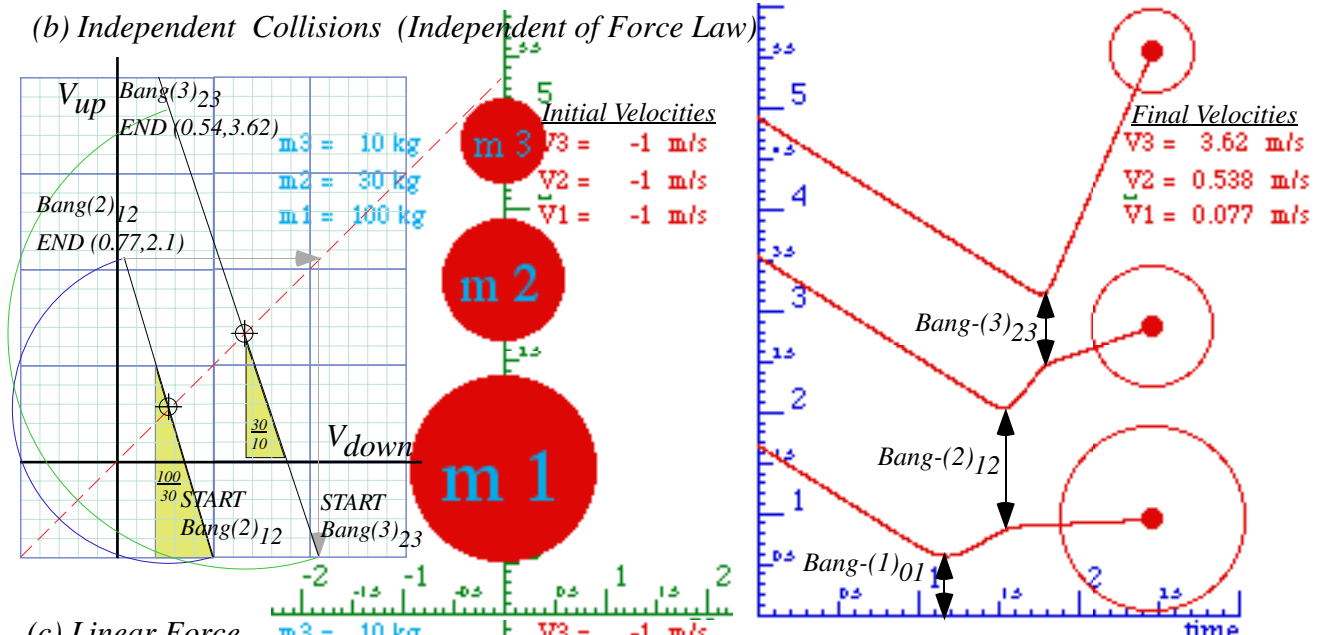
^{††} J. B. Hart and R. B. Herrmann *Am. J. Phys.* **36**, 46 (1968).

(a) Quartic Force

$$F(y) = ky^4$$



(b) Independent Collisions (Independent of Force Law)



(c) Linear Force

$$F(y) = ky$$

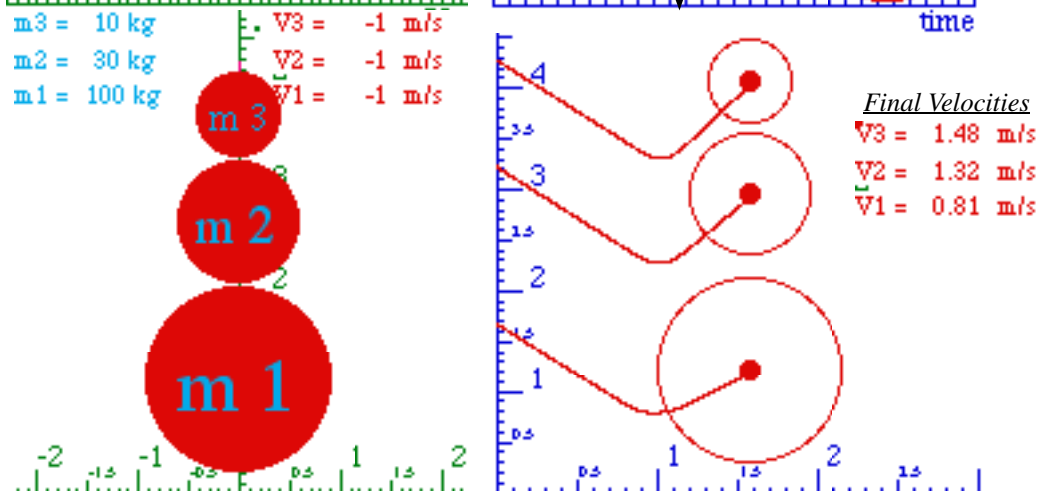


Fig. 8.1 Dropped 3-ball tower. (a) Quartic force (b) Independent (Finite gap) (c) Linear force.

Geometric properties of N -stage collisions

The 3-stage collision construction in Fig. 8.1b uses earlier construction of Fig. 4.4. It begins after the lowest mass $m_1=100$ has rebounded from the floor to the $Bang(2)_{12}$ START point ($V_1=1, V_2=-1$) where it meets mass $m_2=30$ and bangs up to $Bang(2)_{12}$ END point ($V_1=0.77, V_2=2.1$) on a slope $^{100}/_{30}$ line. The second velocity ($V_2=2.1$) of mass $m_2=30$ is then transferred (See gray arrows.) to the first component of $Bang(3)_{23}$ START point ($V_2=2.1, V_3=-1$). There m_2 meets mass $m_3=10$ and bangs it up to $Bang(3)_{23}$ END point ($V_2=0.54, V_3=3.62$) on a slope $^{30}/_{10}$ line, giving final top m_3 velocity $V_3=3.62$.

A 4-stage collision tower sequence with nearly the same mass ratios is constructed in Fig. 8.2(a). Here each mass $m_1, m_2,$ and $m_3,$ is exactly 3-times the one above it, and the top mass m_4 gets the biggest boost of nearly 5.8. Recall *Maximum Energy Transfer (MET)* case in Fig. 4.5 where a mass ratio of three ($m_1/m_2=3$) leaves the lowest ball stopped ($V_1=0$). In Fig. 8.1b m_1 is nearly stopped. ($V_1=0.077$).

The same arrangement with a higher mass ratio $m_k/m_{k+1}=7$ is constructed in Fig. 8.2b. Here the top mass m_4 gets a boost of over 9.0. That is a kinetic energy boost factor of $(V_4)^2=81$ and an altitude bounce of four or five hundred feet if dropped from arm's length. (Friction is being seriously neglected!)

Supernovae super-duper-elastic bounce (SSDEB)

Imagine dropping two towers like the ones in Fig. 8.2a-b from either side of a tunnel through the Earth so the two lowest m_1 -masses run into each other at the center. If the resulting collisions were elastic, they could send the other masses to infinity with energy to spare! Later we see escape from Earth's surface takes only three times the energy it takes to sit there. (*Starlet escapes!*) Energy factors for a conservative 3:1-tower are $2^2=4, 3.5^2=12.3,$ and $5.8^2=34.8$ and more than enough for a free ride to kingdom come. Astrophysical modeling of Type-II supernovae reveals just such a high speed SSDEB when a star, like a spherical layer-cake with lighter elements above heavier ones, collapses. *Boom!* It appears that most of our bodily stuff has come along on such a ride! As Carl Sagan remarked, we are of blown-up stars.

Newton's balls

Novelty stores have simple examples of multistage collisions made by hanging identical ball bearings in line as sketched in Fig. 8.2c-d. These are also common lecture demos, and they have been called "Newton's balls" to elicit giggles from otherwise boring lectures.

Few teachers explain the details of the cool pop-up-single in Fig. 8.2d. In fact, it won't work unless all the collisions are *independent*, and this requires *non-linearity* of the sphere-on-sphere force function, as we saw in Fig. 8.1. Cooler still, is an elastic 4-ball column-bounce in Fig. 8.3c. N -balls need $N(N+1)/2(=10$ if $N=4)$ independent bangs to get all N balls back with the same speed. Given this, it seems a wonder that solid objects can bounce elastically. (In fact, they cannot, quite!)

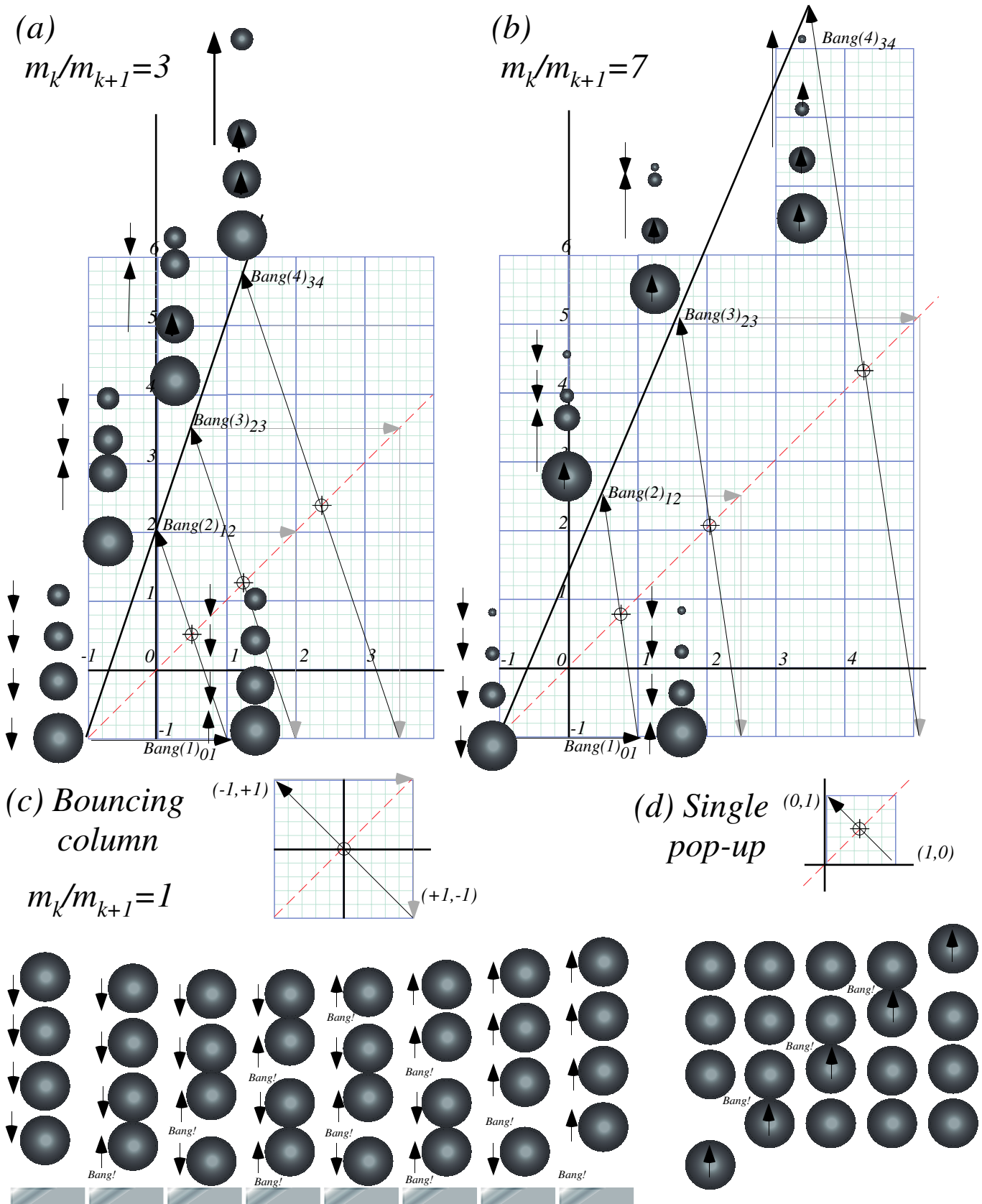


Fig. 8.2 4-ball towers. Mass-ratios m_k/m_{k+1} (a) 3, (b) 7, (c-d) 1. Independent bangs needed for all.

Friction, again: Inelastic energy-momentum quadratic equations

Perhaps, you noticed that *FINAL* velocity values could be found from *INITIAL* values by two different ways. Back in Fig. 2.1 we noted an easy way using a momentum conserving straight line and a circle through \mathbf{V}^{COM} from \mathbf{v}^{IN} to the answer \mathbf{v}^{FIN} . But, Fig. 3.1 showed another way using an energy-conserving ellipse to connect \mathbf{v}^{IN} to the answer \mathbf{v}^{FIN} . The first way uses simple linear equations and the second way uses more complex quadratic equations.

Why are there two ways? Often this means that situations exist where both are needed. Here friction or *inelastic* collisions make total kinetic energy decrease. (Recall our 60.2-gazillion thieves? They're *baa-ck!*) Such a situation is plotted in Fig. 8.3b with the energy decrease indicated by a smaller ellipse inside the initial ellipse in Fig. 8.3a. This is similar to an earlier Fig. 3.2.

The idea is that momentum conservation is still true even if the two masses are exerting sticky, energy-wasteful, forces on each other. No matter how wasteful those inter-particle forces may be, they still must obey Newton's 3rd axiom demanding equal-and-opposite forces on each other. So the final answer for \mathbf{v}^{FIN} must be at an intersection of the *old* momentum line with a *new and smaller* ellipse.

However, intersecting an ellipse and a line uses a *quadratic* equation. And, in Fig. 8.3, there appear *two* solutions to the quadratic equation. One \mathbf{u}^{FIN} we want is near the old energy-conserving \mathbf{v}^{FIN} . But, the other one that we now *don't* want is a \mathbf{u}^{IN} , which is nearer to the old \mathbf{v}^{IN} .

Let's look at a quadratic equation for u_I^{FIN} . There are two given constants $KE(u)$ and MV^{COM} .

$$m_1 u_1 + m_2 u_2 = MV^{COM} = p_u = \text{const.} \quad (8.1) \qquad \frac{1}{2} m_1 u_1^2 + \frac{1}{2} m_2 u_2^2 = KE(u) = k_u \quad (8.2)$$

The COM momentum p_u in (8.1) is a constant during the entire collision. Not so for the kinetic energy k_u in (8.2). It's just a given loss parameter that is quite difficult to predict. We first solve p_u for u_2 .

$$u_2 = \frac{p_u - m_1 u_1}{m_2} \quad (8.4a)$$

Then we insert the u_2 result into k_u equation (8.2) to get the needed quadratic equation for just u_1 .

$$\frac{1}{2} m_1 u_1^2 + \frac{1}{2} m_2 \left(\frac{p_u - m_1 u_1}{m_2} \right)^2 = k_u \quad \text{or:} \quad m_1 \left(\frac{m_1 + m_2}{m_2} \right) u_1^2 - 2 p_u \frac{m_1}{m_2} u_1 + \frac{p_u^2}{m_2} - 2 k_u = 0 \quad (8.4b)$$

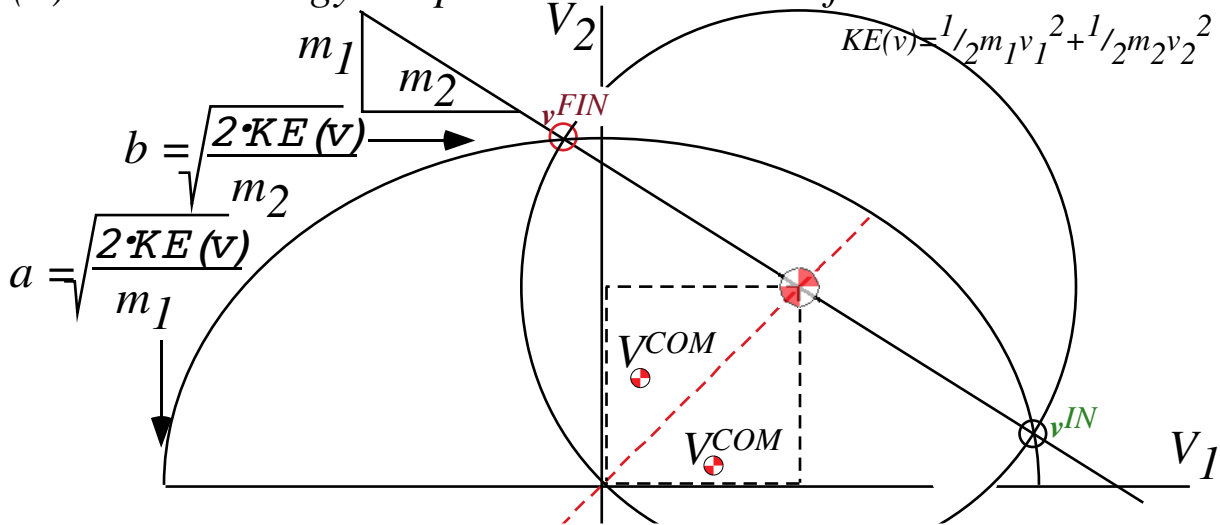
The solution isn't pretty but its \pm gives both u_I^{FIN} and u_I^{IN} shown in Fig. 8.3b.

$$u_1 = \frac{2 p_u (m_1 / m_2) \pm \sqrt{(2 p_u)^2 - 4 (m_1 / m_2) (m_1 + m_2) \left[(p_u^2 / m_2) - 2 k_u \right]}}{2 (m_1 / m_2) (m_1 + m_2)} = v^{COM} \pm \frac{\sqrt{p_u^2 - (m_1 / m_2) (m_1 + m_2) \left[(p_u^2 / m_2) - 2 k_u \right]}}{(m_1 / m_2) (m_1 + m_2)} \quad (8.5a)$$

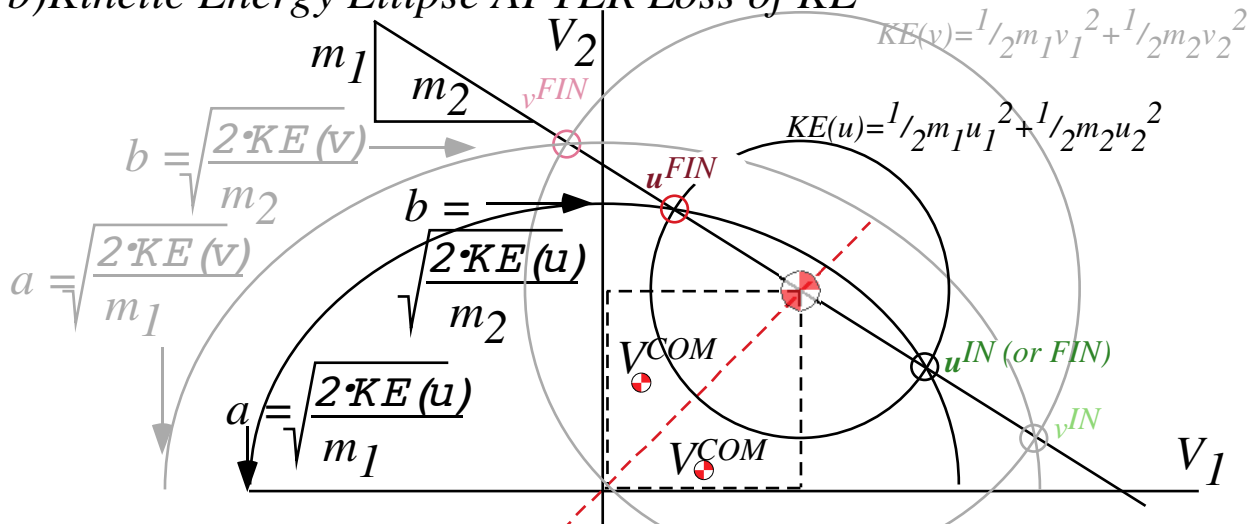
$$(8.5b)$$

The unwanted (+) solution u_I^{IN} (given that we started with v_I^{IN}) means the two balls "wiffle" through each other. In classical physics, only u_I^{FIN} makes sense starting with v_I^{IN} and only u_I^{IN} makes sense starting with v_I^{FIN} . In quantum theory, masses can "wiffle." Then *both* solutions make sense (sort of).

(a) Kinetic Energy Ellipse BEFORE Loss of KE



(b) Kinetic Energy Ellipse AFTER Loss of KE



(c) Kinetic Energy Ellipse AFTER M aximum Loss of KE

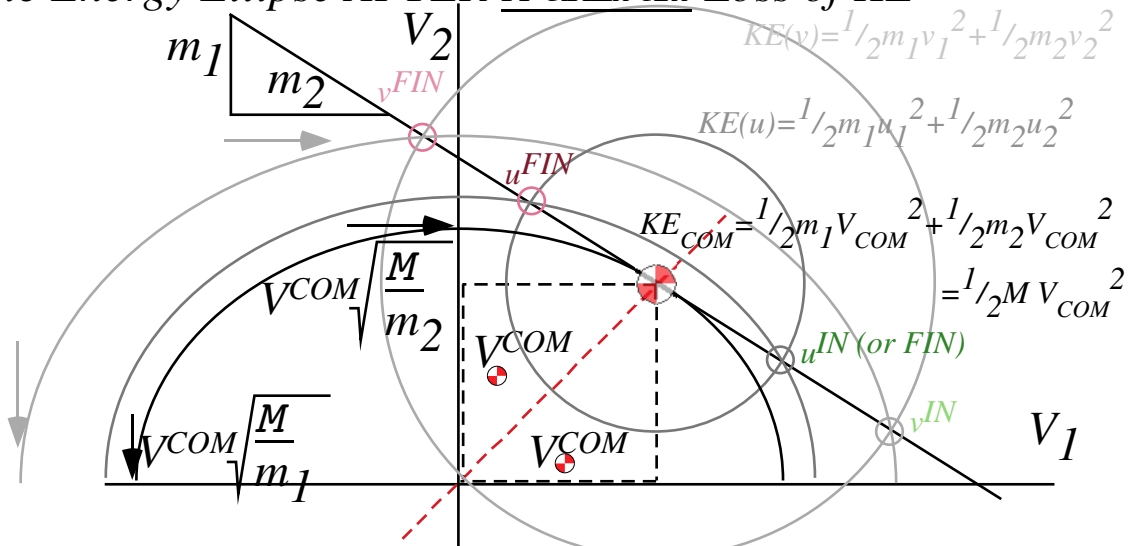


Fig. 8.3 KE-Ellipse shrinks by frictional loss. (a) Elastic (No loss). (b) Inelastic. (c) Totally inelastic.

Geometric construction of elastic and inelastic energy ellipses

Can you do quadratic solutions (8.5) with a ruler and compass? At first this seems difficult, but the energy ellipse construction in Fig. 3.5 and geo-mean square root construction in Fig. 1.8 can be used.

As shown in Fig. 3.6, an ellipse has two radii, a *major radius* a giving x -coordinate $x=acos\theta$, and a *minor radius* b giving y -coordinate $y=bsin\theta$. The Cartesian ellipse equation (3.7) is satisfied by these x and y , and polar angle parameter θ is eliminated. (x and y may switch places.)

$$\frac{x^2}{a^2} + \frac{y^2}{b^2} = 1 = \frac{m_1}{2 \cdot KE} (V_1)^2 + \frac{m_2}{2 \cdot KE} (V_2)^2 \quad (3.7)_{\text{repeated}}$$

Velocity values $x=V_1$ and $y=V_2$ have equal magnitude for initial *Bang(0)* ($V_1=-V^{IN}$, $V_2=-V^{IN}$) or *Bang(1)* (V^{IN} , $-V^{IN}$), and for a totally inelastic final state ($V_1=V^{COM}$, $V_2=V^{COM}$). The geometry needed to solve for the initial elliptic radii (a^{IN} , b^{IN}) in Fig. 8.3a or totally inelastic radii (a^{COM} , b^{COM}) in Fig 8.3c is described in Fig. 8.4. Then an energy ellipse in (V_1 , V_2)-space such as sketched in Fig. 8.3b may be constructed for any radii ($a^{FIN}\sqrt{R}$, $b^{FIN}\sqrt{R}$) where the *energy retention ratio* $R=KE^{FIN}/KE^{IN}$ ranges from $R=1$ down to $R_{min}=(a^{COM}/a)^2=(b^{COM}/b)^2$ as (a^{FIN} , b^{FIN}) range from initial radii (a^{IN} , b^{IN}) to totally inelastic (a^{COM} , b^{COM}) at the lowest KE allowed by momentum conservation.

The roots (8.5) are two points where energy ellipse and momentum line intersect. For totally inelastic collision they coalesce and the momentum line is tangent at (v^{COM} , v^{COM}) as in Fig. 8.3c. The slope $m_1/m_2=a^2/b^2$ of the momentum line is fixed no matter how much energy is wasted. So is ellipse aspect ratio $a/b=\sqrt{(m_1/m_2)}$. Square root construction (from Fig. 1.8) finds a/b from a^2/b^2 in Fig. 8.4a-c.

The construction begins by boxing the momentum line in the 1st quadrant and doubling it using a semi-circular arc around its upper left hand corner. An extended box including the arc is drawn in Fig. 8.4b. The center of the extended box is the center of a second arc that finds the square root $\sqrt{(m_1/m_2)}$ of the momentum line slope in Fig. 8.4c that is the desired ellipse aspect ratio a/b of all possible energy ellipses for the masses m_1 and m_2 . The basis of this construction is the mean geometry of Fig. 1.8.

Location of radii a^{COM} and b^{COM} in Fig. 8.4d uses vertical and horizontal projections of $pt-(V^{COM}, V^{COM})$ to the $(\sqrt{(m_1/m_2)}=a/b)$ -line. This is helped by the fact that $pt-(V^{COM}, V^{COM})$ lies on the ellipse *and* on the 45° line so that its x -coordinate ($x=acos\theta$) and y -coordinate ($y=bsin\theta$) are equal. Thus angle parameter is $\tan^{-1}a/b=\theta$, the a/b line slope. So x and y projections of (v^{COM} , v^{COM}) onto the θ -line yield hypotenuse lengths a^{COM} and b^{COM} in Fig. 8.4d. Concentric circles of radii a^{COM} and b^{COM} let us construct the ellipse as in Fig. 3.5.

Initial $pt-(V^{IN}, V^{IN})$ gives initial elliptic radii a^{IN} and b^{IN} in Fig. 8.4e. Square-radii ratio $(a^{COM}/a^{IN})^2=(b^{COM}/b^{IN})^2$ or ratio $(a^{COM}b^{COM})/(a^{IN}b^{IN})$ of the two ellipse areas lets us find the lowest possible kinetic energy retention ratio R_{min} . You should prove (geometrically *and* algebraically) that minimum ratio is given as follows.

$$\sqrt{R_{min}} = \frac{V^{COM}}{V^{IN}} = \frac{m_1 - m_2}{m_1 + m_2} \quad (8.6a)$$

$$\frac{m_2}{m_1} = \frac{V^{IN} - V^{COM}}{V^{IN} + V^{COM}} = \sqrt{\frac{1 - \sqrt{R_{min}}}{1 + \sqrt{R_{min}}}} \quad (8.6b)$$

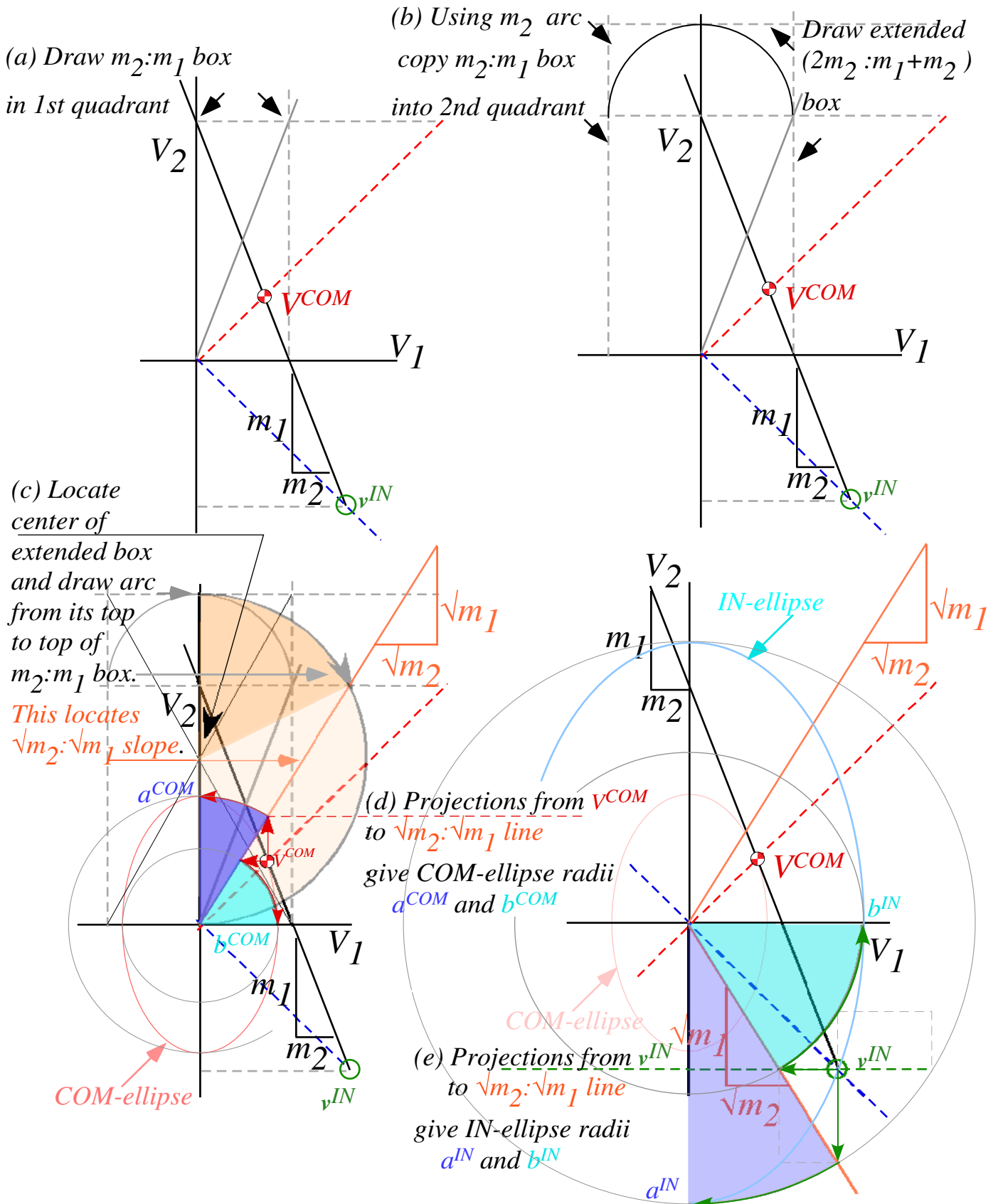


Fig. 8.4 Energy ellipse geometry. (a-c) Axes ratio $\sqrt{m_2}:\sqrt{m_1}$. (d) a^{COM} and b^{COM} . (e) a^{IN} and b^{IN} .

Ka-Runch-Ka-Runch-Ka-Runch-Ka-Runch...:Inelastic pile-ups

N-body collisions described so far have been mostly elastic. That's not true for California freeway pile-ups. California pile-up chains start when a cell-phony driver enters a fog at 60 mph and rear-ends a vehicle or vehicles that have slowed down or stopped. Cars drive bumper-to-bumper so dozens may be involved.

Pile-up mass grows with each car added to it by a series of inelastic "Ka-runch" collisions like Fig. 2.1 of Ch. 2. Cars may be added to a pile-up's rear or to its front or even to both ends. Fig. 8.5 shows a single 60 mph car piling up a line of five stationary cars and, *vice versa*, Fig. 8.6 shows a line of five 60 mph cars piling up on a single stationary car. Each pile-up collision loses as much energy as it can while keeping momentum constant. It makes the smallest ellipse that touches the momentum line in Fig. 3.2c and Fig. 8.3c.

In each case the sequence of velocity-velocity slopes is an *arithmetic progression* 1:1, 2:1, 3:1, 4:1,... similar to velocity sequences in Fig. 6.4 and Fig. 6.5. Both have lines that intersect on a single point and inverse or complimentary slope sequence 1/1, 1/2, 1/3, 1/4,..., known as a *harmonic progression*.

The incoming car in Fig. 8.5 has momentum $P^{IN}=mv=60$ and energy $KE^{IN}=\frac{1}{2}mv^2=1800$ with $v=v^{IN}=60$. The final pile-up mass $M=6$ has the same momentum $P^{FIN}=MV=60$ but reduced velocity $V=v^{FIN}=10$ and energy $KE^{FIN}=\frac{1}{2}MV^2=300$ down by 1500 units. (These are (very) Old English units. We take unit mass ($m=1$) cars.)

The incoming cars in Fig. 8.6 together have momentum $P^{IN}=5mv=300$ and energy $KE^{IN}=5\frac{1}{2}mv^2=9000$. The final pile-up mass $M=6$ has the same momentum $P^{FIN}=MV=300$ with increased velocity $V=v^{FIN}=50$ but reduced energy $KE^{IN}=\frac{1}{2}MV^2=7500$. The same energy deficit of 1500 units is seen in Fig. 8.5 and Fig. 8.6.

Of these two equal-energy-loss nightmares the latter is worse since it began with five times the kinetic energy and still has 7500 units to dissipate. Worse nightmares combine the two as shown in Fig. 8.7. This is a particularly troubling set of nightmares since there are many possible outcomes that have different orders of combination with differing results.

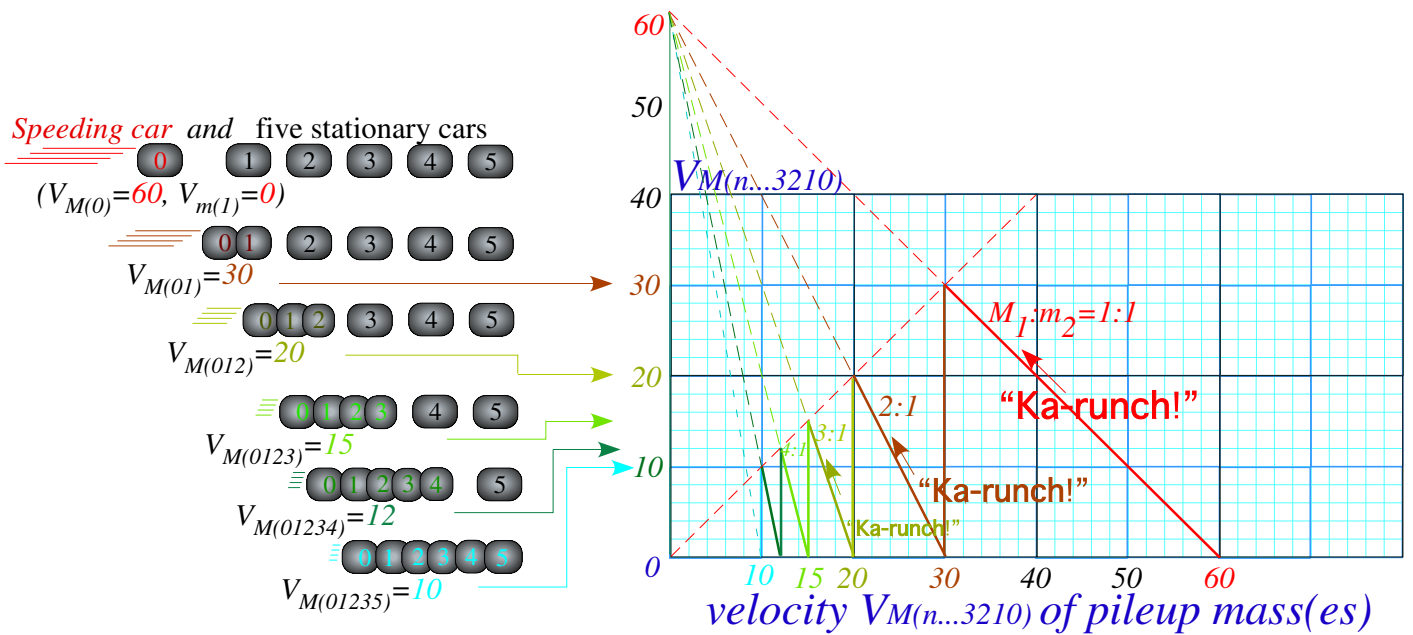


Fig. 8.5 Pile-up due to one 60 mph car hitting stationary line of five cars

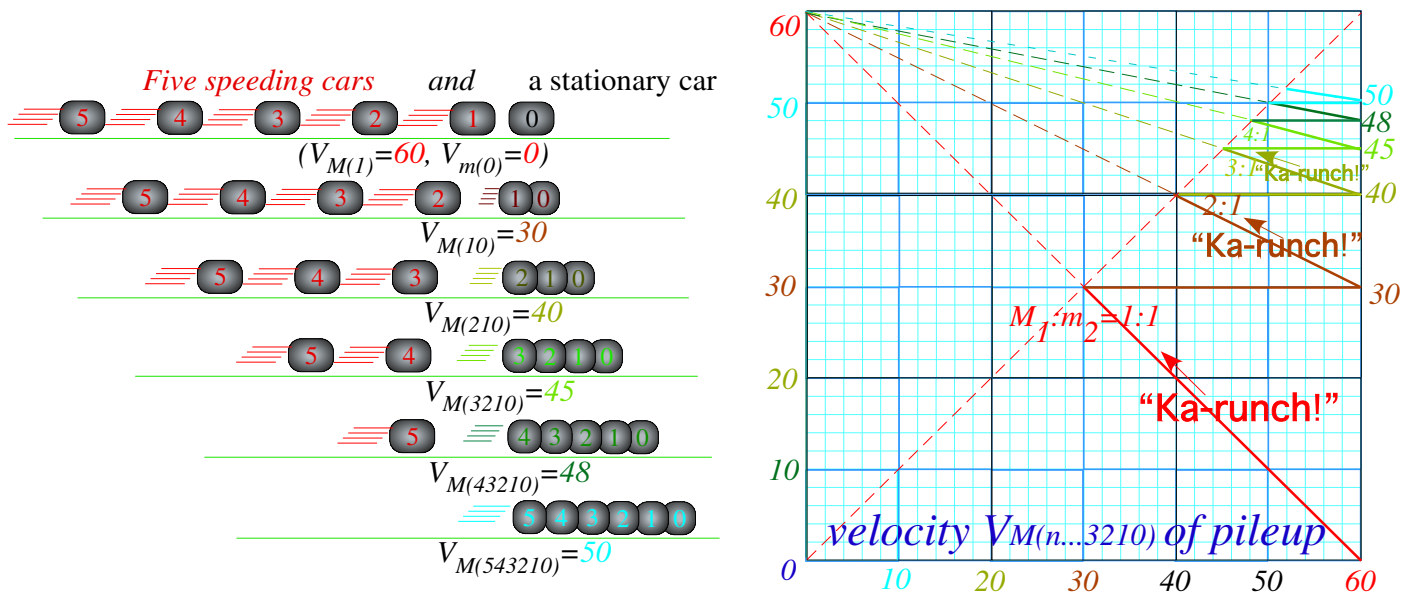


Fig. 8.6 Pile-up due to a line of five 60 mph cars hitting one stationary car

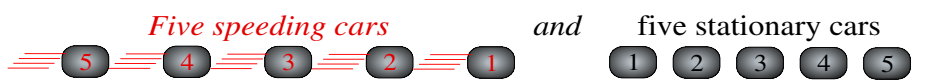


Fig. 8.7 A worse nightmare: Line of five 60 mph cars hitting five stationary cars.

Ka-pow-Ka-pow-Ka-pow-Ka-pow-...:Rocket science

An N -body model of rocket propulsion can be made by “time-reversing” pile-ups. Let us imagine a line of $N=11$ equal ($m=1$)-masses separated by explosive charges that go “pow!” in just the right sequence to blow one fuel-pellet at a time backwards off the rear end of a rocket and propel the remaining rocket mass forward.

Fig. 8.8 is a velocity-velocity plot of seven such “pow!”-blasts after which a rocket with just three masses numbered 8, 9, and 10 speeds off the page to the right. Presumably, the *payload* of this rocket is in the ball labeled 10 at the head of the line. For $N=11$ balls, there are ten $pow(b)$ -blasts numbered by $b=0$ to 9.

The velocity unit in Fig. 8.8 is the relative exhaust velocity $\Delta v_e=-1$ of each $pow(b)$ -blast. The 0^{th} -blast at the bottom of Fig. 8.8a starts with eleven stationary balls and blows ball-0 away from the line of ten balls 1-2-3...8-9-10. To conserve momentum (initially zero) the 10-ball rocket of mass ($M=10m=10$) has final velocity $\Delta V_M=+1/10$ to cancel momentum $\Delta P_0=m\cdot\Delta v_0=-1$ of fuel-pellet ball-0 in a zero-sum $pow(0)$ -blast.

$$m\cdot\Delta v_0+10m\cdot\Delta V_M(0)=0 \tag{8.7a}$$

The 0^{th} -blast line begins at the origin ($V_M=0, v_e=0$) of the V_M-v_e -plot in Fig. 8.8b and extends one unit down and $1/10^{th}$ unit right to point ($V_M(0)=1/10, v_e=-1$). $Pow(0)$ -line slope is mass ratio ($-m/M=-1/10$). It is a COM line of a *time reversed* totally *inelastic* collision, a *super-elastic* collision.

The $0^{th}, 1^{st}, 2^{nd}, 3^{rd}, \dots$, or 9^{th} blast blows off fuel pellet-ball $b=0, 1, 2, 3, \dots$, or 9, respectively. Each blast gives a larger rocket velocity boost $\Delta V_M(1)=1/9, \Delta V_M(2)=1/8, \Delta V_M(3)=1/7 \dots \Delta V_M(b)=1/(10-b)$ since rocket mass is less by $m=1$ after each blast but the exhaust momentum impulse $m\cdot\Delta v_e=-1$ is the same each time.

$$m\cdot\Delta v_1+9m\cdot\Delta V_M(1)=0 \quad m\cdot\Delta v_2+8m\cdot\Delta V_M(2)=0 \quad \dots \quad m\cdot\Delta v_b+(10-b)m\cdot\Delta V_M(b)=0 \tag{8.7b}$$

The *harmonic progression* $1/10, 1/9, 1/8 \dots 1/5, 1/4, 1/3, 1/2, 1$ in Fig. 8.8a contains momentum impulse terms $\Delta V_M(b)$ in a 10-term *harmonic series* $1/10+1/9+1/8 \dots 1/5+1/4+1/3+1/2+1$. Rocket velocity after its b^{th} $pow(b)$ -blast is a partial sum of the first $b+1$ harmonic terms. The (V_M, v_e) -plots in Fig. 8.8b show this.

$$\begin{aligned} 0^{th}: V(0) &= 1/10 = 0.1 & 1^{st}: V(1) &= 1/10 + 1/9 = 0.211 & 2^{nd}: V(2) &= 1/10 + 1/9 + 1/8 = 0.336 \\ 3^{rd}: V(3) &= V(2) + 1/7 = 0.478 & 4^{th}: V(4) &= V(3) + 1/6 = 0.646 & 5^{th}: V(5) &= V(4) + 1/5 = 0.846 \\ 6^{th}: V(6) &= V(5) + 1/4 = 1.096 & 7^{th}: V(7) &= V(6) + 1/3 = 1.429 & 8^{th}: V(8) &= V(7) + 1/2 = 1.929 \end{aligned}$$

On its 9^{th} and final $pow(9)$ the rocket is boosted by a whole unit exhaust velocity to $V(9)=V(8)+1=2.929$.

A 10-blast rocket exceeds exhaust velocity ($|v_e|=1$) on its 6^{th} $pow(6)$ -blast with $V(6)=1.096$. This is plotted on the extreme lower right hand side of Fig. 8.8b. The COM frame sees exhaust mass 6 thru 9 moving *forward* but the rocket sees each exhaust mass leave it moving *backward* at exactly $v_e=-1$ until it gets another blast-boost. Finally exhaust masses numbered 0-9 separate from each other and from payload mass-10. Total COM momentum is always zero, and so all eleven balls always “balance” on the COM origin.

N -blast velocity is a *logarithm* function if N is large. Momentum is still conserved for each blast.

$$M\cdot\Delta V = -v_e\cdot\Delta M \quad \text{becomes:} \quad M\cdot dV = -v_e\cdot dM \quad \text{or:} \quad dV = -v_e \frac{dM}{M} \tag{8.8a}$$

We integrate this from initial rocket mass M_{IN} to final payload M_{FIN} and from rocket V_{IN} to final V_{FIN} .

$$\int_{V_{IN}}^{V_{FIN}} dV = -v_e \int_{M_{IN}}^{M_{FIN}} \frac{dM}{M} \quad \text{becomes:} \quad V_{FIN} - V_{IN} = -v_e \left[\ln M_{FIN} - \ln M_{IN} \right] = v_e \left[\ln \frac{M_{IN}}{M_{FIN}} \right] \tag{8.8b}$$

This is the famous *rocket equation*. It gives discouraging predictions for interstellar travel. (See exercises.)

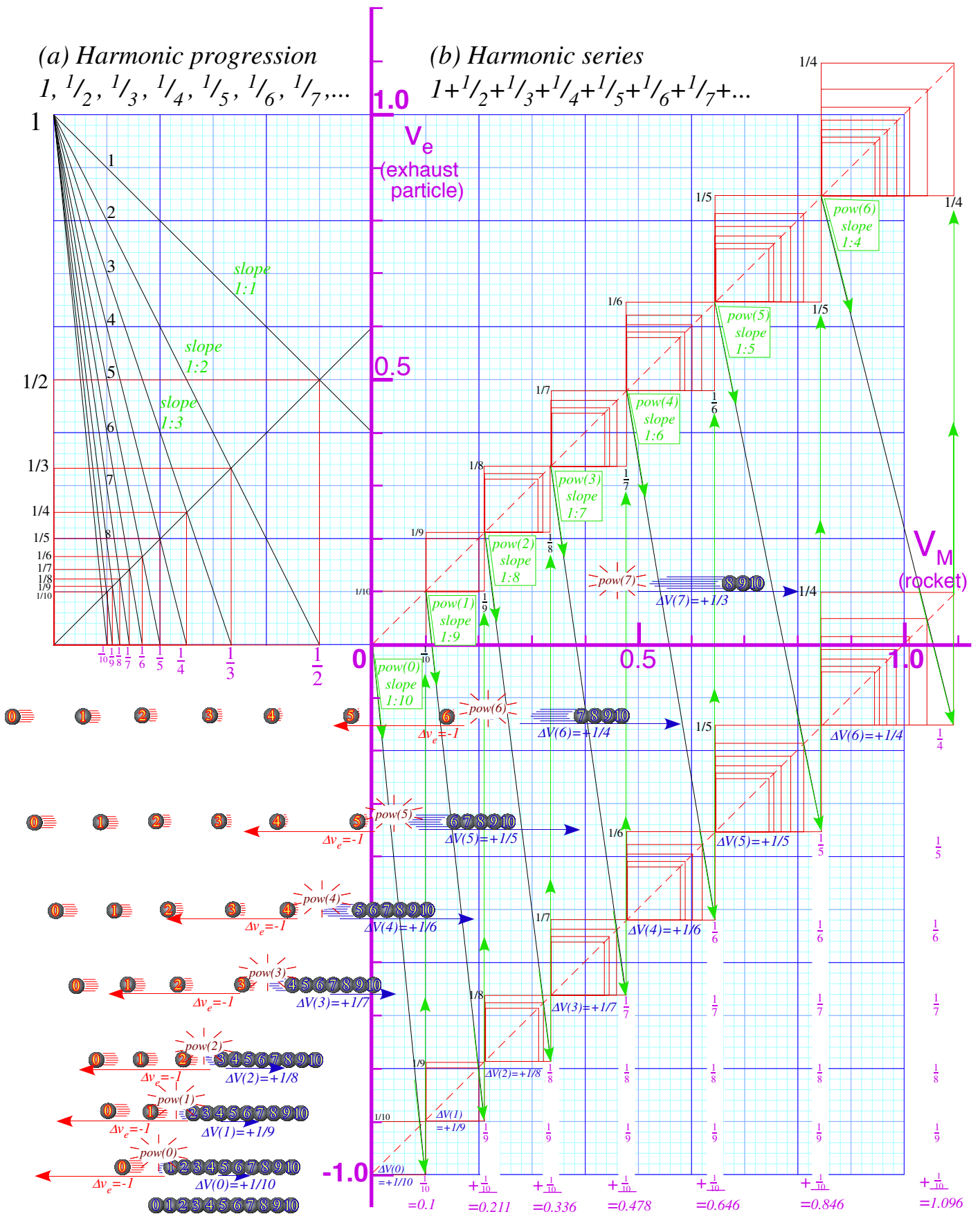


Fig. 8.8 Rocket science by harmonic series geometry.

Exercises

Chapter 9 Geometry and physics of common potential fields

Physical and geometric aspects of elementary force and potential fields are introduced in this section. The two most important are the oscillator and Coulomb fields that will later occupy Units 2 and 3.

Geometric multiplication and power sequences

The most common *power-law potentials* are $U(x) = Ax^2$ (*Oscillator potential*) in Fig. 9.1, $U(x) = Ax$ (*Uniform field potential*), and $U(x) = Ax^{-1}$ (*Coulomb potential*) shown later. Power-law potentials and their force laws have simple geometric constructions. Exponential or logarithmic fields (shown later) do not.

Multiplicative power operations are done using a staircase of similar triangles as shown in Fig. 9.2. A geometric progression $\{1=s^0, s=s^1, s^2, s^3, \dots\}$ and an inverse progression $\{1=s^0, 1/s=s^{-1}, s^{-2}, s^{-3}, \dots\}$ lie on either side of the unit stair step $1=s^0$. A slope or scale factor $s=2$ or $s=1/2$ is used in Fig. 9.2a or Fig. 9.2b. They resemble perspective drawings of school hallways. (Elementary School is (a) and High School is (b).) Each stair zigzags between slope-1 line- $(y=x)$ and slope- s line- $(y=s \cdot x)$ or between line- $(y=-x)$ and line- $(y=x/s)$. The line- $(y=s \cdot x)$ and line- $(y=x/s)$ are perpendicular or *normal* to each other. So are line- $(y=x)$ and line- $(y=-x)$.

A two-step triangle in Fig. 9.1a gives each point on the oscillator potential, a parabola $y=x^2$. To find where the parabola hits vertical line- $(x=2.2)$, for example, we go up that line to the 45° line- $(y=x)$ and then go across to vertical line- $(x=1)$. A dashed blue line is drawn from origin thru that point to an arrow intersecting line- $(x=2.2)$ at $pt-(x=2.2, y=2.2^2)$ on parabola- $(y=x^2)$. A similar zigzag gives $pt-(x=-2, y=4)$ or any point on the parabola $(y=U(x)=x^2)$ below.

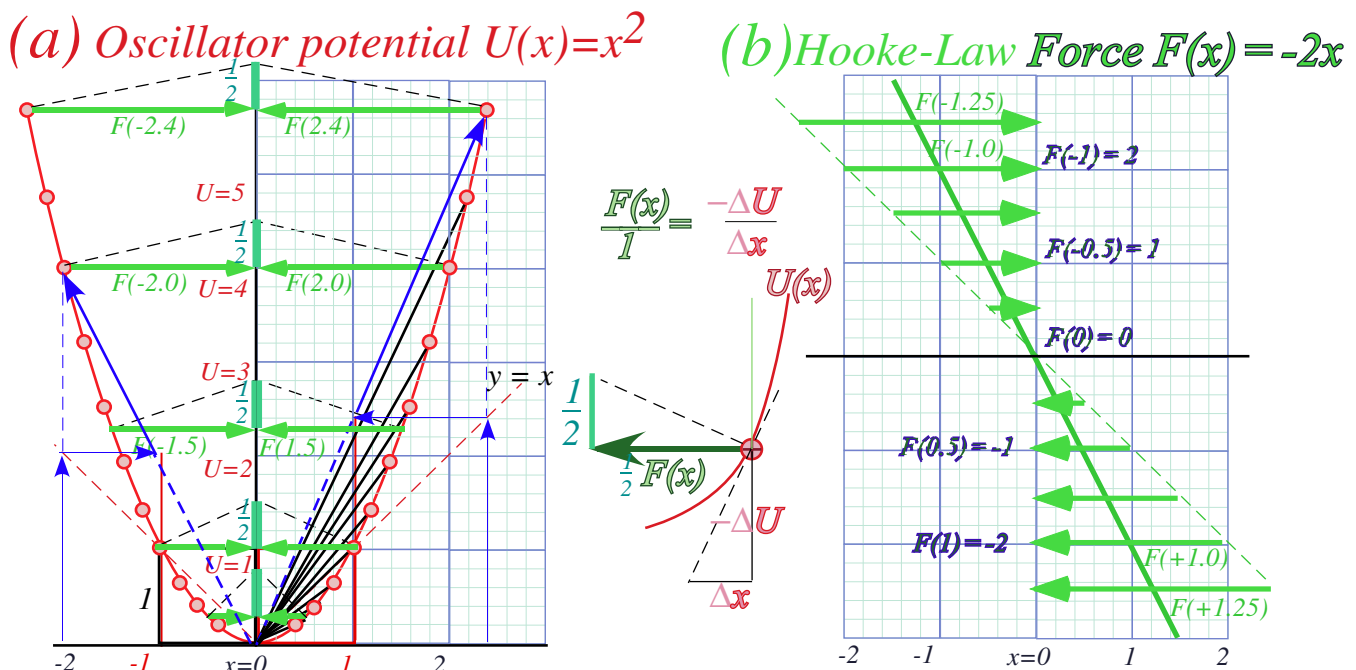


Fig. 9.1 Geometric construction of $U(x)=x^2$ potential and Hooke's force law $F(x)=-2x$.

Parabolic geometry

A parabola $U(x)=Ax^2$ has a *focal point* at $y=U=A/4$ where vertical rays meet if reflected by parabola tangents as in Fig. 9.3b. A parabolic radius is its half-width λ at the focus. For $y=x^2$ we have $\lambda=1/2$. (Note how $F(\pm 0.5)$ vectors point at the focus in Fig. 9.1a.) An old name for λ is *latus rectum*. A circle through the focus about any parabolic point will be tangent to a line called the *directrix* located at a distance λ from the focus. Focus and directrix define a parabola that passes midway between them thru the tip-point **M** of the parabola where its focal radius and equal distance-to-directrix both reach their minimum value $\lambda/2$.

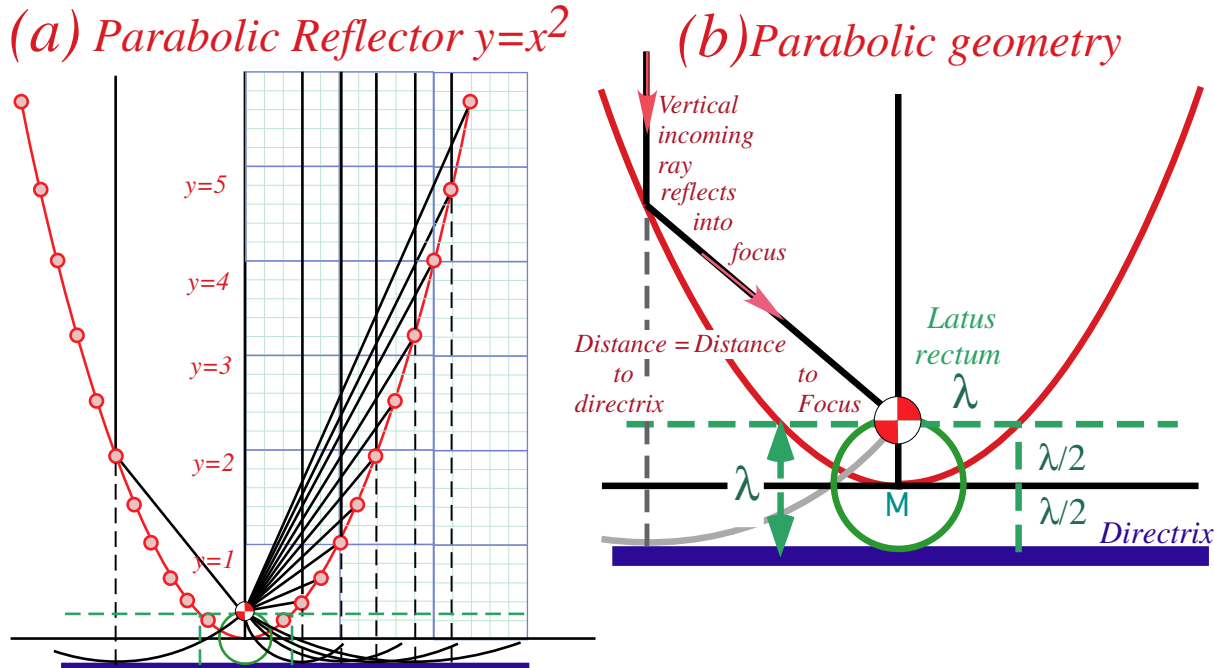


Fig. 9.3 Parabola and analytic geometry (a) Rays converging on focus. (b) λ -geometry of tangent reflection.

Directrix is a so named because it “directs” both the rays and wave phase of an optical reflector. Since the *focal radius* (length of each sloping ray line in Fig. 9.3a) equals the perpendicular *directrix distance* (length of corresponding dashed vertical line), waves are guaranteed to be plane waves. Also, the equality of angle of incidence and reflection off the parabola bisecting the dashed and solid lines, guarantees vertical parallel rays for all which leave the focus and bounce off the inside of the parabola. It also guarantees that parallel vertical rays bouncing off the *outside* will go away from the focus. Either side of a parabolic surface converts plane waves to spherical ones or *vice-versa*.

To better understand the parabola’s geometric optics we draw examples of the *tangent-kite* for four different tangent slope values. The blue kite of *slope=2* in Fig. 9.4a and yellow kite of *slope=5/2* in Fig. 9.4b have equal focal radius and perpendicular distance-to-directrix forming the major isoscoles triangle of the kite. A minor isoscoles triangle (upside down in Fig. 9.4) shares a base with the major one. Their perpendicular bisector is the tangent line. The bisection point is slope $\frac{dy}{dx} = \frac{x}{\lambda} = \frac{x}{2p}$ in units of λ as indicated by vertical arrows.

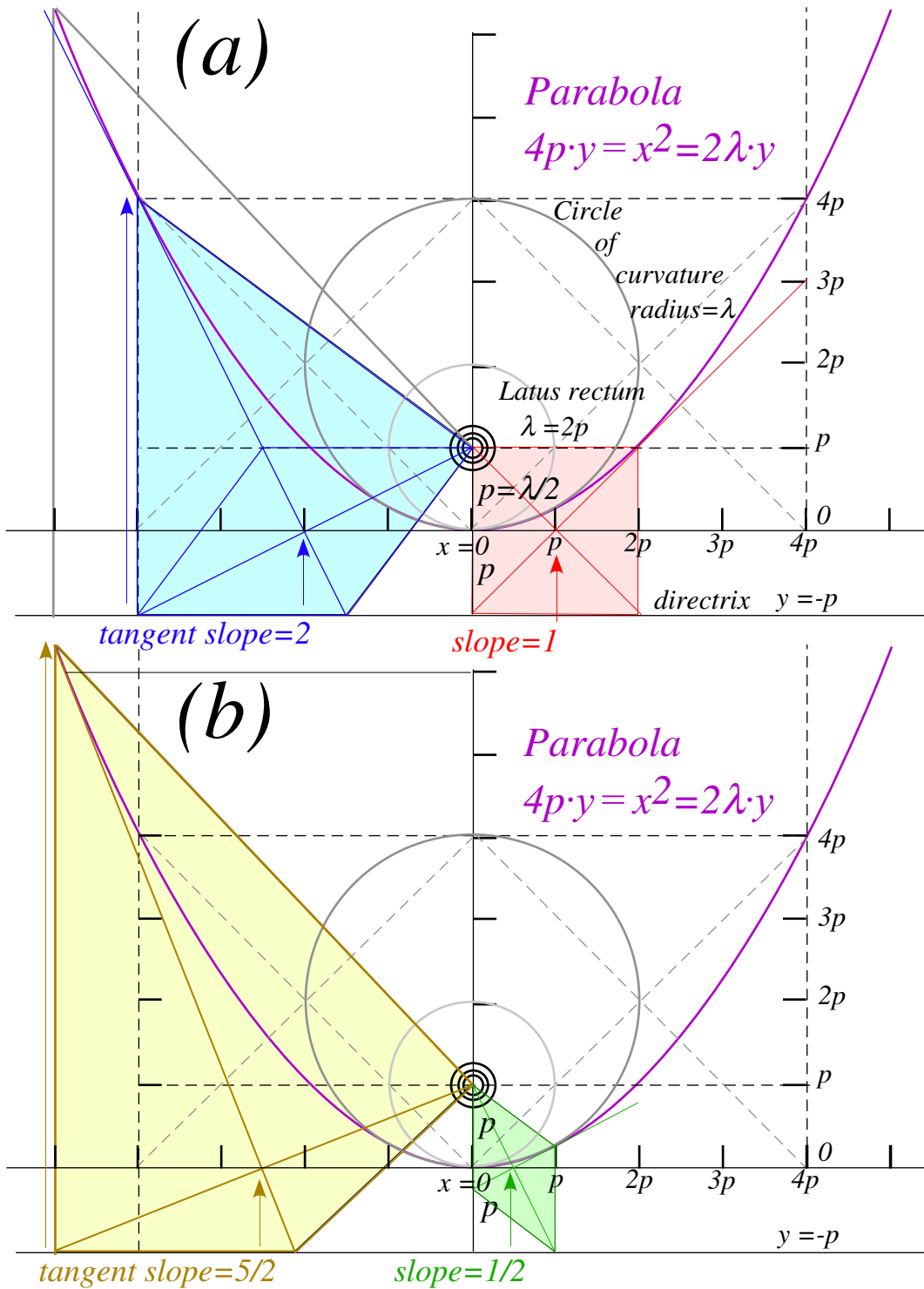


Fig. 9.4 Parabola and geometry of curvature and slope of tangent-kites.

A singular case is the red kite of *slope=1* that is square. Lesser *slope=1/2* gives a rhomboidal green kite with one side on the vertical parabolic axis instead of on the horizontal directrix. Points of *slope=±1* on the $(4py=x^2=2\lambda y)$ -parabola lie on either side of its focus at distance $\lambda=2p$ from it. $\lambda=2p$ is also the (minimum) *radius of curvature* of the parabola at its tip (minimum y at $x=0$) that lies a distance $\lambda/2=p$ below the focus.

Coulomb and oscillator force fields

Our atoms and molecules depend on the electrostatic Coulomb field to have stable chemistry and biology. Like charges repel and opposites attract with a force that varies inversely with the square of distance r between them. A simple version of the electric Coulomb force law (axiom) is:

$$F(r) = \frac{1}{4\pi\epsilon_0} \frac{qQ}{r^2} \quad \text{where: } \frac{1}{4\pi\epsilon_0} = 9,000,000,000 \frac{\text{Newtons} \cdot \text{meter} \cdot \text{square}}{\text{per square Coulomb}} \quad (9.1)$$

The units and notation are standard but the size of this is *mind boggling*. It's nine *billion Newtons* for just two charge-units a meter apart. (To be precise it's $8.99 \cdot 10^9 \text{ Nm}^2/\text{C}^2$.) OK, a 1N is only about $\frac{1}{4} \text{ lb}$, but are you able to hold up a billion sticks of butter? Also, you have *thousands* of Coulomb charge units in each fingertip with only a centimeter separation so add another factor of *(100)-squared*. Make that ninety *trillion* Newtons for each Coulomb or about a *million trillion* Newtons trying their darndest to blow your pinkie to bits!

But, still we're underestimating this monster force. Most of the electronic charge in the world is crammed into atoms and molecules with at most a nanometer (10^{-9} meter) across and some are an *Angstrom* (10^{-10} meter) or a tenth of a *nano*. So put on another factor of *(10⁻⁹)-squared* or million-billion trying to undo your pinkie, that's a *trillion-trillion-billion*. Does your manicurist know about this?

Sometimes these forces get loose as in a TNT blast, but usually, tiny nuclei with an equal positive charge hold down potentially rebellious electrons. Still, what's holding nuclei together? Nuclear radii are *femto*-meters (10^{-15} meter) or *Fermi*. (Note: both *fm* and *Fm* are abbreviations for $10^{-15} \text{ m} = 10^{-13} \text{ cm}$.)

Oops! That's another factor of *(10⁻¹⁵)²* or another million-trillion-trillion to increase our stress level. Nuclear charge is 10^5 times more pent-up than its atomic electronic counterpart with a grand total of about a *trillion-trillion-trillion-trillion* Newtons hankering to blow up your fingertip nuclei. Cancel the manicure!

When nuclei do blow up, the result is more than 10^5 times more devastating than any TNT bang. We don't use *force* to estimate the devastation of a nuclear fission bomb or the yield of nuclear power plant fuel. Rather we use electric *potential energy*, that varies as $1/r$ not $1/r^2$. (Slope of a $U(r)=1/r$ -curve is $F(r)=1/r^2$.)

$$U(r) = \frac{1}{4\pi\epsilon_0} \frac{qQ}{r} \quad \text{where: } \frac{1}{4\pi\epsilon_0} = 9,000,000,000 \frac{\text{Joule}}{\text{per square Coulomb}} \quad (9.2a)$$

Energy or *(Force)-times-(distance)-unit* is *Joule* or *Newton meter (N·m)*. Like superball potential field $U(r)$ in (6.9), force $F(r)$ (9.1) is a (-)derivative of potential $U(r)$ that in turn is (-)integral of force $F(r)$. (Recall (7.5).)

$$F(r) = -\frac{dU(r)}{dr} = -\frac{qQ}{4\pi\epsilon_0} \frac{d}{dr} r^{-1} = \frac{qQ}{4\pi\epsilon_0} r^{-2} \quad (9.2b)$$

$$U(R) = -\int_{\infty}^R F(r) \cdot dr = \frac{qQ}{4\pi\epsilon_0} r^{-1} \Big|_{\infty}^R = \frac{qQ}{4\pi\epsilon_0} R^{-1} \quad (9.2c)$$

Potential nuclear energy yield is about a million times greater than for the same number of chemical energy sources since *femto*-meter nuclei are a million times smaller ($R_{\text{NUC}} \sim 10^{-15}$) than *nano*-meter molecules ($R_{\text{MOL}} \sim 10^{-9}$). Nuclear forces would then be a trillion times greater than typical atomic and molecular forces.

Fig. 9.5 plots attractive Coulomb force $F(r)=-1/r^2$ and potential $U(r)=-1/r$ of *negative* charge $-q$ to a *positive* $+Q$ nucleus. (Negative force points toward the $+Q$ origin ($x=0$.) It uses zigzag geometry of Fig. 9.4.

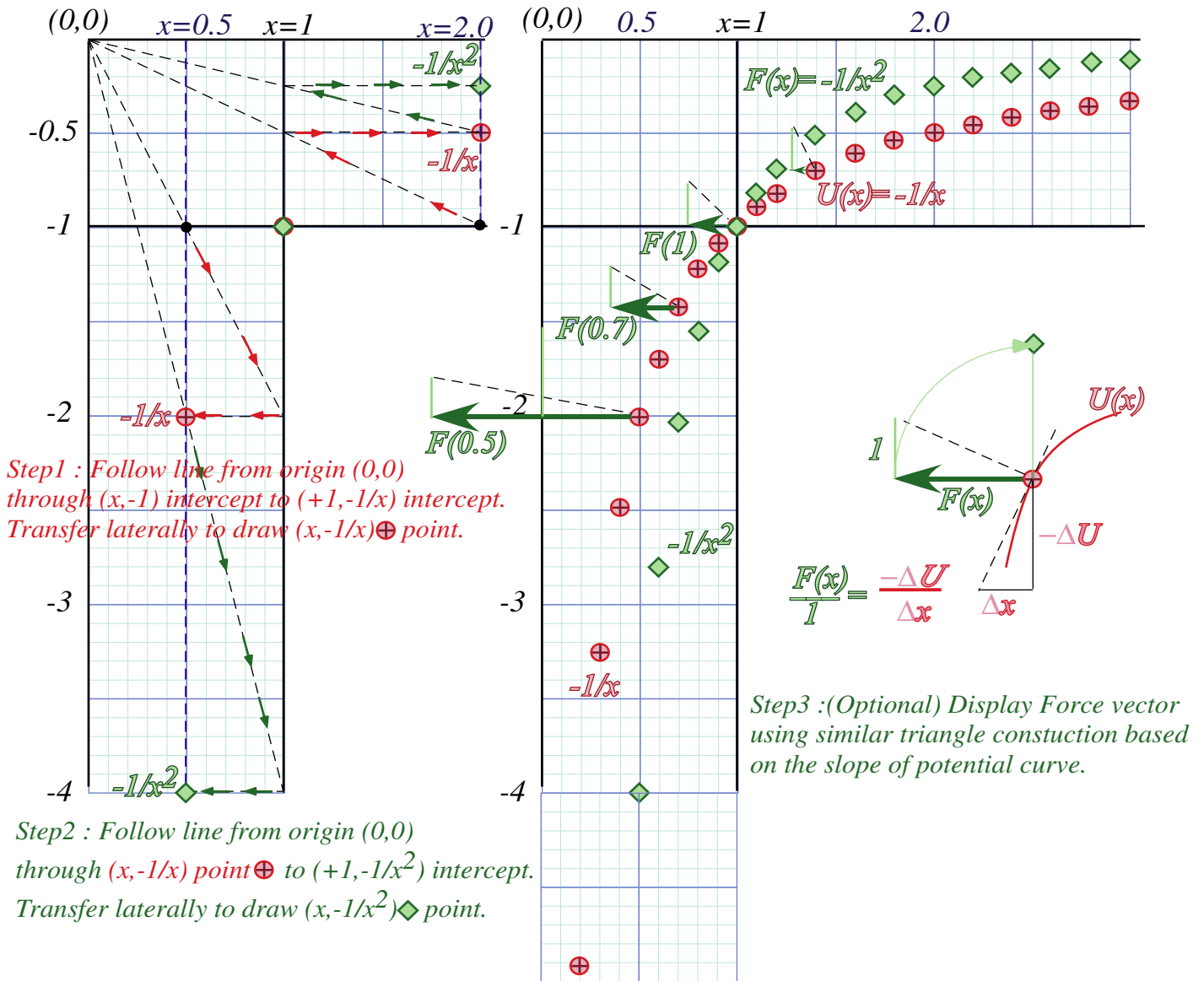


Fig. 9.5 Attractive Coulomb force $F(x)$ and potential $U(x)$ curves. ($F(x)$ vectors drawn at 1/4-scale.)

Could the Coulomb $F(r) \sim 1/r^2$ force field be derived like the superball force $F(Y) \sim 1/Y^3$ in (6.10) by counting momentum bangs? Indeed, if a charge ejected a cloud of little “bang-balls” then the number of bangs scored at distance r would vary inversely with area $4\pi r^2$ of a radius r sphere. But, that idea doesn’t explain very well attraction of a charge $+Q$ to a $-q$ or of a mass M to a mass m in Newton’s gravity law.

$$F_{grav}(r) = -GMm / r^2, \text{ where: } G=0.00000000067 \text{ N m/kg}^2 \quad (9.3)$$

Gravity is universally attractive (no “negative” matter readily available) but much weaker than the electric one since G constant $6.672E-11$ ($\frac{2}{3} \cdot 10^{-10}$ in mks units) is smaller (by 10^{20} times!) than the $9 \cdot 10^{+9}$ in (9.2).

As of this writing it is still a mystery why these are so different. We really do not yet understand either of these forces at a fundamental level. They are still very much in the axiom box.

Tunneling to Australia: Earth gravity inside and out

Imagine $x=1$ in Fig. 9.5 is the Earth radius $R_{\oplus}=6.4E6m$. The $F(r)$ plot shows gravity falling off for $r>R_{\oplus}$ or $x>1$. But it's wrong for subterranean radii ($r<R_{\oplus}$) unless Earth is compressed. $F(r)=-1/r^2$ doesn't apply everywhere unless Earth is squashed to a 10 millimeter radius "black hole." (More on this later.)

If you were to be at sub- R_{\oplus} levels all Earth mass at radii above your radius r can be completely ignored in figuring your weight! As you might expect, you're weightless at the center ($r=0$) since the pull of all Earth's mass exactly cancels there. But, so also does your attraction to a spherical mass shell cancel anywhere inside it. One could float weightlessly anywhere therein regardless of the shell's size or weight.

Such a cancellation is a geometric peculiarity of an inverse square law. (It also underlies a Gauss law explanation of why you're safe inside a car struck by lightning.) Any direction you look inside a uniform mass shell has a mass element m whose force is cancelled by another element M behind you. (See Fig. 9.6.)

The shell tangent to the m -point you're facing intersects the tangent to the M -point behind you to make an isosceles triangle whose sides make an angle Θ with your line of sight along the base. This means a narrow cone of sight will include shell mass $m=Ad^2$ at a distance d in front of you and shell mass $M=AD^2$ at a distance D directly behind you, where the angular factor $A\sim 1/\sin\Theta$ is the same for both. That assures perfect cancellation of gravity m/d^2 in front with $-M/D^2$ behind you. This applies for *all directions* in Fig. 9.6.

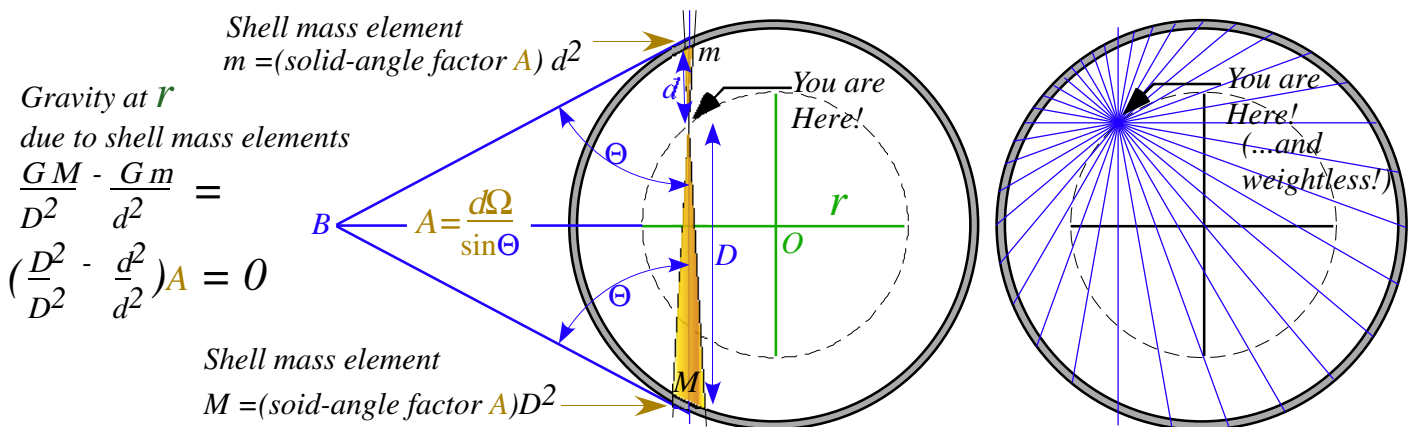


Fig. 9.6 Equal-opposite attraction. Geometry for you floating weightless inside a spherical shell.

A mass m at radius r inside Earth feels gravity attraction $GmM_{<}/r^2$ where $M_{<}$ is Earth mass *inside* the radius r indicated by the dashed circle in Fig. 9.6. If Earth is uniform density ρ , then that inside-mass is $M_{<}=4\pi\rho r^3/3$. Force law r^{-2} cancels all but one r of the r^3 in mass $M_{<}$. We then get a *linear* force law.

$$F_{inside}(r)=GmM_{<}/r^2=m(G4\pi\rho/3)r=mg(r/R_{\oplus})=mgx \tag{9.4a}$$

$$(Earth\ surface\ gravity:\ g=GR_{\oplus}4\pi\rho/3=9.8ms^{-2}) \tag{9.4b}$$

The linear force law (9.4) is like that of a harmonic oscillator in Fig. 9.1b and so the inside-Earth potential must be a parabola like Fig. 9.1a. Force $F(1)=-1$ is continuous as we cross $x=1$ and so must be the slope of potential $U(x)$ as U changes from $-1/x^2$ to parabola. Terrestrial beings such as ourselves live in a nearly-constant-field ($\frac{dF}{dx}\sim 0$)-region near $x=1$. In Fig. 9.7 we find the potential parabola geometrically by its focal

point and directrix using the tangent at $x=1$. Recall a tangent at $x=\lambda=2p$ in Fig. 9.4a has $slope=1$ or 45° . So does the parabola at $x=1$ in Fig. 9.7 below have a slope of $(+1)$ and a force of (-1) (That's $-mg$ in mks units.)

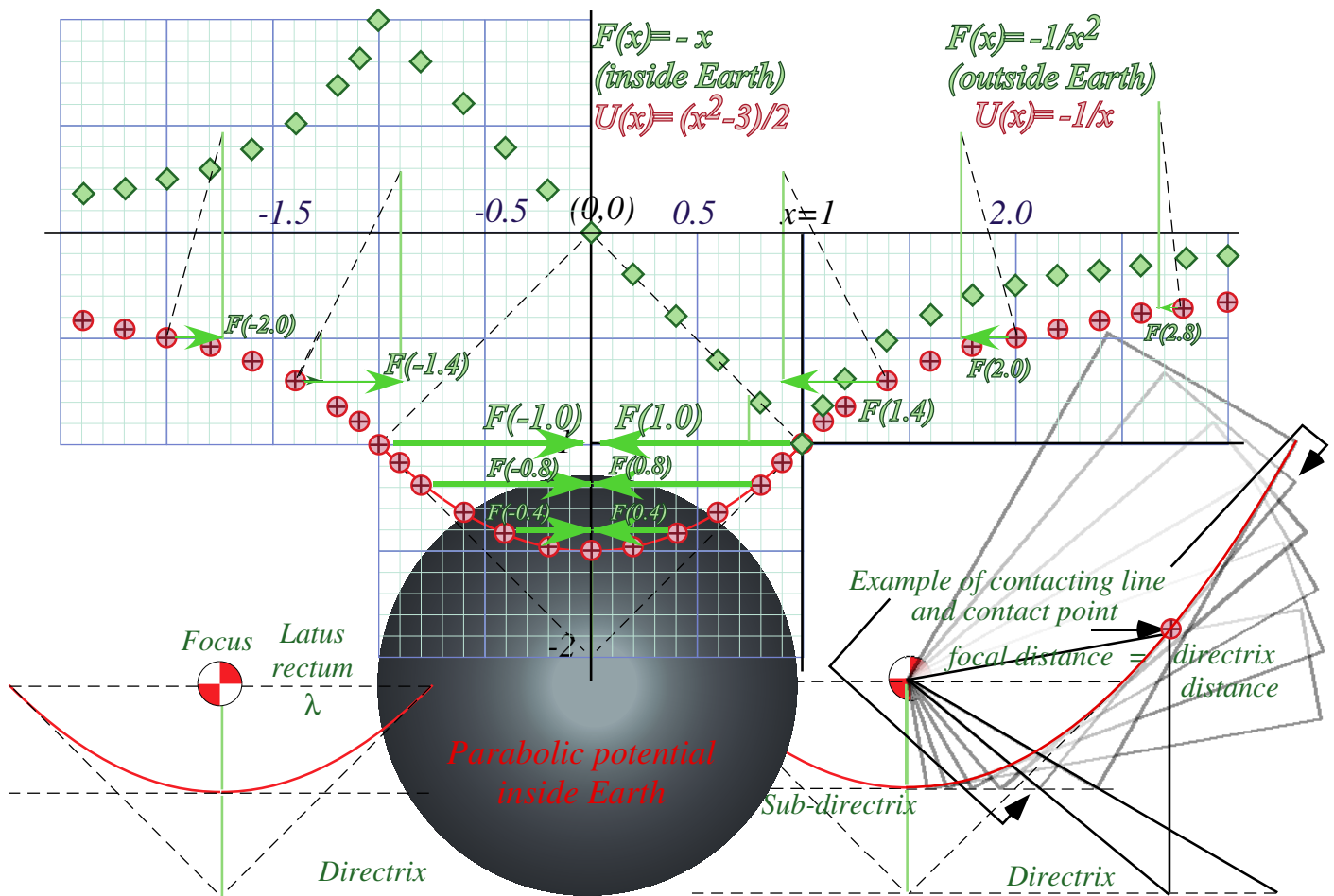


Fig. 9.7 Construction of Earth gravitational fields inside and outside. (units of x : R_\oplus ; F : mg ; U : mgR_\oplus)

A parabola tangent bisects the angle between the line to the focus and the directrix drop-line as in Fig. 9.4. Twice 45° gives 90° . The focus is $\lambda=1.0$ units straight across and the directrix is $\lambda=1.0$ units below as shown in Fig. 9.7 (lower-left). Using this we may construct the parabola by rotating a square corner of a piece of graph paper around the focus so the corner touches a line halfway to the directrix. (We can call this half-way line the *sub-directrix*. It is the line of tangent intersections indicated by arrows in Fig. 9.4.)

The parabola so constructed is $y=x^2/2 - 3/2$. That is the *interior* potential $U^{IN}(x)$ ($-1 < x < 1$). It meets the curve $y=-1/x$ that is the *exterior* potential $U^{EX}(x)$ ($1 < x < \infty$) at $x=1$ where they are equal ($U^{IN}(1)=-1=U^{EX}(1)$) as is slope, which is the force ($F^{IN}(1)=-1=F^{EX}(1)$). (However, the slope of the *force* curve takes a *big* jump!)

Adding a constant to a potential won't alter slope or force. We added $-3/2$ to $x^2/2$ to make it equal $-1/x$ at $x=1$.

To catch a falling neutron starlet

The “glue” that holds in the rebellious nuclear proton charge is called *nuclear matter*, a mix of neutrons, mesons, and their ingredients. Let’s imagine a fingertip (1cc) of neutrons as densely packed as they are in a nucleus or neutron star and estimate how such a neutron starlet might travel through Earth. First, we find the density of nuclear matter. Let’s say a nucleus of atomic weight 50 has a radius of 3 fm, so it has 50 nucleons each with a mass $2 \cdot 10^{-27} \text{kg}$. (It’s actually more like $1.67 \cdot 10^{-27}$, but roughly $2 \cdot 10^{-27}$.)

That is $100 \cdot 10^{-27} = 10^{-25} \text{kg}$ packed into a volume of $\frac{4\pi}{3}r^3 = \frac{4\pi}{3}(3 \cdot 10^{-15})^3 \text{m}^3$ or about 10^{-43}m^3 . That gives a whopping density of $10^{-25+43} = 10^{18} \text{kg per m}^3$ or a *trillion* kilograms in the size of a fingertip.

That’s a pretty heavy fingertip! Its weight mg is ten trillion Newtons. (Well, actually 9.8 trillion Newtons. No need to exaggerate here!) In spite of this, its gravitational attraction to nearby rocks on the Earth is comparatively moderate. A (10cm)³ 1kg rock would cling to the starlet with a force of about

$$F_{rock} = Gm(1\text{kg})/r^2 = 100Gm = 100(6.7E-11)1E12 = 6,700 \text{ N}, \quad (m = M_{starlet} = 10^{12} \text{kg})$$

or less than a ton and small change for a starlet weighing billions of tons and cutting into the Earth like a bullet going through cotton candy. Let’s see what speed it might gain falling from the surface.

Starlet energy is assumed constant since friction would be tiny compared to its enormous weight.

$$E = KE + PE = \frac{1}{2} m v^2 + U(x) = \frac{1}{2} m v^2 + \frac{1}{2} mg (x^2 - 3) = \text{const.} \quad (9.5)$$

Let it be released at Earth surface ($x=1$) with zero velocity. This sets the energy constant.

$$E = \frac{1}{2} m 0^2 + \frac{1}{2} mg (1^2 - 3) = \text{const.} = -mg \quad (9.6)$$

At Earth center ($x=0$) we solve for the velocity there. (The starlet mass m cancels out.)

$$E = \frac{1}{2} m v^2 + \frac{1}{2} mg (0^2 - 3) = \text{const.} = -mg \quad \text{or: } v^2 = g, \quad (9.7a)$$

$$v = \sqrt{g} \quad (\text{In mks units: } v^2 = gR_{\oplus}, \text{ or: } v_0 = \sqrt{gR_{\oplus}} = 8 \text{ km/s}) \quad (9.7b)$$

$v_0 = 8 \text{ km/s}$ is also Earth’s minimum *orbital insertion speed*. A mass dropped down the tunnel flies with the same x -coordinate as one shot with the speed v_0 into circular orbit. One flies above the other and they meet each other on the other side 42 minutes later as shown in Fig. 9.8. We now show this synchrony of orbital timing holds for all pairs of starlets sent from anywhere inside the Earth!

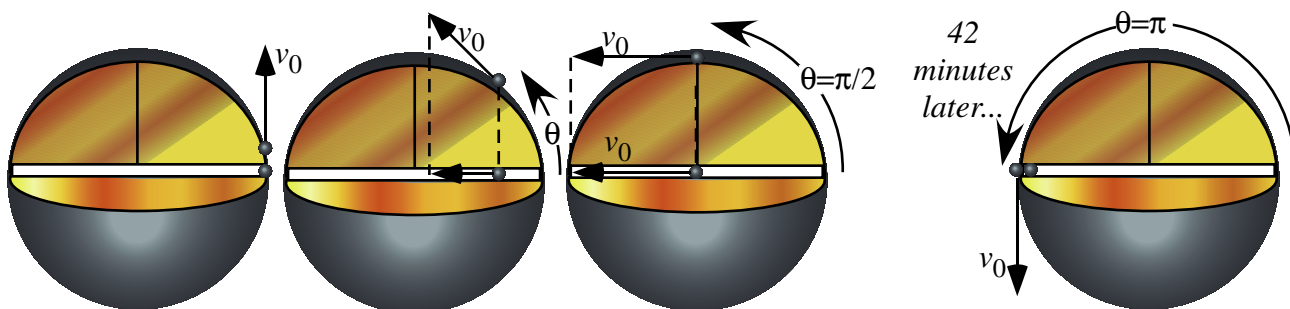


Fig. 9.8 Neutron starlet penetrates Earth as satellite orbits to meet 1/2-way around in 42 minutes.

This synchrony involves a physicist's most favored type of potential energy $U=1/2kx^2$. When $PE=U$ is a square like kinetic energy $KE=1/2mv^2$ we have a wonderful symmetry between position x and velocity v .

$$E=KE + PE= const. = 1/2mv^2 + 1/2kx^2$$

We make any constant-sum-of-squares into a *Pythagorean relation* $1=\sin^2\theta+\cos^2\theta$ just as we did to analyze the sum (5.10) of super-ball KE . Here (9.5) is a sum $E=KE+PE$ and the constant k is starlet weight mg .

$$1=(m v^2/2E) + (k x^2/2E) =\sin^2\theta+\cos^2\theta \tag{9.8a}$$

Position x and velocity v are then expressed in terms sine and cosine of a *phase angle* θ .

$$x= \sqrt{2E/k} \sin\theta \tag{9.8b}$$

$$v= \sqrt{2E/m} \cos\theta \tag{9.8c}$$

Velocity v is proportional to $\cos\theta$ and θ has a constant *angular velocity* $\omega=d\theta/dt$ so that $\theta=\omega t+\alpha$. ($\alpha=\theta_0=const.$)

$$v=\frac{dx}{dt}=\frac{dx}{d\theta}\frac{d\theta}{dt}=\frac{dx}{d\theta}\omega=\omega\sqrt{\frac{2E}{k}}\cos\theta=\sqrt{\frac{2E}{m}}\cos\theta \tag{9.9a} \quad \text{where:} \quad \omega=\frac{d\theta}{dt}=\sqrt{\frac{k}{m}} \tag{9.9b}$$

Angle θ is a polar angle in $(x,v/\omega)$ -*phasor-space* of Fig. 9.10a. $(x,v/\omega)$ -orbits are circular-*clockwise* ($\omega=-|\omega|$) if positive phasor v -axis is *up* and positive- x axis is to the *right*. Earth xy -orbits may be elliptical with a polar angle ϕ that can orbit either way in Fig. 9.10. Each spatial dimension x and y has a constant sub-total energy.

$$KE_{Total}=e_x+e_y \quad \text{where:} \quad e_x=const.=1/2mv_x^2 + 1/2kx^2 \quad \text{and:} \quad e_y=const.=1/2mv_y^2 + 1/2ky^2 \tag{9.10}$$

Equal constants ($e_x=e_y$) give the circular orbit in Fig. 9.8. Frequency ω (9.9) is independent of energy value e_x or e_y and so orbit and x -tunnel motion each have frequency $\omega=\sqrt{g}$, but tunnel motion, with same e_x but zero e_y , has half the energy. All motions of the starlet inside the Earth have the same 84-minute period. That is a *fundamental harmonic period* of a uniform Earth and approximates behavior of the real Earth.

To depict the force vector \mathbf{F} on the starlet simply draw an arrow from it to origin as in Fig. 9.9a since \mathbf{F} is proportional to coordinate vector $-\mathbf{r}$. (In Fig. 9.7, F is equal to $-r$.) It's projection on x or y -axes are the forces components driving the 84-minute oscillations along x or y -axes. Perhaps, there is a starlet deep below us swishing out 84-minute elliptical orbits as in Fig. 9.9b.

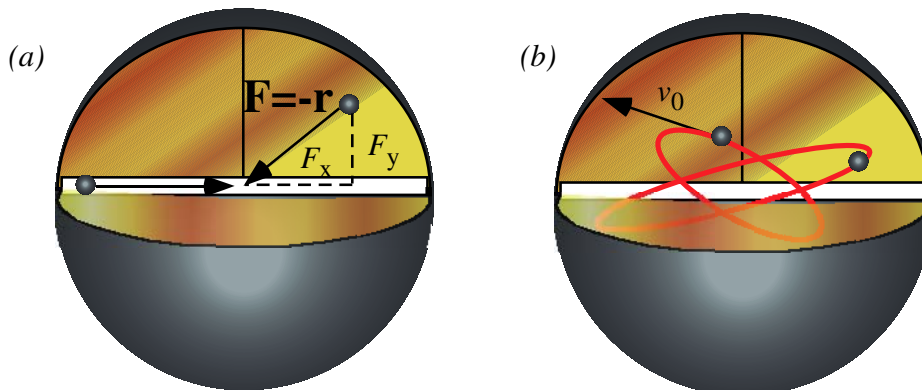


Fig. 9.9 Force and orbits inside Earth. (a) \mathbf{F} is minus the coordinate vector (b) Typical orbits.

Starlet escapes! (In 3 equal steps)

Imagine starlet- m has decayed to where it sits at the bottom of the $U(x)=\frac{1}{2}mg(x^2-3)$ curve in Fig. 9.7. How much energy does it take for it to escape from Earth center and go back whence it came? The plot of $U(x)$ in Fig. 9.7 and discussions above suggest three equal steps of $1/2$ that bring energy $-3/2$ at $x=0$ up *zero* at $x=\infty$

Step-1 is to drag or shoot the starlet- m to the Earth's surface. That takes energy $\Delta E_1=\frac{1}{2}$. (That's $\frac{1}{2}mgR_\oplus$ in *mks* units.) Shooting radially at velocity $v_0 = \sqrt{(gR_\oplus)}$ given by (9.7b) would do this first step. It would then come to rest (momentarily) at the Earth surface at $r=R_\oplus$.

Step-2 is to launch starlet- m into a minimal circular orbit from the Earth's surface. That takes dollop of energy $\Delta E_2=\frac{1}{2}$ equal to the first. (Again, that's $\frac{1}{2}mgR_\oplus$ in *mks* units.) Shooting tangentially with minimum orbital insertion velocity $v_0 = \sqrt{(gR_\oplus)}$ given by (9.7b) does this second step.

Step-3 involves a final energy jump $\Delta E_3=\frac{1}{2}$ equal to each of the first two by increasing from the orbital insertion velocity $v_0 = \sqrt{(gR_\oplus)}$ to the *escape velocity* V_e from Earth's surface $r=R_\oplus$.

$$V_e = v_0\sqrt{2} = \sqrt{(2gR_\oplus)} = 11.3 \text{ km/s} = 7 \text{ mile/s} \quad (9.11a)$$

In terms of fundamental potential $U_{grav}(R_\oplus) = -GMm/R_\oplus$ at a planets surface $r=R_\oplus$ the escape velocity is

$$V_e = v_0\sqrt{2} = \sqrt{(2GM/R_\oplus)}. \quad (9.11b)$$

Orbital threshold velocity v_0 of radius R_\oplus is $\sqrt{2}=0.707$ or about *71%* of the escape velocity V_e from there.

No escape: A black-hole Earth!

By uniformly compressing Earth, we imagine extending the region of the Coulomb potential $-1/r$ in Fig. 9.5 to lower values of r while making the harmonic potential $U(r)=\frac{1}{2}kr^2$ inside the body occupy a smaller and smaller radius R_\oplus and take on narrower, deeper, and more negative energy values.

The plot in Fig. 9.5 maintains its shape but we rescale to accommodate a squashed Earth. The escape velocity in (9.11b) grows as we consider a decreasing squashed-planet radius R_\oplus . Finally there comes a particular radius R_\oplus where the escape velocity (9.11b) is the speed c of light.

$$c = \sqrt{(2GM/R_\oplus)} \quad (9.12a)$$

That radius is called the *Schwarschild radius* or "black hole" radius since light cannot escape.

$$R_\oplus = 2GM/c^2 \quad (9.12b)$$

For the earth of mass $M_\oplus = 6 \cdot 10^{24}$ kg the radius R_\oplus is about nine *mm*, or the size of a fingertip. It is hard to imagine our world so squashed! Things may be collapsing all around, but not *that* much.

Oscillator phasor plots and elliptic orbits

The oscillator functions in (9.8) suggest a coordinate-velocity plot or *phase-space* plot. By (9.9) the phase angle $\theta=\omega t+\alpha$ is a product of angular frequency ω and time. To get a circle starting on the x -axis, we set initial phase to $\alpha=\theta_0=\pi/2$ and plot $(x = X \cos \omega t, v/\omega = -X \sin \omega t)$ for the "clock" or *phasor plot* in Fig. 9.10a.

So that positive v versus x defines its 1st quadrant, a phasor rotates *clockwise* like a clock hand so angle $\theta = -\omega t$ has a minus sign. (This is quite *apropos* since our clocks now *are* waves and harmonic oscillators.)

Each dimension x and y has its phasor plot as indicated by Fig. 9.10b. In other words there are four phase-space or phasor dimensions $(x, v_x/\omega, y, v_y/\omega)$ being plotted. Here the frequency ω for each dimension x and y is identical due to symmetry or *isotropy* of the Earth model. But, initial phases α_x and α_y of x and y are independent. In Fig. 9.10b we set x -oscillator phase to 2 o'clock (on a 16-hour clock) and y -oscillator 2 hours ahead to 4 o'clock so the ellipse orbit is *clockwise* and have a *left-handed* symmetry. Setting x to be 2 hours ahead of y makes the same orbit but it will go *counter-clockwise* and have a *right-handed* symmetry.

The x versus y plot with x always two hours or 45° behind y , is an inclined elliptical xy -orbit path in Fig. 9.10b. It might represent a typical neutron starlet path in the Earth. Or else, it might represent an optical polarization ellipse described in Unit 2. Below is a discussion of some special cases of orbit ellipses.

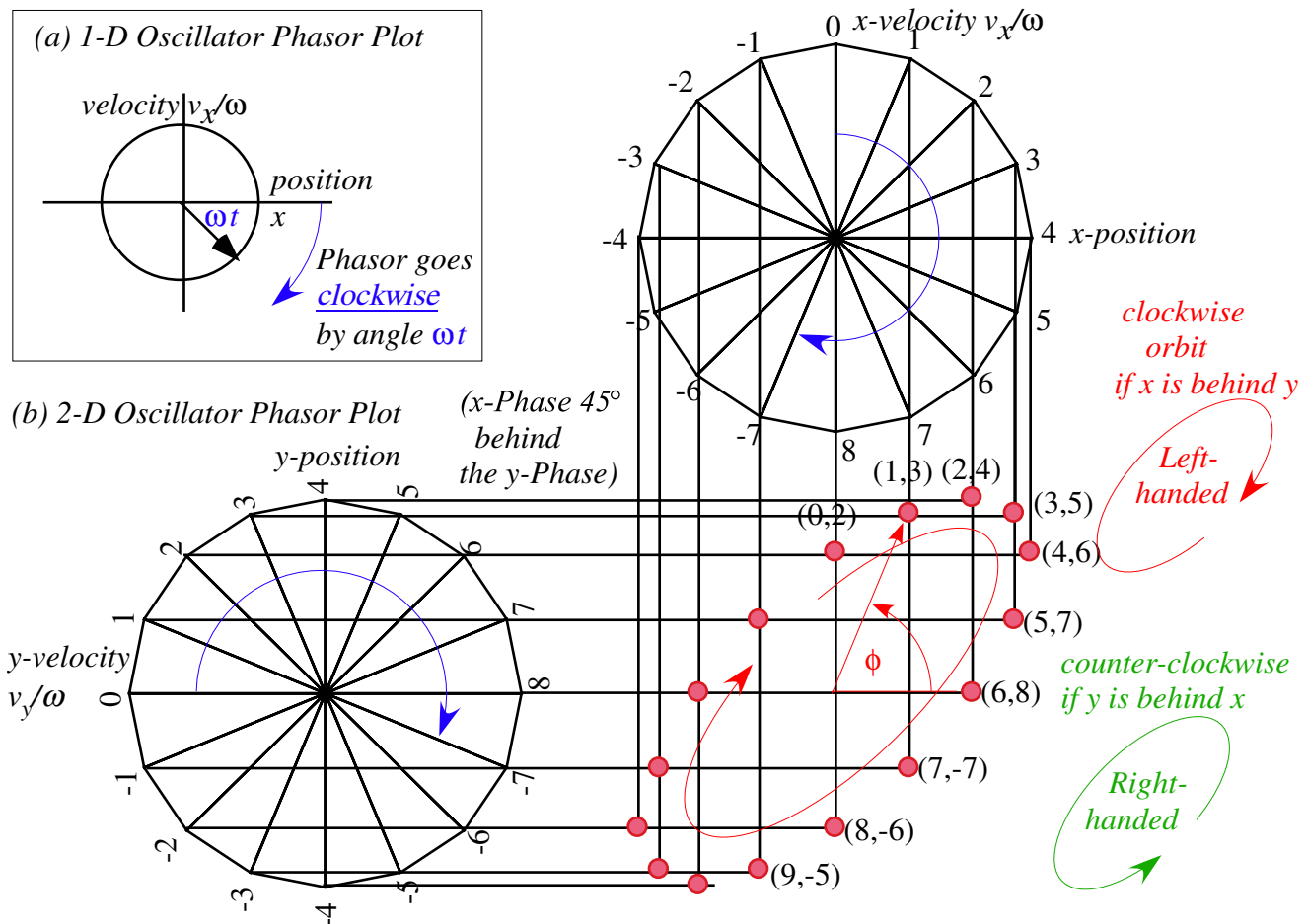


Fig. 9.10 Oscillator plots. (a) 1D-HO phasor plot. (b) Isotropic 2D-oscillator phasors and xy -path.

First we verify by algebra that orbits in Fig. 9.11 are ellipses. Fig. 9.11a has x running 90° behind y with a *relative phase lag* $\Delta\alpha=\alpha_x-\alpha_y=\pi/2$ that is 4 hours or $1/4$ -period behind in phase on a 16-hour clock. We say such a 90° -lagging- x -motion is *in-quadrature* to y -motion. It gives an un-tilted ellipse with a left-handed orbit, and if $e_x=a=b=e_y$, then it gives a circular orbit or *left-circular polarization*. (See Fig. 9.11a on right.) For right-handed orbits x -motion and x -motion switch leads to $\Delta\alpha=\alpha_x-\alpha_y=-\pi/2$.

Quadrature xy -motion is a *cosine* and *sine* projection on a -side and b -side of an ellipse, respectively, based on expressions (9.8).

$$x = a \cos \omega t, \quad (9.13a) \quad y = b \cos(\pi/2 - \omega t) = b \sin \omega t. \quad (9.13b)$$

Squaring and adding cosine and sine expressions gives a standard xy -ellipse equation.

$$x^2 / a^2 + y^2 / b^2 = 1 \quad (9.13c)$$

Zero phase lag $\Delta\alpha=0$ or *in-phase* motion gives *linear* polarization in Fig. 9.11b. In the case of Fig. 9.11b where x and y -motions are *in-phase* we have

$$x = a \cos \omega t, \quad (9.14a) \quad y = b \cos \omega t. \quad (9.14b)$$

Combining these two gives a trajectory that follows a straight line of slope (b/a) seen in the figure.

$$y = (b/a) x \quad (9.14c)$$

Lag $\Delta\alpha=\pm\pi$ or *pi-out-of-phase* is a linear polarized motion, too.

$$x = a \cos \omega t, \quad (9.15a) \quad y = -b \cos \omega t. \quad (9.15b)$$

It is simply a horizontal mirror reflection of the in-phase path.

$$y = -(b/a) x \quad (9.15c)$$

In each of the figures we could imagine *three* starlets going in unison. The first starlet obeys the y -equation (9.13b) with $x=0$. The second starlet obeys the x -equation (9.13a) with $y=0$ like the tunneling starlet in Fig. 9.8. A third starlet obeys *both* the x and y equations like the starlet orbiting above the tunneling one(s).

A *linear force field* $\mathbf{F}=-k\mathbf{r}$ is the only field whose Cartesian components oscillate sinusoidally at the same frequency.

$$\mathbf{F}=-k\mathbf{r} \quad \text{implies : } F_x=-kx, \quad F_y=-ky, \quad F_z=-kz \quad (9.15)$$

Neither the coulomb field $\mathbf{F}=-k\mathbf{r}/r^3$ nor any other power-law field $\mathbf{F}=-k\mathbf{r}r^p$ is so convenient!

As shown in later units, negative energy orbits in Coulomb fields are elliptic, too. However, Coulomb ellipses are symmetric about origin only for circular orbits. All other Coulomb orbits are eccentric since they orbit about one off-center focal point and not the ellipse center like a Hooke's law oscillator orbit.

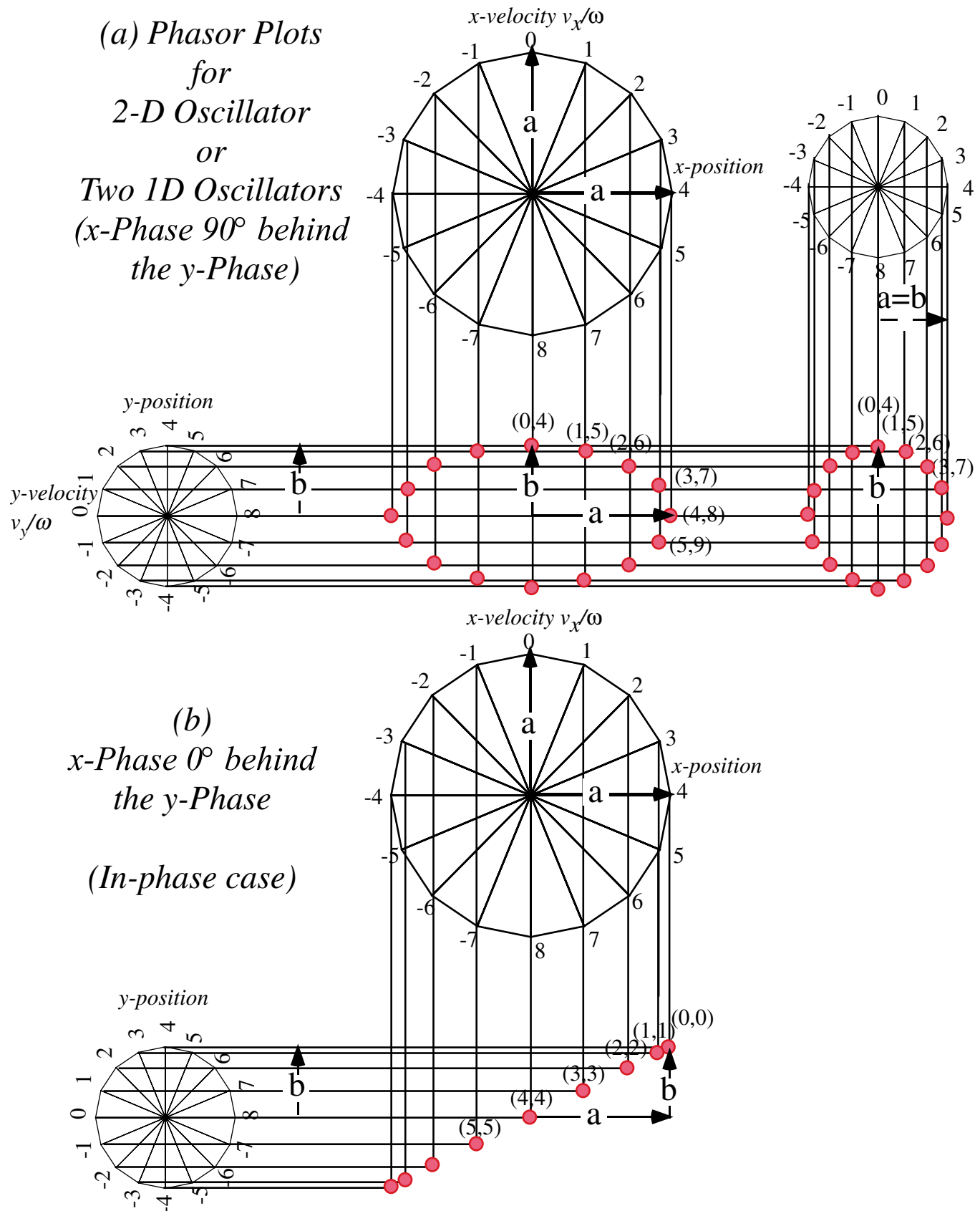


Fig. 9.11 Two 1-D oscillator phasor plots combine to give 2D-oscillator xy -trajectory.

Chapter 10 Exponentials, logarithms, and complex phasors

A *logarithmic* potential curve $U=\ln(y)=\log_e y$ was given by (6.11). Our first example is the flip or inverse *exponential* curve $y=e^U$ since that function is so important for making the *complex phasor* $e^{-i(\omega+\Gamma)t}$.

Also, the *population growth function* $y=e^t=\exp(t)$ is one of the most used if not *the* most useful of *transcendental* functions. Roughly, *transcendental* means not expressed by finite algebra or constructed by Euclid's strict rules. (However, like transcendental spirituality, it is easily *approximated!*) Later in this section we will prove that the exponential is the only function that is equal to its slope or *derivative*.

$$\frac{d}{dx} f(x) = f(x) \quad \text{if and only if:} \quad f(x) = e^x \quad \text{where: } e = 2.7182818\dots \quad (10.1)$$

In other words, if e^x is a force or potential curve then $F(x)$ and $U(x)$ are similar, in fact, identical.

$$F^{\text{math}}(x) = \frac{dU}{dx} = U(x). \text{ if and only if: } U(x) = e^x \quad (10.2a)$$

For physicist's definition (6.9) of force, e^{-x} is the one for which potential and force are identical.

$$F^{\text{phys}}(x) = -\frac{dU}{dx} = U(x). \text{ if and only if: } U(x) = e^{-x} \quad (10.2b)$$

For now we use these slope-function relations to construct the exponential curve approximately. Starting from origin ($x=0$) we use the fact that any positive number to zero power is 1. ($e^0=1$) From that point we draw a right triangle made of a unit altitude, a unit base, and a hypotenuse line of slope-1 as indicated in *Step-0* of Fig. 9.12. The hypotenuse line gives approximately the points just above and just below $x=0$. Then subsequent steps move the right triangle Δx to a point on the previously constructed line to make the next line. Since the slope is equal to the new function value, the base stays fixed at 1, but the altitude grows with the function value and makes the new line and a new point up the e^x -curve.

This approximation is a rough one. It underestimates a concave curve and overestimates convex ones because it puts the next point $x+\Delta x$ on a tangent from the previous point x . That's OK only if the curve is pretty straight and tangent slope is about the same at $x+\Delta x$. A better approximation uses the tangent halfway between neighboring tangents and extends that new slope to $x+\Delta x$ to find the next point.

Now if you rotate your $y = e^x$ -graph by 90° you get a *logarithm* $U(y)=-\ln(y)$ graph as shown in Fig. 10.1 (lower right). Each $U(y)$ -curve-normal defines a unit-altitude triangle whose base is the force $F(y)=1/y$.

The story of e : A tale of great intrest

Long ago banks would pay simple intrest at some rate r such as $r=0.03$ (3%) based on a 1 year period. You gave a principal $p(0)$ to the bank and some time t later they would pay you $p(t)=(1+r \cdot t)p(0)$. If you put in \$1.00 at rate $r=1$ (like Israel that once had 100% intrest.) you got \$2.00 at $t=1$ year.

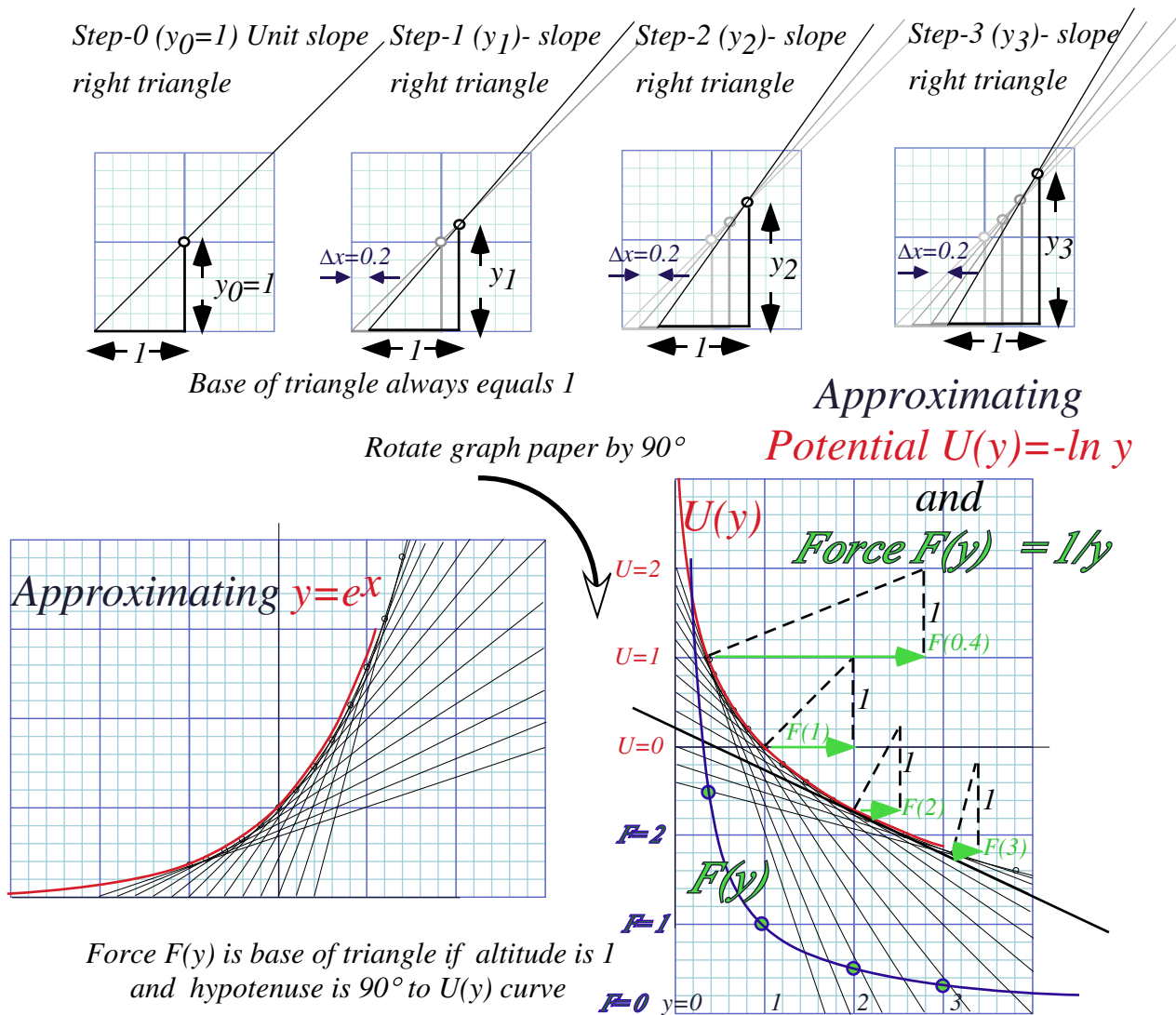


Fig. 10.1 Rough constructions (a) exponential curve $y=e^x=\exp(x)$. (b) Log potential. (c) $1/y$ -Force.

Later on fancy banks would pay *semester compounded* interest $p(\frac{t}{2}) = (1+r \cdot \frac{t}{2})p(0)$ at the half-period $\frac{t}{2}$ and then use $p(\frac{t}{2})$ during the last half to figure final payment. Now \$1.00 at rate $r=1$ earns \$2.25.

$$p^{\frac{1}{2}}(t) = (1+r \cdot \frac{t}{2})p(\frac{t}{2}) = (1+r \cdot \frac{t}{2}) \cdot (1+r \cdot \frac{t}{2})p(0) = \frac{3}{2} \cdot \frac{3}{2} \cdot 1 = \frac{9}{4} = 2.25$$

Fancier banks would pay *trimester compounded* interest $p(\frac{t}{3}) = (1+r \cdot \frac{t}{3})p(0)$ at the $1/3^{rd}$ -period $\frac{t}{3}$ or 1^{st} trimester and then use that to figure the 2^{nd} trimester and so on. Now \$1.00 at rate $r=1$ earns \$2.37.

$$p^{\frac{1}{3}}(t) = (1+r \cdot \frac{t}{3})p(2\frac{t}{3}) = (1+r \cdot \frac{t}{3}) \cdot (1+r \cdot \frac{t}{3})p(\frac{t}{3}) = (1+r \cdot \frac{t}{3}) \cdot (1+r \cdot \frac{t}{3}) \cdot (1+r \cdot \frac{t}{3})p(0) = \frac{4}{3} \cdot \frac{4}{3} \cdot \frac{4}{3} \cdot 1 = \frac{64}{27} = 2.37$$

Still fancier banks would pay *quarterly, monthly, weekly, daily*, and so on. The race was on to give better earnings at a given interest rate r . Let's compare some different earnings on \$1.00 at rate $r=1$. At first it looks like you gain a lot by compounding more often. Then earnings slow to a halt just shy of \$2.72.

$$\begin{aligned}
 p^{\frac{1}{1}}(t) &= (1+r\cdot\frac{t}{1})^1 p(0) = \left(\frac{2}{1}\right)^1 \cdot 1 = \frac{2}{1} = 2.00 & \text{Monthly: } p^{\frac{1}{12}}(t) &= (1+r\cdot\frac{t}{12})^{12} p(0) = \left(\frac{13}{12}\right)^{12} \cdot 1 = 2.613 \\
 p^{\frac{1}{2}}(t) &= (1+r\cdot\frac{t}{2})^2 p(0) = \left(\frac{3}{2}\right)^2 \cdot 1 = \frac{9}{4} = 2.25 & \text{Weekly: } p^{\frac{1}{52}}(t) &= (1+r\cdot\frac{t}{52})^{52} p(0) = \left(\frac{53}{52}\right)^{52} \cdot 1 = 2.693 \\
 p^{\frac{1}{3}}(t) &= (1+r\cdot\frac{t}{3})^3 p(0) = \left(\frac{4}{3}\right)^3 \cdot 1 = \frac{64}{27} = 2.37 & \text{Daily: } p^{\frac{1}{365}}(t) &= (1+r\cdot\frac{t}{365})^{365} p(0) = \left(\frac{366}{365}\right)^{365} \cdot 1 = \mathbf{2.7145} \\
 p^{\frac{1}{4}}(t) &= (1+r\cdot\frac{t}{4})^4 p(0) = \left(\frac{5}{4}\right)^4 \cdot 1 = \frac{625}{256} = 2.44 & \text{Hrly: } p^{\frac{1}{8760}}(t) &= (1+r\cdot\frac{t}{8760})^{8760} p(0) = \left(\frac{8761}{8760}\right)^{8760} \cdot 1 = \mathbf{2.7181}
 \end{aligned}$$

That halting point is *Euler's growth constant* $e=2.718281828459\dots$ that we're after. Let's try huge numbers (m) of multiplications in $p^{1/m}(1) = (1+\frac{1}{m})^m$. (Get out a calculator. Rule & compass is useless now!)

$$\begin{aligned}
 p^{1/m}(1) &= \mathbf{2.7169239322} & \text{for } m &= 1,000 \\
 p^{1/m}(1) &= \mathbf{2.7181459268} & \text{for } m &= 10,000 \\
 p^{1/m}(1) &= \mathbf{2.7182682372} & \text{for } m &= 100,000 \\
 p^{1/m}(1) &= \mathbf{2.7182804693} & \text{for } m &= 1,000,000 \\
 p^{1/m}(1) &= \mathbf{2.7182816925} & \text{for } m &= 10,000,000 \\
 p^{1/m}(1) &= \mathbf{2.7182818149} & \text{for } m &= 100,000,000 \\
 p^{1/m}(1) &= \mathbf{2.7182818271} & \text{for } m &= 1,000,000,000
 \end{aligned} \tag{10.3}$$

The **solid figures** represent numbers that stay the same as we raise m . It's still a torturous way to find e . We do a *Billion* (That's "B" as in "Boy!") multiplications ($m=10^9$) just to get 6 **solid figures** beyond **2.71**.

A better way expands binomial $e = \lim_{m \rightarrow \infty} (1+\frac{1}{m})^m$ or its power $e^{rt} = \lim_{m \rightarrow \infty} (1+\frac{1}{m})^{mr \cdot t}$ for all rates r and times t . We let $mr \cdot t = n$ and $m = n/r \cdot t$ to simplify it for huge multiplication numbers m or n .

$$e^{rt} = \lim_{m \rightarrow \infty} (1+\frac{1}{m})^{mr \cdot t} = \lim_{n \rightarrow \infty} (1+\frac{r \cdot t}{n})^n \tag{10.4}$$

The general *binomial expansion* turns exponential function e^{rt} into a power series in $y = \frac{r \cdot t}{n}$ with $x=1$.

$$(x+y)^n = x^n + n \cdot x^{n-1}y + \frac{n(n-1)}{2!} x^{n-2}y^2 + \frac{n(n-1)(n-2)}{3!} x^{n-3}y^3 + \dots + n \cdot xy^{n-1} + y^n$$

We actually *save* work as multiplication number n gets huge! ("Huge" means "as close to ∞ as you like.")

$$\left(1 + \frac{r \cdot t}{n}\right)^n = 1 + n \cdot \left(\frac{r \cdot t}{n}\right) + \frac{n(n-1)}{2!} \left(\frac{r \cdot t}{n}\right)^2 + \frac{n(n-1)(n-2)}{3!} \left(\frac{r \cdot t}{n}\right)^3 + \dots \quad \text{(Note factorials: } 0!=1=1!, 2!=1 \cdot 2, 3!=1 \cdot 2 \cdot 3, \text{ etc.)}$$

Huge n makes $n(n-1)$ cancel n^2 , and $n(n-1)(n-2)$ cancel n^3 , and so on. The exponential e^{rt} series is born.

$$e^{rt} = 1 + r \cdot t + \frac{1}{2!} (r \cdot t)^2 + \frac{1}{3!} (r \cdot t)^3 + \dots = \sum_{p=0}^o \frac{(r \cdot t)^p}{p!} \tag{10.5a} \qquad e = 1 + 1 + \frac{1}{2!} + \frac{1}{3!} + \dots = \sum_{p=0}^o \frac{1}{p!} \tag{10.5b}$$

Let's try it out for $r \cdot t = 1$ to evaluate e to order- o . (The *precision order* o is the power of highest term used.)

$$\begin{aligned}
 \text{Precision order: } (o=1)\text{-}e\text{-series} &= \mathbf{2.00000} = 1+1 \\
 (o=2)\text{-}e\text{-series} &= \mathbf{2.50000} = 1+1+1/2 \\
 (o=3)\text{-}e\text{-series} &= \mathbf{2.66667} = 1+1+1/2+1/6 \\
 (o=4)\text{-}e\text{-series} &= \mathbf{2.70833} = 1+1+1/2+1/6+1/24 \\
 (o=5)\text{-}e\text{-series} &= \mathbf{2.71667} = 1+1+1/2+1/6+1/24+1/120 \\
 (o=6)\text{-}e\text{-series} &= \mathbf{2.71805} = 1+1+1/2+1/6+1/24+1/120+1/720 \\
 (o=7)\text{-}e\text{-series} &= \mathbf{2.71825} \\
 (o=8)\text{-}e\text{-series} &= \mathbf{2.71828}
 \end{aligned} \tag{10.6}$$

Nine terms in series (10.5) give 5-figure accuracy (10.6) and do the work of a million products in (10.3). That's a *million* reduced to 8 sums and half-dozen or so divisions. It's a *big* savings of arithmetic labor!

Derivatives, rates, and rate equations

Binomial expansions provide ways to find calculus formulas for *slope* or *velocity* introduced geometrically in Ch. 1. Soon we will do the same for *curvature* or *acceleration* and other higher order calculus concepts.

Suppose someone gives you a plot of formula like $x(t)=t^2$ or $x(t)=\sin 4t$ or an exponential plot of $x(t)=e^t$ that we just did in Fig. 10.1. You should be able to *estimate* its slope at any point from its x versus t graph. However, a binomial expansion may let you find an *exact* formula for its slope.

Consider a parabola $x(t)=t^2$ for example. Let's find the slope $\frac{\Delta x}{\Delta t}$ of a line that goes through point $x(t)$ and a point $x(t+\Delta t)=(t+\Delta t)^2$ that is a *tiny* time interval Δt later. Binomial expansion gives $\Delta x=x(t+\Delta t)-x(t)$.

$$\Delta x=x(t+\Delta t)-x(t)=(t+\Delta t)^2-t^2=t^2+2t\cdot\Delta t+(\Delta t)^2-t^2=2t\cdot\Delta t+(\Delta t)^2$$

Slope ratio $\frac{\Delta x}{\Delta t}$ follows. If Δt is *tiny* we ignore it. Then *tangent slope* $v(t)=\frac{dx}{dt}$ is the *1st derivative* of $x(t)=t^2$.

$$\frac{\Delta x}{\Delta t}=\frac{2t\cdot\Delta t+(\Delta t)^2}{\Delta t}=2t+\Delta t \tag{10.7a}$$

$$\frac{dx}{dt}=v(t)=2t=\frac{d}{dt}t^2 \tag{10.7b}$$

This checks the geometry of parabola $2\lambda y=x^2$ in Fig. 9.4. Slope is $\frac{dy}{dx}=\frac{2x}{2\lambda}=\frac{x}{\lambda}$, twice the x -value in units of 2λ .

Consider an n -power curve $x(t)=At^n$. Binomial expansion of $\Delta x=x(t+\Delta t)-x(t)$ has n terms, most in $+\dots+$.

$$\Delta x=x(t+\Delta t)-x(t)=A(t+\Delta t)^n-At^n=At^n+Ant^{n-1}\cdot\Delta t+\dots+A(\Delta t)^n-At^n=Ant^{n-1}\cdot\Delta t+\dots+A(\Delta t)^n$$

If Δt is *tiny*, only *1st* term Ant^{n-1} in slope ratio $\frac{\Delta x}{\Delta t}$ is not *tiny-tiny*. That *1st* term is *1st derivative* of $x(t)=At^n$.

$$\frac{\Delta x}{\Delta t}=A\frac{nt^{n-1}\cdot\Delta t+\dots+(\Delta t)^n}{\Delta t}=Ant^{n-1}+\dots+A(\Delta t)^{n-1} \tag{10.8a}$$

$$\frac{dx}{dt}=v(t)=Ant^{n-1}=\frac{d}{dt}At^n \tag{10.8b}$$

Series for $x(t)=Ae^t$ is unchanged (for $r=1$) by $\frac{d}{dt}$. It does kill term number- ∞ , but $\frac{1}{\infty!}r^\infty t^\infty$ is *tiny-tiny-tiny* anyway.

$$\begin{aligned} \frac{d}{dt}e^{rt} &= \frac{d}{dt}1 + \frac{d}{dt}rt + \frac{d}{dt}\frac{1}{2!}r^2t^2 + \frac{d}{dt}\frac{1}{3!}r^3t^3 + \frac{d}{dt}\frac{1}{4!}r^4t^4 + \dots && \text{(From (10.5a) and linearity)} \\ &= 0 + r + \frac{2}{2!}r^2t + \frac{3}{3!}r^3t^2 + \frac{4}{4!}r^4t^3 + \dots && \text{(From (10.8b))} \\ &= 0 + r + r^2t + \frac{1}{2!}r^3t^2 + \frac{1}{3!}r^4t^3 + \dots && \text{(Factorial } n!=n\cdot(n-1)\cdot(n-2)\cdot\dots\cdot 1 \text{)} \\ &= r(1 + rt + \frac{1}{2!}r^2t^2 + \frac{1}{3!}r^3t^3 + \dots) = re^{rt} && \text{(From (10.5a) again)} \end{aligned} \tag{10.9}$$

For 100% interest ($r=1$), growth rate-of- Ae^t equals Ae^t . Otherwise, growth rate of Ae^{rt} is *proportional* to Ae^{rt} . To state that the growth rate of a function $x(t)$ equals a constant "*interest rate*" r times current value of $x(t)$ is to write a *differential rate equation* whose "*solution*" is $x(t)=Ae^{rt}$. (The constant A is "*initial capital*" $A=x(0)$.)

$$\text{Rate equation: } \frac{dx}{dt}=r\cdot x(t) \text{ has solution: } x(t)=x(0)e^{rt} \tag{10.10}$$

It is *Malthus's population explosion equation* for positive rate $r>0$! It is *radioactive decay equation* for $r<0$.

General power series approximations

Are power series like (10.5) useful for functions other than exponentials? Well, Mr. Maclaurin and Mr. Taylor thought so. Series that bear their names are *de rigueur* in good math books. (And, in this one, too!)

Let's start with a general power series like (10.5) but with arbitrary constant coefficients $c_0, c_1, \text{etc.}$

$$x(t) = c_0 + c_1 t + c_2 t^2 + c_3 t^3 + c_4 t^4 + c_5 t^5 + \dots + c_n t^n + \quad (10.11a)$$

We derive c_0 by setting time t to an *initial time* $t=0$. (Like C-programmers, we count “uh-zero, uh-one, uh-two...”)

$$c_0 = x(0) \quad (10.11b)$$

So the 0th coefficient c_0 is *initial position* $x(0)$. Now we use (10.8b) to find a derivative of each term.

$$v(t) = \frac{d}{dt} x(t) = 0 + c_1 + 2c_2 t + 3c_3 t^2 + 4c_4 t^3 + 5c_5 t^4 + \dots + n c_n t^{n-1} + \quad (10.11c)$$

Rate of change of position $x(t)$ is *velocity* $v(t)$. Setting $t=0$ derives c_1 .

$$c_1 = v(0) \quad (10.11d)$$

So the 1st coefficient c_1 is *initial velocity* $v(0)$. Now find a 2nd derivative using (10.8b).

$$a(t) = \frac{d}{dt} v(t) = 0 + 2c_2 + 2 \cdot 3c_3 t + 3 \cdot 4c_4 t^2 + 4 \cdot 5c_5 t^3 + \dots + n(n-1)c_n t^{n-2} + \quad (10.11c)$$

Change of velocity $v(t)$ is *acceleration* $a(t)$. Set $t=0$ to get c_2 .

$$c_2 = \frac{1}{2} a(0) \quad (10.11d)$$

So the 2nd coefficient c_2 is half the *initial acceleration* $a(0)$. Now a 3rd derivative:

$$j(t) = \frac{d}{dt} a(t) = 0 + 2 \cdot 3c_3 + 2 \cdot 3 \cdot 4c_4 t + 3 \cdot 4 \cdot 5c_5 t^2 + \dots + n(n-1)(n-2)c_n t^{n-3} + \quad (10.11e)$$

Change of acceleration $a(t)$ is *jerk* $j(t)$. (*Jerk* is a NASA sanctioned term!) Set $t=0$ to get c_3 .

$$c_3 = \frac{1}{3!} j(0) \quad (10.11f)$$

So the 3rd coefficient c_3 is *initial jerk* $j(0)$ over $3!$. Now a 4th derivative:

$$i(t) = \frac{d}{dt} j(t) = 0 + 2 \cdot 3 \cdot 4c_4 + 2 \cdot 3 \cdot 4 \cdot 5c_5 t + \dots + n(n-1)(n-2)(n-3)c_n t^{n-4} + \quad (10.11g)$$

Change of jerk $j(t)$ is *inauguration* $i(t)$. (If NASA can be silly, so can we!) Set $t=0$ to get c_4 .

$$c_4 = \frac{1}{4!} i(0) \quad (10.11h)$$

So the 4th coefficient c_4 is *initial inauguration* $i(0)$ over $4!$. Now a 5th derivative.

$$r(t) = \frac{d}{dt} i(t) = 0 + 2 \cdot 3 \cdot 4 \cdot 5c_5 + \dots + n(n-1)(n-2)(n-3)(n-4)c_n t^{n-5} + \quad (10.11i)$$

Change of inauguration $i(t)$ is *revolution* $r(t)$. (Ooops! Politically incorrect!) Quick set $t=0$ to get c_5 .

$$c_5 = \frac{1}{5!} r(0) \quad (10.11j)$$

That's enough iterations to show the Maclaurin series of any function $x(t)$ that has decent derivatives.

$$x(t) = x(0) + v(0)t + \frac{1}{2!} a(0)t^2 + \frac{1}{3!} j(0)t^3 + \frac{1}{4!} i(0)t^4 + \frac{1}{5!} r(0)t^5 + \dots + \frac{1}{n!} x^{(n)}t^n + \dots \tag{10.12a}$$

By “decent” we mean the non-exploding types that we can deal with. The following is a list that shows some of the notations used for the higher order derivatives discussed so far.

$$\begin{aligned} v(t) &= \frac{d}{dt} x(t) = \dot{x}(t) \\ a(t) &= \frac{d}{dt} v(t) = \dot{v}(t) = \frac{d^2}{dt^2} x(t) = \ddot{x}(t) \\ j(t) &= \frac{d}{dt} a(t) = \dot{a}(t) = \frac{d^2}{dt^2} v(t) = \ddot{v}(t) = \frac{d^3}{dt^3} x(t) = \dddot{x}(t) \\ i(t) &= \frac{d}{dt} j(t) = \dot{j}(t) = \frac{d^2}{dt^2} a(t) = \ddot{a}(t) = \frac{d^3}{dt^3} v(t) = \ddot{v}(t) = \frac{d^4}{dt^4} x(t) = \ddddot{x}(t) \end{aligned} \tag{10.12b}$$

The “dot” notation writes n -derivatives of $x(t)$ by putting n -dots over x . This may help prevent writer's cramp. But, j -dot looks, well, kind of jerky. It's common to use primes ($y' = \frac{dy}{dx}, y'' = \frac{d^2y}{dx^2}, etc.$) for x -derivatives.

How good is a power series (10.5) at faking $x=e^t$ beyond $t=1$ listed in (10.6)? We plot various orders of approximation in Fig. 10.2. The 1st order (2-terms of (10.5a)) is just a straight line of slope 1. A 2nd order (3-term) parabola, 3rd order cubic, 4th order quartic, etc. each peel off $x=e^t$ in succession. All meet at $(t=0, x=1)$.

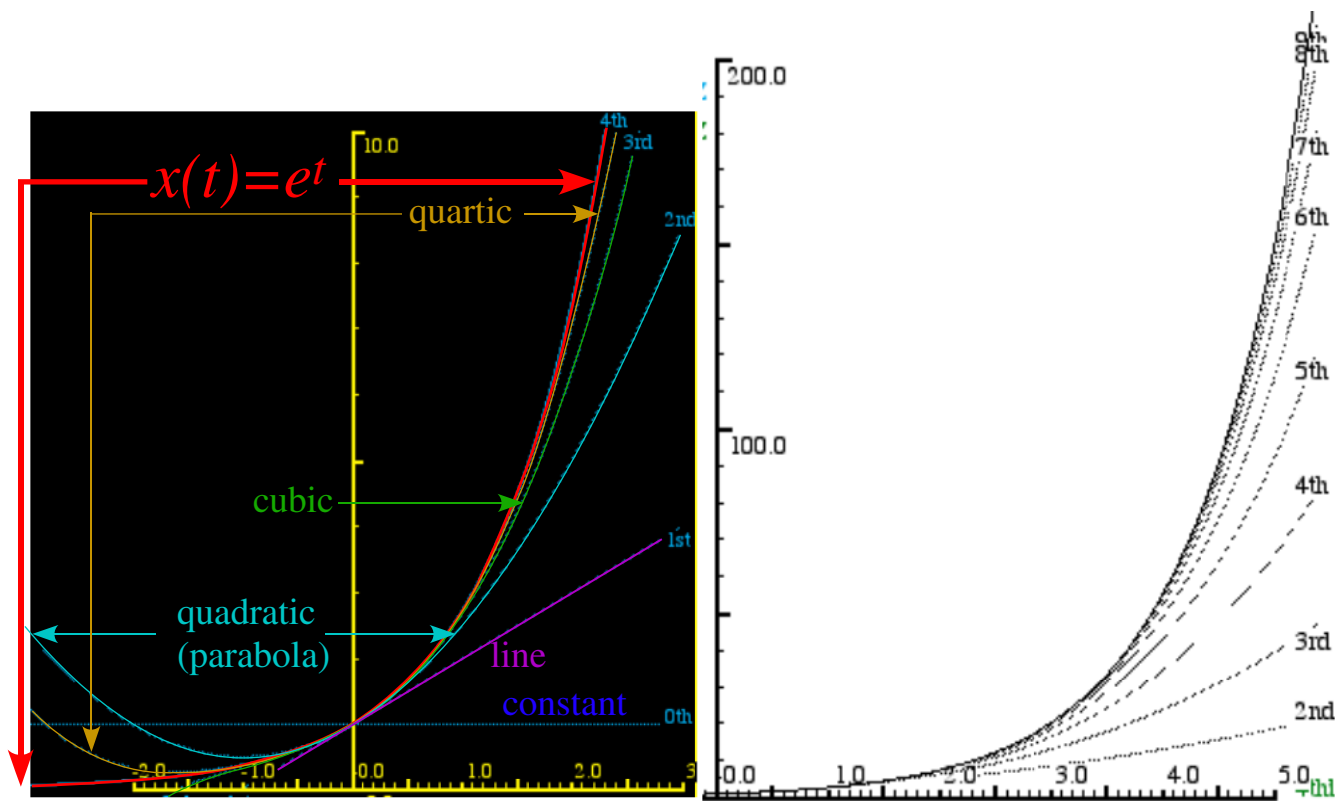


Fig. 10.2 Comparing $x=e^t$ with its n^{th} -order approximate power series.

Sine-wave power series

A severe test of power series is their ability to fake sine waves. The derivative and rate equation for the sine function $x(t)=\sin\omega t$ uses expansion $x(t+\Delta t)=\sin\omega(t+\Delta t)$. To expand $\sin(a+b)$ or $\cos(a+b)$ we use Fig. 10.3.

$$\sin(a+b) = \cos a \sin b + \sin a \cos b \quad (10.13a)$$

$$\cos(a+b) = \cos a \cos b - \sin a \sin b \quad (10.13b)$$

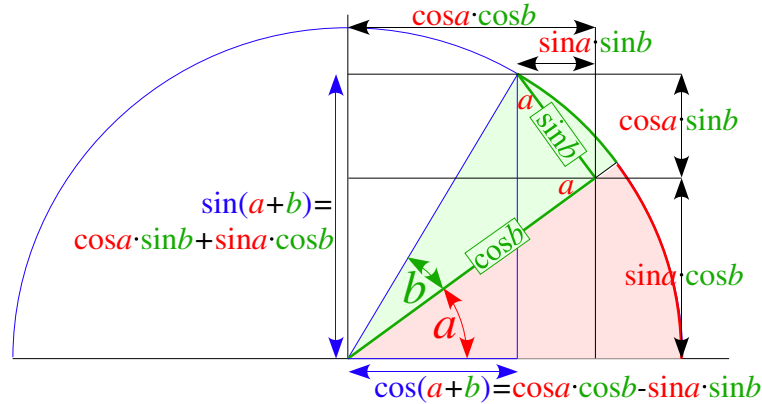


Fig. 10.3 Geometry of sine and cosine expansion identities.

Expansion of $\Delta x = x(t+\Delta t) - x(t)$ for sine or cosine is easy since $\sin\omega\Delta t = \omega\Delta t$ and $\cos\omega\Delta t = 1$ for tiny Δt .

$$\begin{aligned} \sin\omega(t+\Delta t) - \sin\omega t &= \cos\omega t \sin\omega\Delta t + \sin\omega t \cos\omega\Delta t - \sin\omega t \\ &= \cos\omega t (\omega\Delta t) + \sin\omega t (1) - \sin\omega t \\ &= (\omega\Delta t)\cos\omega t \end{aligned} \quad (10.14a)$$

$$\begin{aligned} \cos\omega(t+\Delta t) - \cos\omega t &= \cos\omega t \cos\omega\Delta t - \sin\omega t \sin\omega\Delta t - \cos\omega t \\ &= \cos\omega t (1) - \sin\omega t (\omega\Delta t) - \cos\omega t \\ &= -(\omega\Delta t)\sin\omega t \end{aligned} \quad (10.14b)$$

We will need the sine and cosine slope (derivative) formulas that follow from this.

$$\begin{aligned} \frac{d}{dt}\sin\omega t &= \frac{\sin\omega(t+\Delta t) - \sin\omega t}{\Delta t} \\ &= \omega \cdot \cos\omega t \end{aligned} \quad (10.15a)$$

$$\begin{aligned} \frac{d}{dt}\cos\omega t &= \frac{\cos\omega(t+\Delta t) - \cos\omega t}{\Delta t} \\ &= -\omega \cdot \sin\omega t \end{aligned} \quad (10.15b)$$

A list of series coefficients $c_n = \frac{1}{n!} \frac{d^n x}{dt^n}$ in (10.12) for sine $x = \sin\omega t$ and cosine $x = \cos\omega t$ is worked out below.

$$\begin{aligned} c_0 &= x(0) = \sin\omega \cdot 0 = 0 \\ c_1 &= v(0) = +\omega \cdot \cos\omega \cdot 0 = +\omega \\ c_2 &= \frac{a(0)}{2!} = -\frac{\omega^2}{2!} \cdot \sin\omega \cdot 0 = 0 \\ c_3 &= \frac{j(0)}{3!} = -\frac{\omega^3}{3!} \cdot \cos\omega \cdot 0 = -\frac{\omega^3}{3!} \\ c_4 &= \frac{i(0)}{4!} = +\frac{\omega^4}{4!} \cdot \sin\omega \cdot 0 = 0 \\ c_5 &= \frac{r(0)}{5!} = +\frac{\omega^5}{5!} \cdot \cos\omega \cdot 0 = +\frac{\omega^5}{5!} \end{aligned}$$

$$\begin{aligned} c_0 &= x(0) = \cos\omega \cdot 0 = 1 \\ c_1 &= v(0) = -\omega \cdot \sin\omega \cdot 0 = 0 \\ c_2 &= \frac{a(0)}{2!} = -\frac{\omega^2}{2!} \cdot \cos\omega \cdot 0 = -\frac{\omega^2}{2!} \\ c_3 &= \frac{j(0)}{3!} = +\frac{\omega^3}{3!} \cdot \sin\omega \cdot 0 = 0 \\ c_4 &= \frac{i(0)}{4!} = +\frac{\omega^4}{4!} \cdot \cos\omega \cdot 0 = +\frac{\omega^4}{4!} \\ c_5 &= \frac{r(0)}{5!} = -\frac{\omega^5}{5!} \cdot \sin\omega \cdot 0 = 0 \end{aligned}$$

A sine derivative repeats after four orders: ...sin t, cos t, -sin t, -cos t, (again) sin t, cos t, -sin t, -cos t, (etc.) .

The resulting sine and cosine series show this *repeat-after-4-pattern* of factors 0,1,0,-1 of $\frac{(\omega t)^n}{n!}$ terms.

$$\sin \omega t = 0 + \omega t + 0 - \frac{(\omega t)^3}{3!} + 0 + \frac{(\omega t)^5}{5!} + 0 - \dots$$

(10.16a)

$$\cos \omega t = 1 + 0 - \frac{(\omega t)^2}{2!} + 0 + \frac{(\omega t)^4}{4!} + 0 - \dots$$

(10.16b)

The sine is an *odd* function to time reversal ($\sin(-t) = -\sin(t)$), but cosine is *even* ($\cos(-t) = +\cos(t)$). Thus sine has only odd powers $p=1,3,5,\dots$ of time and cosine has only even powers $p=0,2,4,\dots$. Series plots (10.16) in Fig. 10.4 have highest power or *order* $o=1^{st}, 2^{nd}, 3^{rd}, 4^{th}, \text{etc.}$. Number n of terms is $\frac{o+1}{2}$ for sine and $\frac{o+2}{2}$ for cosine.

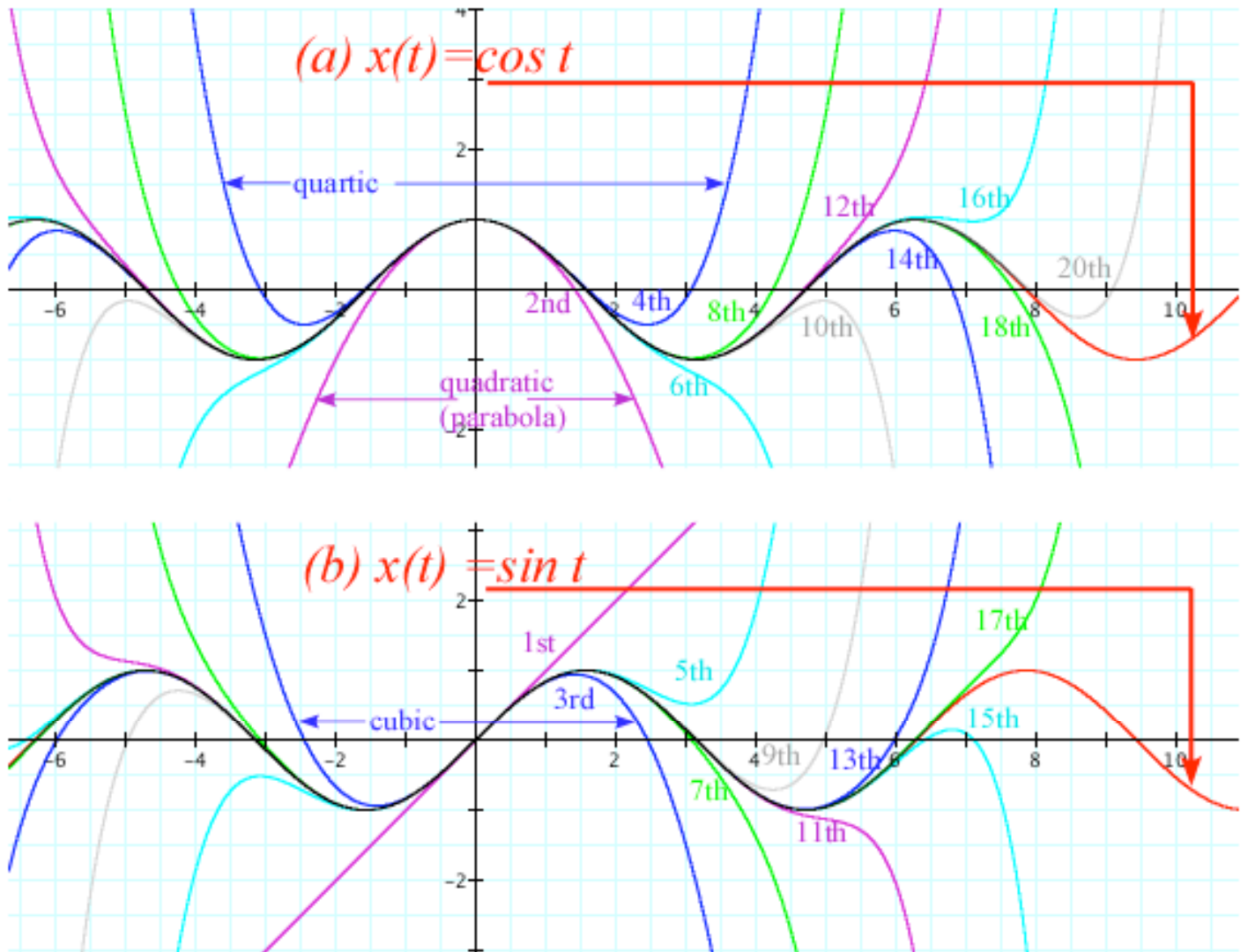


Fig. 10.4 Comparing (a) $x=\sin t$ and (b) $x=\cos t$ with their n^{th} -order approximate power series.

It takes a 9^{th} (for $\sin t$) or 10^{th} (for $\cos t$) order series of 5 terms to get one full oscillation with 5% or better precision. Then 10 terms gives two oscillations, and so on. Fig. 10.4 shows that precision breaks down quite explosively. Polynomials are *exponentially degrading* approximations of wave motion.

Euler's theorem and relations

Sine, cosine, and e^{rt} power series (10.16) and (10.9) lead to an 18th Century crown jewel of mathematics. It is due to a close relation of these series and the functions they represent. It is hard to imagine, but exponential interest rate growth and simple harmonic oscillation are related. As it turns out, the relation *is* quite imaginary!

Suppose the fancy bankers really went bonkers and made interest rate r an *imaginary number* $r=i\theta$.

Imaginary number $i = \sqrt{-1}$ has powers with a *repeat-after-4-pattern*: $i^0=1, i^1=i, i^2=-1, i^3=-i, i^4=1, etc...$ It fits the pattern leading to $\cos\theta$ and $\sin\theta$ series (10.16). Series (10.9) with imaginary $rt=i\theta$ joins the (10.16) series.

$$\begin{aligned}
 e^{i\theta} &= 1 + i\theta + \frac{(i\theta)^2}{2!} + \frac{(i\theta)^3}{3!} + \frac{(i\theta)^4}{4!} + \frac{(i\theta)^5}{5!} + \dots && \text{(From series (10.9))} \\
 &= 1 + i\theta - \frac{\theta^2}{2!} - i\frac{\theta^3}{3!} + \frac{\theta^4}{4!} + i\frac{\theta^5}{5!} - \dots && (i = \sqrt{-1} \text{ implies: } i^1=i, i^2=-1, i^3=-i, i^4=+1, i^5=i, \dots) \\
 &= \left(1 - \frac{\theta^2}{2!} + \frac{\theta^4}{4!} - \dots \right) + \left(i\theta - i\frac{\theta^3}{3!} + i\frac{\theta^5}{5!} - \dots \right) && \text{(To match series (10.16))} \\
 e^{i\theta} &= \cos\theta + i\sin\theta && \text{Euler - DeMoivre Theorem} \tag{10.17}
 \end{aligned}$$

The resulting *Euler-DeMoivre Theorem* is a beautiful identity and a very powerful tool as we shall see. First and foremost it is a *complex wave phasor function* $\psi = Ae^{-i\omega t}$ that we will use from now on. (Note: $\theta = -\omega t$.)

$$\psi = Ae^{-i\omega t} = A \cos \omega t - i A \sin \omega t = \text{Re } \psi + i \text{Im } \psi = \psi_x + i\psi_y \tag{10.18}$$

Fig. 10.5a plots $e^{i\theta}$ in the *complex plane*, a real-vs-imaginary graph. Fig. 10.5b shows $\psi = Ae^{-i\omega t}$ as a *complex phasor clock*. Its *real part* is position $\text{Re}\psi = x(t)$ and its *imaginary part* is ω -scaled velocity $\text{Im}\psi = v(t)/\omega$. Polar-to-Cartesian conversion (10.19a) and *vice-versa* (10.19b) are easy by scientific calculator. (*Recall end of Ch. 1.*)

$$\begin{aligned}
 \text{Cartesian } \begin{cases} \psi_x = \text{Re } \psi(t) = x(t) = A \cos \omega t \\ \psi_y = \text{Im } \psi(t) = \frac{v(t)}{\omega} = -A \sin \omega t \end{cases} && \text{(10.19a)} && \text{Polar } \begin{cases} r = A = |\psi| = \sqrt{\psi_x^2 + \psi_y^2} \\ \theta = -\omega t = \arctan(\psi_y / \psi_x) \end{cases} && \text{(10.19b)}
 \end{aligned}$$

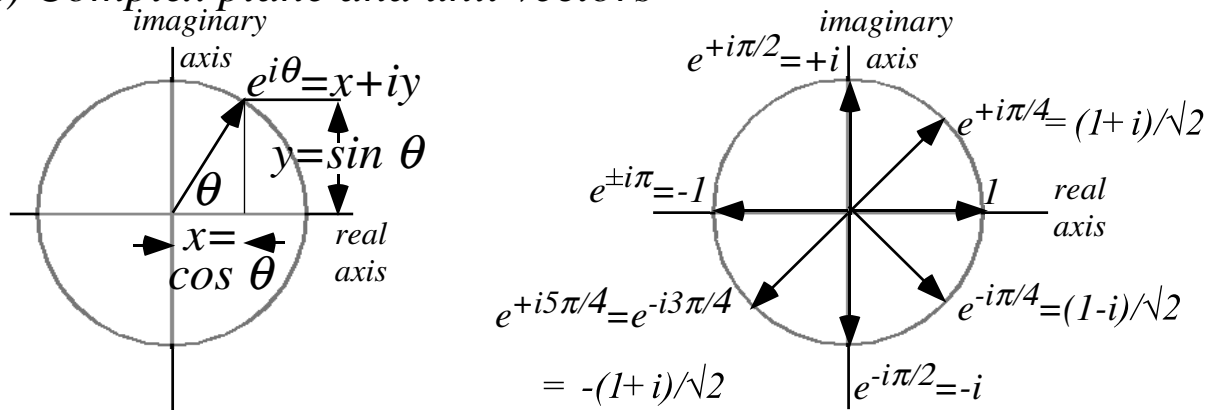
Real part $\text{Re}\psi$ is the “*is*” (*that Clinton sought in 1997*) and $\text{Im}\psi$ is what $\text{Re}\psi$ is “*gonna-be*” in $\frac{1}{4}$ -cycle (*as in “gonna be in trouble!”* A mantra, “*Imagination precedes reality by one quarter*” works here as in US corporate world.) *Euler expo-sino conversion identities* relate $\cos\theta, \sin\theta$, and $e^{\pm i\theta}$. A *conjugate* ψ^* reflects i with $-i$.

$$\begin{aligned}
 \psi &= re^{+i\theta} = re^{-i\omega t} = r(\cos \omega t - i \sin \omega t) && \text{(10.20a)} && \cos\theta = \frac{1}{2}(e^{+i\theta} + e^{-i\theta}) && \text{(10.20b)} \\
 \psi^* &= re^{-i\theta} = re^{+i\omega t} = r(\cos \omega t + i \sin \omega t) && && \sin\theta = \frac{1}{2i}(e^{+i\theta} - e^{-i\theta}) &&
 \end{aligned}$$

A special case is $e^{-i\pi} = -1$. (We’ll also use a *real* π -exponential: $e^{-\pi} = 0.04321$.) Other special cases are noted.

$$e^{-i\pi} = -1 = e^{+i\pi}, \quad e^{+i\frac{\pi}{2}} = i = -e^{-i\frac{\pi}{2}}, \quad e^{+i\frac{\pi}{4}} = \frac{1}{\sqrt{2}}(1+i) = -e^{-i\frac{3\pi}{4}} = -e^{+i\frac{5\pi}{4}}. \tag{10.21}$$

(a) Complex plane and unit vectors



(b) Quantum Phasor Clock $\psi = Ae^{-i\omega t} = A\cos\omega t - iA\sin\omega t = x + iy$

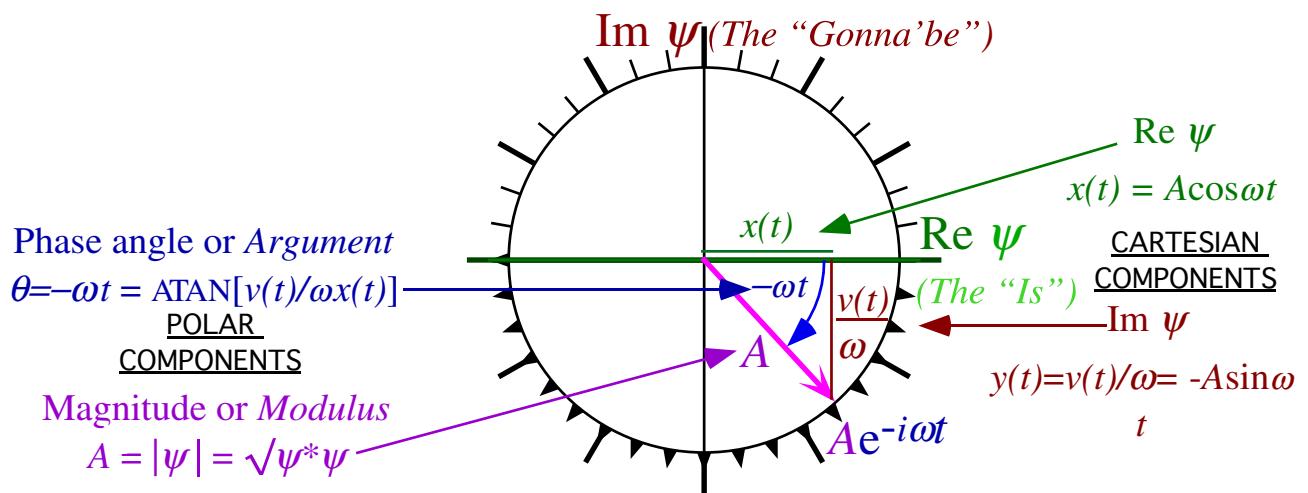


Fig. 10.5 (a) Complex plane. (b) Phasor clock. Cartesian form uses $(\text{Re}\psi, \text{Im}\psi)$. Polar form uses $(|\psi|, \theta)$.

Wages of imaginary interest: Phasor oscillation dynamics

By now bankers should know what happens when you use *imaginary interest*. The accounts *oscillate* up and down and the imagineering bankers *oscillate* in and out of the slammer. (At least that was the way until 2001 when the Bush administration passed the *No Banker Left on His Behind Act* that also outlawed reality.)

Consider exponential rate equation (10.15) with negative imaginary rate $r = -i\omega$.

$$\text{Imaginary rate equation: } \frac{dx}{dt} = -i\omega \cdot x(t) \text{ has solution: } x(t) = x(0)e^{-i\omega t} \tag{10.22a}$$

It becomes a real 2nd order equation if we apply the derivative operation to both sides.

$$\frac{d}{dt} \frac{dx(t)}{dt} = \frac{d^2x}{dt^2} = -i\omega \cdot \frac{d}{dt} x(t) = -i\omega \cdot (-i\omega \cdot x(t)) = -\omega^2 x(t) \tag{10.22b}$$

It is the *Newton-Hooke simple harmonic oscillator equation*, but it has the same solution as (10.19) above.

$$\text{Newton-Hooke HO equation: } \frac{d^2x}{dt^2} = -\omega^2 x(t) \text{ has solution: } x(t) = x(0)e^{-i\omega t} \quad (10.23a)$$

It combines Newton's force law $F=m \cdot a=m \ddot{x}$ and Hooke's force law $F=-k \cdot x$. The ω value repeats (9.9b).

$$m \frac{d^2x}{dt^2} = -k \cdot x(t) \text{ has angular frequency: } \omega = \sqrt{\frac{k}{m}} \quad (10.23b)$$

What Good Are Complex Exponentials?

Complex Exponentials are used to describe oscillation, resonance, waves and fields. We don't use them just to be cute! Let's look at some compelling reasons for using imaginary or complex arithmetic.

Complex numbers provide "automatic trigonometry"

If you have trouble remembering trigonometric identities then this is a good reason all by itself to use complex numbers. For example, if you're taking a test and you can't remember what is $\cos(a+b)$, then just factor $e^{i(a+b)} = e^{ia}e^{ib}$, expand exponentials into $e^{ia} = \cos a + i \sin a$ and multiply them out.

$$\begin{aligned} e^{i(a+b)} &= e^{ia}e^{ib} \\ \cos(a+b) + i \sin(a+b) &= (\cos a + i \sin a) (\cos b + i \sin b) \\ \cos(a+b) + i \sin(a+b) &= [\cos a \cos b - \sin a \sin b] + i[\sin a \cos b + \cos a \sin b] \end{aligned} \quad (10.24a)$$

That's two trig identities for the price of one! The real part gives the cosine relation (10.13b).

$$\cos(a+b) = [\cos a \cos b - \sin a \sin b] \quad (10.24b)$$

The imaginary part gives the sine relation (10.13a).

$$\sin(a+b) = [\sin a \cos b + \cos a \sin b]. \quad (10.24c)$$

Complex exponentials $Ae^{-i\omega t}$ tracks position and velocity using Phasor Clock.

Recall discussion of phasor diagram in Fig. 10.5b. Real and imaginary give position and velocity.

Complex numbers add like vectors.

Physics of *wave interference* involves the addition or subtraction of oscillating signals. If the signals are represented by complex numbers then you simply add (or subtract) their Cartesian components.

$$\begin{aligned} z_{sum} &= z + z' = (x + iy) + (x' + iy') = (x + x') + i(y + y') \\ z_{diff} &= z - z' = (x + iy) - (x' + iy') = (x - x') + i(y - y') \end{aligned}$$

Before adding, convert z and z' to Cartesian (x,y) form if given in polar form $z=re^{i\phi}$ and $z'=r'e^{i\phi'}$. Radius r of a vector z is its *magnitude* or *complex absolute value* $|z|$. Square $|z|^2$ is proportional to energy or *intensity*.

$$|z| = r = \sqrt{(x^2 + y^2)} = \sqrt{([x - iy][x + iy])} = \sqrt{(z^*z)}$$

We write $|z|^2$ as product of z and its *complex conjugate* $z^* = x - iy = re^{-i\phi}$ to derive radius $|z_{sum}|$ of a vector sum z_{sum} or radius $|z_{diff}|$ of a difference z_{diff} . It is an easy way to get the well-known *cosine laws*.

$$|z_{SUM}| = \sqrt{(z+z')^*(z+z')} = \sqrt{(re^{i\phi} + r'e^{i\phi'})^*(re^{i\phi} + r'e^{i\phi'})} = \sqrt{(re^{-i\phi} + r'e^{-i\phi'})(re^{i\phi} + r'e^{i\phi'})}$$

$$= \sqrt{r^2 + r'^2 + rr'(e^{i(\phi-\phi')} + e^{-i(\phi-\phi')})} = \sqrt{r^2 + r'^2 + 2rr' \cos(\phi - \phi')} \tag{10.25a}$$

$$|z_{DIFF}| = \sqrt{(z-z')^*(z-z')} = \sqrt{r^2 + r'^2 - 2rr' \cos(\phi - \phi')} \tag{10.25b}$$

Vector diagrams of sum, difference, and product of complex z and z' are shown in Fig. 10.6.

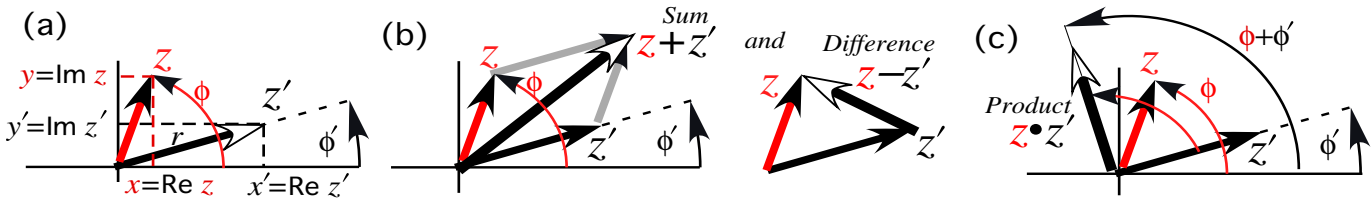


Fig. 10.6 Parallelogram diagonals are sum $z_{sum}=z+z'$ and difference $z_{diff}=z-z'$ vectors.

Complex products provide 2D rotation operations.

A product zz' of two complex numbers expressed in Cartesian form as $z = x + iy$ and $z' = x' + iy'$ is

$$z z' = (x + iy)(x' + iy') = [xx' - yy'] + i[xy' + yx'].$$

It is simpler if the numbers are expressed in polar form as $z = r e^{i\phi}$ and $z' = r' e^{i\phi'}$.

$$z z' = (r e^{i\phi})(r' e^{i\phi'}) = r r' e^{i(\phi+\phi')}. \tag{10.26}$$

Note that multiplication results in addition of exponents and a sum of polar angles. Radii multiply to give a product rr' but angles add to give a sum $(\phi+\phi')$. You might imagine z rotating vector z' by ϕ radians or that z' rotates z by ϕ' radians. Consider in detail a *rotational operator* $e^{i\phi}$ on a vector $z = (x + iy)$.

$$e^{i\phi} \cdot z = (\cos\phi + i \sin\phi) \cdot (x + iy) = x \cos\phi - y \sin\phi + i(x \sin\phi + y \cos\phi) \tag{10.27a}$$

Ch. 5 2-by-2 rotation matrix \mathbf{R}_ϕ (Fig. 5.3d) acts on a 2D vector \mathbf{r} to give results precisely similar to $e^{i\phi} \cdot z$.

$$\mathbf{R}_{+\phi} \cdot \mathbf{r} = (x \cos\phi - y \sin\phi)\hat{e}_x + (x \sin\phi + y \cos\phi)\hat{e}_y \tag{10.27b}$$

$$\begin{pmatrix} \cos\phi & -\sin\phi \\ \sin\phi & \cos\phi \end{pmatrix} \cdot \begin{pmatrix} x \\ y \end{pmatrix} = \begin{pmatrix} x \cos\phi - y \sin\phi \\ x \sin\phi + y \cos\phi \end{pmatrix} \tag{10.27c}$$

Complex products set initial values

Phase angle $-\omega t$ of phasor $e^{-i\omega t}$ rotates clockwise with time. Multiplying $e^{-i\omega t}$ by a complex amplitude $A = |A|e^{i\rho}$ sets its phase *back* by angle ρ and its radius to $|A|$. Amplitude A is the *initial value* $x(0) = |A|e^{i\rho}$.

$$x(t) = Ae^{-i\omega t} = x(0)e^{-i\omega t} = |A|e^{i\rho}e^{-i\omega t} = |A|e^{-i(\omega t - \rho)} \tag{10.28}$$

Such products set initial values of oscillator clocks. A positive angle ρ is a *phase lag* since it moves the phasor counter-clockwise and sets its clock back. A negative angle $\rho = -|\rho|$ gives a *phase lead*.

Complex products provide 2D “dot”(•) and “cross”(×) products.

Consider any two vectors $A=A_x+iA_y$ and $B=B_x+iB_y$ and their “star” (*)-product $A*B$.

$$\begin{aligned} A*B &= (A_x + iA_y)^* (B_x + iB_y) = (A_x - iA_y)(B_x + iB_y) \\ &= (A_x B_x + A_y B_y) + i(A_x B_y - A_y B_x) = \mathbf{A} \cdot \mathbf{B} + i |\mathbf{A} \times \mathbf{B}|_{Z \perp(x,y)} \end{aligned} \tag{10.29}$$

Real part is scalar or “dot”(•) product $\mathbf{A} \cdot \mathbf{B}$. Imaginary part is vector or “cross”(×) product, but just the Z-component normal to xy-plane. To better understand this math trickery, we rewrite $A*B$ in polar form.

$$\begin{aligned} A*B &= (|A|e^{i\theta_A})^* (|B|e^{i\theta_B}) = |A|e^{-i\theta_A} |B|e^{i\theta_B} = |A||B|e^{i(\theta_B-\theta_A)} \\ &= |A||B|\cos(\theta_B - \theta_A) + i|A||B|\sin(\theta_B - \theta_A) = \mathbf{A} \cdot \mathbf{B} + i |\mathbf{A} \times \mathbf{B}|_{Z \perp(x,y)} \end{aligned} \tag{10.30a}$$

Standard 3D definitions of dot(•) and cross(×) products of 3D vectors are precisely similar.

$$\mathbf{A} \cdot \mathbf{B} = |A||B|\cos(\angle_A^B) \qquad |\mathbf{A} \times \mathbf{B}| = |A||B|\sin(\angle_A^B) \tag{10.30b}$$

Expansion (10.24) of Δ-angle $a + b = \angle_A^B = \theta_B - \theta_A$ relates $re^{i\theta}$ forms (10.30) to xy -forms in (10.29).

$$\begin{aligned} \mathbf{A} \cdot \mathbf{B} &= |A||B|\cos(\theta_B - \theta_A) & |\mathbf{A} \times \mathbf{B}| &= |A||B|\sin(\theta_B - \theta_A) \\ &= |A|\cos\theta_A |B|\cos\theta_B + |A|\sin\theta_A |B|\sin\theta_B & &= |A|\cos\theta_A |B|\sin\theta_B - |A|\sin\theta_A |B|\cos\theta_B \\ &= A_x B_x + A_y B_y & &= A_x B_y - A_y B_x \end{aligned}$$

Complex derivative contains “divergence”(∇•F) and “curl”(∇×F) of 2D vector field

By relating (z, z^*) to $(x=\text{Re}z, y=\text{Im}z)$ we may define a z -derivative $\frac{df}{dz}$ and “star” z^* -derivative $\frac{df}{dz^*}$.

$$\begin{aligned} z &= x + iy & x &= \frac{1}{2}(z + z^*) & \frac{df}{dz} &= \frac{\partial x}{\partial z} \frac{\partial f}{\partial x} + \frac{\partial y}{\partial z} \frac{\partial f}{\partial y} = \frac{1}{2} \frac{\partial f}{\partial x} - \frac{i}{2} \frac{\partial f}{\partial y} \\ z^* &= x - iy & y &= \frac{1}{2i}(z - z^*) & \frac{df}{dz^*} &= \frac{\partial x}{\partial z^*} \frac{\partial f}{\partial x} + \frac{\partial y}{\partial z^*} \frac{\partial f}{\partial y} = \frac{1}{2} \frac{\partial f}{\partial x} + \frac{i}{2} \frac{\partial f}{\partial y} \end{aligned} \tag{10.31}$$

Derivative chain-rule shows real part of $\frac{df}{dz}$ has 2D divergence $\nabla \cdot \mathbf{F}$ and imaginary part has curl $\nabla \times \mathbf{F}$.

$$\frac{df}{dz} = \frac{d}{dz} (f_x + i f_y) = \frac{1}{2} (\frac{\partial f}{\partial x} - i \frac{\partial f}{\partial y}) (f_x + i f_y) = \frac{1}{2} (\frac{\partial f_x}{\partial x} + \frac{\partial f_y}{\partial y}) + \frac{i}{2} (\frac{\partial f_y}{\partial x} - \frac{\partial f_x}{\partial y}) = \frac{1}{2} \nabla \cdot \mathbf{F} + \frac{i}{2} |\nabla \times \mathbf{F}| \tag{10.32}$$

Now we can invent *source-free 2D vector fields* that are both zero-divergence and zero-curl by taking any function $f(z)$ and conjugating it (change all i 's to $-i$) to give $f^*(z^*)$ for which $\frac{df^*}{dz^*} = 0$. For example, if $f(z)=a \cdot z$ then $f^*(z^*)=a \cdot z^*=a(x-iy)$ is not a function of z so it has zero z -derivative, hence zero $\nabla \cdot \mathbf{F}$ and zero $|\nabla \times \mathbf{F}|$.

$$\mathbf{F}=(F_x, F_y)=(f^*_{,x}, f^*_{,y})=(a \cdot x, -a \cdot y) \text{ has zero divergence: } \nabla \cdot \mathbf{F}=0 \text{ and has zero curl: } |\nabla \times \mathbf{F}|=0. \tag{10.32}$$

A plot of vector field $\mathbf{F}=(f^*_{,x}, f^*_{,y})=(a \cdot x, -a \cdot y)$ in Fig. 10.7 shows a *divergence-free laminar (DFL) flow field*.

Complex potential ϕ contains “scalar”(F=∇Φ) and “vector”(F=∇×A) potentials

Any DFL flow field \mathbf{F} is a gradient of a *scalar potential field* Φ or a curl of a *vector potential field* \mathbf{A} .

$$\mathbf{F} = \nabla \Phi \qquad \mathbf{F} = \nabla \times \mathbf{A}$$

There is a *complex potential* $\phi(z)=\Phi(x,y)+i\mathbf{A}(x,y)$ whose z -derivative is $f(z)$ and it comes with its complex conjugate $\phi^*(z^*)=\Phi(x,y)-i\mathbf{A}(x,y)$ whose z^* -derivative is the $f^*(z^*)$ that we use to plot DFL flow fields \mathbf{F} .

$$f(z) = \frac{d\phi}{dz} \quad (10.33a)$$

$$f^*(z^*) = \frac{d\phi^*}{dz^*} \quad (10.33b)$$

Derivative $\frac{d\phi^*}{dz^*}$ by (10.31) has 2D gradient $\nabla\Phi = \begin{pmatrix} \frac{\partial\Phi}{\partial x} \\ \frac{\partial\Phi}{\partial y} \end{pmatrix}$ of scalar Φ and curl $\nabla \times \mathbf{A} = \begin{pmatrix} \frac{\partial\mathbf{A}}{\partial y} \\ -\frac{\partial\mathbf{A}}{\partial x} \end{pmatrix}$ of vector \mathbf{A} .

$$\frac{d}{dz^*} \phi^* = \frac{d}{dz^*} (\Phi - i\mathbf{A}) = \frac{1}{2} \left(\frac{\partial}{\partial x} + i \frac{\partial}{\partial y} \right) (\Phi - i\mathbf{A}) = \frac{1}{2} \left(\frac{\partial\Phi}{\partial x} + i \frac{\partial\Phi}{\partial y} \right) + \frac{1}{2} \left(\frac{\partial\mathbf{A}}{\partial y} - i \frac{\partial\mathbf{A}}{\partial x} \right) = \frac{1}{2} \nabla\Phi + \frac{1}{2} \nabla \times \mathbf{A} \quad (10.34)$$

Some more math trickery has “vector- \mathbf{A} ” be just a “Z-component” $\mathbf{A} = A_z \mathbf{e}_z$ normal to the complex (x,y) -plane. So $\mathbf{A}(x,y) = A_z(x,y)$ is treated as a *single* function of (x,y) like scalar $\Phi(x,y)$. Also, a *mathematician definition* for force field $\mathbf{F} = +\nabla\Phi$ replaces our usual physicist’s definition $\mathbf{F} = -\nabla U$ of (6.9). (No annoying $(-)$ -sign for us now!)

To find $\phi = \Phi + i\mathbf{A}$ we integrate $f(z) = a \cdot z$ to get ϕ and isolate real ($\text{Re}\phi = \Phi$) and imaginary ($\text{Im}\phi = \mathbf{A}$) parts.

$$\begin{aligned} \phi &= \Phi + i\mathbf{A} = \int f \cdot dz = \int a z \cdot dz = \frac{1}{2} a z^2 = \frac{1}{2} a(x + iy)^2 \\ &= \frac{1}{2} a(x^2 - y^2) + i axy \end{aligned} \quad (10.35a)$$

Note that *either* part gives the *whole* field \mathbf{F} . The factors $\frac{1}{2}$ in (10.34) reflect this elegant symmetry.

$$\nabla\Phi = \begin{pmatrix} \frac{\partial\Phi}{\partial x} \\ \frac{\partial\Phi}{\partial y} \end{pmatrix} = \begin{pmatrix} \frac{\partial}{\partial x} \frac{a}{2}(x^2 - y^2) \\ \frac{\partial}{\partial y} \frac{a}{2}(x^2 - y^2) \end{pmatrix} = \begin{pmatrix} ax \\ -ay \end{pmatrix} = \mathbf{F} \quad (10.35b) \quad \nabla \times \mathbf{A} = \begin{pmatrix} \frac{\partial\mathbf{A}}{\partial y} \\ -\frac{\partial\mathbf{A}}{\partial x} \end{pmatrix} = \begin{pmatrix} \frac{\partial}{\partial y} axy \\ -\frac{\partial}{\partial x} axy \end{pmatrix} = \begin{pmatrix} ax \\ -ay \end{pmatrix} = \mathbf{F} \quad (10.35c)$$

Scalar *static potential lines* $\Phi = \text{const.}$ and vector *flux potential lines* $\mathbf{A} = \text{const.}$ define a *field-net* in Fig.10.7.

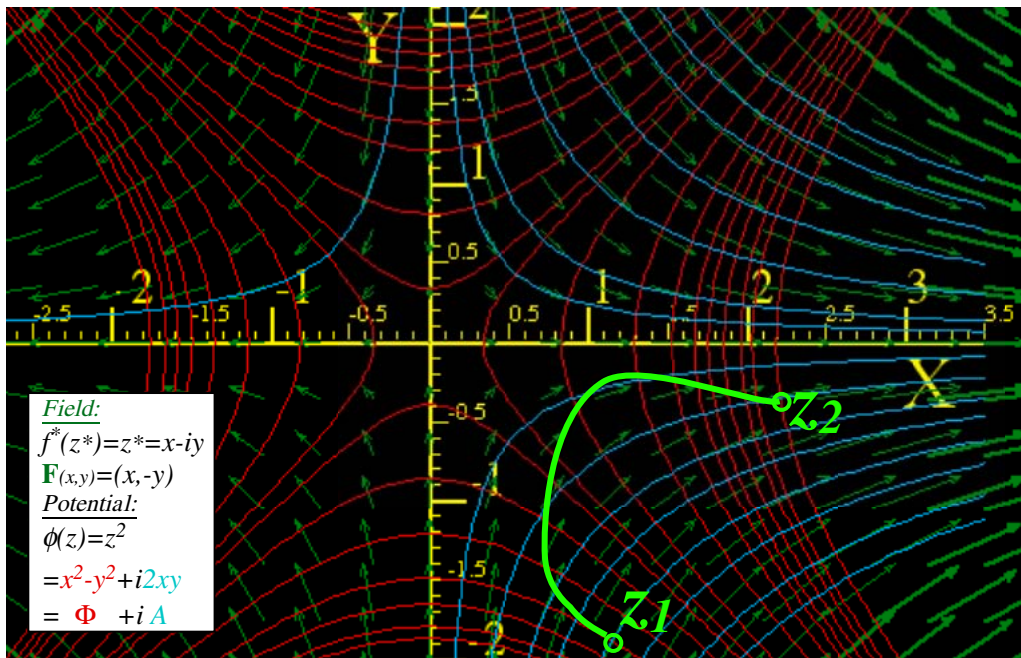


Fig.10.7 Complex field $f(z)=z$ of $\mathbf{F}=(x,-y)$ vectors on potentials of static $\Phi=(x^2-y^2)/2$ and flux $\mathbf{A}=xy$.

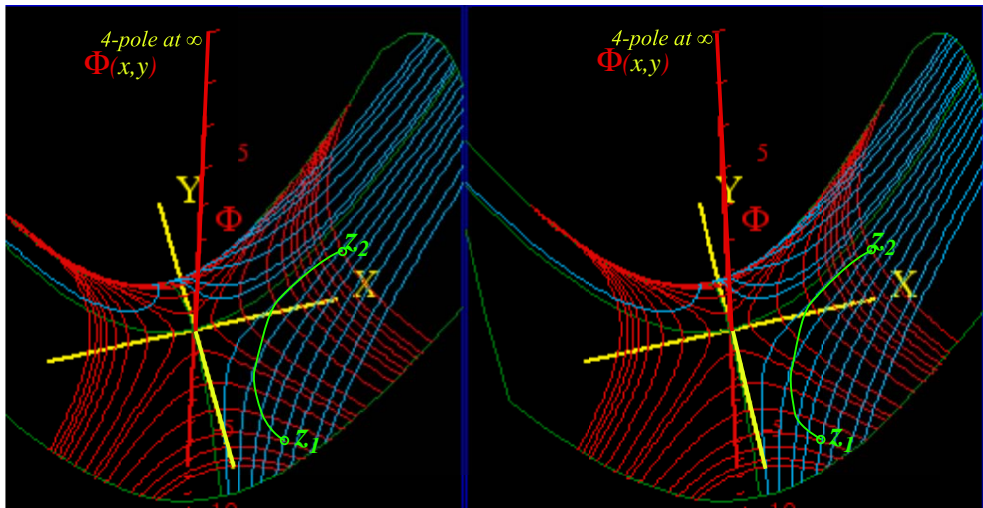


Fig. 10.8 Stereo-3D view of Fig. 10.7($\phi(z)=z^2/2$) plots static potential Φ normal to xy -axes.

Complex integrals $\int f(z)dz$ count “flux”($\int \mathbf{F} \cdot d\mathbf{r}$) and “vorticity”($\int \mathbf{F} \cdot d\mathbf{r}$)

Integral $f(z)$ (10.35a) between point z_1 and point z_2 in Fig. 10.8 is potential difference $\Delta\phi = \phi(z_2) - \phi(z_1)$ between the end-points. In DFL fields, $\Delta\phi$ is independent of the integration path $z(t)$ connecting z_1 and z_2 .

$$\Delta\phi = \phi(z_2) - \phi(z_1) = \int_{z_1}^{z_2} f(z)dz = \Phi(x_2, y_2) - \Phi(x_1, y_1) + i[\mathbf{A}(x_2, y_2) - \mathbf{A}(x_1, y_1)] \tag{10.36}$$

$$\Delta\phi = \quad \Delta\Phi \quad + i \quad \Delta\mathbf{A}$$

The real part $\Delta\Phi$ of $\Delta\phi$ is work $\int_1^2 \mathbf{F} \cdot d\mathbf{r}$ done pushing \mathbf{r} up a hill in Fig. 10.8. (Now force $\mathbf{F} = \nabla\Phi$ points up-slope.) Since $\mathbf{F} = (f_x^*, f_y^*)$ is plotted using $f^*(z^*)$, we set $f(z) = (f^*(z^*))^*$ to get real and imaginary parts of $f(z)dz$.

$$\begin{aligned} \int f(z)dz &= \int (f^*(z^*))^* dz = \int (f^*(z^*))^* (dx + i dy) = \int (f_x^* + i f_y^*)^* (dx + i dy) = \int (f_x^* - i f_y^*) (dx + i dy) \\ &= \int (f_x^* dx + f_y^* dy) + i \int (f_x^* dy - f_y^* dx) \\ &= \int \mathbf{F} \cdot d\mathbf{r} + i \int \mathbf{F} \times d\mathbf{r} \cdot \hat{\mathbf{e}}_z = \int \mathbf{F} \cdot d\mathbf{r} + i \int \mathbf{F} \cdot d\mathbf{r} \times \hat{\mathbf{e}}_z \\ &= \int \mathbf{F} \cdot d\mathbf{r} + i \int \mathbf{F} \cdot d\mathbf{S} \quad \text{where: } d\mathbf{S} = d\mathbf{r} \times \hat{\mathbf{e}}_z \end{aligned} \tag{10.37}$$

Real part $\int_1^2 \mathbf{F} \cdot d\mathbf{r}$ sums \mathbf{F} projections along path vectors $d\mathbf{r}$ to get $\Delta\Phi$ in (10.36). Imaginary part $\int_1^2 \mathbf{F} \cdot d\mathbf{S} = \Delta\mathbf{A}$ sums \mathbf{F} projection across $d\mathbf{r}$ that is, it sums flux thru surface elements $d\mathbf{S} = d\mathbf{r} \times \hat{\mathbf{e}}_z$ normal to $d\mathbf{r}$ to get $\Delta\mathbf{A}$.

One power-law field $f(z) = az^n$ lacks a power-law potential $\phi(z) = \frac{a}{n+1} z^{n+1}$. It is $f(z) = \frac{a}{z} = az^{-1}$. Its integral is a logarithmic potential $\phi(z) = a \cdot \ln(z) = a \cdot \ln(x + iy)$. (Recall (6.11).) Use $\ln(a \cdot b) = \ln(a) + \ln(b)$, $\ln(e^{i\theta}) = i\theta$, and $z = re^{i\theta}$.

$$\phi(z) = \Phi + i\mathbf{A} = \int f(z)dz = \int \frac{a}{z} dz = a \ln(z) = a \ln(re^{i\theta}) = a \ln(r) + i a \theta \tag{10.38}$$

Potential $a \cdot \ln(z)$ is the field of a line of charge q if $a = q$ is real and a line of current J if $a = iJ$ is imaginary. Fig. 10.9a is a diverging \mathbf{F} -field of unit charge ($q=1$) and Fig. 10.9b is a curling \mathbf{F} -field of unit current ($J=1$). Line charge \mathbf{F} -field is like an electric \mathbf{E} -field. Line current \mathbf{F} -field is like a magnetic \mathbf{B} -field of a wire. It is a vortex.

(a) Unit Z-line-flux field $f(z)=1/z$

(b) Unit Z-line-vortex field $f(z)=i/z$

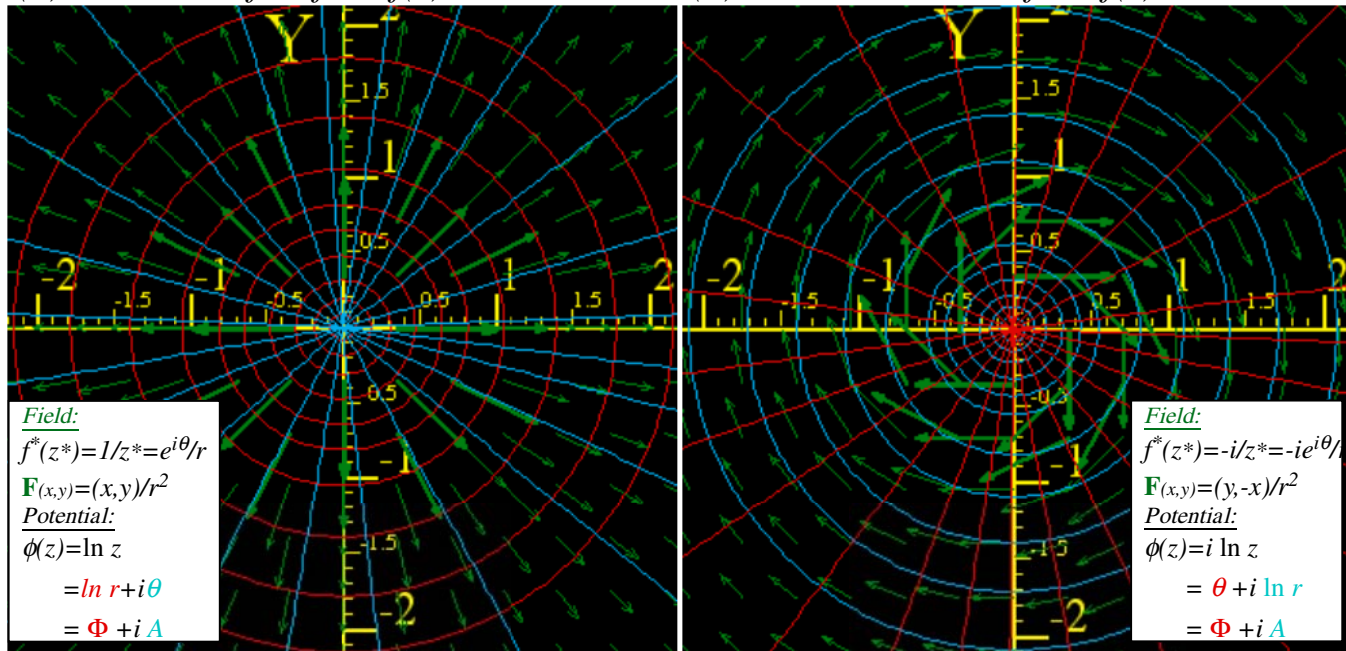


Fig. 10.9 Fields due to a unit Z-line-source normal to center. (a) Real source $a=q=1$. (b) Imaginary $a=iJ=i$.

F-field and radial streamlines ($A=\theta=const.$) diverge normal to equal- Φ circles ($\Phi=r=const.$) in Fig. a. **F**-field and circular streamlines ($A=r=const.$) curl clockwise normal to radial equal- Φ lines ($\Phi=\theta=const.$) in Fig. b. (The clockwise ($-i$)-sense of rotation results from plotting $f^*(z^*)=-i/z^*$ as our $(^*)$ -convention requires.)

Stereo-3D potential plots of real-line-source field shown in Fig. 10.10a show mathematical structure of its Φ and A potentials that lets us compare them to imaginary-line-source potentials in Fig. 10.10b. Real part $\Phi=\ln(r)$ of (10.38) for real ($a=1$)-source in Fig10.10a is a surface like a *morning-glory*. Blue- $(A=\theta=const.)$ -streamlines stream down its throat normal to $(\Phi=r=const.)$ level circles.

Below that Φ -vs- (x,y) -plot is a 3D A -vs- (x,y) -plot for the same real source in Fig. 10.10a. Imaginary part $A=\theta$ of (10.38) gives radial steps that are level lines of a single helix or *helicoid*. Red- $(\Phi=r=const.)$ -lines stream up its spiral staircase normal to $(A=\theta=const.)$ steps. At the top step $A=\theta=\pi$, above the $-X$ -axis, is a “waterfall” of red lines falling by $\Delta A=2\pi$ straight to bottom helical step $A=\theta=-\pi$. This $2\pi i$ -fall of complex potential $\phi(z)$ by $\Delta\phi=i\Delta A=2\pi i$ at $\theta=\pm\pi$ equals the *loop integral* of $f(z)$ from $\theta=-\pi$ to $\theta=+\pi$.

$$\Delta\phi = i\Delta A = \oint f(z)dz = \oint \frac{dz}{z} = 2\pi i \tag{10.39}$$

Imaginary part ΔA of a loop integral counts real source (“flux”) since loop flux is $\text{Im} \oint f(z)dz$ in (10.37). Real part $\Delta\Phi = \text{Re} \oint f(z)dz = \oint \mathbf{F} \cdot d\mathbf{r}$ counts imaginary source (“vorticity”) since only that makes work around a loop, that is, *perpetual motion*! In Fig. 10.10b, Φ and A switch roles to make imaginary-line-source-potentials.

(a) Unit Z-line-flux field $f(z)=1/z$

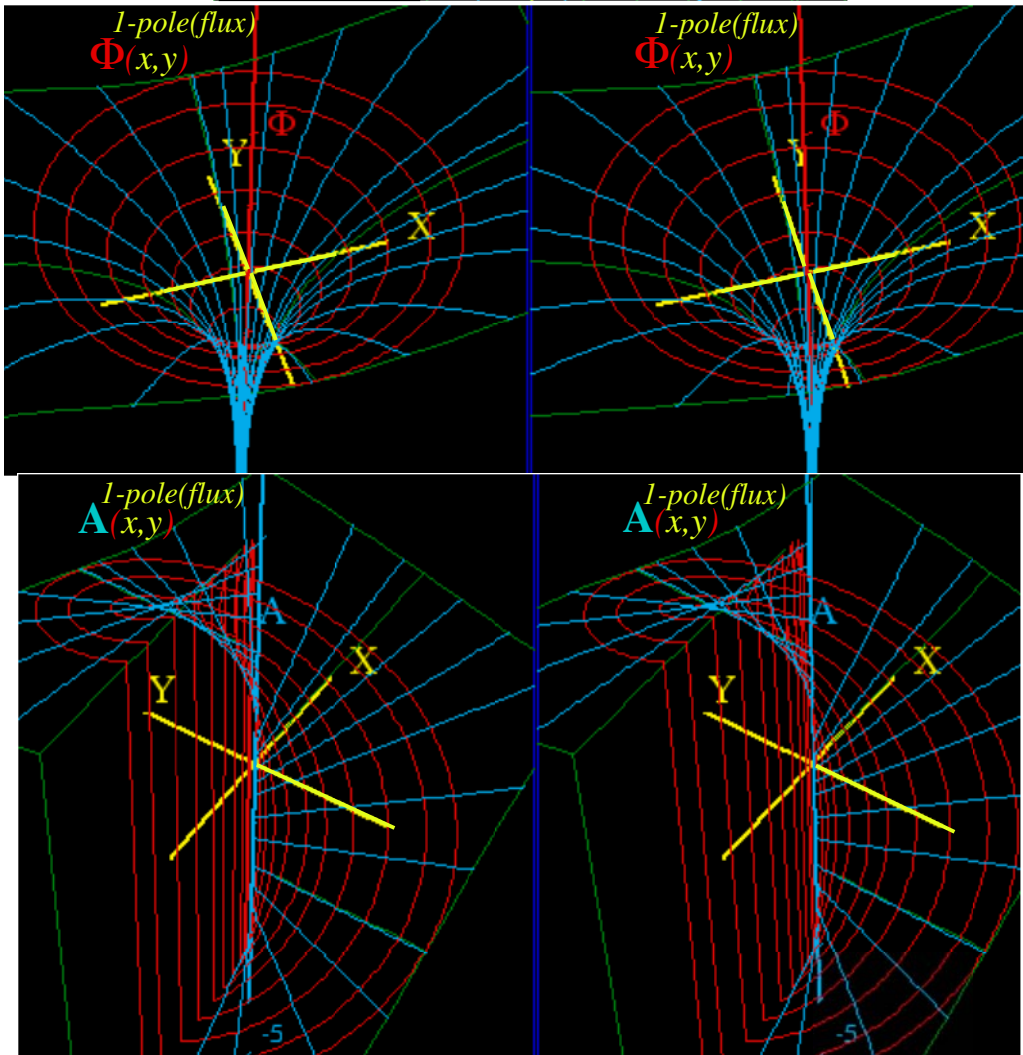
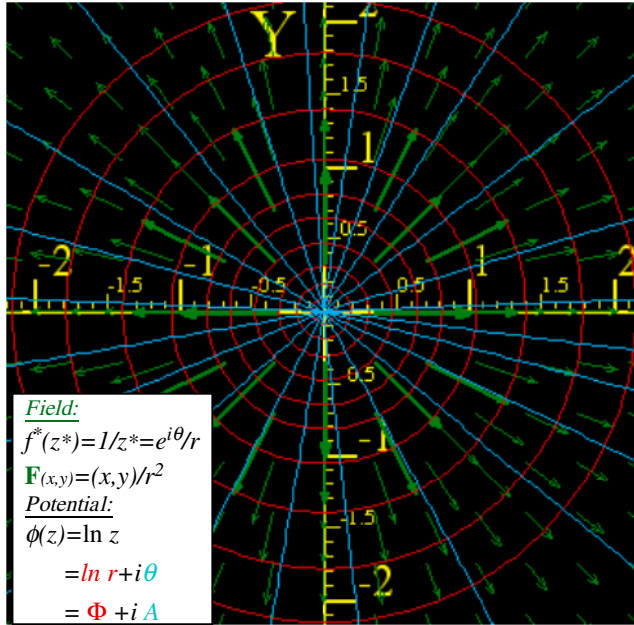


Fig. 10.10(a) Real unit line-source ($a=1$) with diverging \mathbf{F} -field resembling \mathbf{E} -field of electric line-charge.

(b) Unit Z-line-vortex field $f(z)=i/z$

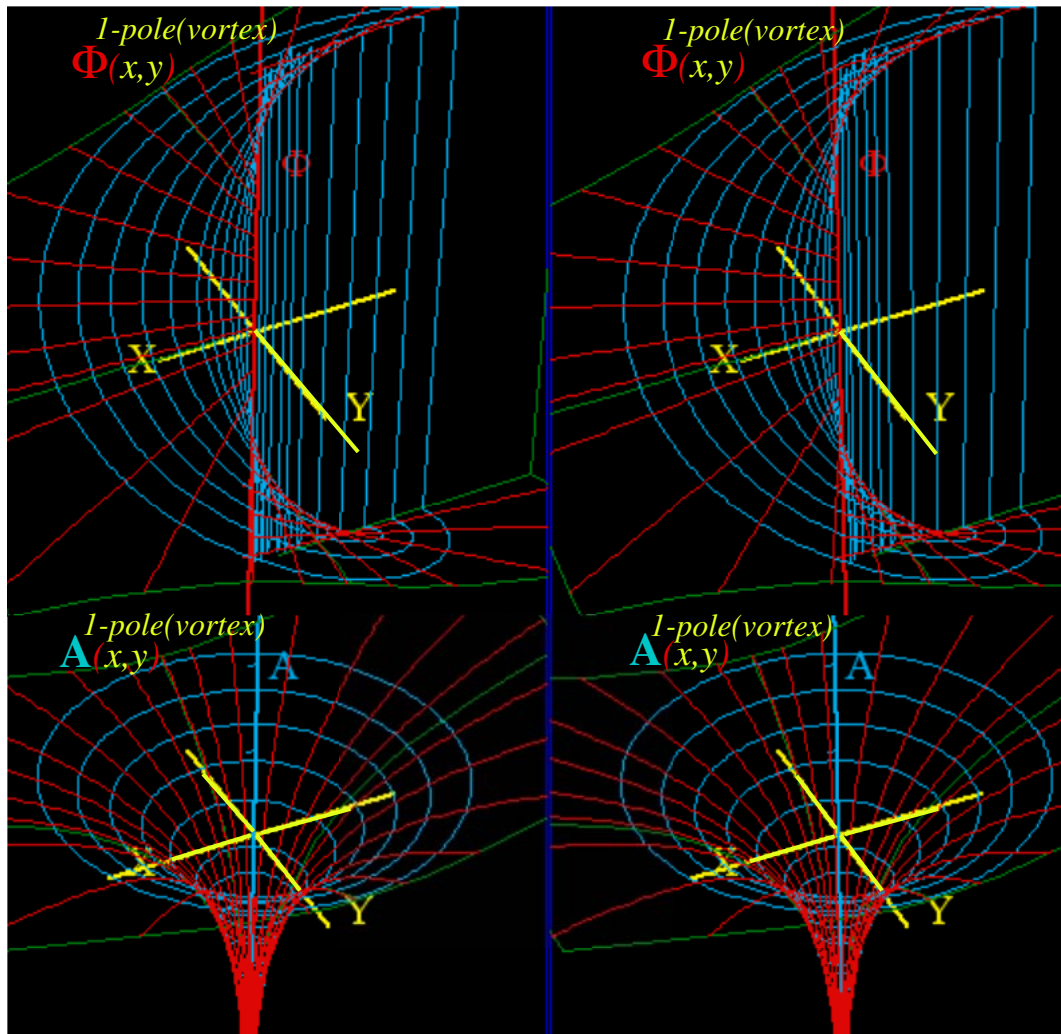
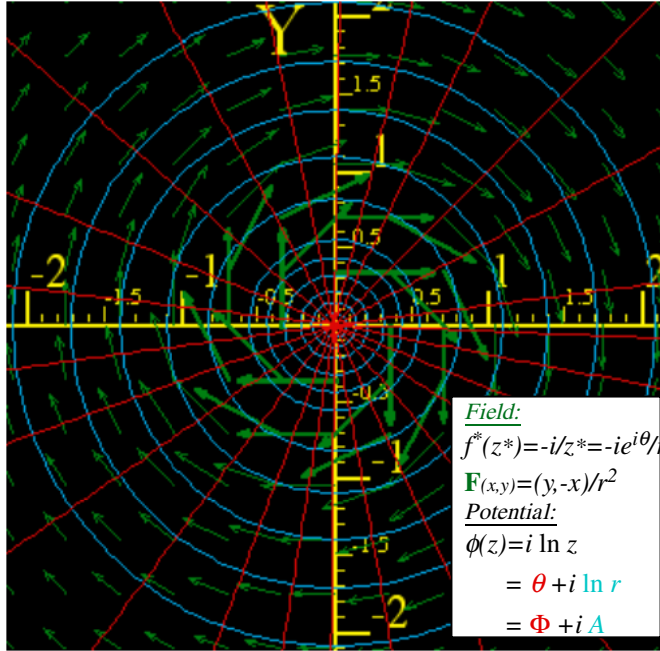


Fig. 10.10(b) Imaginary line-source ($a=i$) with curling \mathbf{F} -field resembling \mathbf{B} -field of electric line-current.

Complex derivatives give 2D multipole fields

Of all integer-power-law field functions $f(z)=z^n$ of z only $a/z =az^{-1}$ has a non-power-law multi-valued integral and potential $\phi(z)=\int az^{-1}dz = a \ln z$ (10.38) and non-zero flux-work-loop integral $\oint az^{-1}dz=2\pi ia$ (10.39). This special $f(z)=az^{-1}$ is a 2D line *monopole field* and $\phi(z)=a \ln z$ is its *monopole potential* of source strength a .

$$f^{1-pole}(z) = \frac{a}{z} = \frac{d\phi^{1-pole}}{dz} \quad (10.40a)$$

$$\phi^{1-pole}(z) = a \ln z \quad (10.40b)$$

Now let these two line-sources of equal but opposite source constants $+a$ and $-a$ be located at $z=\pm\Delta/2$ thus separated by a small interval Δ . This sum (actually difference) of f^{1-pole} -fields is called a *dipole field*.

$$f^{dipole}(z) = \frac{a}{z+\frac{\Delta}{2}} - \frac{a}{z-\frac{\Delta}{2}} = \frac{-a \cdot \Delta}{z^2 - \frac{\Delta^2}{4}} \quad \phi^{dipole}(z) = a \ln(z - \frac{\Delta}{2}) - a \ln(z + \frac{\Delta}{2}) = a \ln \frac{z - \frac{\Delta}{2}}{z + \frac{\Delta}{2}}$$

If interval Δ is *tiny* and is divided out we get a *point-dipole field* f^{2-pole} that is the z -derivative of f^{1-pole} .

$$f^{2-pole} = \frac{-a}{z^2} = \frac{df^{1-pole}}{dz} = \frac{d\phi^{2-pole}}{dz} \quad (10.41a)$$

$$\phi^{2-pole} = \frac{a}{z} = \frac{d\phi^{1-pole}}{dz} \quad (10.41b)$$

A *point-dipole potential* ϕ^{2-pole} (whose z -derivative is f^{2-pole}) is a z -derivative of ϕ^{1-pole} . Pair (10.41) looks like a Coulomb force (9.1) and potential (9.2) of 3D point monopoles. However, 2D dipole field (10.41a) is quite different as is 2D potential (10.41b) whose $\Phi=const.$ and $A=const.$ lines make a circle-net in Fig. 10.11.

$$\begin{aligned} \phi^{2-pole} = \frac{a}{z} &= \frac{a}{x+iy} = \frac{a}{x+iy} \frac{x-iy}{x-iy} = \frac{ax}{x^2+y^2} + i \frac{-ay}{x^2+y^2} = \frac{a}{r} \cos \theta - i \frac{a}{r} \sin \theta \\ &= \Phi^{2-pole} + i A^{2-pole} \end{aligned} \quad (10.42)$$

(Note that complex $z=x+iy$ is cleared from the denominator by using $z^* = x-iy$ to give real $r^2 = z^*z = x^2 + y^2$.)

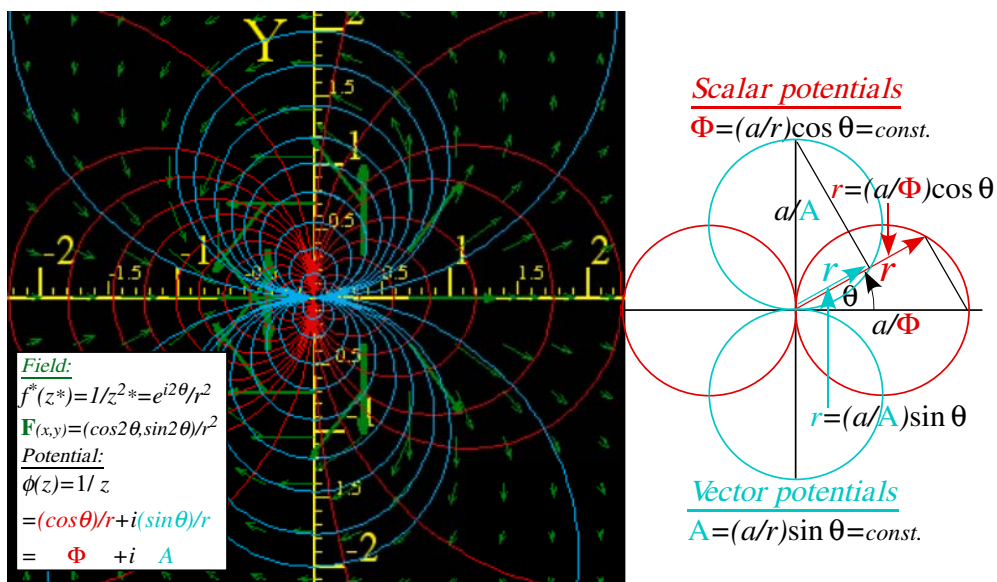


Fig. 10.11 Dipole \mathbf{F} -field $f(z)=1/z^2$ and scalar potential ($\Phi=const.$)-circles orthogonal to ($A=const.$)-circles.

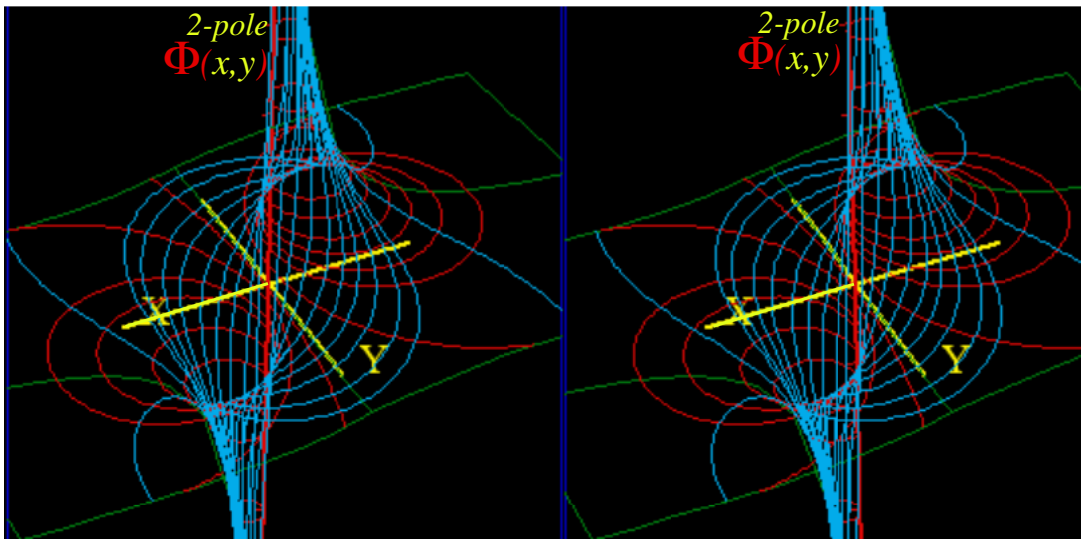


Fig. 10.12 Stereo 3D plot of dipole $\phi(z)=1/z$ scalar potential $\Phi(x,y)$ with Δ -streamlines between poles.

Complex power series are 2D multipole expansions

A z -derivative turns 1-pole fields into 2-pole fields in (10. 41). It makes a copy of 1-pole in (10. 40) with a sign change and puts the (-)copy very near the original. What if we put a (-)copy of a 2-pole near its original? Well, the result is 4-pole or *quadrupole* field f^{4-pole} and potential ϕ^{4-pole} , each a z -derivative of f^{2-pole} and ϕ^{2-pole} .

$$f^{4-pole} = \frac{a}{z^3} = \frac{1}{2} \frac{df^{2-pole}}{dz} = \frac{d\phi^{4-pole}}{dz} \quad (10.43a)$$

$$\phi^{4-pole} = -\frac{a}{2z^2} = \frac{1}{2} \frac{d\phi^{2-pole}}{dz} \quad (10.43b)$$

Fig. 10.13 shows 4-pole structure. Two $+\infty$ -poles loom above Y-axis and two $-\infty$ -poles lurk below X-axis . The \mathbf{F} -field vectors and their Δ -streamlines are shown running at 90° to Φ -equipotential lines in Fig. 10.13.

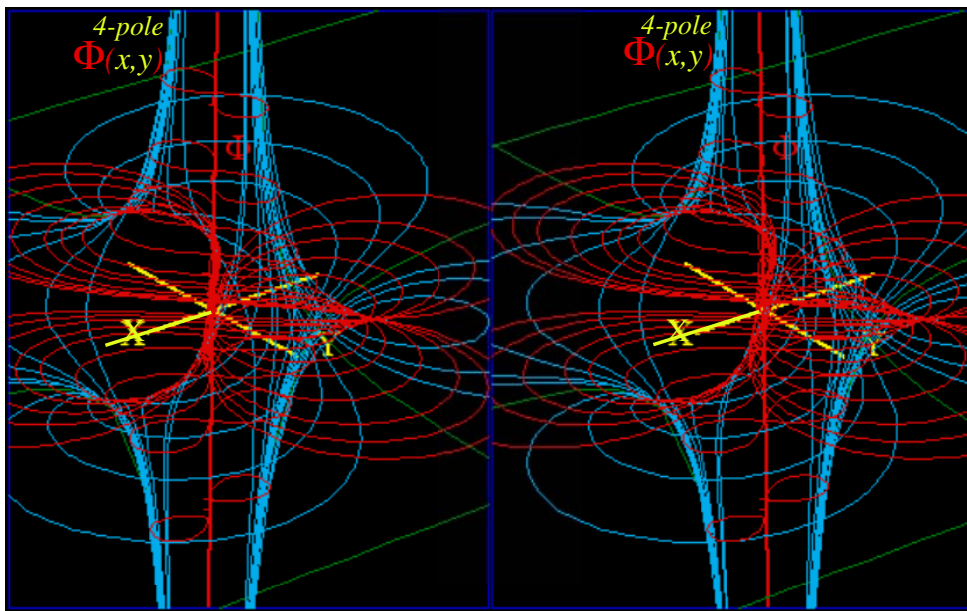


Fig. 10.13 Stereo 3D plot of quadrupole $\phi(z)=1/z^2$ scalar potential $\Phi(x,y)$ with Δ -streamlines between poles.

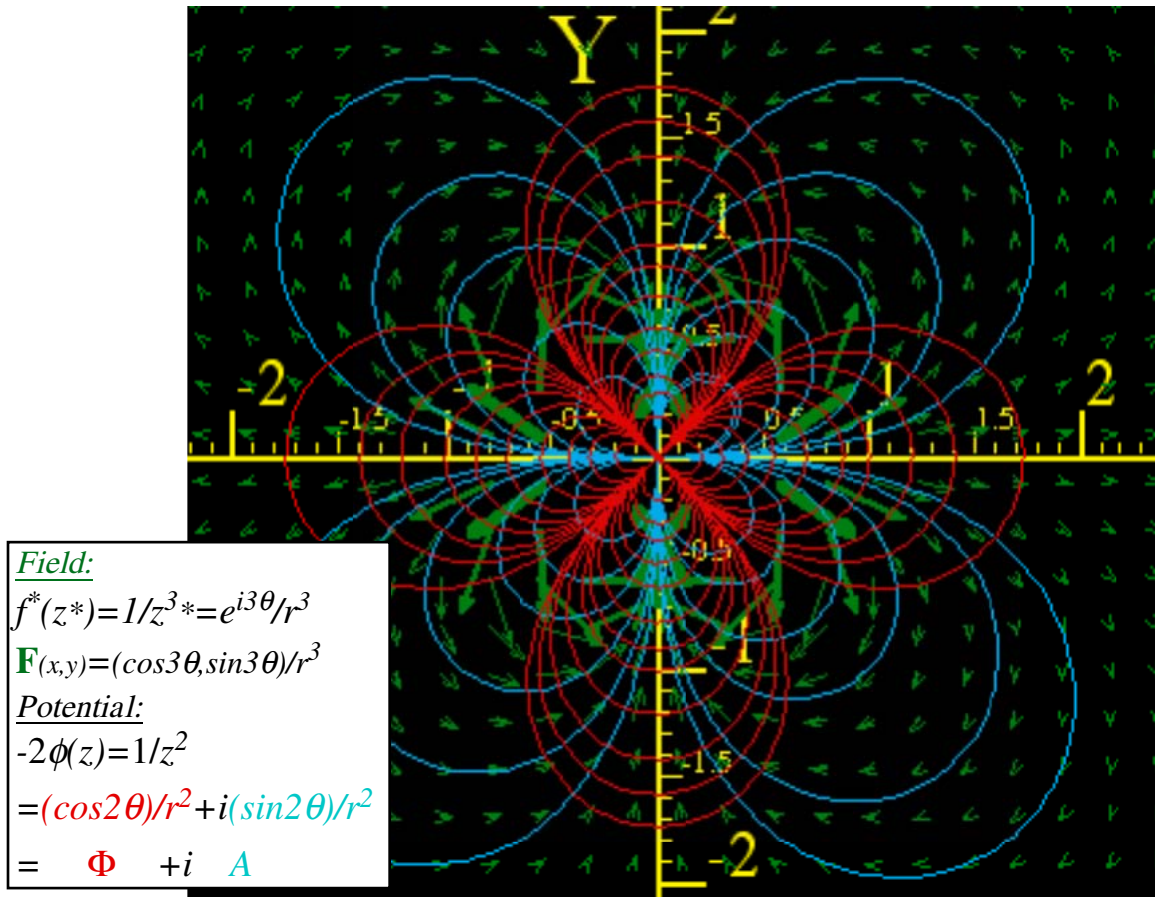


Fig. 10.14 \mathbf{F} -field $f(z)=1/z^3$ of 4-pole with scalar ($\Phi=const.$)-equipotentials normal to ($A=const.$)-streamlines.

A field $f(z)$ with sources only at origin ($z=0$) or at infinity ($z=\infty$) may be given by power series that generalize Maclaurin series derived in (10.11) by using both positive and negative powers $z^{\pm n}$. Series $\Sigma a_{\pm n}z^{\pm n}$ is called a *Laurent series* or *multipole expansion* (10.44) of a given complex field function $f(z)$ around $z=0$. All field terms $a_{m-1}z^{m-1}$ except *1-pole* $\frac{a_{-1}}{z}$ have potential term $a_{m-1}z^m/m$ of a 2^m -pole at $z=0$ ($z=\infty$) for $m<0$ ($m>0$).

$$\begin{aligned}
 f(z) = & \dots a_{-3}z^{-3} + a_{-2}z^{-2} + a_{-1}z^{-1} + a_0 + a_1z + a_2z^2 + a_3z^3 + a_4z^4 + a_5z^5 + \dots \\
 & \dots \text{2}^2\text{-pole} \quad \text{2}^1\text{-pole} \quad \text{2}^0\text{-pole} \quad \text{2}^1\text{-pole} \quad \text{2}^2\text{-pole} \quad \text{2}^3\text{-pole} \quad \text{2}^4\text{-pole} \quad \text{2}^5\text{-pole} \quad \text{2}^6\text{-pole} \dots \\
 & \text{at } z=0 \quad \text{at } z=0 \quad \text{at } z=0 \quad \text{at } z=\infty \quad \text{at } z=\infty
 \end{aligned} \tag{10.44}$$

$$\phi(z) = \dots \frac{a_{-3}}{-2} z^{-2} + \frac{a_{-2}}{-1} z^{-1} + a_{-1} \ln z + a_0 z + \frac{a_1}{2} z^2 + \frac{a_2}{3} z^3 + \frac{a_3}{4} z^4 + \frac{a_4}{5} z^5 + \frac{a_5}{6} z^6 + \dots$$

The unique *1-pole*(*2*⁰-pole) ϕ -term $a_{-1} \ln z$ is *not* a constant $a_{-1}z^0 = a_{-1}$. (Constant- ϕ has no field: $f = \frac{d\phi}{dz} = \frac{da_{-1}}{dz} = 0$) Also a *1-pole* at $z=\infty$ gives zero field near $z=0$. However, a *2*¹-pole at $z=\infty$ gives a constant field $f(z)=a_0$ near $z=0$. A quadrupole (*2*²-pole) at $z=\infty$ gives the linear field $f(z)=a_1z$ shown in Fig. 10.7, but a *2*²-pole at $z=0$ gives the field $a_{-3}z^{-3}$ in Fig. 10.14. Octupoles (*2*³-poles) at $z=\infty$ (or $z=0$) give a_2z^2 (or $a_{-4}z^{-4}$), and so on for $m=4,5,\dots$

The potential ϕ -expansion is most useful for revealing multi-pole structure. A negative power ϕ -term $a_{-m-1}z^m/m$ belongs to a 2^m -pole at $z=0$. A positive power ϕ -term $a_{m-1}z^m/m$ belong to a 2^m -pole at $z=\infty$. Pole field geometry involves mapping z -points onto a sphere so $z=0$ is its North Pole and $z=\infty$ is its South Pole in Fig. 10.15. There a *stereographic projection* maps a point $z=x+iy$ on the z -plane tangent to North Pole into a point $w=1/z=u+iv$ in the inverse w -plane tangent to the South Pole. The map geometry uses an inscribed rectangle. A pair of red unit circles $|z|=1$ and $|w|=1$ map into each other. Any point z inside the $|z|=1$ circle maps into a point w outside the $|w|=1$ circle as shown and *vice-versa* outside z maps to inside w .

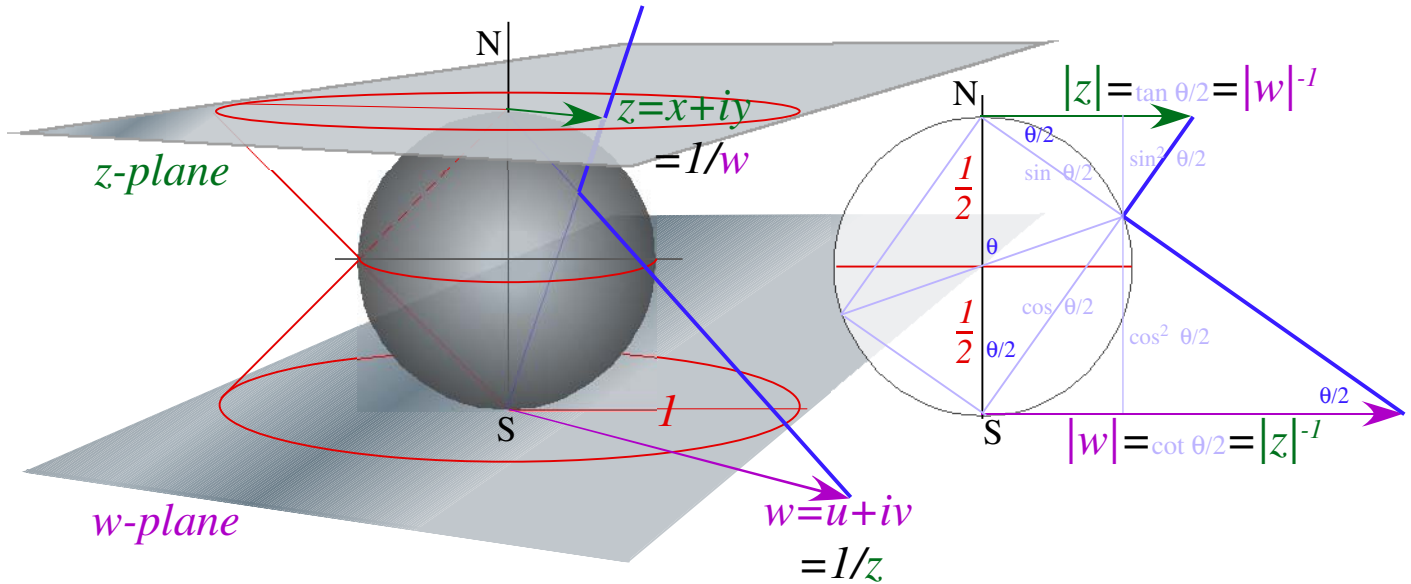


Fig. 10.15 Stereographic projection of z -plane through a unit-diameter sphere to inverse $1/z=w$ -plane.

Replacing z with $w=z^{-1}$ in (10.13) switches positive multi-pole- m terms in potential ϕ with negative ones.

$$\phi(z) = \dots \frac{a_{-3}}{-2} z^{-2} + \frac{a_{-2}}{-1} z^{-1} + a_{-1} \ln z + a_0 z + \frac{a_1}{2} z^2 + \frac{a_2}{3} z^3 + \dots \text{ (from (10.44))}$$

$$\phi(w) = \dots \frac{a_{-3}}{-2} w^{-2} + \frac{a_{-2}}{-1} w^{-1} + a_{-1} \ln w + a_0 w + \frac{a_1}{2} w^2 + \frac{a_2}{3} w^3 + \dots \text{ (with } z=w^{-1}\text{)}$$

$$= \dots \frac{a_2}{3} z^{-2} + \frac{a_1}{2} z^{-1} + a_0 z - a_{-1} \ln z + \frac{a_{-2}}{-1} z + \frac{a_{-3}}{-2} z^2 + \frac{a_{-3}}{-2} z^3 + \dots \text{ (with } w=z^{-1}\text{)}$$

But, the unique monopole source term stays put with only a sign change ($\ln \frac{1}{z} = -\ln z$) as seen in Fig. 10.16a.

Constant field $f=a_0$ in (10.44) appears if there is a dipole at the South Pole and, *vice-versa*, a dipole field at the North Pole appears to be a constant field near the South Pole as seen in Fig. 10.16b.

Of all 2^m -pole field terms $a_{m-1}z^{m-1}$, only the $m=0$ monopole $a_{-1}z^{-1}$ has a non-zero loop integral (10.39).

$$\oint f(z)dz = \oint a_{-1}z^{-1}dz = 2\pi ia_{-1} \qquad a_{-1} = \frac{1}{2\pi i} \oint f(z)dz$$

This $m=1$ -pole constant- a_{-1} formula is just the first in a series of Laurent coefficient expressions.

$$\dots a_{-3} = \frac{1}{2\pi i} \oint z^2 f(z) dz, \quad a_{-2} = \frac{1}{2\pi i} \oint z^1 f(z) dz, \quad a_{-1} = \frac{1}{2\pi i} \oint f(z) dz, \quad a_0 = \frac{1}{2\pi i} \oint \frac{f(z)}{z} dz, \quad a_1 = \frac{1}{2\pi i} \oint \frac{f(z)}{z^2} dz, \dots$$

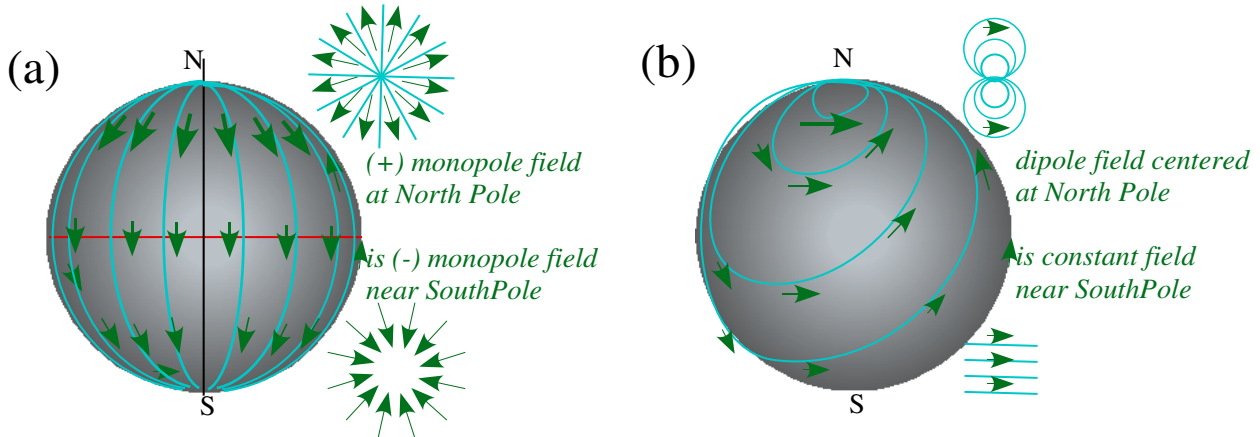


Fig. 10.16 Projective sphere view of North Pole ($z=0$) sources. (a) monopole (b) dipole.

Cauchy integrals

Source analysis starts with 1-pole loop integrals $\oint z^{-1} dz = 2\pi i$ or, with origin shifted $\oint (z-a)^{-1} dz = 2\pi i$. They hold for any loop around point- a . A continuous function $f(z)$ is just $f(a)$ on a tiny circle around point- a .

$$\oint \frac{f(z)}{z-a} dz = \oint \frac{f(a)}{z-a} dz = f(a) \oint \frac{1}{z-a} dz = 2\pi i f(a) \quad (10.45a) \qquad f(a) = \frac{1}{2\pi i} \oint \frac{f(z)}{z-a} dz \quad (10.45b)$$

The $f(a)$ result is called a *Cauchy integral*. Then repeated a -derivatives gives a sequence of them.

$$\frac{df(a)}{da} = \frac{1}{2\pi i} \oint \frac{f(z)}{(z-a)^2} dz, \quad \frac{d^2 f(a)}{da^2} = \frac{2}{2\pi i} \oint \frac{f(z)}{(z-a)^3} dz, \quad \frac{d^3 f(a)}{da^3} = \frac{3!}{2\pi i} \oint \frac{f(z)}{(z-a)^4} dz, \dots, \frac{d^n f(a)}{da^n} = \frac{n!}{2\pi i} \oint \frac{f(z)}{(z-a)^{n+1}} dz$$

This leads to a general *Taylor-Laurent* power series expansion of function $f(z)$ around point- a .

$$f(z) = \sum_{n=-\infty}^{\infty} a_n (z-a)^n \quad \text{where: } a_n = \frac{1}{2\pi i} \oint \frac{f(z)}{(z-a)^{n+1}} dz \left(= \frac{1}{n!} \frac{d^n f(a)}{da^n} \text{ for: } n \geq 0 \right) \quad (10.45c)$$

If the function $f(z)$ has no poles inside the contour then only positive powers $n > 0$ are needed in its expansion and the series above reduces to a Taylor series or (if $a=0$) a Maclaurin series like (10.12) derived previously. There the n^{th} expansion coefficient a_n is given by n^{th} derivative of $f(z)$ as in (10.45c) above. Otherwise, negative powers are needed with coefficients given by n^{th} order pole loop integrals above.

This represents just a “tip of an iceberg” for an enormous subject of complex analysis. We shall use only tiny portions of this grand mathematical subject, and later we will consider generalizations of complex numbers to hyper-complex *quaternions* and *spinor* operators. This takes the analysis from a 2D framework into a 3D and 4D description that is more like the one we live in.

Complex damped oscillator

In (10.22) and (10.23) are oscillator equations with complex $e^{-i\Omega t}$ solutions. Here is one more example.

$$\text{Damped HO equation : } \frac{d^2x}{dt^2} + 2\Gamma \frac{dx}{dt} + \omega_0^2 x(t) = 0 \text{ has solution : } x(t) = x(0)e^{-i\Omega t} \tag{10.46a}$$

Now a *complex phase rate* Ω depends on *friction damping coefficient* 2Γ as well as *natural frequency* ω_0 .

$$\left(\frac{d^2}{dt^2} + 2\Gamma \frac{d}{dt} + \omega_0^2\right)x(0)e^{-i\Omega t} = 0 = (-\Omega^2 - 2\Gamma i\Omega + \omega_0^2)x(0)e^{-i\Omega t} \text{ has solutions : } \Omega_{\pm} = -i\Gamma \pm \sqrt{\omega_0^2 - \Gamma^2} = -i\Gamma \pm \omega_{\Gamma}$$

Complex rate Ω gives both a Γ -*slowed frequency* $\omega_{\Gamma} = \sqrt{\omega_0^2 - \Gamma^2}$ and Γ -*decaying amplitude* $|x(t)| = |x(0)|e^{-\Gamma t}$.

$$x(t) = (\text{decaying amplitude})e^{-i(\text{slowed frequency})t} = (x(0)e^{-\Gamma t})e^{-i(\omega_{\Gamma})t} \text{ where: } \omega_{\Gamma} = \sqrt{\omega_0^2 - \Gamma^2} \tag{10.46b}$$

We choose the first root Ω_+ so phase $e^{-i\omega_{\Gamma}t}$ moves clockwise like the phasor clock in Fig. 10.5b.

If damping is $\Gamma = 0.2$ then a 1Hz oscillator ($\omega_0 = 2\pi$) is slowed by only .05% of 2π to $\omega_{\Gamma} = 6.280$.

$$\omega_{\Gamma} = \sqrt{\omega_0^2 - \Gamma^2} = \omega_0 - \frac{1}{2}(\Gamma^2 / \omega_0) + \dots = 6.2831853 - 0.003183 + \dots = 6.280002 + \dots = 6.280001 \tag{10.46c}$$

More significant is *exponential decay* of amplitude $|x(t)|$ down to 5% of $|x(0)|$ in time interval $t_{5\%} = 15 \text{ sec}$.

$$t_{5\%} = \frac{3}{\Gamma} = \frac{3}{0.2} = 15 \tag{10.46d} \qquad t_{4.321\%} = \frac{\pi}{\Gamma} = \frac{\pi}{0.2} = 15.708 \tag{10.46d}$$

Fig. 10.17 shows the exponential decay envelope. An easy-to-recall 5% approximation is $e^{-3} \cong 0.05$. A more precise one is $e^{-\pi} \cong 0.04321$. *Decay rate* sounds negative so we use *lifetime*, usually a $e^{-3} = 5\%$ lifetime. For more precise calculation, we use $e^{-\pi} = 4.321\%$ -lifetime such as $\pi/\Gamma = 15.708 \text{ sec}$. in (10.46d).

A damping of $\Gamma = 0.2$ reduces its natural 1Hz frequency only by about 0.05% to 0.9995Hz. This tiny frequency lag could be noticeable in a graph like Fig. 10.17 only after about 200 seconds, at which point it is well off the page and way too damped-out to see.

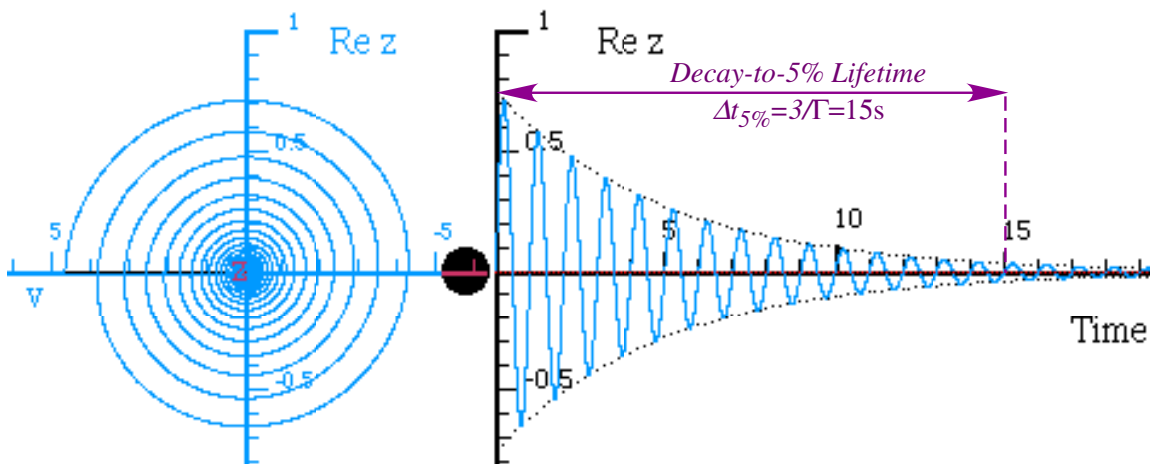


Fig. 10.17 Phasor z and corresponding coordinate versus time plot for $\omega_0 = 2\pi$ and $\Gamma = 0.2$

Complex response to stimulus: Lorentz-Green's function

A complex phasor $e^{-i\omega t}$ also describes stimulated damped harmonic oscillation (SDHO). Consider a *monochromatic* (single-frequency ω_s) accelerative stimulus $a_s(t) = A_s e^{-i\omega_s t}$ added to motion equation (10.46).

$$\begin{aligned}
 \text{SDHO equation : } \frac{d^2 x_s}{dt^2} + 2\Gamma \frac{dx_s}{dt} + \omega_0^2 x_s(t) &= A_s e^{-i\omega_s t} & \text{has solution : } x_s(t) &= G_{\omega_0}(\omega_s) A_s e^{-i\omega_s t} \\
 (-\omega_s^2 - 2\Gamma i \omega_s + \omega_0^2) G_{\omega_0}(\omega_s) A_s e^{-i\omega_s t} &= A_s e^{-i\omega_s t} & \text{where : } G_{\omega_0}(\omega_s) &= \frac{1}{\omega_0^2 - \omega_s^2 - 2\Gamma i \omega_s}
 \end{aligned}
 \tag{10.47a}$$

This implies a response of the same frequency and an amplitude proportional to the stimulus. The proportionality factor G is supposed to depend upon the stimulus frequency ω_s , the natural frequency ω_0 , and damping constant Γ , and not on the amplitude A_s of the stimulus since (10.47) is linear and (ω_0, Γ, A_s) are constant. The oscillator is a 'black box' in Fig. 10.18 with response output due to input stimuli.

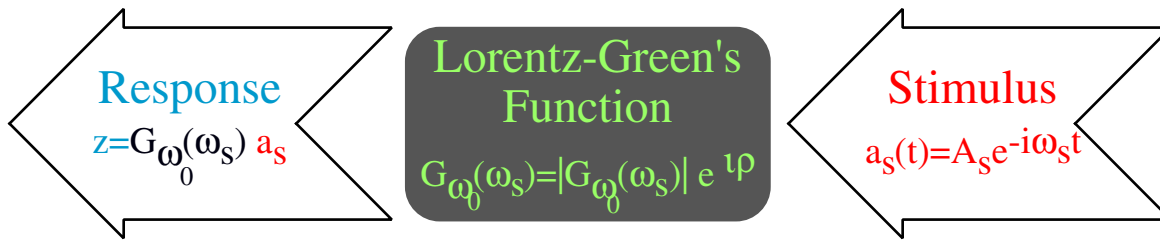


Fig. 10.18 Black-box diagram of oscillator response to monochromatic stimulus

The G_{ω_0} is the *Lorentz response function or classical Green's function* of the stimulus frequency ω_s .

$$G_{\omega_0}(\omega_s) = \frac{1}{\omega_0^2 - \omega_s^2 - 2\Gamma i \omega_s} = \text{Re } G_{\omega_0}(\omega_s) + i \text{Im } G_{\omega_0}(\omega_s) = |G_{\omega_0}(\omega_s)| e^{i\rho}
 \tag{10.47b}$$

The Lorentz-Green's function G is a constant amplitude for fixed stimulating frequency ω_s and natural ω_0 , so $x_s(t)$ is called the *steady-state stimulated response*. The real and imaginary parts of the Green's function are the two parts of the following *Cartesian form* of the Green's function G .

$$\text{Re } G_{\omega_0}(\omega_s) = \frac{\omega_0^2 - \omega_s^2}{(\omega_0^2 - \omega_s^2)^2 + (2\Gamma \omega_s)^2}
 \tag{10.48a}$$

$$\text{Im } G_{\omega_0}(\omega_s) = \frac{2\Gamma \omega_s}{(\omega_0^2 - \omega_s^2)^2 + (2\Gamma \omega_s)^2}
 \tag{10.48b}$$

Then the magnitude $|G_{\omega_0}(\omega_s)|$ and polar angle ρ of the *polar form* of G are the following:

$$|G_{\omega_0}(\omega_s)| = \frac{1}{\sqrt{(\omega_0^2 - \omega_s^2)^2 + (2\Gamma \omega_s)^2}}
 \tag{10.48c}$$

$$\rho = \tan^{-1} \left(\frac{2\Gamma \omega_s}{\omega_0^2 - \omega_s^2} \right)
 \tag{10.48d}$$

The angle ρ is the response *phase lag*, that is, the phase angle by which the response oscillation lags continually behind the phase $(-\omega_s t)$ of the stimulating oscillation.

$$x_s(t) = |G_{\omega_0}(\omega_s)| A_s e^{-i(\omega_s t - \rho)}
 \tag{10.48e}$$

We visualize stimulus and response phasors as a pair rigidly rotating at rate ω_s as shown in Fig. 10.19 with fixed response amplitude $|G|A_s$ and fixed angle ρ between them.

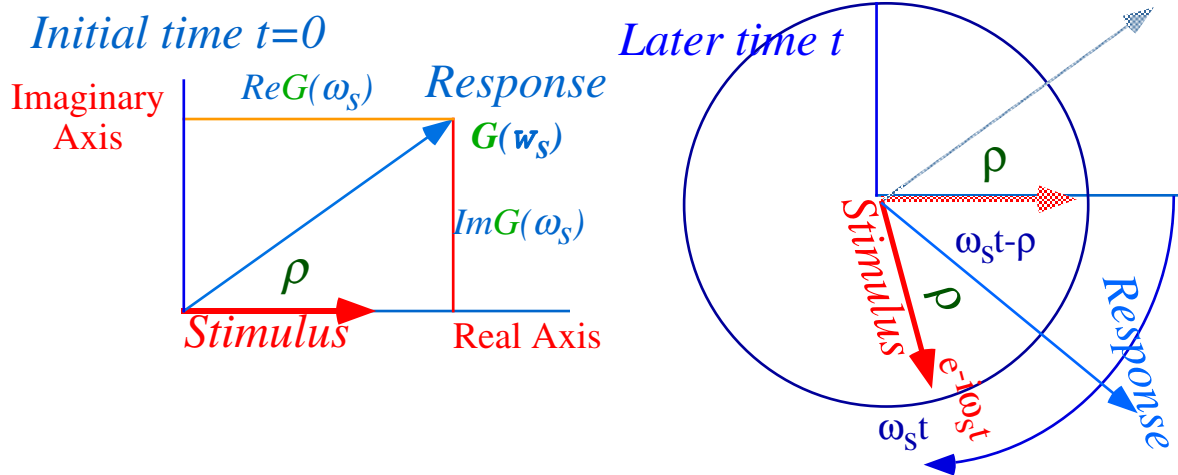


Fig. 10.19 Oscillator response and stimulus phasors rotate rigidly at angular rate ω_s .

Several views of the Lorentz Green's function (10.48) are shown in Fig. 10.20 for a 1 Hz oscillator with natural angular frequency $\omega_0 = 2\pi = 6.283(\text{radian})/\text{s}$ and decay constant $\Gamma = 0.2/\text{s}$. The complex $G(\omega_s)$ phasor is plotted $\text{Re}G$ vs. $\text{Im}G$ in Fig. 10.20a for a range ($0 < \omega_s < 13$) of stimulus angular frequency (or $0 < \nu_s < 2$ Hz of standard frequency). In Fig. 10.20b the response $R = G(\omega_s)a_s$ due to three G -function parts $\text{Re}G(\omega_s)$ (blue), $\text{Im}G(\omega_s)$ (green), and $|G(\omega_s)|$ (gray dots) are plotted for the same range.

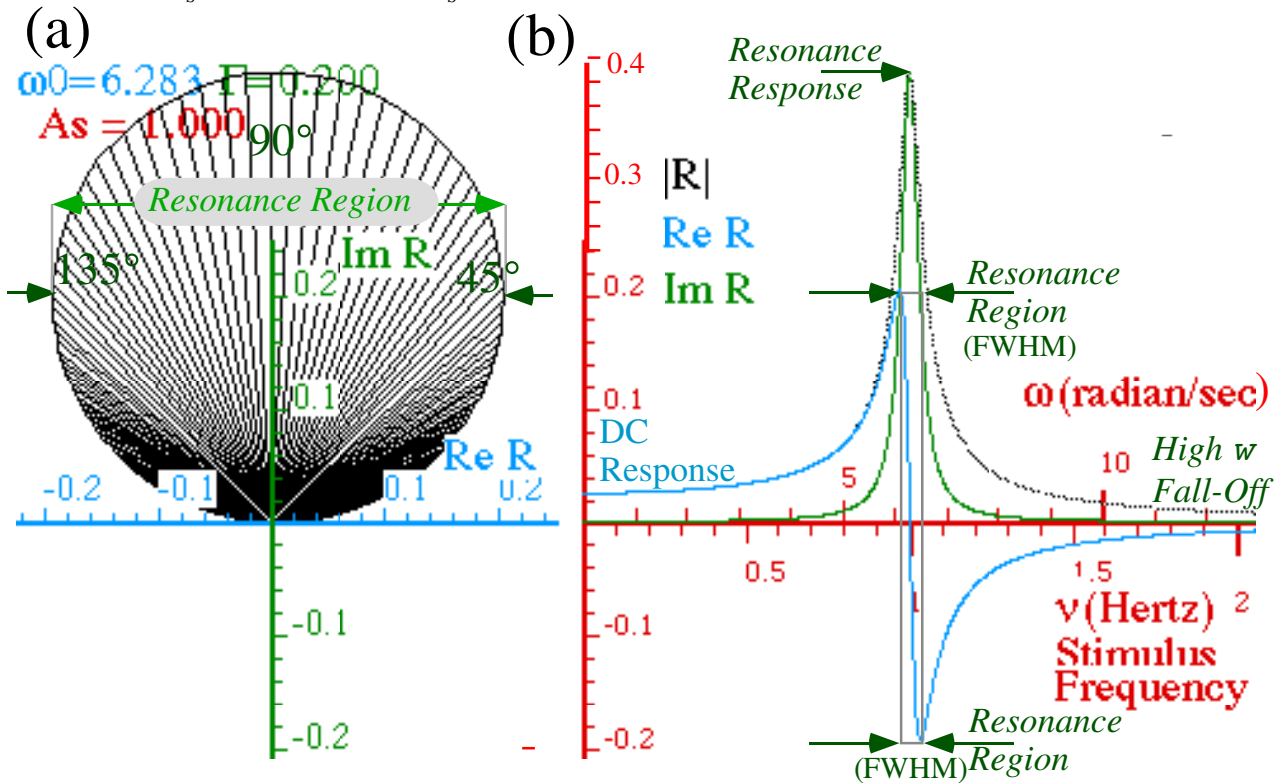


Fig. 10.20 Anatomy of oscillator Green-Lorentz response function plots

The response magnitude $|G(\omega_s)|$ is a dotted curve enveloping the others in Fig. 10.20b. It starts at $\omega_s = 0$ small and fairly flat ($\omega_s \ll \omega_0$ is called the *DC response* region.) and peaks near *resonance point* $\omega_s = \omega_0$ and falls to zero for $\omega_s \gg \omega_0$ (*high frequency fall-off*). Real part $\text{Re}G(\omega_s)$ dominates in the DC region. $\text{Re}G(\omega_s)$ reaches a peak just shy of where it intersects the rising imaginary part $\text{Im}G(\omega_s)$. $\text{Im}G(\omega_0)$ achieves its peak value near *resonance point* $\omega_s = \omega_0$ where $\text{Re}G(\omega_0)=0$ in the center of the *resonance region* between two *Full Width at Half-Maximum (FWHM)* points $\omega_s^{\text{FWHM}}(\pm) = \omega_0 \pm \Gamma$ shown in Fig. 10.21. These $\omega_s^{\text{FWHM}}(\pm)$ points are near ones that give max or min $\text{Re}G(\omega_s)$, half-max $\text{Im}G(\omega_s)$, and half-max $|G(\omega_s)|$.

Ratio of resonant response $|G(\omega_0)|$ to DC-response $|G(0)|$ is an important number from (10.48).

$$AAF = \frac{\text{Resonant response}}{\text{DC response}} = \frac{|G_{\omega_0}(\omega_0)|}{|G_{\omega_0}(0)|} = \frac{1/(2\Gamma\omega_0)}{1/\omega_0^2} = \frac{\omega_0}{2\Gamma} \equiv q \tag{10.49}$$

This ratio is about 15 in Fig. 10.20. We will call this ratio the *amplitude amplification factor (AAF)* or *angular quality (q) factor* of an oscillator. A *Standard Quality Factor* $Q = \nu_0/2\Gamma = q/2\pi$ is more commonly known[†] just as standard frequency $\nu = \omega/2\pi$ is more common than angular frequency $\omega = 2\pi\nu$.

When physicists speak of a Lorentzian function they generally mean an ideal version of Lorentz response (10.47b) with very high-Q or *near-resonant* $\omega_s \rightarrow \omega_0$ *conditions* $\omega_0^2 - \omega_s^2 \equiv (\omega_0 - \omega_s)2\omega_s$.

$$G_{\omega_0}(\omega_s) = \frac{1}{\omega_0^2 - \omega_s^2 - i2\Gamma\omega_s} \xrightarrow{\omega_s \rightarrow \omega_0} \frac{1}{2\omega_s} \frac{1}{\omega_0 - \omega_s - i\Gamma} \approx \frac{1}{2\omega_0} \frac{1}{\Delta - i\Gamma} = \frac{1}{2\omega_0} L(\Delta - i\Gamma) \tag{10.50a}$$

A *complex detuning-decay* $\delta = \Delta - i\Gamma$ variable δ is defined with the *real detuning* $\Delta = \omega_0 - \omega_s$ defined as before to give an *ideal Lorentzian* $L(\delta) = 1/\delta$ below. Imaginary part $\Gamma / (\Delta^2 + \Gamma^2)$ is the common “real Lorentzian.” The ideal complex Lorentzian $L(\delta) = 1/\delta$ (10.50) is like the complex dipole function (10.42). The $1/z$ -plots in Fig. 10.21 are known as *Smith plots* and are like the dipole net in Fig. 10.11 or 10.12.

$$L(\Delta - i\Gamma) = \frac{1}{\Delta - i\Gamma} = \text{Re } L + i \text{Im } L = \frac{\Delta}{\Delta^2 + \Gamma^2} + i \frac{\Gamma}{\Delta^2 + \Gamma^2} = |L|^2 \Delta + i |L|^2 \Gamma \tag{10.50b}$$

$$= |L| e^{i\rho} = |L| \cos \rho + i |L| \sin \rho = \frac{\cos \rho}{\sqrt{\Delta^2 + \Gamma^2}} + i \frac{\sin \rho}{\sqrt{\Delta^2 + \Gamma^2}} \text{ where: } |L| = \frac{1}{\sqrt{\Delta^2 + \Gamma^2}} \tag{10.50c}$$

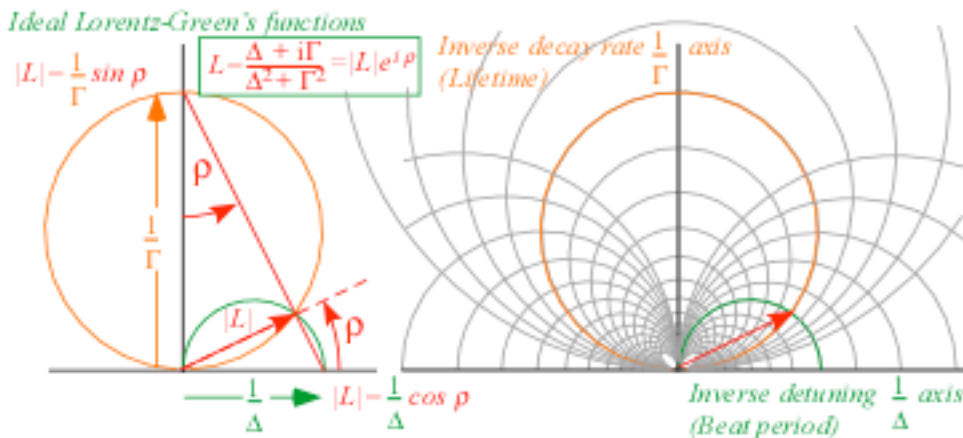


Fig. 10.21 Ideal Lorentzian in inverse rate space. (Smith life-time $1/\Gamma$ vs. beat-period $1/\Delta$ coordinates)

[†] Peter W. Milonni, private communication.

A circle of constant decay rate Γ and varying detuning frequency Δ has a diameter of $1/\Gamma$ along the vertical of the inverse frequency space in Fig. 10.21. As detuning approaches zero (perfect tuning) the polar phase-lag angle ρ approaches $\pi/2$ and the inverse detuning or beat-period $1/\Delta$ approaches infinity.

There appears to be circle of constant decay rate $\Gamma=0.2$ in Fig. 10.20, however, it cannot be a perfect circle, particularly in the DC region around origin. Ideal Lorentzian (10.50), unlike the real one, does not have an extended flat DC response region. Near-resonant condition $\omega_s \rightarrow \omega_0$ is broken if ω_s is allowed to go to zero.

As decay rate Γ increases the $1/\Gamma$ circle shrinks and becomes distorted by its DC “flat” at $\omega=0$ as shown in a rather low quality ($Q=1/4$)-example having $\Gamma=2.0$ and $\omega=2\pi$ in Fig. 10.22 below. Low quality response does not have the intersection of $\text{Re}G(\omega_s)$ and $\text{Im}G(\omega_s)$ near FWHM points of $\text{Im}G(\omega_s)$ or min-max points of $\text{Re}G(\omega_s)$ as is nearly the case for Fig. 10.20 and *exactly* the case for an ideal Lorentzian.

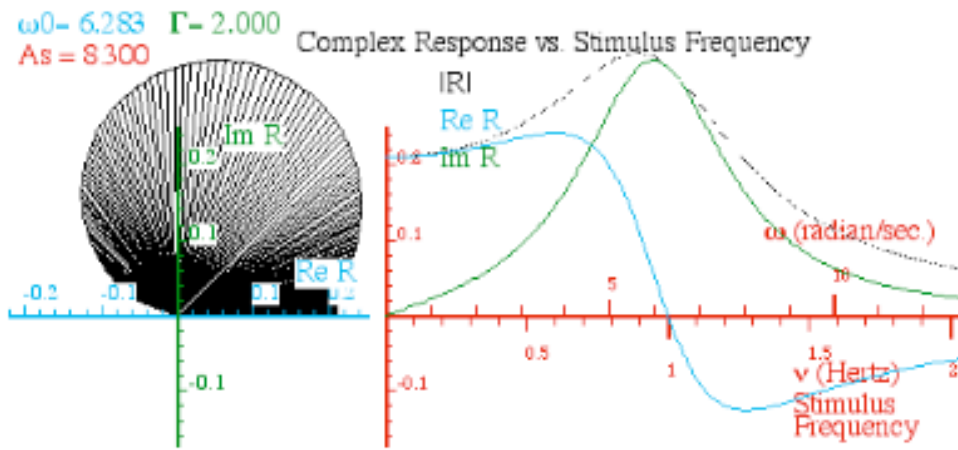


Fig. 10.22 Highly damped Lorentz-Green function plots with $\Gamma=2.0$ and $\omega=2\pi$.

Beats and lifetimes

Suppose at $t = 0$ a stimulus of angular frequency ω_s and amplitude $a(0)$ is applied to a ‘cold’ oscillator ($z(0) = 0$). Then a sum of decaying solution (10.46b) and stimulated response (10.48d) applies.

$$z(t) = z_{\text{transient}}(t) + z_{\text{response}}(t) \equiv z_{\text{decaying}}(t) + z_{\text{steady state}}(t)$$

$$= Ae^{-\Gamma t} e^{-i\omega_r t} + G_{\omega_0}(\omega_s) a(0) e^{-i\omega_s t} \tag{10.51a}$$

$$= Ae^{-\Gamma t} e^{-i\omega_r t} + |G_{\omega_0}(\omega_s)| a(0) e^{-i(\omega_s t - \rho)} \tag{10.51b}$$

The initial condition ($z(0) = 0$) demands that the complex transient amplitude A be given by:

$$A = -|G_{\omega_0}(\omega_s)| a(0) e^{i\rho} \quad \text{for } z(0) = 0 \tag{10.51c}$$

Then A cancels the stimulated response at $t=0$. But, as time progresses, the *transient amplitude* $z_{\text{transient}}(t)$ dies at rate Γ and the solution eventually grows up to be the *steady state* $z_{\text{response}}(t)$ alone. An example with a resonant stimulus ($\omega_s = \omega_0 = 2\pi$) is shown below in Fig. 10.23(a-b). Sub-resonant stimulus ($\omega_s < \omega_0$) is shown in Fig. 10.23(c-d) and super-resonant stimulus ($\omega_s > \omega_0$) is shown in Fig. 10.24(a-b).

Stimulus: $A_s = 0.5000$ $\omega = 6.2832$
 Response: $R = 0.1989$ $\rho = 1.5708$

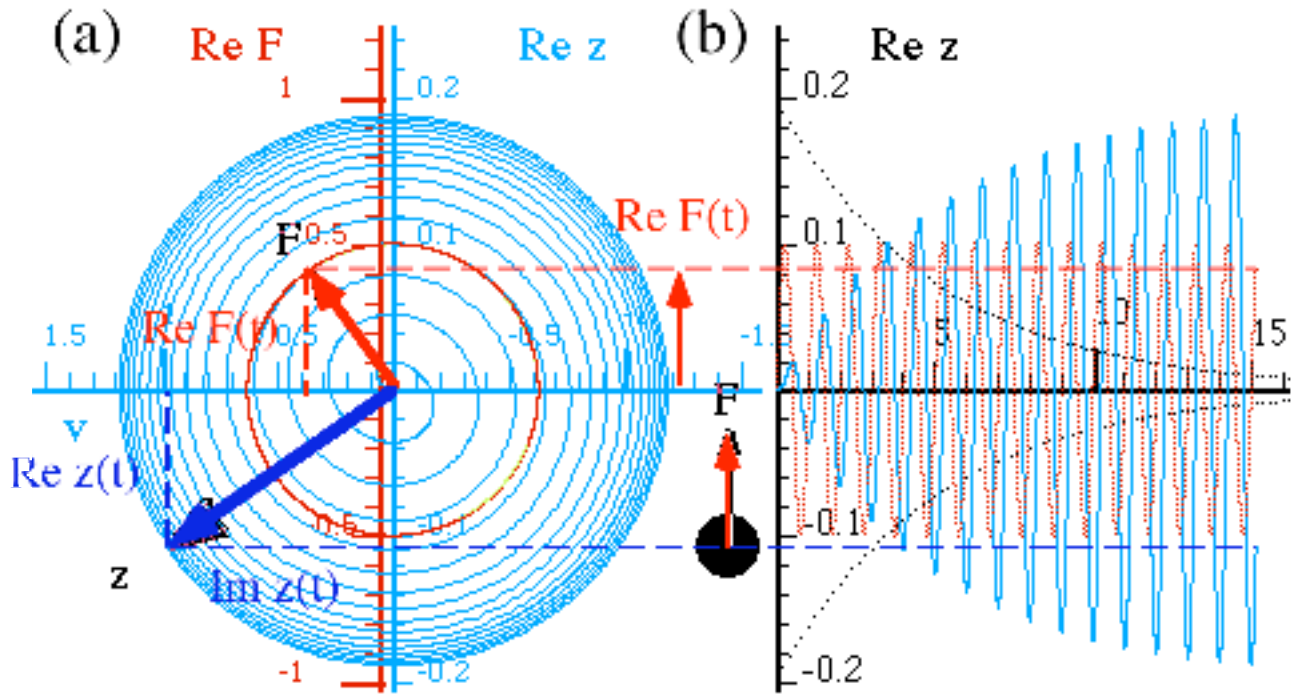


Fig. 10.23 On Resonance (a) Response z -phasor lags $\rho = 90^\circ$ behind stimulus F -phasor.

($\omega_s = \omega_0 = 2\pi$ and $\Gamma = 0.2$). (b) Time plots of $\text{Re } z(t)$ and $\text{Re } F(t)$

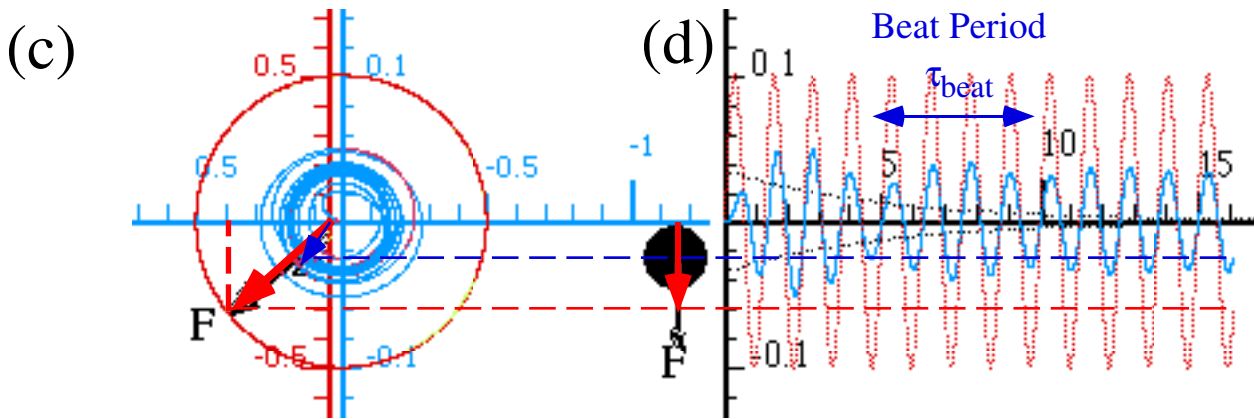


Fig. 10.23 Below Resonance (c) Response z -phasor lags $\rho = 8.05^\circ$ behind stimulus F -phasor.

($\omega_s = 5.03, \omega_0 = 2\pi, \Gamma = 0.2$). (d) Time plots of $\text{Re } z(t)$ and $\text{Re } F(t)$. Beats are barely visible.

The length of time it takes $z(t)$ to approach the steady state oscillation $z_{\text{response}}(t)$ is the same as the time it takes the transient part to die. So, after the 5% lifetime, the solution is more than 95% steady state response. In Fig. 10.23b the transient dies after about $t = 15$ sec. or about 15 oscillations. The angular quality factor $q = 15$ also gives the number of oscillations needed for the transient to decay to less than 5% and establish 95% of a resonance. Dotted outline traces of the hidden transient are shown in Fig. 10.23 and are proportional to the outline of the plot in Fig. 10.17.

Note that each resonant response oscillation is $1/4$ -period to the right of its stimulating oscillation in Fig. 10.23b, that is, it *lags* by $1/4$ -period. That is shown more clearly by the phasor diagram in Fig. 10.23a where the z phasor is behind the stimulus $F = a(0)e^{-i\omega_s t}$ by 90° ($\rho = \pi / 2$). This is consistent with (10.48a) that has real part of the response vanish at resonance ($\text{Re}G(\omega_s)=0$), leaving response at $\omega_s=\omega_0$ to be purely imaginary ($|G_{\omega_0}(\omega_0)| |a(0)| = \text{Im}G_{\omega_0}(\omega_0)$).

A stimulus frequency below resonance causes transient oscillatory *beat modulation*. In Fig. 10.24a-d the angular frequency ($\omega_s = 5.026$) of stimulus and steady state response is less than that of the transient ($\omega_\Gamma \cong \omega_0 = 2\pi = 6.28..$). So, the transient phasor $z_{transient}$ turns faster than response phasor $z_{ss-response}$ by $\omega_0 - \omega_s = 1.25$ radian / s, and it will " 2π -lap" the slower phasor every $1.25/(2\pi)$ seconds. This lap rate is called the *beat frequency* $\nu_{beat} = \omega_{beat}/2\pi$.

$$\nu_{beat} = |\nu_s - \nu_0| = |\omega_s - \omega_0| / (2\pi) = 0.199s^{-1} \tag{10.52}$$

The corresponding *beat period* $\tau_{beat} = 1/\nu_{beat}$ is the frequency inverse.

$$\tau_{beat} = 1/|\nu_s - \nu_0| = 2\pi / |\omega_s - \omega_0| = 5.01s \tag{10.53}$$

A beat period of about 5 sec. is seen in Fig. 10.23d. Beats are visible until the transient decays below about 5%. Then the poor $z(t)$ phasor has lost 95% of its faster transient part and can no longer "lap" the stimulus F -phasor. It is left with only the steady-state response part of (10.51a) and forced to "settle down" and lag dutifully at angle ρ behind the all-powerful stimulating F -phasor.

In its "younger days" the transient phasor $z_{transient}$ is big enough that the phasor sum $z(t) = z_{transient} + z_{ss-response}$ swells up as $z_{transient}$ passes the stimulus F -phasor and $z_{ss-response}$ (beat max) but then $z(t)$ shrinks as $z_{transient}$ goes on to be opposite $z_{ss-response}$ and nearly cancel it (beat min). The interference sum $z(t)$ experiences a beat every time $z_{transient}$ laps $z_{ss-response}$, as shown in Fig. 10.25.

However, note how much smaller the transient phasor has become just in the time it takes to make a beat. It is "aging" at rate Γ while the steady-state response-phasor $z_{ss-response}$ is just stuck ρ behind its stimulus F -phasor according to $z_{ss} = G \cdot F_{stimulus}$. Soon $z(t)$ falls into $z_{ss-response}$ to stay as long as F_s lasts.

Number of beats per second measures the magnitude of the relative *detuning* $\nu_s - \nu_0 = \Delta$, but not the sign of Δ . The following example in Fig. 10.24 has the stimulus faster than resonance by $|\Delta|=0.199s^{-1}$ but with $\nu_0 - \nu_s = -0.199/s$ Δ is the negative of (10.52). The beat number is the same but *not the phase!*

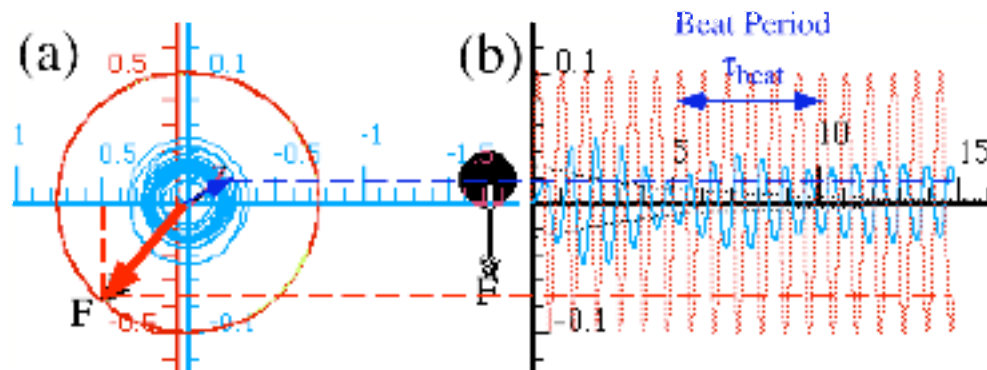


Fig. 10.24 Above Resonance (a)Response z -phasor lags $\rho=170.2^\circ$ behind stimulus F -phasor. ($\omega_s=7.53, \omega_0=2\pi, \Gamma=0.2$). (b) Time plots of $\text{Re} z(t)$ and $\text{Re} F(t)$ show decaying beats.

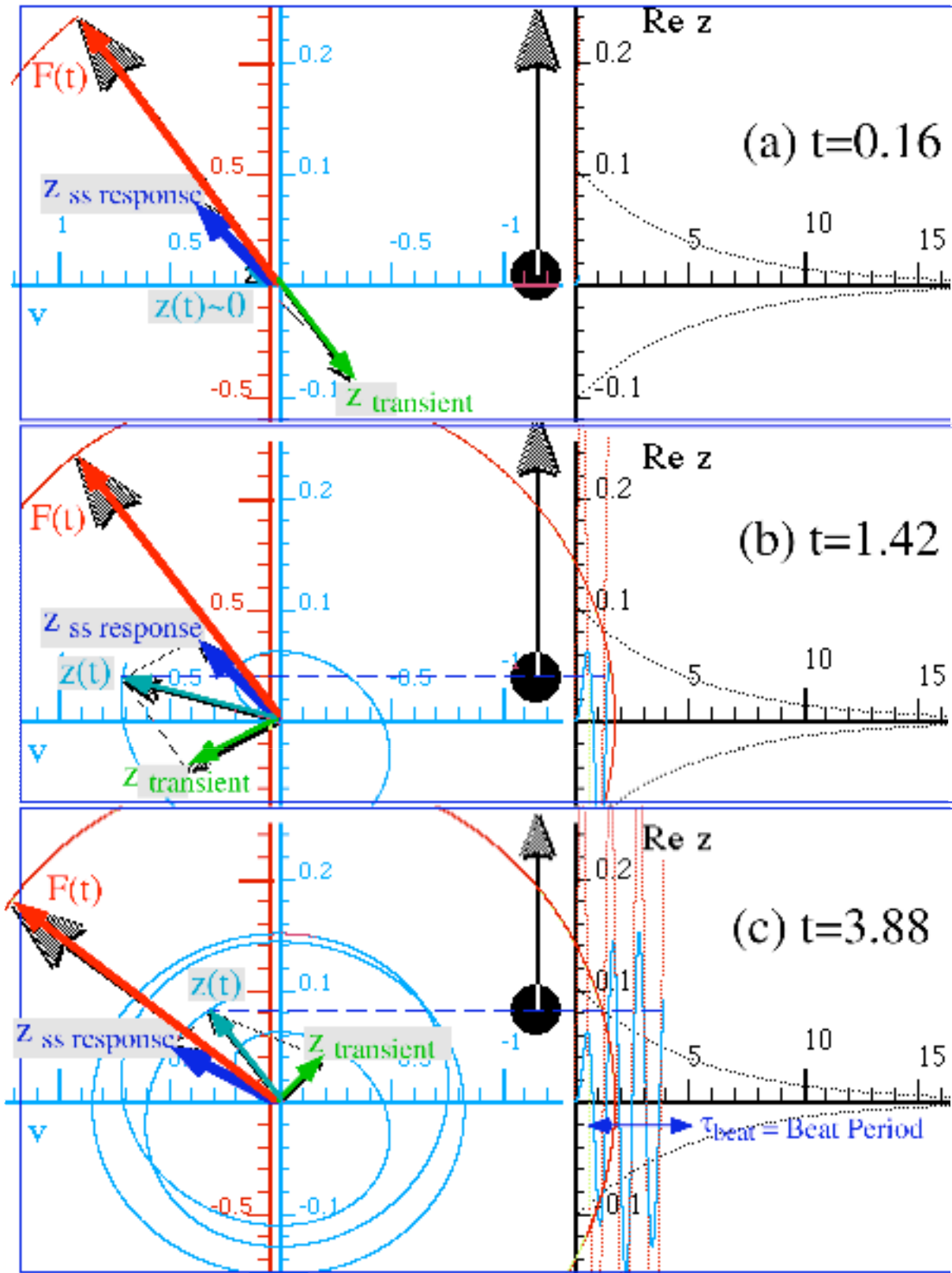


Fig. 10.25 Beat formation. Beat maximum occurs as transient phasor $z_{\text{transient}}$ catches up with F -phasor and passes it. The next beat maximum will be smaller since $z_{\text{transient}}$ is decaying.

Comparing resonant and non-resonant cases

For the below-resonance case in Fig. 10.23c and Fig. 10.25, the response phase lag according to (10.48d) is $\rho = 0.1405$, so $z_{ss \text{ response}}$ (and eventually $z(t)$ itself) is only 8.05° behind the stimulus. For the above-resonance case in Fig. 10.24, the response $z_{ss \text{ response}}$ and $z(t)$ lag behind by about 180° ($\rho = 170.2^\circ$). This is the signature of high frequency response $G(\infty)$: it becomes nearly π out of phase with the stimulus. In contrast the low frequency or DC response $G(0)$ is very nearly in phase with the stimulus.

Another difference between high and low frequency response is that high frequency response goes to zero $G(\infty) \sim 1/\omega_s^2 \rightarrow 0$ (as $\omega_s \rightarrow \infty$) and this helps explain the transparency of most materials to X-rays. Only heavy metals have electrons whose resonant frequencies are high enough to respond significantly to X-rays.

In contrast the low frequency response approaches a constant value, namely

$$\text{DC response} = G(0) = 1/\omega_0^2. \quad (10.54)$$

$G(0)$ is just the response due to a static (DC) unit force. For high frequency oscillators, $G(0)$ will be very small, but if you multiply little $G(0)$ by the big angular quality factor ($q = \omega_0 / 2\Gamma$ is the number of oscillations in the time needed to achieve 95% of a resonance) then the result $1/2\omega_0 \Gamma$ is exactly the resonant response amplitude $G(\omega_0)$. (Recall (10.49).) In other words, the DC response (10.54) is the average amplitude increase that is achieved during each cycle of a unit resonant stimulus before the damping Γ really takes effect.

High- q resonant and non-resonant cases

For very high q quality oscillators (very low Γ) the resonant region ($\omega_0 \pm \Gamma$) is so small that it may be considered non-existent. Let us note that typical atomic values for the angular quality q -factor approach 10^8 . An atomic resonance beginning in Fig. 10.26b has a hundred million oscillations to go! Atoms and molecules provide truly enormous resonant amplification factors!

In classical Hamiltonian systems we deal with this limiting case exclusively since damping is zero by definition. For infinite q there are really only two values for the response phase lag angle: in-phase ($\rho = 0$) and out-of-phase ($\rho = \pi$). The out-of-phase ($\rho = \pi$) occurs above resonance ($\omega_s > \omega_0$) as shown in Fig. 10.26a. The in-phase ($\rho = 0$) case occurs below resonance ($\omega_s < \omega_0$) as shown in Fig. 10.26c. Exactly at resonance where ($\omega_s = \omega_0$) the steady state response and the transient are both infinite and opposite so they cancel each other, and the $z(t)$ builds up forever as shown in Fig. 10.26b. Each cycle of revolution adds another bit of amplitude equal to the DC response (10.54) just as we explained above.

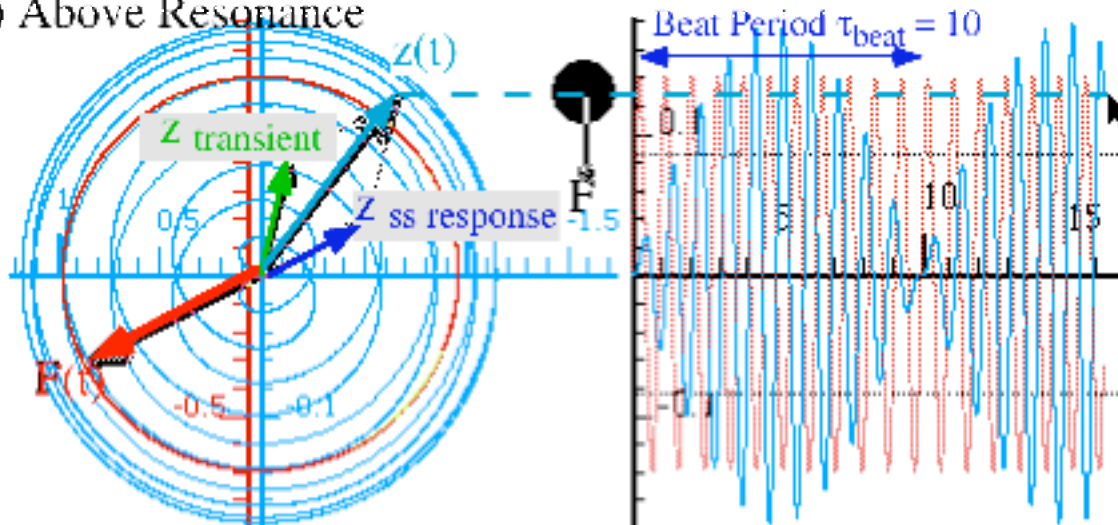
Fig. 10.26 Zero damping response ($\omega_0 = 2\pi, \Gamma = 0$) (Next page)

(a) Above resonance ($\omega_s = 6.91$)

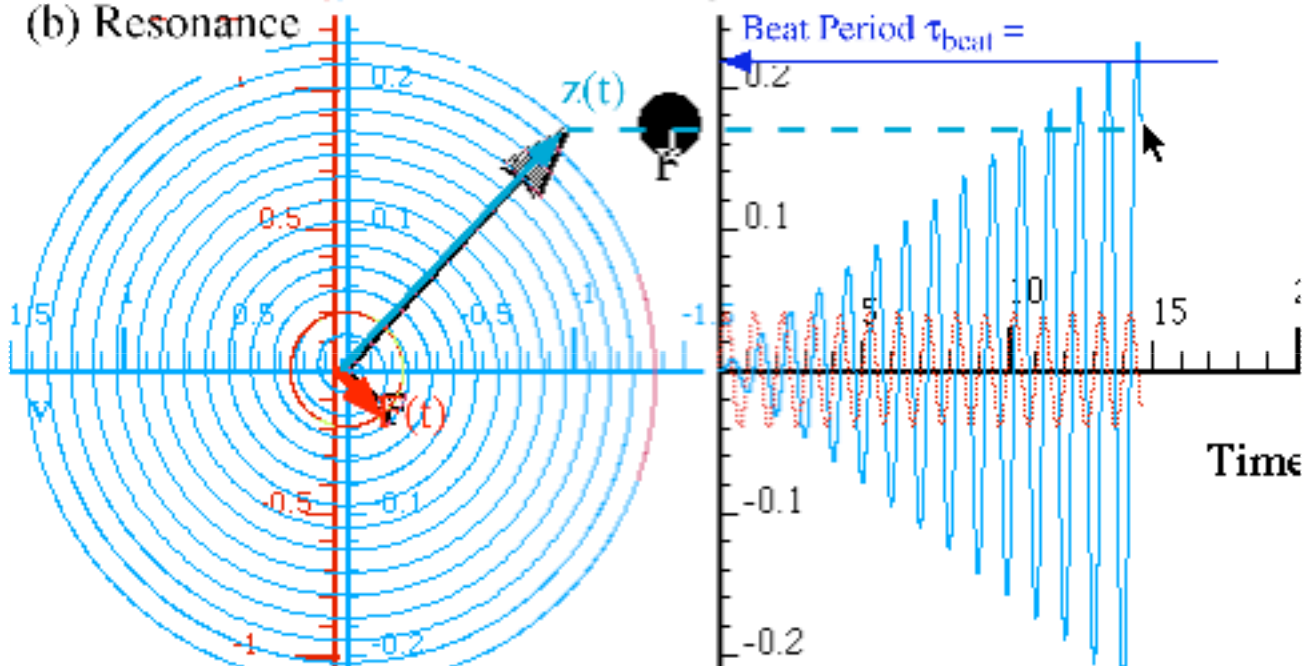
(b) Resonance ($\omega_s = 6.28$) (Stimulus amplitude reduced to show response.)

(c) Below resonance ($\omega_s = 5.65$)

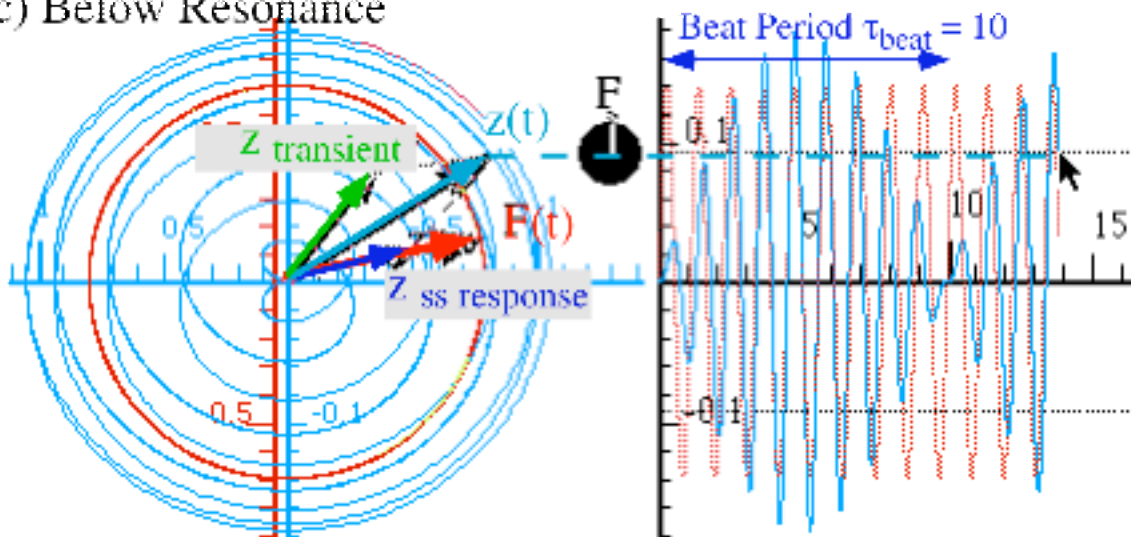
(a) Above Resonance



(b) Resonance



(c) Below Resonance



Appendix 1.A Vector product geometry

Vectors have *relative* projections onto each other. Components x , y , or z are projections of \mathbf{r} onto unit \mathbf{i} , \mathbf{j} , and \mathbf{k} . Power $\mathbf{F} \cdot \mathbf{v} = Fv \cos \theta$ is a *dot product* cosine projection of \mathbf{F} on \mathbf{v} . Coriolis $a = |\boldsymbol{\omega} \times \mathbf{v}| = \omega v \sin \theta$ is a sine-like transverse projection called the *cross product*. Product $\mathbf{A} \cdot \mathbf{B}$ (or $|\mathbf{A} \times \mathbf{B}|$) is cosine (or sine) of a relative angle $(\theta_B - \theta_A)$ times length factor AB as drawn in Fig. 1.A.1.

The cosine or dot-projection may be given in Cartesian lab components $(A_x = A \cos \phi_A) A_y = A \sin \phi_A$.

$$\mathbf{A} \cdot \mathbf{B} = AB \cos(\phi_B - \phi_A) = A \cos \phi_A B \cos \phi_B + A \sin \phi_A B \sin \phi_B = A_x B_x + A_y B_y \tag{1.A.1a}$$

The sine or cross-projection has a somewhat different or “crossed-up” form.

$$\mathbf{A} \times \mathbf{B} = AB \sin(\phi_B - \phi_A) = A \cos \phi_A B \sin \phi_B - A \sin \phi_A B \cos \phi_B = A_x B_y - A_y B_x \tag{1.A.1b}$$

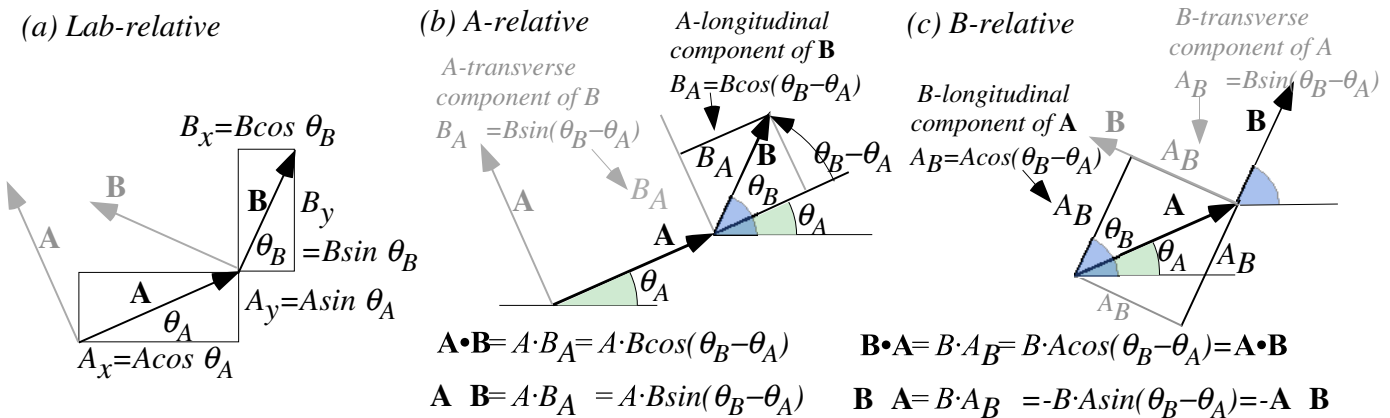


Fig. 1.A.1 Vector component geometry (a) Lab-relative. (b) A-relative. (c) B-relative.

Here $\mathbf{A} \cdot \mathbf{B}$ and $\mathbf{A} \times \mathbf{B}$ are numbers or *scalars*. Full $\mathbf{A} \times \mathbf{B}$ definition ((1.A.4b) below) is a vector perpendicular to both \mathbf{A} and \mathbf{B} . (In Fig. 1.A.1, it would stick out of the page.) Also it happens that $\mathbf{A} \times \mathbf{B}$ is the area of the vector parallelogram and $1/2 \mathbf{A} \times \mathbf{B}$ is the area of the $\mathbf{A} + \mathbf{B}$ or $\mathbf{A} - \mathbf{B}$ triangle as shown in Fig. 1.A.2.

In Fig. 1.A.1b vector \mathbf{B} refers to axes made of vector \mathbf{A} and its perpendicular copy \mathbf{A}_\perp and *vice-versa* in Fig. 1.A.1(c). Dot products are *reflexive* ($\mathbf{A} \cdot \mathbf{B} = \mathbf{B} \cdot \mathbf{A}$), but cross products must be *anti-reflexive* ($\mathbf{A} \times \mathbf{B} = -\mathbf{B} \times \mathbf{A}$) since the \mathbf{B}_\perp vector is in a negative direction relative to \mathbf{A} in Fig. 1.A.1(c). One way to display the relation between the pair $(\mathbf{A}, \mathbf{A}_\perp)$ and the pair $(\mathbf{B}, \mathbf{B}_\perp)$ is in a *rotation matrix*.

$$\begin{pmatrix} A_B & A_{B_\perp} \\ A_{\perp B} & A_{\perp \perp B} \end{pmatrix} = \begin{pmatrix} \cos \theta_{BA} & -\sin \theta_{BA} \\ \sin \theta_{BA} & \cos \theta_{BA} \end{pmatrix} = \begin{pmatrix} B_A & B_{A_\perp} \\ B_{\perp A} & B_{\perp \perp A} \end{pmatrix}^{-1} = \begin{pmatrix} \cos \theta_{BA} & \sin \theta_{BA} \\ -\sin \theta_{BA} & \cos \theta_{BA} \end{pmatrix}^{-1} \tag{1.A.2}$$

Algebraic definitions of $\mathbf{A} \cdot \mathbf{B}$ and $\mathbf{A} \times \mathbf{B}$ are based on the symmetric *Kronecker function* δ_{ij} and the totally *anti-symmetric Levi-Civita function* ϵ_{ijk} defined as follows.

$$\delta_i^j = \delta_{ij} = \begin{cases} 1 & \text{if: } i = j \\ 0 & \text{if: } i \neq j \end{cases} \tag{1.A.3a} \quad \epsilon^{ijk} = \epsilon_{ijk} = \begin{cases} +1 & \text{if } \{ijk\} \text{ is EVEN permutation of } \{123\}, \\ -1 & \text{if } \{ijk\} \text{ is ODD permutation of } \{123\}, \\ 0 & \text{otherwise.} \end{cases} \tag{1.A.3a}$$

These are fundamental to tensor analysis and exterior calculus that will be introduced in Unit 3. They also define scalar $\mathbf{A} \cdot \mathbf{B}$ and vector $\mathbf{A} \times \mathbf{B}$ products in useful ways for fast computer logic, as follows.

$$\mathbf{A} \cdot \mathbf{B} = \sum_{i=1}^3 \sum_{j=1}^3 \delta_{ij} A_i B_j = \sum_{i=1}^3 A_i B_i \quad (1.A.4a)$$

$$(\mathbf{A} \times \mathbf{B})_k = \sum_{i=1}^3 \sum_{j=1}^3 \epsilon_{ijk} A_i B_j = \sum_{i=1}^3 \sum_{j=1}^3 \epsilon_{kij} A_i B_j \quad (1.A.4b)$$

The notation $C_k=(\mathbf{C})_k$ denotes the k^{th} component of a vector \mathbf{C} .

Determinants and triple products

Levi-Civita sums define the *determinant detU* of a matrix U_{ij} . An *expansion by minors* is shown here.

$$\det U = \begin{vmatrix} U_{11} & U_{12} & U_{13} \\ U_{21} & U_{22} & U_{23} \\ U_{31} & U_{32} & U_{33} \end{vmatrix} = \sum_{i,j,k} \epsilon_{ijk} U_{1i} U_{2j} U_{3k} = U_{11} \begin{vmatrix} U_{22} & U_{23} \\ U_{32} & U_{33} \end{vmatrix} - U_{12} \begin{vmatrix} U_{21} & U_{23} \\ U_{31} & U_{33} \end{vmatrix} + U_{13} \begin{vmatrix} U_{21} & U_{22} \\ U_{31} & U_{32} \end{vmatrix} \quad (1.A.5)$$

A *triple vector product $\mathbf{A} \times \mathbf{B} \cdot \mathbf{C}$* is such a determinant made from a matrix of three vector components.

$$\mathbf{A} \cdot \mathbf{B} \times \mathbf{C} = \begin{vmatrix} A_1 & A_2 & A_3 \\ B_1 & B_2 & B_3 \\ C_1 & C_2 & C_3 \end{vmatrix} = \sum_{i,j,k} \epsilon_{ijk} A_i B_j C_k = A_1 \begin{vmatrix} B_2 & B_3 \\ C_2 & C_3 \end{vmatrix} - A_2 \begin{vmatrix} B_1 & B_3 \\ C_1 & C_3 \end{vmatrix} + A_3 \begin{vmatrix} B_1 & B_2 \\ C_1 & C_2 \end{vmatrix} \quad (1.A.6a)$$

$$= A_1 (\mathbf{B} \times \mathbf{C})_1 + A_2 (\mathbf{B} \times \mathbf{C})_2 + A_3 (\mathbf{B} \times \mathbf{C})_3 \quad (1.A.6b)$$

Minor expansion (1.A.5) is a (\bullet) -product of \mathbf{A} with (\times) -product vector $\mathbf{B} \times \mathbf{C}$. Base area $|\mathbf{B} \times \mathbf{C}|$ times altitude (\mathbf{A} projected onto normal $\mathbf{B} \times \mathbf{C}$) equals the parallelepiped volume enclosed by \mathbf{A} , \mathbf{B} , and \mathbf{C} .

Anti-symmetric ϵ -forms let us generalize geometry from 2-and 3-dimensions to N -dimensions.

Advanced mechanics has *many* dimensions. One mole ($6 \cdot 10^{23}$ particles) has at least $6 \cdot 10^{23}$ dimensions and two or three times that if the atoms move in 2D or 3D. So ϵ -forms are necessary!

Products of anti-symmetric ϵ -forms reduce to symmetric δ -forms by a *LeviCivita identity*.

$$\sum_{k=1}^3 \epsilon_{ijk} \epsilon_{mnk} = \delta_{im} \delta_{jn} - \delta_{in} \delta_{jm} = \sum_{k=1}^3 \epsilon_{kij} \epsilon_{kmn} \quad (1.A.7)$$

A triple-cross-product formula $\mathbf{A} \times (\mathbf{B} \times \mathbf{C}) = (\mathbf{A} \cdot \mathbf{C})\mathbf{B} - (\mathbf{A} \cdot \mathbf{B})\mathbf{C}$ is a first application.

$$\begin{aligned} (\mathbf{A} \times (\mathbf{B} \times \mathbf{C}))_i &= \sum_{j,k} \epsilon_{ijk} A_j (\mathbf{B} \times \mathbf{C})_k = \sum_{j,k,m,n} \epsilon_{ijk} \epsilon_{mnk} A_j B_m C_n = \sum_{j,m,n} (\delta_{im} \delta_{jn} - \delta_{in} \delta_{jm}) A_j B_m C_n \\ &= \sum_n A_n B_i C_n - \sum_m A_m B_m C_i = (\mathbf{A} \cdot \mathbf{C})(\mathbf{B})_i - (\mathbf{A} \cdot \mathbf{B})(\mathbf{C})_i \end{aligned}$$

The LC-identity (1.A.7) reduces each sum over k to dot-product terms.

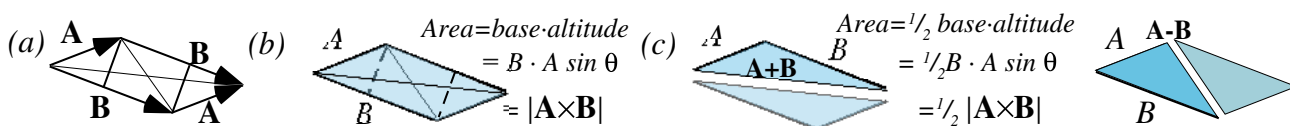


Fig. 1.A.2 Cross-product and area of (a)-(b) Parallelogram, (c) Sum triangle, (d) Difference triangle.

